University of Brasília

Department of Cell Biology

Postgraduate in Molecular Biology

PhD Thesis

Analysis of the effect of Ischemia and Reperfusion on Neutrophil Proteome in Rats

Muhammad Tahir

Supervisor: Prof. Dr. Wagner Fontes

Brasilia, June – 2014

University of Brasília

Department of Cell Biology

Postgraduate in Molecular Biology

Muhammad Tahir

PhD Thesis

Analysis of the effect of Ischemia and Reperfusion on Neutrophil Proteome in Rats

Thesis presented as partial requirement for the degree of Doctor of Philosophy in Molecular Biology, to the Department of Cell Biology at the Institute of Biological Sciences, University of Brasilia.

Supervisor: Prof. Dr. Wagner Fontes

Brasilia, June – 2014

This work was performed in the laboratory of Biochemistry and Protein Chemistry (LBQP) University of Brasilia in collaboration with Laboratory of Surgical Physiopathology (LIM-62), Faculty of Medicine University of São Paulo and Protein Research Group (PRG) Southern Denmark University, Odense, Denmark.

ACKNOWLEDGMENT

*All praises for **Almighty Allah** the most compassionate, the most beneficent and ever merciful, who gives me the power to do, the sight to observe and mind to think and judge. Peace and blessings of **Almighty Allah** be upon **His Prophet Hazrat Muhammad (P.B.U.H)** who exhorted his followers to seek knowledge from cradle to grave.*

This thesis is based on results from Laboratório de Bioquímica e Química de Proteínas (LBQP), University of Brasília, Brazil, Laboratory of Surgical Physiopathology (LIM-62), of the Faculty of Medicine (LIM-62), University of São Paulo, Brazil, Protein Research Group of Southern Denmark University (SDU), Odense.

*I want to express my deepest gratitude for my supervisor, **Prof. Dr. Wagner Fontes**, for his kind supervision, useful suggestions, consistent encouragement, friendly behavior and dynamic supervision which enabled me to perform my research work in ensuring my academic, professional and moral well being.*

*I would like to extend my vehement sense of gratitude and sincere feelings of reverence and regards to **Prof. Dr. Peter Roepstorff** to receive me in his research group under his supervision, for his co-operation in providing me all possible facilities during my research at Protein Research Group, (SDU). Many thanks also go to my honorable teachers, especially **Prof. Dr. Belchor Fontes** and **Prof. Dr. Edna Montero** for their support and providing me all possible facilities during research at LIM 62.*

I am grateful to TWAS-CNPq for the financial assistance in the form of PhD Fellowship.

*Also many thanks to my wife **Samina Arshid**, a PhD student at FMUSP, for her kind cooperation and help during my research.*

Furthermore, I am deeply obliged and thankful to my lab fellows at LBQP and LIM62 especially to Alison da Silva Alexandre, Adelson Silva, Rayner Queiroz, Muhammad Faheem, Michaella Pereira, Carlos Garcia, Everton da Rosa, Diana Gomez, Elaine Nascimento, Anne Dian, Nuno Domingues, Ana Maria Cattani, Marcos, Mario, Luci, and others for their co-operation and sympathetic attitude during my study.

Also, during my stay at SDU, Odense, I am very much thankful to Simone Sidoli and Giuseppe Palmisano for their help in Mass Spectrometric Analysis, Veit Schwämmle for statistical analysis of data, Lene Jakobsen for my initial training at SDU, Odense, Maria Ibáñez-Vea for nice discussions and guidelines for the sample preparation, Prof. Dr. Martin Larsen, Karin Hjernø, Helle Marquard Mortensen, Marco Milioli, Philipp Holzinger, Marcela Braga, Thiago Braga, Richard Hemmi Valente and other members of PR-Group.

Finally, I wish to express my deepest gratitude to my family for continuous support and love during these years. I wish special thanks to my dear parents especially to my father ***Taj Merin*** *for his love, encouragement and support in every part of my life and my son* ***Ayan Tahir*** *for unconditional love, patience and encouragement.*

May ***Almighty Allah*** *shower* ***His*** *blessings and prosperity on all those who assisted me in any way during my work.*

Muhammad Tahir

ABSTRACT

Intestinal Ischemia and reperfusion injury are widely used models, which results into tissue dysfunction and organ failure especially after trauma and surgery. Whereas neutrophils play an important role in the mechanism of injuries caused by ischemia and reperfusion. However, the effect of intestinal ischemia and reperfusion on stimulation and activation of neutrophils is still unclear. Proteomic analysis has been ratified as an appropriate tool to studying complex systems, such as stimulation and activation of neutrophils, so the objective of this work was to evaluate the effect of ischemia and reperfusion on neutrophil proteome in Wistar rats. For proteomic neutrophils from three groups; control, laparotomy, and intestinal ischemia/reperfusion were separated. Protein was extracted according to FASP protocol, trypsin digested, iTRAQ-labeled. Phosphopeptides were enriched by TiO_2-SIMAC-HILIC procedure. Non-phosphorylated and mono-phosphorylated peptides were HILIC fractionated prior to LC-MS/MS analysis. LC-MS/MS and bioinformatics procedures were applied to peptides for their quantitation, phosphosite assignment and protein identification. A total of 3816 proteins containing 2231 non-phosphorylated unique proteins and 892 unique phosphorylated proteins whereas 693 phosphorylated proteins were identified in both total and phosphoproteome. In total 1585 phosphorylated proteins were identified, representing 41.5% of protein phosphorylation of the total neutrophil proteome identified in this study. We aimed to bring further light to this process by analyzing hematological parameters after ischemia and preconditioning. Gene ontologies for all the regulated proteins represented changes confer by the experimental groups on neutrophil proteome. We could identify the relevant predicted enzyme activities and pathways involved in neutrophils activation after intestinal ischemia and reperfusion. Most of the regulated predicted enzymes of the rat neutrophil proteome are transferases, hydrolases and oxidoreductases. Important pathways from KEGG analysis include ribosomal, regulation of actin cytoskeleton, Fc gamma R-mediated phagocytosis, chemokine signaling, metabolic and oxidative phosphorylation pathways. We also aimed to bring further light to this process by analyzing hematological parameters after ischemia and preconditioning. Our findings provide platform for the first time to understand the effects

of intestinal ischemia and reperfusion on neutrophil proteome and mechanism involve in this process.

Keywords: Ischemia Reperfusion, Neutrophils, Proteomics, Systemic Inflammatory Response, Phosphoproteomics.

RESUMO

Lesão por isquemia e reperfusão é um modelos amplamente usados que resulta em disfunção tecidual e falha do órgão especialmente após trauma e cirurgia, enquanto que neutrófilos desempenham papel importante no mecanismo de lesão causada por isquemia e reperfusão. No entanto, o efeito da isquemia e reperfusão na estimulação e ativação de neutrófilos ainda não é claro. A análise proteômica tem sido ratificada como uma ferramenta adequada no estudo de sistemas complexos, tais como a estimulação e ativação de neutrófilos, portanto o objetivo desse trabalho foi avaliar os efeitos da isquemia e reperfusão no proteoma de neutrófilos e nos parâmetros hematológicos em ratos Wistar. Três grupos de neutrófilos foram separados: controle, laparotomia e isquemia/reperfusão intestinal. Proteínas foram extraídas de acordo com o protocolo FASP, digeridas com tripsina e marcadas com iTRAQ. Fosfopeptídios foram enriquecidos pelo procedimento TiO_2-SIMAC-HILIC. Peptídios fosforilados e não fosforilados foram fracionados por HILIC antes da análise por LC-MS/MS. Procedimentos de LC-MS/MS e bioinformática foram aplicados para quantificação dos peptídeos, designação do sitio de fosforilação e identificação proteica. Foi identificado um total de 3816 proteínas contendo 2231 proteínas exclusivamente não fosforiladas, 892 exclusivamente fosforiladas e 693 presentes tanto no proteoma total quanto no fosfoproteoma. No total 1585 proteínas fosforiladas foram identificadas, representando 41,5% da fosforilação de proteínas no proteoma total de neutrófilos identificado nesse estudo. A classificação das proteínas reguladas por ontologia genética mostrou mudanças no proteoma de neutrófilos conferidas pelos grupos experimentais. Nós pudemos identificar atividades enzimáticas e vias de sinalização relevantes envolvidas na ativação de neutrófilos após isquemia intestinal e reperfusão. A maior parte das enzimas reguladas no proteoma de neutrófilos de rato são transferases, hidrolases e oxidoredutases. Vias identificadas na base de dados KEGG e contendo diversas proteínas reguladas incluem a ribossomal, regulação de actina do citoesqueleto, fagocitose mediada por Fc-gama-R, sinalização por quimocina, vias de fosforilação oxidativa e metabólica. Nossos resultados fornecem base para compreender pela primeira vez os efeitos de isquemia e reperfusão no proteoma de neutrófilos e os mecanismos envolvidos no processo.

Palavras-chave: Isquemia/Reperfusão, Neutrófilos, Proteômica, Resposta Inflamatória Sistêmica, Fosfoproteômica.

CONTENTS

List of Figures

List of Tables

List of Abbreviations

1DE	One-dimensional gel electrophoresis
2DE	Two-dimensional gel electrophoresis
6PGDH	6-phosphogluconate dehydrogenase
AA	Arachidonic acid
AdoRA2B	Adenosine A2B-receptors
ALI	Acute Lung Injury
AMI	Acute mesenteric ischemia
AR	Aldose reductase
ARTs	Adp-ribosyl transferase
ATP	Adenosine triphosphate
BAL	Bronchoalveolar lavage
BLT-1	Leukotriene B (4) receptors.
BPI	Permeability-increasing protein
BTK	Bruton tyrosine kinase
C3a	Complement 3a
CaMKs	Calmodulin-dependent protein kinase
CG	Cathepsin
CI	Chemical ionization
CID	Collision-induced dissociation
CINC-1	Cytokine-induced neutrophil chemoattractant-1
COX	Cyclooxygenase

CXCR	CXC chemokine receptors
CyPs	Cyclophilins
DEGs	Differentially expressed genes
DGKζ	Diacylglycerol kinase ζ
DIGE	Differential gel electrophoresis
ECD	Electron capture dissociation
ECs	Endothelial cells
ERK1/2	Extracellular signal-regulated protein kinase-1/2
ESI	Electrospray ionization
ESI-MS/MS	Electrospray tandem mass spectrometry
ETD	Electron transfer dissociation
FAB	Fast atom bombardment
FAK	Focal adhesion kinase
FGAM	Phosphoribosyl formyl glycin amidine
Fhs	Formate tetrahydrofolate ligase
fMLP	Formyl-Methionyl-Leucyl-Phenylalanine
G-CSF	Granulocyte colony-stimulating factor
GAPDH	Glyceraldehyde-3-phosphate dehydrogenase
GROs	Growth-related oncogenes
Gsr	Glutathione reductase
H2O2	Hydrogen peroxide
HIF-1	Hypoxia-inducible factor 1

HK3	Hexokinase-3
HNP-1	Human neutrophil peptides
HPLC	High-performance liquid chromatography
ICAMs	Intercellular Adhesion Molecule
ICAT	Isotope coded affinity tag
ILs	Interleukins
IMAC	Immobilized metal affinity chromatography
IPC	Ischemic Preconditioning
IRAK-4	Interleukin-1 receptor-associated kinase-4
iTRAQ	Isobaric tags for relative and absolute quantitation
KATP channel	ATP-sensitive potassium channel
KEGG	Kyoto Encyclopedia of Gens and Genomes
LDH	Lactate dehydrogenase
LPS	Lipopolysaccharide
LSI-MS	Liquid secondary ion mass spectrometry
LTB4	Leukotriene B4
LTQ	Linear ion trap
MALDI-TOF	Matrix-assisted laser desorption/ionization tandem mass spectrometry
MAPK	Mitogen-activated protein kinase
MAPKAPK 2	Map kinase-activated protein kinase 2
MIF	Macrophage migration inhibitory factor
MIPs	Macrophage inflammatory protein

MOAC	Metal oxide affinity chromatography
MOF	Multiple organ failure
MPO	Myeloperoxidase
MRP-14	Myeloid-related protein-14
MTP	Mitochondrial transition pore
NADPH oxidase	Nicotinamide adenine dinucleotide phosphate-oxidase
NAP2	Neutrophil activating peptide-2
NE	Neutrophil elastase
NF-κB	Nuclear factor-κB
NQO1	Nad(p)h quinone oxidoreductase 1
PAF	Platelet-activating factor
PAK2	P21-activated kinase
PAR1	Proteinase-activated receptor 1
PD	Plasma desorption
PDI	Protein disulfide-isomerase
PECAM-1	Platelet endothelial cell adhesion molecule
PGE	Prostaglandin-e synthase
PGG2	Prostaglandin g2
PGH2	Prostaglandin h2
PIP5K	Phosphatidylinositol 4 phosphate 5 kinase
PMNs	Polymorphonuclear Neutrophils
PQD	Pulsed Q Dissociation

PR3	Proteinase 3
PSGL-1	P-selectin glycoprotein ligand-1
PTM	Post translational modifications
RA	Rheumatoid arthritis
Raf-1	Serine/threonine-specific protein kinases
RALDH	Retinal dehydrogenase
RANTES	Regulated on Activation Normal T-cell Expressed and Secreted
ROS	Reactive oxygen specie
RPLC	Reversed Phase liquid chromatoraphy
SDC	Sodium deoxycholate
SDS	Sodium dodecyl sulfate
SDSPAGE	Polyacrylamide gel electrophoresis
SILAC	Stable isotope labeling of Amino acids in cell culture
SIMAC	Sequential elution from IMAC
SIRS	Systemic inflammatory response syndrome
SMAO	Superior mesenteric artery occlusion
SOD	Superoxide dismutase
Sph	Serine residue
TEAB	Triethylammonium bicarbonate
TEM	Trans endothelial migration
TFA	Trifluoroacetic acid
TiO2	Titanium dioxide affinity chromatography-

TLR	Toll like receptors
TMT	Tandem Mass Tags
TNF-α	Tumor necrosis factor α
Tph	Threonine
TrxR	NADPH-dependent thioredoxin reductases
VEGF	Vascular endothelial growth factor
XDH	Xanthine dehydrogenase
XO	Xanthine oxidase

INTRODUCTION

1.1 Polymorphonuclear Neutrophils (PMNs)

Neutrophils are part of peripheral blood and play important role in microbe clearance and participate in systemic inflammatory response after activation [1]. As soon as pathogen invasion occurs neutrophil become activated and infiltrate to site of injury. To control infection neutrophil take part in phagocytosis and produce free radicals. These cells can be primes by hypoxia, microbial products, and cytokines, and on complete activation results into superoxide production, endothelial adherence, and membrane receptor expression [2]. Neutrophil recruitment is multistep process and requires three classes of adhesion receptors, including selectins, integrins and adhesion receptors of the immunoglobulin superfamily [3]. These steps are as shown the figure 1.

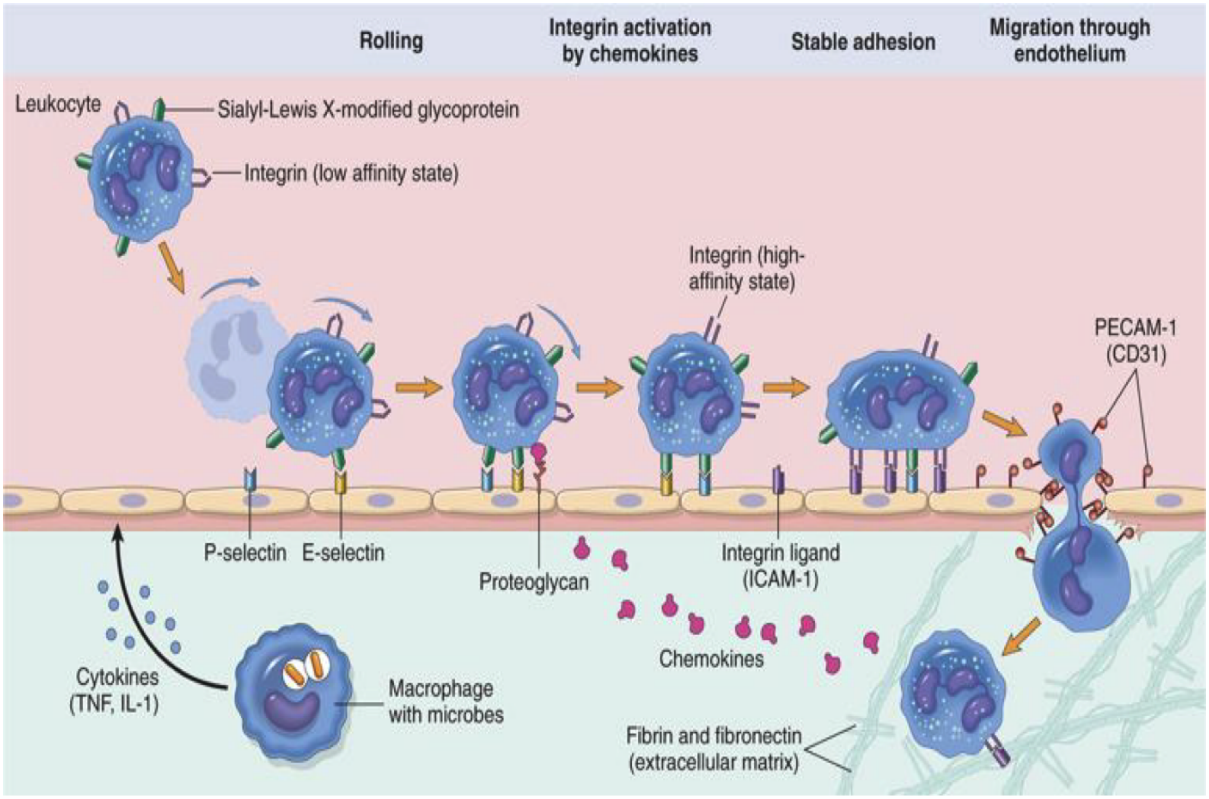

Figure 1 Neutrophil recruitment to sites of inflammation

A step-wise process involving leukocytes rolling, activation, and adherence to endothelium, transmigration across endothelium and pierce basement membrane migrate towards chemoattractants emanating from source of injury. Adapted from [4].

1.1.1 Rolling

Selectins are glycoprotein surface adhesion molecules, as L-selectin (leukocytes), E-selectin (endothelial cells (EC)), and P-selectin (platelets and EC) which not only take part in rolling but also has impact on adherance [5]. The ligands for neutrophil L-selectin are multiple sialylated carbohydrate determinants, which are linked to mucin-like molecules [5]. Activation of toll like receptor (TLR-2) and complement system, ROS and thrombin production and a high intracellular calcium concentration causes maximum increase in expression of endothelial P-selectin from Weibel–Palade within 10-20 min of reperfusion. Interaction of P-selectin with P-selectin glycoprotein ligand-1 (PSGL-1) expressed by neutrophils results into weak and reversible interaction between neutrophil and endothelium i-e, adherence followed by rolling [6, 7]. In an ischemia/reperfusion model experiment blocking of L-selectin and/or P-selectins has decreased both neutrophil rolling and adherence [8].

1.1.2 Tight adhesion

Integrins are heterodimeric proteins, having α-subunits and β-subunits that are expressed on cell surface. β2 integrins expresses on leukocytes and consist of three distinct α-subunits such as CD11a, CD11b, and CD11c, which bind to a common β-subunit such as CD18. Relative expression of α-subunit differs according to the stimulus causing leukocyte adherence and transmigration [9]. Endothelial cells molecules like intercellular adhesion molecule (ICAM-1) act as the ligand for both CD11a/CD18 and CD11b/CD18, but ICAM-2 binds only with CD11a resulting into strong adhesion of neutrophils to endothelium [10]. Increase in adhesion and migration of PMNs to post capillary venules has been noticed during study of tissue underwent IRI [11]. ROS, platelet-activating factor (PAF), IL-1, TNF-α and leukotriene B4 (LTB4) released by endothelium and immune cells after reperfusion causes increase in expression of neutrophil β2 integrins from intracellular granules resulting into tight adhesion [12, 13].

1.1.3 Tansendothelial Migration/Diapedesis

Platelet endothelial cell adhesion molecule (PECAM-1) expresses on the lateral borders of EC as well as on neutrophil and is involved in transfer of neutrophils towards the interstitium called as diapedesis. Blocking PECAM-1, lead to inhibition of diapedesis but stronger

adhesion between neutrophil and endothelium [14]. In another study, up-regulation of adhesion molecules have been observed following IRI which can promote diapedesis of neutrophil by further contributing to muscle dysfunction [15]. CD11/CD18–ICAM-1 interaction and ROS also facilitate diapedesis by decreasing the expression of cadherin and inducing phosphorylation of vascular endothelial-cadherin and catenin which lead to loosening of intercellular junctions resulting into neutrophil transmigration [16, 17].

1.1.4 Chemotaxis

Transmigrating cells moves towards increasing gradient of chemoattractants in a process known as chemotaxis [18]. Chemoattractants for different leukocyte population include N-formylated peptides produced by bacteria, such as Formyl-Methionyl-Leucyl-Phenylalanine (fMLP), polypeptides (e.g. C5a), and lipids (e.g. leukotriene-B4) [19]. Cytokines, or chemokines, are a novel family of include IL-8 [20], neutrophil activating peptide-2; growth-related oncogene (GRO)-α, GRO-β and GRO-δ; and macrophage inflammatory protein MIP-2α and MIP-2β. These chemokines belongs to CXC chemokines/α chemokines and are similar in structure. Another family of chemokines is the CC chemokines/β chemokines, that includes RANTES/CCL5 (regulated on activation, normal T cell expressed and secreted), Monocyte chemoattractant protein-1, -2 and -3 (MCP-1/2/3); and Macrophage inflammatory proteins, MIP-1α and MIP-1β [21].

Along with massive ROS production, proteases released from neutrophilic granules and metabolites of arachidonic acid (AA) such as PAF and LTB4 are also involve in neutrophil related tissue injury. PAF and LTB4 are strong chemokines that stimulate neutrophil degranulation [22].

1.2 Neutrophils Granules and Degranulation

There are four fundamental types of granules in neutrophils (Fig-2) as below.

1.2.1 Azurophilic granules

Azurophilic granules or primary granules are produced first during neutrophil maturation, and contain myeloperoxidase (MPO) which is very important enzyme of oxidative burst [23]. Defensins, lysozyme, permeability-increasing protein (BPI), and a number of serine

proteases: neutrophil elastase (NE), proteinase 3 (PR3), and cathepsin G (CG) are also stored in primary granules [24].

1.2.2 Specific (or secondary) granules

Specific granules contain the glycoprotein lactoferrin and different antimicrobial compounds including neutrophil gelatinase-associated lipocalin (NGAL), human cathelicidin antimicrobial protein (hCAP-18), and lysozyme [23, 24].

1.2.3 Gelatinase (tertiary) granules

The gelatinase granules contain few antimicrobials, and stores metalloproteases, such as gelatinase and leukolysin [25].

1.2.4 Secretory vesicles:

Secretory vesicles consist of albumin and stores membrane-bound molecules required during neutrophil migration [26].

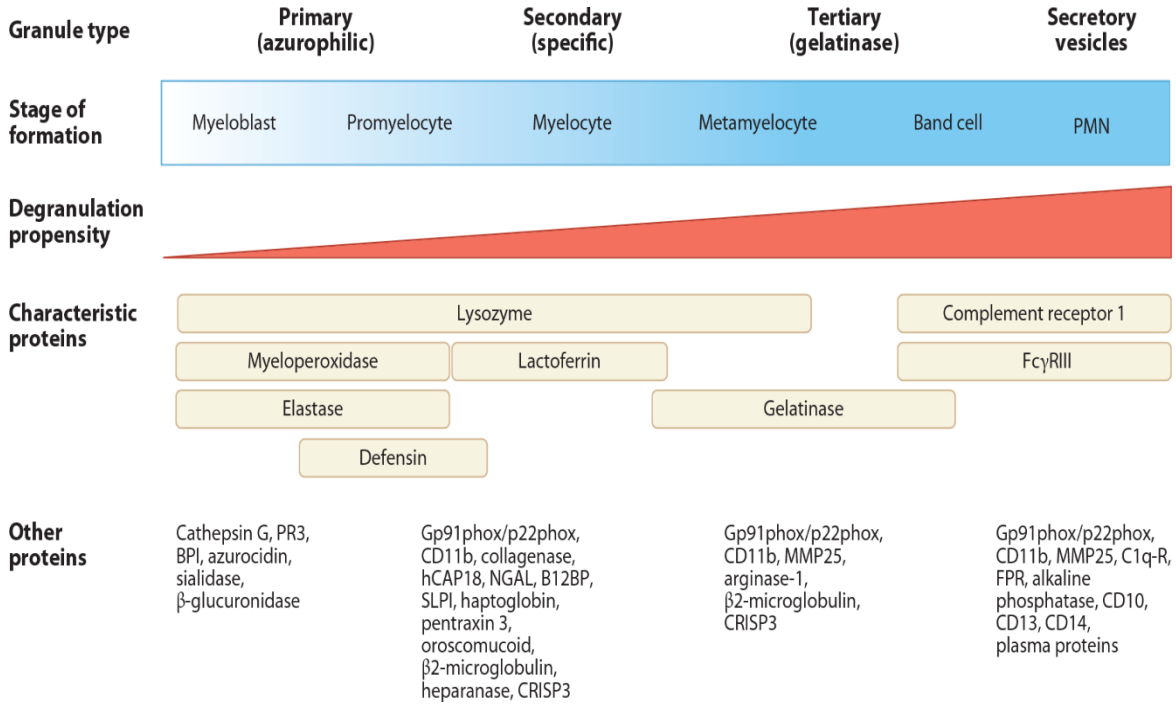

Figure 2 Neutrophil granules and their characteristic proteins.

Neutrophil granules carry a rich variety of antimicrobials and signaling molecules. Adapted from [27].

1.2.5 Degranulation

Neutrophil activation, causes alteration in molecular composition of membrane of granules resulting into mobilization of granules, fusion with the plasma membrane or the phagosome and secretion of the contents to outside of neutrophil. The order of mobilization is first secretory, tertiary, primary and then secondary granules while intera-cellular calcium level play role in this type of mobilization [28].

Mobilization of secretory vesicles, is necessary for continued activation of the neutrophil because its membrane contains the β2 integrins, complement and fMLP receptors, as well as the FcγRIII receptor [25]. This results into firm adhesion of neutrophil with endothelium further mobilizing gelatinase granules, which releases metalloproteases [29].

After extravasation, oxidative burst starts with mobilization of the azurophilic and specific granules, which contain flavocytochrome b558, a component of the NADPH oxidase machinery. As a result assembly of the NADPH oxidase complex and production of ROS takes place inside the phagolysosome and outside the cell creating antimicrobial environment [30].

1.3 Ischemia

Ischemia is insufficient blood supply to an organ that leads to cellular dysfunction and necrosis. It occurs mostly in case of trauma, shock, surgery, or organ transplantation [31].

1.3.1 Cellular effects of Ischemia

Prolonged ischemia results in a variety of cellular metabolic and ultra-structural changes (fig-3A). During ischemia, anaerobic metabolism produces a decrease in cell pH by accumulating hydrogen ions, and then Na+/H+ exchanger excretes excess hydrogen ions, resulting into large influx of sodium ions [32]. Cellular ATP depletes which inactivates ATPases, reduces active Ca^{2+} efflux, and limits the re-uptake of calcium by the endoplasmic reticulum, thereby produce calcium overload in the cell. As a result mitochondrial permeability transition (MPT) pore open that further disrupt ATP production by interrupting mitochondrial membrane potential. Magnitude of blood flow

and duration of ischemia effect the degree of tissue injury [33] (fig-3A). Hypoxia-inducible factor 1 (HIF-1) induces increase in transcription of vascular endothelial growth factor (VEGF), which also plays important role in angiogenesis [34, 35].

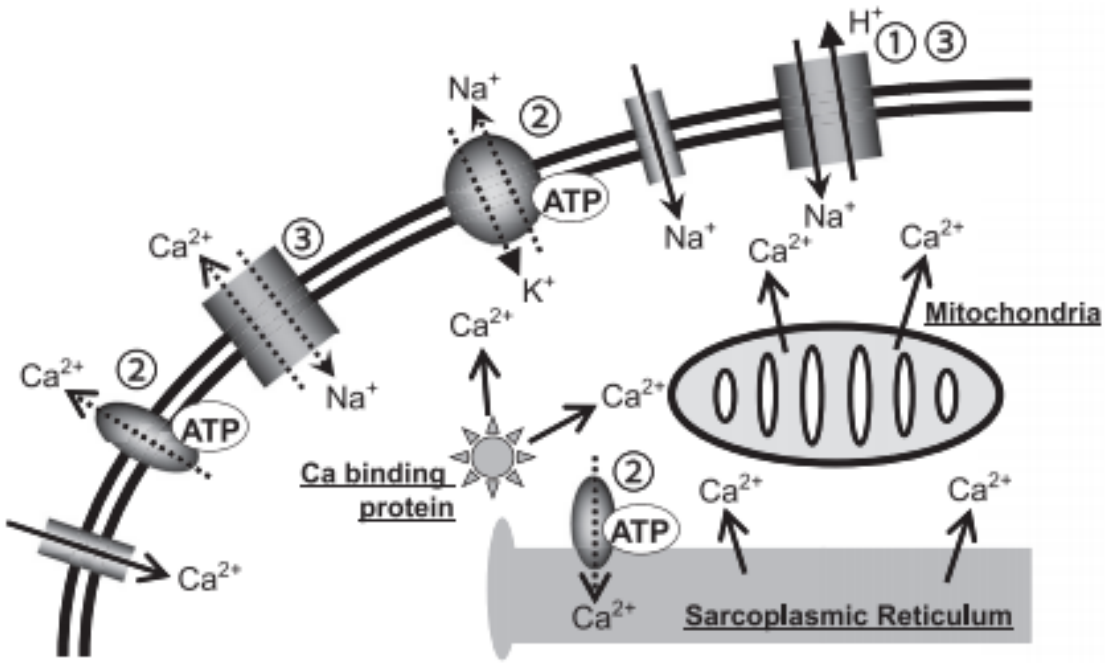

Figure 3 A Cellular effect of Ischemia.

Modified from [32]. (1) Excretion of H^+ due to pH lowering, (2) deactivation due to loss of ATP, and (3) reduction of Na^+/Ca^{2+} exchange due to lowered extracellular pH and intracellular accumulation of Na^+.

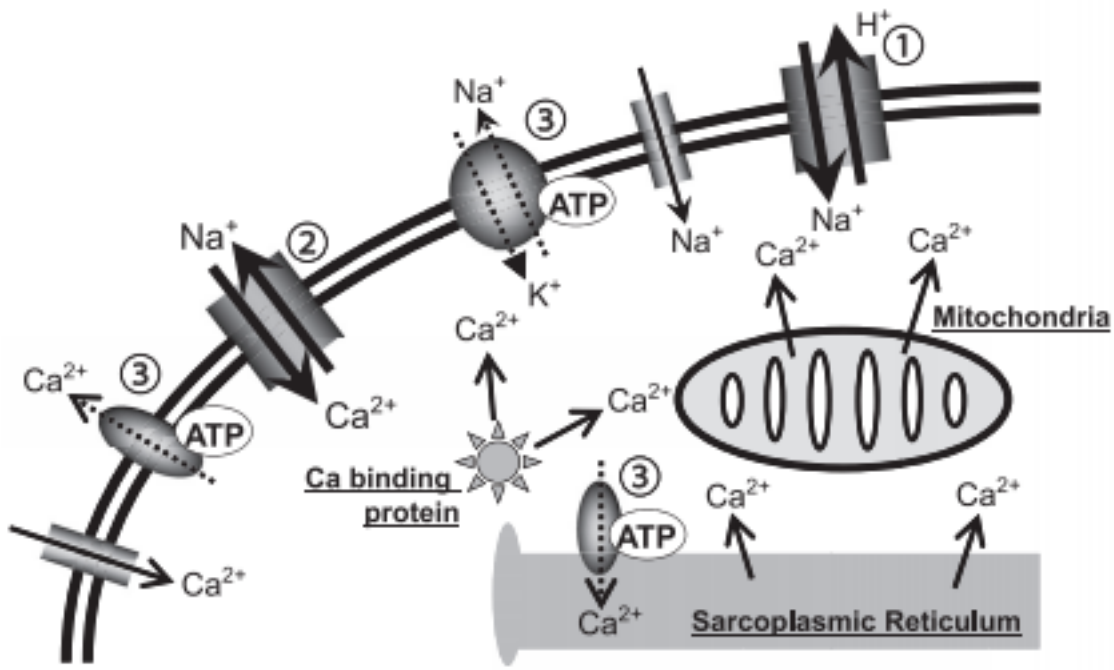

Figure 3-B: Cellular effect of Reperfusion.

Modified from [32]. (1) Robust excretion of H+ due to prompt recovery of extracellular pH, (2) "reverse mode" excretion of accumulated Na+ and Ca^{2+} influx in turn, and (3) re-excretion of Ca^{2+} followed by recovery of ATP synthesis.

1.4 Ischemic Reperfusion injury (IRI)

Reperfusion results into infiltration of activated neutrophil to site of injury which participate along with acute inflammatory response [36]. The mechanism underlying reperfusion injury is complex, multi-factorial (Fig-3B) and involve

1. Generation of reactive oxygen species (ROS) upon re-introduction of molecular oxygen,
2. Calcium overload,
3. Opening of the MPT pore,
4. Endothelial dysfunction,
5. Hypoxanthine accumulation,

6. Expression of certain pro-inflammatory gene products such as leukocyte adhesion molecules, cytokines,

7. Repression of protective gene products like constitutive nitric oxide synthase, thrombomodulin and bioactive agents i-e prostacyclin, nitric oxide [37].

Vasoconstriction after reperfusion injury occurs as a result of reduction in bioavailability of endothelial mediators that results into more production of adhesion molecules and cytokines. These adhesion molecules and cytokines supports recruitment of inflammatory cells which release more inflammatory mediator leading to more endothelial dysfunction and tissue damage [38, 39].

1.5 Intestinal Ischemic Reperfusion injury and PMNs

Intestine is most sensitive organ to IRI and is caused by many clinical conditions like acute mesenteric ischemia, intestinal obstruction, incarcerated hernia, small intestine transplantation, neonatal necrotizing enterocolitis, trauma, and shock which can result into severe clinical syndrome, even death [40, 41]. For example acute mesenteric ischemia (AMI) has overall mortality of 60% to 80%, and the reported incidence are increasing with time because the major reason is the continued difficulty in recognizing the condition [42, 43].

IRI of intestines alters absorption of intestines resulting into inadequate absorption of nutrients causing infarction of the bowel, short-bowel syndrome and even death [44]. Bacterial translocation through epithelial mucosa to extra-intestinal sites can occur after IRI which subsequently can produce sepsis, shock, or multiple organ failure (MOF). Bacterial translocation has been noticed in 44% of the pediatric patients after small bowel transplantation [45, 46]. Similarly endotoxin lipopolysaccharide (LPS), (part of outer membrane of gram-negative bacteria) binds to TLR4 and at the end amplify the production of cytokines [47-49]. Reactive oxygen species such as hydrogen peroxide, superoxide, and cytokines leads to the development of systemic inflammatory response syndrome (SIRS), which can progress to Multiple organ failure (MOF) [50]. Pulmonary infiltration of neutrophils is another well studies process, which contributes to the development of acute respiratory distress syndrome (ARDS) and Acute Lung Injury (ALI) [51].

The intestine consists of labile cells that are sensitive and easily injured by ischemia and reperfusion [52]. Mucosa of the intestine becomes the site for the production of various acute-phase proteins [53], gut hormones [54], cytokines [55], reactive oxygen species [11], nitric oxide [56], AA derivatives [57], and cell adhesion molecules [58]. Molecular and cellular inflammatory responses like transcription of nuclear factor-κB (NF-κB) [59], induction of granulocyte colony-stimulating factor (G-CSF) and interleukin (IL)-6, and recruitment of neutrophils to the intestinal muscularis takes place after IRI [55].

Following studies prove that PMNs are involved in the pathophysiology of IRI. Intestinal reperfusion injury is primarily due to leukocyte and EC interactions in the mucosa of the transplanted intestine [60]. Depletion of PMNs from blood before reperfusion has shown decrease IRI in the human small bowel [61]. Intra-vital microscopic studies of tissues following IRI showed an acute inflammatory response due to increase protein efflux and PMNs adhesion in post capillary venules [11]. Riaz *et al.* showed that following IRI of the mouse intestine, both P- and E-selectins were over expressed. Blocking of P-selectin reduced PMN rolling and adhesion, so attenuating the injury [62]. PMNs causes damage by different ways like secretion of proteolytic enzymes from cytoplasmic granules [63], free radicals production by respiratory burst [64], and damage to microcirculation and extension of ischemia [65]. A study confirmed that PMNs are the initial source of free radicals in a rat model of IRI of the intestine [66]. This intestinal reperfusion injury causes not only local acute inflammatory response, but also noteworthy pulmonary injury and systemic inflammatory changes [67]. Pharmacological strategies that reduced neutrophil infiltration also reduce IRI [67, 68]. Although numerous modalities and substances have been tested to reduce ischemia/reperfusion-induced mortality, none has been entirely successful. Furthermore, the molecular mechanisms and networks underlying IRI are still poorly known. Neutrophil is an important player in IRI and how the neutrophil takes part in whole story is still not known. For a better understanding of the molecular mechanisms taking place during IRI, further understanding of the neutrophil biology is necessary. That would benefit from the knowledge of the neutrophil proteome.

1.6 Mediators and receptors of IRI

1.6.1 Leukotriene (LT) B4

Leukotriene (LT) B4 is one of the inflammatory mediators known to activate neutrophils and induce their recruitment in intestinal tissues following severe ischemia and reperfusion injury of the superior mesenteric artery. But pharmacological study using LTB4 receptor antagonist, showed no effect on neutrophil hence BLT receptor plays a minor role in the local, remote and systemic injuries after severe IRI in rats [69]. LTB4 is produced as a result of arachidonic acid (AA) metabolism. It is produced by a reaction catalyze by 5-lipoxygenase and leukotriene A4 hydrolase [70] binds to the G protein-coupled receptor BLT-1 and promotes chemotaxis in neutrophils [71, 72].

1.6.2 TNF-α

TNF-α is released during IRI and mediates inflammatory cascade. Decrease in neutrophil recruitment and tissue injury has been observed after inhibition of TNF-α [73]. TNF-α also induced apoptosis in neutrophils [74]. In a study TNF-α and IL-1β production has been found associated with inflammatory response mediated in part by Toll-like receptor (TLR) signaling in IR model. This pulmonary and intestinal inflammation was dependent on TLR/MyD88 signaling suggesting involvement of p38 kinase and NF-kB [75].

1.6.3 Thrombin

Thrombin induces leukocyte rolling and adhesion after IR and antithrombin markedly decreased the lung injury characterized by decrease extravasation, leukocyte sequestration, and MPO activity [76]. It induce PAR1 pathway via G protein-coupled receptors resulting into release of rat cytokine-induced neutrophil chemoattractant-1 (CINC-1) (chemokine) during IR [77].

1.6.4 Potassium channels (KATP)

In epithelial cells of small intestine, K^+ channels provide the driving force for electrogenic transport processes across the plasma membrane, and they are involved in cell volume regulation. Fine-tuning of salt and water transport and of K^+ homeostasis

occurs in colonic epithelia cells, where K^+ channels are involved in secretory and reabsorptive processes [78].

Potassium channels (KATP) blockers, has been shown to suppress neutrophil migration and chemotaxis during acute inflammatory responses. Local, remote and systemic injury was prevented after treatment with glibenclamide (KATP blocker) suggesting important role of KATP channels in neutrophil associated injury in intestine rat model [79].

1.6.5 Complement system

Complement system is a well-known mediator involved in ischemia/reperfusion (I/R) injury and exerts its effects in a number of ways. For example, anaphylatoxins (C3a and C5a) and membrane attack complement complex (C5b-9) induce increased expression of ICAM-1, endothelial E-selectin, P-selectin, IL-8, MCP-1, and ROS. As a result neutrophil attraction and aggregation, chemotaxis, cytotoxic activity, and the release of RO metabolites and proteases occur [80, 81]. In addition, C5a is a potent chemoattractant for other immune cells and leads to the up-regulation of vascular adhesion molecules [82]. C5a receptor (C5aR) knockout in mice before SMA occlusion leads to protection of intestinal injury and diminishes intestine-derived pulmonary neutrophil sequestration [83].

1.6.6 CXC receptors 1 and 2 (CXCR1/2)

CXCR1 and CXCR2 belong to G protein-coupled receptors (GPCR), act as receptors for C5a, LTB4, PAF, and fMLP [84]. Blockage of CXCR1 and CXCR2 significantly reduced neutrophil infiltration of the jejunal lamina and lung parenchyma, and vascular leakage into the airways (BAL protein) but had no effects on expression of myeloperoxidase, IL-1, IL-6, GRO, MIP-2 and MMP-9 [85, 86].

1.6.7 Reactive oxygen species (ROS)

ROS such as superoxide anion ($O_2^{-\bullet}$), hydrogen peroxide (H_2O_2) and hydroxyl radical (OH−) can cause oxidation of proteins, DNA, phospholipids and other biological structures. During reperfusion, PAF, TNF-α, IL-6, IL-1β, GMCSF, C5a and the ROS themselves stimulate endothelial and neutrophil ROS production [87, 88]. The main

sources of ROS in neutrophils are NADPH-oxidase, xanthine oxidase (XO), mitochondria and the Arachidonic acid metabolism after reperfusion [89, 90]. ROS directly lead to structural damage, enhance MTP opening, activate immune and ECs and induce apoptosis [91].

1.7 Mass Spectrometry Based Proteomics

1.7.1 Introduction to mass spectrometry

The mass spectrometer is an instrument that measures the mass-to-charge ratios (m/z) of ions in order to find molecular mass. A typical mass spectrometer consists of an ion source, a mass analyzer and a detector. The ion source creates gas phase ions from different analytes. The mass analyzer resolves the ions according to their mass to charge ratio (m/z). The detector sequentially detects the ions. Fig.4 is a scheme graph of the mass spectrometer.

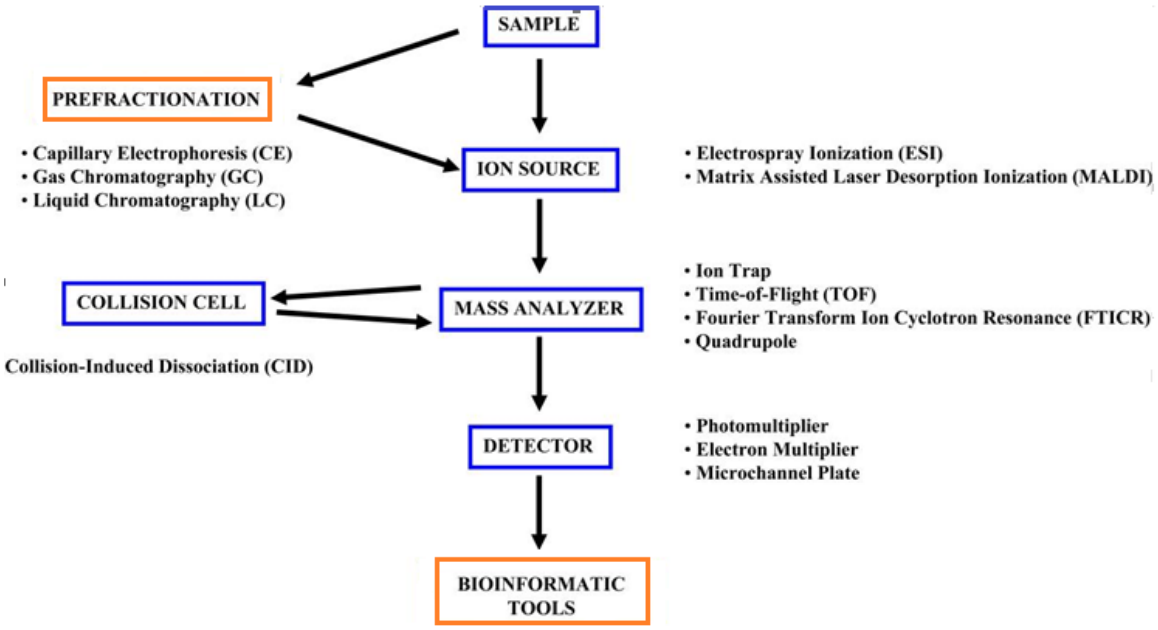

Figure 4 Scheme representing the steps performed in a mass spectrometer

(blue boxes) and some steps related to sample preparation and data analysis (orange boxes). Most boxes represent mass spectrometers' components. The boxes named prefractionation and sample represent steps performed to prepare the sample for mass

spectrometry. To the side of the boxes are represented some of the most common types of mass spectrometer components.

Adapted from [92].

1.7.1.1 Ion source

There are many ionization methods including Chemical ionization (CI) and plasma desorption (PD), which were introduced in 1966 and 1974 [93]. Later, fast atom bombardment (FAB) [94], liquid secondary ion mass spectrometry (LSI-MS) [95], electrospray ionization (ESI) (Fig.5-A) [96] and matrix-assisted laser desorption ionization **(**MALDI) (Fig.5-B) [97] were developed, being the last two the predominant methods currently applied to proteomics. In MALDI analysis, the analyte is first co-crystalized with a matrix. Afterwards, laser radiation is applied to this mixture (matrix-analyte) leads to the sublimation of matrix and analyte, and the matrix donates a charge to the analyte [98]. The generated ions from MALDI are mostly singly charged and accelerated by an electrostatic field towards the analyzer. The main disadvantage of MALDI is the lower reproducibility (different from shot-to-shot) due to sample preparation and its non-homogenous deposit on the probe. However, MALDI allows the ionization of analytes with very high molecular mass; up to 300,000 Da. ESI ionizes the analytes in solution. Application of a strong electric field results in the evaporation of the sample solution into gas phase of highly charged electrospray (ES) droplets. While the charged droplets evaporate, the analyte is ionized and transferred to the gas phase and MS lenses with opposite charge attract these ions. ESI has the advantage to produce multiply charged ions from large biomolecules. In addition, coupling pre-fractionation of molecules using high-performance liquid chromatography (HPLC) with the ESI-MS has made this hyphenated technique proficient in analyzing different sizes of molecules with various polarities in a complex sample mixture [99].

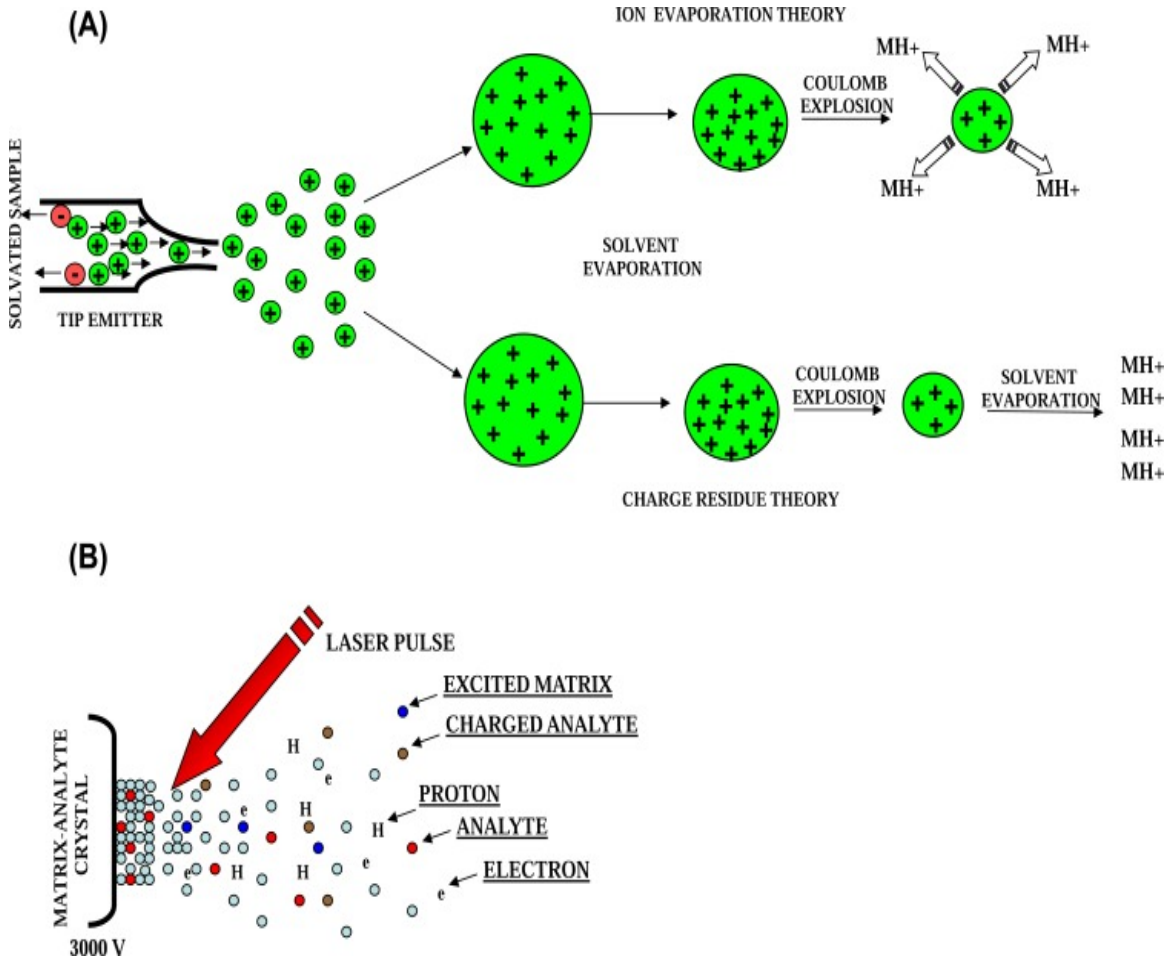

Figure 5 Ionization techniques for MS

A- Ion formation in electrospray ionization technique and B- Matrix-Assisted Laser Desorption Ionization process, Adapted from [92].

1.7.1.2 Mass analyzer

A mass analyzer separates ions according to their m/z values. There are different physical principles used for the separation of ions such as electrically driven traditional analyzers (i.e., magnetic sectors) that employs magnetic field. Currently, widely used mass analyzers are quadrupole (Q), quadrupole ion trap (QIT), time-of-flight (ToF), and Fourier transform ion cyclotrone resonance (FT-ICR) analyzers (Fig. 6).

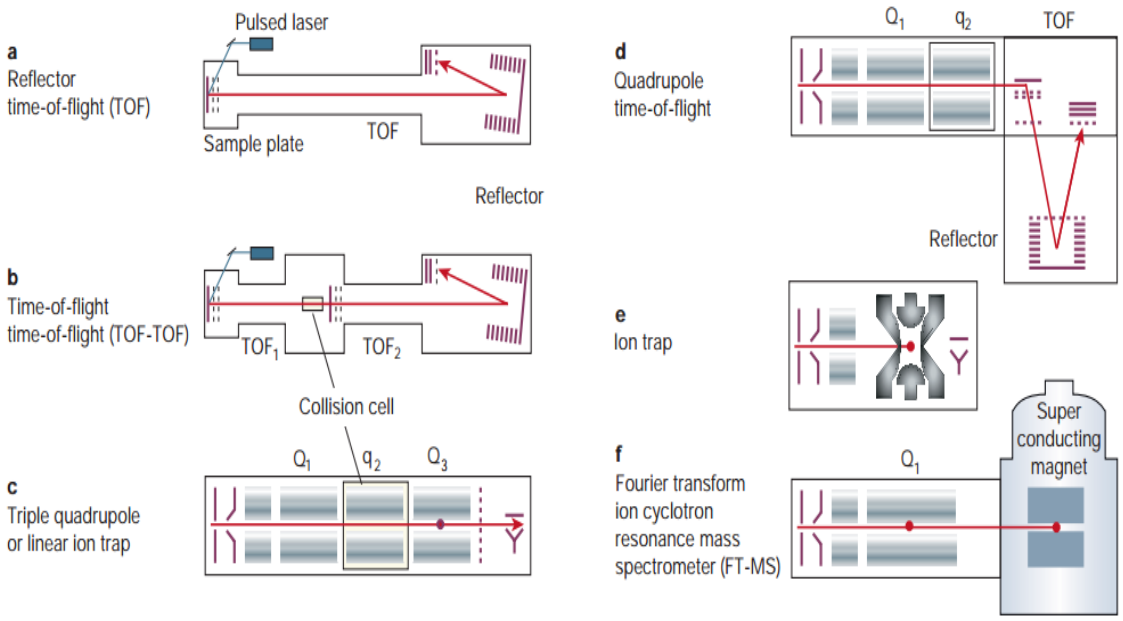

Figure 6 Mass spectrometers used in proteome research.

Adapted from [100]. (a) Time-of-flight (TOF) instruments, (b) TOF-TOF instrument, (c) Quadrupole mass spectrometers, (d) Quadrupole TOF instrument, (e) The (three-dimensional) ion trap and (f) FT-MS instrument.

The characteristics of a mass analyzer are determined by resolution (the ion separation efficiency, through their m/z ratio), mass accuracy (confidence in the m/z values), mass range, MS/MS acquisition and precision (the ability to reproduce a mass measurement of a given compound) including dynamic range (abundance ratio from the most abundant to the least abundant detected ion within a single scan guaranteeing specified mass accuracy). The most recent acquisition of the FT/MS family is the Orbitrap analyzer, which is a modification of the QIT, where the Orbitrap works with static electrostatic fields while the QIT uses a dynamic electric field typically oscillating at ~1 MHz. Orbitrap mass spectrometers fundamentally differ from the most FT-ICR mass spectrometers because of their built in excitation-by-injection mechanism [101]. Orbitraps have a high mass accuracy (1–2 ppm), a high resolving power (up to 240,000 at m/z 400), a high dynamic range (around 5000) and high sensitivity [102-104].

The type of applied mass spectrometry instrument in this PhD research work was a LTQ-

Orbitrap Velos. It includes an electrospray ion source (ESI), and two LTQ ion traps. It can eject the ions in the Orbitrap mass analyzer or in the collision cell (Fig. 8).

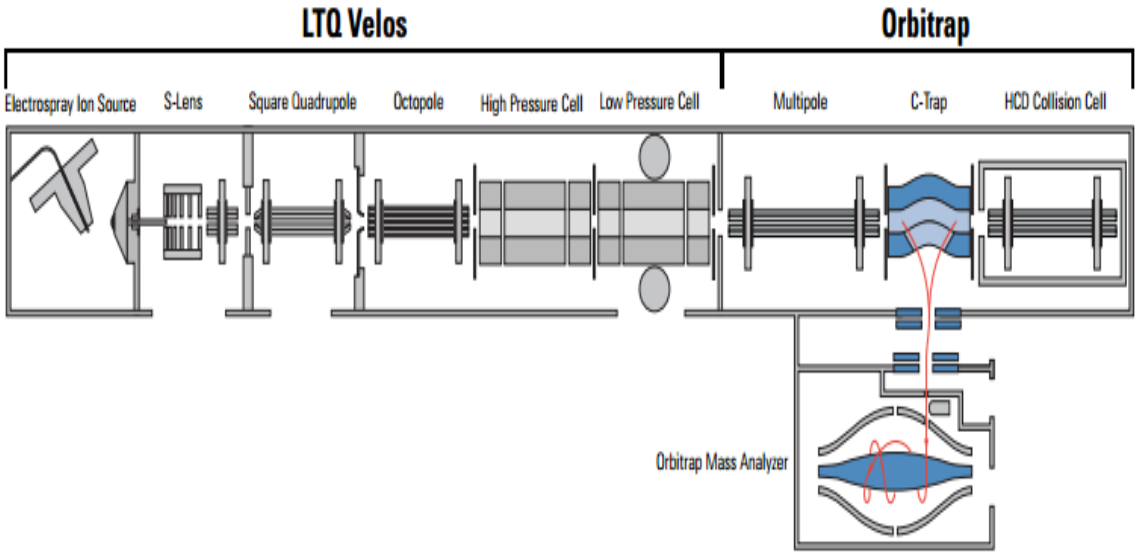

Figure 7 Schematic view of the LTQ Orbitrap Velos

Adapted from [105].

1.7.1.3 Peptide fragmentation

To obtain information about the amino acid sequence of a peptide from a proteolytically digested protein using mass spectrometry, the precursor peptide ion needs to be fragmented into a "ladder" of consecutively smaller fragment ions, each having lost one or more amino acids. The most common peptide fragmentation technique in MS, collision-induced dissociation (CID), leads to N- and C-terminal fragment ions resulting from a cleavage of the C-N bond in the peptide backbone, producing y- and b-ions, respectively (Fig. 8). The other important types of fragmentation methods in peptide analysis are electron capture dissociation (ECD)/electron transfer dissociation (ETD), which produce N- and C-terminal fragments of a backbone bond between the nitrogen and alpha carbon atom, thereby generating c- and z-ions, respectively [106, 107]. ETD fragmentation can identify CID-labile posttranslational modifications (PTMs). Ideally, for peptides with PTMs, it can provide both the sequence information and the localization of the modification sites. Another alternative type of fragmentation method is the beam-

type CID or high-energy collision dissociation (HCD). The fragmentation pattern of HCD is featured with higher activation energy and shorter activation time compared to the traditional ion trap CID. HCD also generates b- and y-type fragment ions. While the higher energy for HCD leads to a predominance of y-ions; b-ions can be further fragmented to a-ions or smaller species. Without the low mass cut-off restriction and with high mass accuracy MS2 spectra, HCD has been successfully applied for *de novo* peptide sequencing, providing more informative ion series. As for PTMs studies, certain diagnostic ions specific for HCD could be recognized for PTMs identification. Efficient fragmentation with detection over a wide m/z range makes HCD a powerful tool for sequencing and quantitation of iTRAQ labeled peptides. In particular, the combination of high quality accurate mass MS/MS spectra with the high abundance and resolution of the iTRAQ reporter ions is well suited for the simultaneous peptide identification and quantitation in complex protein digests [108, 109].

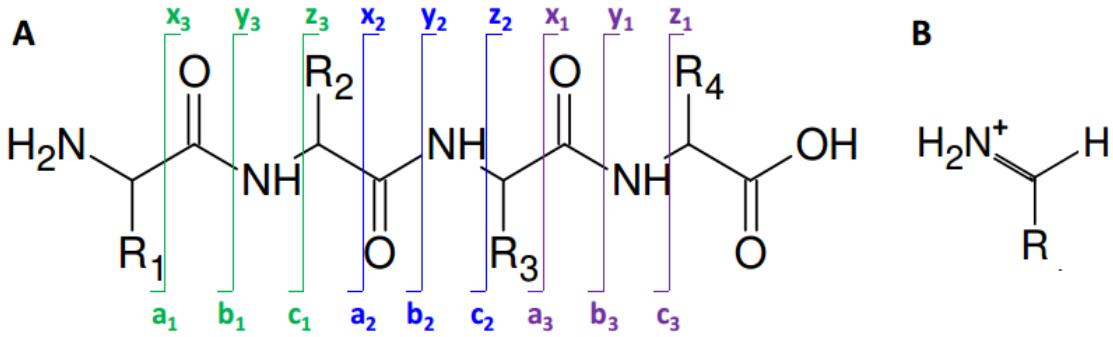

Figure 8 The Roepstorff-Fohlman-Biemann peptide fragment ion nomenclature

[107, 110].

A. Cleavage of a single Cα-C, C-N, or N-C αbond results in a, b, and c-ions, respectively, when the charge is retained on the N-terminal side, while x,y, or z-ions are produced, respectively, if the charge is retained on the C-terminal fragment. B. Double backbone cleavage resulting in an immonium ion only containing a single side chain.

1.8 Quantitative Proteomics

MS based quantitative proteomics is used for biological and clinical research like the

identification of functional modules and pathways or monitoring of disease biomarkers. Quantitative results can be obtained using stable isotope labels or label-free methods [104, 111]. Isotope labels techniques have higher reproducibility whereas label-free techniques require highly reproducible LC-MS/MS platforms [112]. Several labeling methods based on heavy isotopes (2H, 13C, 15N, and 18O) have been developed such as stable isotope labeling by amino acids in cell culture (SILAC) [113], Isotope coded affinity tag (ICAT) [114] and Isobaric tags for relative and absolute quantitation (iTRAQ) [115].

In contrast to ICAT and SILAC, where two or three samples are compared, iTRAQ allows simultaneous labeling and quantitation of four or eight samples [115, 116]. By combining multiple samples in one run, the instrument time for analyses can be reduced, and variations between different LC/MS runs do not affect the results. Comparative studies for different isotope labels including differential gel electrophoresis (DIGE), ICAT, and iTRAQ showed that iTRAQ is more sensitive than ICAT [117]. High-throughput quantitative proteomics experiments produce large datasets [115, 116, 118].

1.8.1 Isobaric tags for relative and absolute quantitation (iTRAQ)

Relative and absolute quantitation can be performed by iTRAQ by using internal standards (for absolute quantitation) [115, 116].

1.8.2 iTRAQ™ reagent chemistry

The iTRAQ™ tags are isobaric labels that can label most of the peptides and proteins in as ample as it reacts with primary amines of amino termini including the N-terminus and the ε-amino group of the lysine side-chain. Each label contains a unique reporter group, a peptide reactive group, and a neutral balance group, these together maintaining a total mass of145Da (Fig. 9). During peptide fragmentation in MS/MS, iTRAQ™ reporter groups separate from isobaric tags and produce distinguishable ions with m/z 114, 115, 116 and 117. In this way, the relative intensities of the reporter ions give the relative abundances of each peptide in the samples. This MS/MS fragmentation of iTRAQ™ - tagged peptides also produces strong y- and b-ion signals for more confident identification [119].

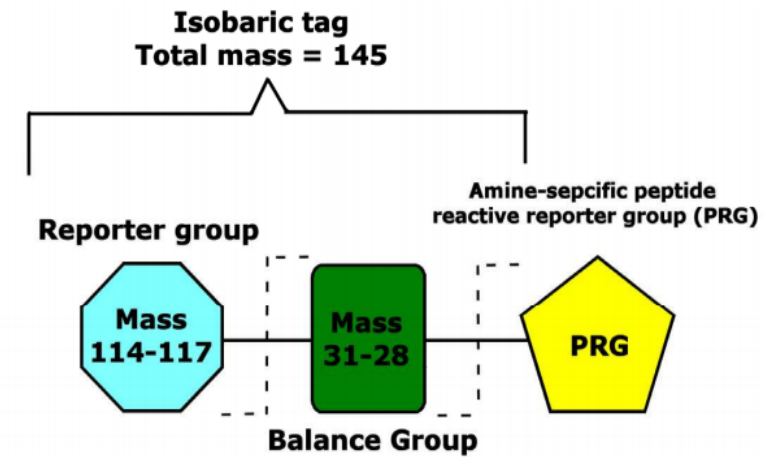

Figure 9 Structure of the iTRAQTM reagents.

Adapted from [120].

1.8.3 iTRAQ^{TM} work-flow

Samples are first reduced, alkylated and then trypsin digested. The set of peptides obtained after digestion are then labeled with one of the four iTRAQ^{TM} tags. Then the labeled peptides are pooled, separated by liquid chromatography (LC), and fractions obtained at the end are analyzed through MS (Fig-10).

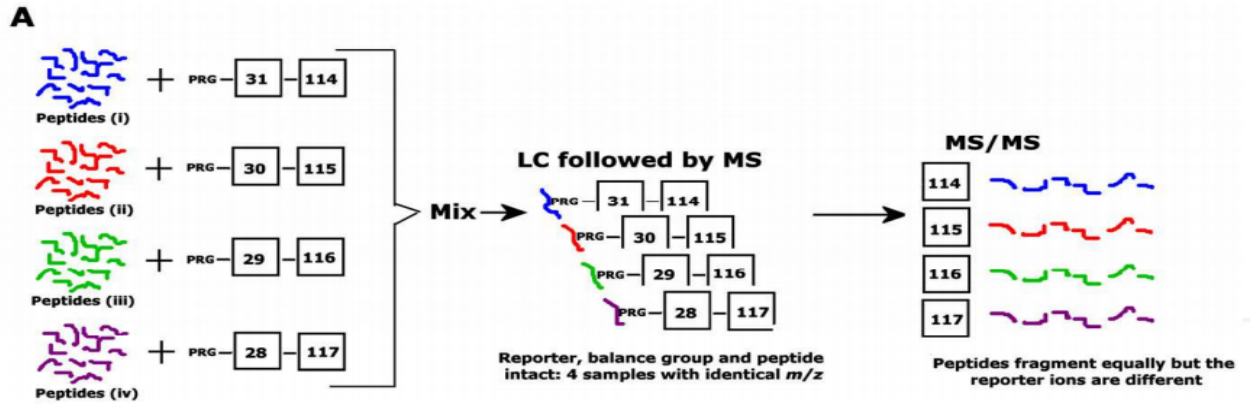

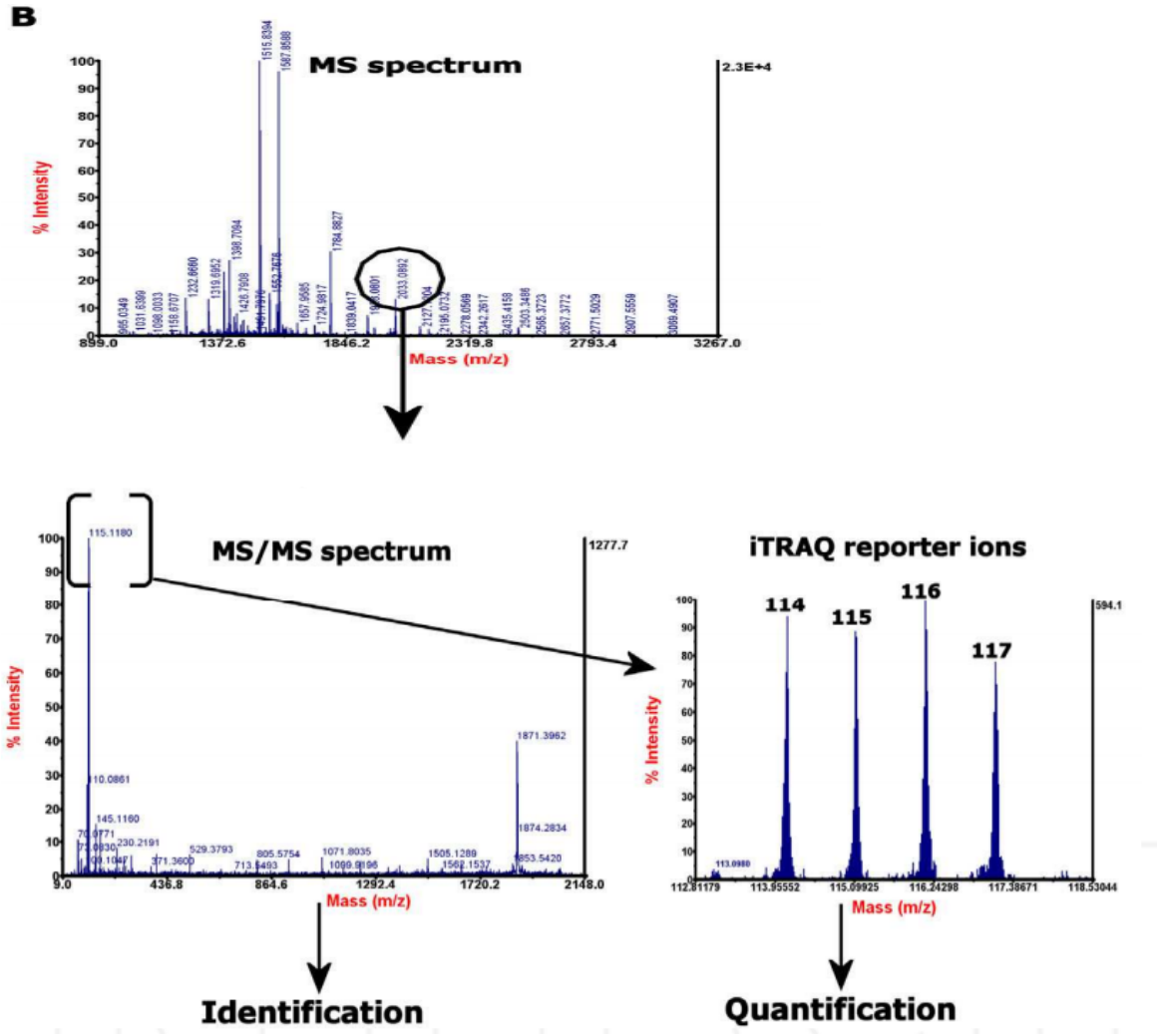

Figure 10 A general scheme and example data for a 4-plex iTRAQ experiment.

Adapted from [120].

iTRAQ™ based quantification can be performed on LTQ-Orbitrap and include Pulsed Q Dissociation (PQD) [121] and higher energy C-trap dissociation (HCD) [122]. Sensitive and accurate iTRAQ™ quantification of a total proteome can be done now using HCD fragmentation method in combination with the CID fragmentation technique [123].

1.9 Phosphoproteomics

Protein phosphorylation, an essential post-translational modification, affects most cellular activities including signal transduction, gene expression, cell cycle progression and other biological functions [124]. Enzymes dedicated to protein phosphorylation are among the

largest class of PTM (post transaltional modification) enzymes. This superfamily of protein kinases has been termed the kinome, with over 500 members in the human kinome. Protein kinases catalyze the transfer of a phosphoryl group from a high-energy organic compound such as adenosine triphosphate (ATP) to the side chain of serine, threonine, tyrosine or histidine amino acid residues in mammalian proteins. Kinases have been predicted to encompass 1.7% of the human genes [125, 126]. It has furthermore been estimated that the relative abundances of phosphoserine, -threonine, and -tyrosine in the human proteome are 90%, 10%, and 0.05%, respectively [127]. By hydrolyzing the covalent phosphoester bond, thereby releasing orthophosphate, protein phosphatases catalyze the enzymatic removal of these phosphate groups from proteins, returning them to their non-phosphorylated state [128]. Phosphorylation affects protein structure by changing the charge and hydrophobicity of the amino acid side chain. Negatively or positively charged amino acids in close proximity to the phosphorylated residue will be repelled or attracted, respectively, and the phosphoryl moiety will furthermore introduce a very hydrophilic and polar region in the affected protein. Thereby, conformational changes can be induced, affecting the properties of the protein [129].

Phosphopeptide analysis is a challenge for mass spectrometry for several main reasons [130]:

1. High activity of phosphatase requires sensitive careful sample preparation to avoid losing the modified proteins;
2. The phosphorylation is a labile PTM, which can be lost during the MS/MS fragmentation process;
3. Incomplete peptide fragmentation complicates the correct localization of the phosphorylation site;
4. The low stoichiometry of phosphopeptides implies the use of enrichment strategies, which have their limitations (see next section);
5. Some of multi-phosphorylated peptides display less ion intensities compared to the less phosphorylated peptides by conventional RPLC-MS/MS analysis [131, 132];

6. The phosphoproteome is dynamic and complex. Currently, it is predicted that more than 100,000 phosphorylated sites are present in mammalian proteins, distributed in a wide dynamic range [133]. However, large-scale studies currently reach no more than 20,000 sites using phosphopeptide enrichment and LC-MS. Different sample fractionation and phosphopeptides enrichment strategies can address the problem of low stoichiometry of the phosphopeptides.

1.9.1 PTM-Specific Enrichment

There are several PTM-specific protein and peptide enrichment methods including PTM-directed affinity chromatography or immune precipitation with PTM specific antibodies. Phosphoproteins can be purified by PTM-specific affinity resins [134] or anti-phospho amino acid antibodies [135]. Subsequent digestion of protein and LC-MS/MS analysis of peptides gives phosphorylation sites in the recovered proteins. However, it is more useful to enrich PTM peptides before MS analysis that can improve sensitivity and specificity. Immobilized metal affinity chromatography (IMAC) [136], or TiO_2 columns [137] are used to recover enriched PTM peptides before MS/MS analysis. Strong cation exchange and anion exchange chromatography methods are also helpful for reducing peptide complexity including phosphopeptides. Combinations of these methods have revealed thousands of phosphorylated sites in proteins from different species. IMAC showed stronger sensitivity for multiply phosphorylated peptides, so, buffer exchange by reversed phase chromatography before IMAC has been used with a high risk of losing phosphorylated peptides [138, 139].

1.9.1.1 Titanium dioxide affinity chromatography-TiO_2:

TiO_2 is a resin that can create an ionic interaction with the phosphate groups of biomolecules and therefore, it is mixed (or used in microcolumns) together with the sample to trap peptides that are phosphorylated. The subsequent washing procedure can eliminate all the non-binding peptides and elution step can create a mixture of peptides containing only the fraction of interest. The approach is comparable to others but it is cheaper, faster, and reproducible and it is also MS compatible due to the buffers used for the elution. Regarding the application of TiO2 for phosphopeptide enrichment, first the ratio between the amount of titanium and the concentration of peptides needs to be

optimized in order to achieve the higher efficiency of enrichment [140]. In this enrichment strategy, the pH value of the loading buffer needs to be acidic to allow the acidic residues in the peptides become neutral while, the phospho groups remain negatively charged. Several studies have been done to achieve the highest selectivity of enrichment by comparing different loading buffers, all of which enable the acidic conditions [141].

1.9.1.2 Sequential elution from IMAC (SIMAC)

SIMAC (Fig. 12) is a phosphopeptide-enriching method combining both MOAC (Metal Oxide Affinity Chromatography) and IMAC [142]. It separates both multiply and singly phosphorylated peptides and first acidic conditions are used to elute monophosphorylated peptides from IMAC material, whereas subsequent basic elution recovers the multiply phosphorylated peptides that are normally not readily detected. Singly phosphorylated peptides as well as flow through peptides then pass on TiO_2-MOAC. Finally the two distinct phosphopeptide pools can now be analyzed separately using tandem mass spectrometry parameters that are optimized for each type of sample [143]. Second TiO_2enrichment help to separate non-phosphorylated peptides in the first eluate and having phosphorylated peptides in the flow-through [143].

SIMAC results into a larger amount of phosphopeptides identification than MOAC itself and broadened the phosphopeptide spectrum [142]. The sequential elution is another advantage, since having a greater amount of less complex phosphopeptide fractions increases the chances for ionization and identification of phosphopeptides by MS [144]. Overall SIMAC schematic workflow is given below in fig.12.

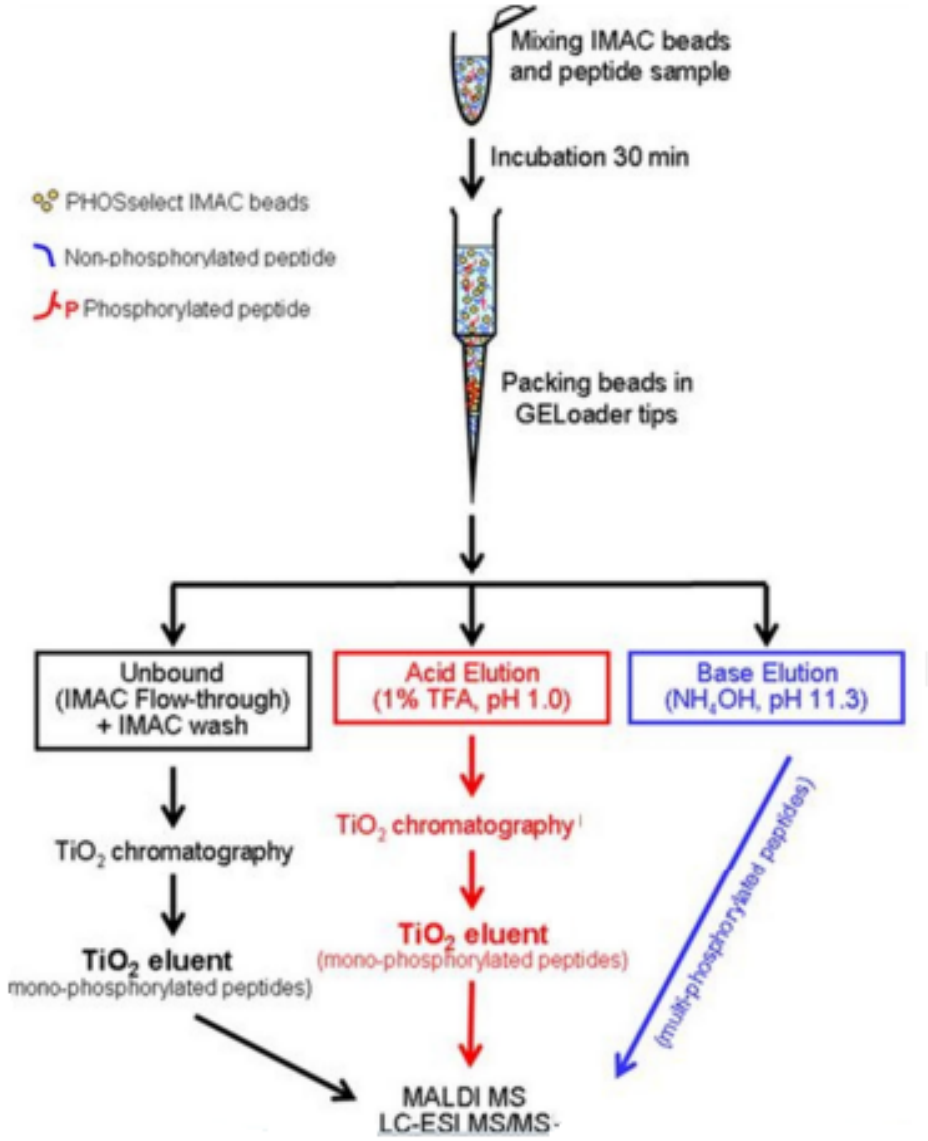

Figure 11 Overall SIMAC workflow

Adapted from [142].

1.10 Proteomics in Neutrophils

There is need to identify protein expression of cells as not all the genes are translated into proteins which is also true for neutrophils, where correlation between mRNA and protein expression is inconsistent too. There are limited proteomic studies of the neutrophil particularly explaining effect of the inflammatory response on the neutrophil proteome [77].

The First global analysis of rat neutrophil proteins analysis done by two-dimensional gel electrophoresis (2DE) and MS approaches identified 52 proteins [145]. Later 250 proteins were identified through a combination of 1DE followed by ESI-MS/MS from bovine neutrophils. Proteins identified belong to cell metabolism, cell motility, immune response, protein synthesis, cell signaling, and membrane trafficking [146].

Proteomic analysis of gelatinase, specific, and azurophil granules by 2DE and MALDI-TOF identified 87 proteins including one membrane-spanning protein. Although the detection ability of 2DE was limited yet it identified differential expression of actin associated with all granules [147]. Cytoskeletal, structural, and membrane fusion proteins (247 Proteins) were identified from human neutrophil azurophil granules lipid rafts by 10% SDSPAGE and LC-MS/MS [148]. A similar study identified total of 23 proteins from plasma membrane lipid rafts using gradient gel electrophoresis and MALDI-MS or MALDI-MS/MS. Nine of the proteins belonging to the cytoskeleton were common to a previous study of human neutrophil azurophil granules lipid rafts [149]. Fessler et al. [150] identified 1200 proteins from neutrophils after exposure to lipopolysaccharide (LPS) for 4 h, which resulted in to 50% increase in expression of 100 proteins, and 50% decrease in expression of another 100 proteins. 2DE followed by MALDI-TOF-MS identified substrates for MMP2 and MMP9 from the BAL fluid of mice. These substrates include Ym1, S100A8, and S100A9, which showed chemotactic activity [151]. Proteomic analysis of rat intestinal mucosa after ischemic preconditioning in IRI model identified 10 proteins using 2DE in combination with MALDI-TOF-MS and these proteins were involved in anti-oxidation, apoptosis inhibition and energy metabolism. This study also revealed up-regulation of aldehyde dehydrogenase and aldose reductase in IPC group [152]. A similar study used 2-DE combined with MALDI-MS to analyze

the proteome of the intestinal mucosa subjected to I/R injury in the absence or presence of IPC pretreatment in rats. Total 16 proteins were differentially expressed belonged to cellular energy metabolism, anti-oxidation and anti-apoptosis of which aldose reductase which removes ROS, was significantly down regulated in IR and up regulated in IPC [153].

Our group has been working on proteomics approach for the identification and characterization of a set of proteins in neutrophils. In order to obtain a broader view of the protein profile in human neutrophils activated by PAF, fMLP and PMA, 2DE and MS of human neutrophils was performed with 22 protein identifications [154]. Comparison of neutrophils proteome from normal individuals and multiple trauma and revealed 114 spots, with 27 up regulated and 87 down regulated in trauma conditions [155].

1.10.1 Phosphorylation of neutrophil Proteins

Eight substrates of MAPKAPK2 (a downstream kinase in the p38 MAPK pathway) were identified by combination of *in vitro* phosphorylation of ^{32}P-orthophosphate-loaded neutrophil lysates, one-dimensional SDS-PAGE, and peptide identification by MADLI-TOF/MS. One of these substrates, 14-3-3ζ was found to be phosphorylated at Ser-58, and this phosphorylation regulated 14-3-3ζ dimerization and binding to Raf-1 [156]. Similar analysis identified the p16-Arc subunit of the Arp2/3 complex as a MAPKAPK2 substrate. The functional consequences of its phosphorylation are not yet known, but may explain the participation of the p38 MAPK pathway in actin-dependent cellular functions [157]. Another similar approach to identify the calcium-binding protein myeloid-related protein-14 (MRP-14) as a target for p38 MAPK phosphorylation in neutrophils stimulated with fMLP, suggesting a role of MRP-14 in stimulated exocytosis [158].

The RhoGTPase regulator, LyGDI, was identified by 2DE, immunoblot and MS/MS and was found to be tyrosine phosphorylated during fibronectin-accelerated TNF-α-mediated neutrophil apoptosis. Phosphorylation was followed by increased caspase-3-mediated LyGDI cleavage, and this cleavage was a signaling event in TNF-α-mediated apoptosis [74]. Pacquelet *et al.* [159] used LC-MS/MS analysis of neutrophil lysates separated by SDS-PAGE to find out that interleukin-1 receptor-associated kinase-4 (IRAK-4) is downstream of TLR-4 and serine and threonine residues were phosphorylated on p47^{phox}

(a component of the NADPH oxidase) directly by IRAK-4 which results into enhanced NADPH oxidase activity.

Using phosphoprotein-specific gel staining (Pro-Q Diamond), changes in expression of each of L-plastin, meosin, cofilin, and strathmin proteins were found due to phosphorylation or dephosphorylation [160]. It was confirmed by MS/MS that p47phox, is phosphorylated on Ser345 by extracellular signal-regulated protein kinase-1/2 (ERK1/2) in response to GM-CSF, and by p38 MAPK in response to TNF-α. This selective phosphorylation is a point of convergence for MAPK signaling that primes the respiratory burst [161]. A combination of IMAC with ESI-MS/MS for analysis of specific granules isolated from unstimulated or fMLP stimulated human neutrophils identified 31 and 49 phopshopeptides respectively. One peptide that contained two phosphoserines was identified as Slp homolog lacking C2 domains b (Slac2-b) was comprised of known p38 MAPK phosphorylation motif and thought to involve in activation of granule exocytosis in human neutrophil [162, 163].

From our observations in the literature, the molecular mechanism by which neutrophil causes tissue injury in IRI is not clear. Proteomic research has been done for better understanding of neutrophil biology in the past but there is still no study available on proteomic analysis of neutrophil after intestinal ischemia and reperfusion in rat model. For a deeper understanding of the neutrophil proteins taking part in molecular pathways involved in IRI we aimed to perform Quantitative iTRAQ and Phospho-Proteomics in a rat model with intestinal ischemia and reperfusion.

1.11 Hematological analysis

Ischemic injury results from the interruption of blood flow, damaging active tissues; ischemic reperfusion injury (IRI) occurs after the restoration of blood flow, leading to additional tissue injury [164]. Parks and Granger [165] in 1986 reported that reperfusion in these processes is more harmful than ischemia alone. The tissue damage caused by ischemia and reperfusion in the intestine is associated with high morbidity and mortality in surgical patients. IRI occurs during abdominal aortic aneurysm surgery, hemorrhagic shock, strangulated hernias, neonatal necrotizing enterocolitis, cardiopulmonary bypass and organ transplantation [166]. Among the internal organs, the most sensitive to IRI is

the intestine [164]. Intestinal IR injury can lead to damage in the intestinal mucosa and the release of various inflammatory mediators, potentially resulting in the development of the Systemic Inflammatory Response Syndrome (SIRS) and further leading to multiple organs failure (MOF), especially acute lung injuries (ALI) [50, 51, 155, 167]. Ischemia-reperfusion causes local and systemic changes in hemodynamics, endothelial function, microcirculation, fluid equilibrium and metabolic homeostasis while also inducing the complement and inflammatory pathways [154, 168-173]. In an attempt to attenuate this damage, several treatment modalities have been applied in various animal models of IRI, such as hypothermia, antioxidants, ischemic preconditioning (IPC), modulation of inflammatory mediators and adhesion molecules. Among these, ischemic preconditioning seems to be the most promising strategy against reperfusion injury, as it increases the bowel's tolerance against the damage caused by ischemia followed by reperfusion [174-176].

Blood is a component of the vertebrate body fluid system which can be easily accessed and analyzed to check the physiological status [177]. All blood cell components such as erythrocytes, leukocytes and thrombocytes originate from stem cells which are found in the bone marrow, that differentiate as a consequence of regulators such as poietins [178, 179]. The purpose of the present study was to obtain a basic knowledge of the hematology after IRI and IPC in rats as there is no study available in literature. The hematological parameters here analyzed include determination of the total erythrocyte count (RBC), total white blood cell count (WBC), hematocrit (HCT), hemoglobin (Hb) concentration, erythrocyte indices (MCV, MCH, MCHC), and white blood cell differential count. In this prospective study we have evaluated the significance of routine blood parameters after intestinal ischemia and preconditioning in rats, which can help in early diagnosis of IRI and in understanding how IPC affects blood components.

OBJECTIVE

2 Global Objective

The objective of Thesis is to evaluate the effect of ischemia-reperfusion on the proteome of rat neutrophils.

2.1 Specific Objectives

1. To analyse the proteome and phosphoproteome of neutrophils in response to ischemia and reperfusion.

2. To analyse mechanisms and pathways underlying IR in neutrophils and to understand the effect of IR on the biology of neutrophils including cellular components, cellular and molecular functions.

3. To analyse the role of predicted enzymes and their phosphorylation sites in neutrophil after IR.

MATERIAL & METHODS

3.1 Experimental Subjects:

Male Wistar rats (*Rattus norvegicus*), presenting no inflammatory disease, weighing 250–350 g were collected from the animal house of the Faculty of Medicine University of Sao Paulo (FMUSP), Sao Paulo State, Brazil. The project was approved by the Ethics Committee of FMUSP (Protocol 8186) for the use of rats as experimental subjects. The animals had access to food and water *ad libitum* until the time of the experiment.

3.1.1 Experimental groups

Thirty rats were randomly allocated into the following three groups for proteomics analysis (fig.13) whereas a fourth group of ischemic preconditioning was included for hematological analysis:

1. The control group (C) (n=10), without any surgical procedure.
2. The sham laparotomy group (SL) (n=10), without clamping of the mesenteric artery, but comprehending the same surgical procedures applied to the I/R group.
3. Ischemia/reperfusion (I/R) group (n=10), submitted to superior mesenteric artery occlusion (SMAO) for 45 min followed by 120min of reperfusion.

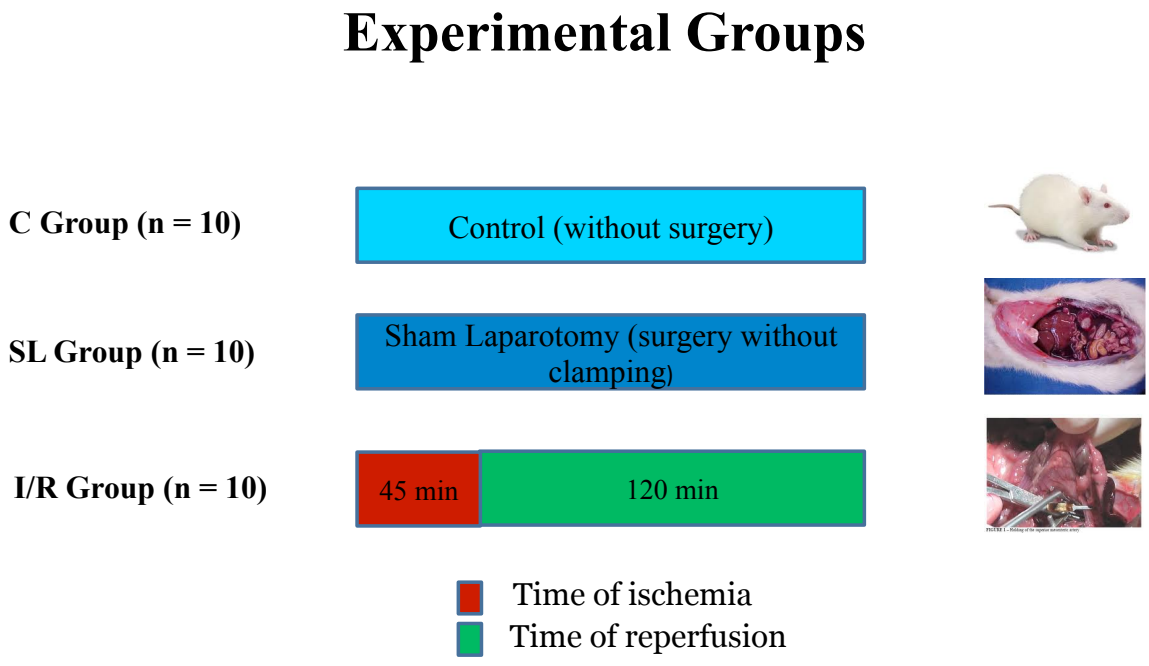

Figure 12 Experimental groups and their time of ischemia and reperfusion.

3.3 Surgical procedures and sample collection:

The Surgical procedures were performed in the Laboratory of Medical Investigation (LIM-62), department of Surgery, FMUSP. Rats from all groups were anesthetized with intraperitoneal (i.p.) injection of sodium pentobarbital (45 mg/kg,)/Ketamine (80mg/kg) + xylazine (7mg/kg), and core body temperature was maintained at 37°C. After midline laparotomy, the superior mesenteric artery was isolated near its aortic origin. During this procedure, the intestinal tract was placed between gauze pads soaked with warmed 0.9% NaCl solution. In rats from groups I/R the superior mesenteric artery was clamped, resulting in total occlusion of the artery for 45 min. After occlusion, the clamps were removed and a blood sample of 20 μl was collected from the animal tail after 120 min of reperfusion and for proteomic analysis (for neutrophils separation) about 10-12 ml of blood was collected from the heart (right ventricle catheter).

3.4 Hematological analyses

We collected 20 μl of blood from the tail of all animals before and after performance of surgery and injected into a veterinary automated cell counter (BC-2800Vet, Shenzhen Mindray Bio-Medical Electronics Co., Nanshan, China). The hematimetric parameters analyzed included the determination of the total erythrocyte count (RBC), total white blood cell count (WBC), hematocrit (HCT), hemoglobin (Hb) concentration, erythrocyte indices (MCV, MCH, MCHC) and white blood cell differential count.

3.4.1 Statistical analysis of hematological data

For statistical analysis, the data were first checked for normality by applying the D'Agostino & Pearson omnibus normality test. Data were normalized, and outliers were removed, based on the Thompson tau technique; then, normality was reconfirmed with the above-mentioned normality test. Variance analysis (One-way ANOVA) was used to determine the difference between the groups, and the Tukey-Kramer test was employed to compare and determine the means that differed significantly from each other, using the Graph Pad Prism program (V.6.0c). Values with $p<0.05$ were considered significant.

3.5 Ficoll Gradient Protocol for Neutrophils separation from Rat Blood:

Rat neutrophils were isolated from the blood as previously described in [180] with some modifications. Blood was collected directly from the heart after the surgery to a heparinized syringe. Ten mililiters of blood were carefully and very slowly layered onto 10 ml of Ficoll in a Falcon tube, making a two-step gradient (ficoll and blood). The samples were centrifuged at 400g for 45 min. At the end of centrifugation there were two distinct phases; the upper phase/layer (containing plasma, mononuclear cells and ficoll gradient) was discarded, and to the lower one (rich in neutrophils and erythrocytes) 4 ml of a 6% dextran solution in 0.15M of NaCl was added. The volume was increased up to 14 ml by adding phosphate buffer solution (PBS) and mixed slowly. After mixing, the samples were incubated for 20 min in incubator/water-bath at 37^{o}C. The supernatant (transparent layer) was collected to another clean Falcon tube and centrifuged at 270g for 10 min. The supernatant was discarded and the pellet was washed by adding 5ml of milli-Q water for 15-20 sec and then 5ml of 2X PBS, mixed slowly and centrifuged at 500g for 10 min. The washing step was repeated to make sure that all the RBCs have been removed/lysed from the neutrophils (if required the step was repeated twice). The pellet was resuspended in 1 ml 1X PBS and neutrophils were counted under the microscope.

3.6 Protein Extraction from the Neutrophils

After counting the neutrophil cells, samples were centrifuged, removed the supernatant and 200 µl of lysis buffer for 3x10^{6} neutrophils (2% SDS, 20mM TEAB, 100mM DTT, Protease inhibitors & PhosSTOP Phosphatase Inhibitor) was added for protein extraction [181]. Neutrophil cells were lysed in the lysis buffer by using tip-sonicator with 40% output, 10 cycles for 15 secs each and 1 min of interval to cool down the sample on ice. After sonication the samples were kept in water bath at 80°C for 10 minutes, centrifuged at 10000 rpm, supernatant was transferred to a new eppendorf tube and were stored at -80°C for further analysis.

3.7 Filter-aided sample preparation (FASP)

The samples were quantified for protein concentration by using Quant-iT™ Protein Assay Kit (Cat. No. Q33210) and aliquots of lysates with 500 µg of proteins were picked and diluted in 1:4 ratio, sample to Urea buffer (8mol/L urea and 20 mM TEAB).

3.7.1 Filter loading & washing:

500 µl of sample, diluted in urea buffer, were added to Vivacon 30kDa spin filter vials and were spun at 14000 x g for 20min and the filtrate was discarded. Two hundred microliters of urea buffer were added to the filter and centrifuged to wash out SDS from the sample. These steps of sample loading and washing with urea buffer were repeated till the entire sample was applied on the filter. 500 µl of DB3 buffer (1% SDC, 20mM/L TEAB) were added to the filter and spun out at 14000g for 20min.

3.7.2 Alkylation:

The samples were then alkylated in the filter (skipping the DTT reduction step as DTT was used in the lysis buffer) with 400ul of Iodoacetamide (IAA) buffer (0.05 mol/L IAA in DB3 buffer). Samples were thermomixed at 600 rpm at room temperature for 1 min and then incubated with no mix for 20 min in dark. Centrifugation was performed and the filtrate was discarded.

3.7.3 Trypsin Digestion:

Before digesting the samples with trypsin, samples were washed twice with 400 µl DB3 buffer. Proteins were digested overnight at 37°C by using Promega Trypsin in 1:50 trypsin to sample ratio in 400 ul of DB3 solution (0.02 ug/ul in DB3 buffer). Vials were sealed with Parafilm and incubation was performed in a wet chamber at 37°C. Filter units were transferred to new collection tubes and spun at 14000 x g for 20min and filtrates having peptides were saved. DB3 buffer (360 µl) was added to the filters, centrifuged as above to ensure the recovery of all the peptides from the filters and the filters were discarded.

3.7.4 Desalting:

The samples were acidified to a final concentration of 0.5% by adding TFA; vortexed and equal amount of ethyl acetate was added and mixed by vortexing. Centrifugation was performed at 15000 x g for 5 min. The upper layer (plus any membranous layer) was discarded, Another 700 µL of ethyl acetate was added to the samples and centrifugation was performed as above. Again, the upper layer (plus any membranous layer) was discarded and samples were transferred to new low-binding eppendorf tubes. A small

aliquot (4 µL) was picked from the sample to find the final concentration of amino acids by performing amino acid analysis (AAA).

3.8 Amino Acid Composition Analysis

An aliquot of 4 µl of the digested sample was lyophilized in a 500 µl low-binding eppendorf tube with holes in the lid of the tube. The sample was placed in a glass cylinder containing 200 µl of hydrolysis buffer (6N HCl/0.1% phenol/0.1% thioglycolic acid). The cylinder was filled with argon, which was subsequently evaporated under vacuum, and the cylinder was incubated at 110°C overnight. After hydrolysis, the AAA was performed on a Biochrome30 amino acid composition analyzer (Cambridge, UK) as described in [182].

3.9 iTRAQ™ Labelling

After amino acid quantification 100 µg of peptides solution for each of the three experimental groups was taken out into new clean tubes, vacuum dried to label by 4-plex iTRAQ ™ Reagent Kit. The iTRAQ reagents were allowed to come at room temperature. The digests of 100 µg for each sample were reconstituted in 20 µl of dissolution buffer according to the manufacturer instruction with little modifications. Samples were vortexed for 10-15 seconds to ensure that all the dried digests have been re-suspended properly and then spun. The iTRAQ reagents were vortexed and spun to bring all the solution to the bottom of the tube. 70 µl of ethanol was added to each of the iTRAQ reagent tube, vortexed and spun down. Samples were labeled from the Control group with 114, Laparotomy with 115 and Ischemia/Reperfusion with 116. All of the iTRAQ labeling contents were transferred to the respective sample vials, vortexed, short spun and the pH was checked to ensure it was between 7.5 and 8.5. Samples were incubated for 1-2hrs at room temperature. Labeling was confirmed by MALDI and, after that, digests from the three experimental groups were mixed in 1:1:1 ratio. Labeled samples were vacuum dried and stored at -20°C (Fig.14).

3.10 Enrichment of Phosphopeptides –

The TiO_2-SIMAC-HILIC procedure

This procedure was performed in the following steps:

1. First TiO_2 purification
2. Deglycosylation (to remove sialylated glycans from peptides)
3. SIMAC purification
4. Second TiO_2 purification to separate mono-phosphopeptides from deglycosylated peptides

3.10.1 First TiO_2 Purification

Purification of phosphorylated peptides was performed with little modifications in batch mode using Titanium dioxide chromatography as previously described [137, 183, 184]. Briefly, 300 µg of tryptic labeled digests (obtained after mixing 100 µg from each of the three iTRAQ labeled conditions) were reconstituted in 600 µl loading buffer (5% TFA (v/v), 1M Glycolic acid and 80% acetonitrile (v/v) (ACN)) in low binding polypropylene tubes containing 0.6 mg TiO_2 beads per 100 µg peptide solution and incubated with constant shaking at room temperature for 15 min. Samples were centrifuged (table centrifuge <15 sec), the supernatant was incubated with half of the amount of TiO_2 used in the first incubation in another low-binding tube. This was repeated in total three times to recover as much phosphopeptides and sialylated glycopeptides as possible. The flow-through from TiO_2 incubations was collected in a low-binding eppendorf tube and saved for further analysis of unmodified and glycopeptides. The TiO_2 beads from all the three incubations were pooled using 100 µl loading buffer and transferred to a new low-binding eppendorf tube. The TiO_2 beads were washed with 50 µL washing buffer-1 (1% TFA (v/v) and 80% ACN (v/v)) and 50 µL washing buffer-2 (0.2% TFA (v/v) and 10% ACN (v/v)) and vacuum dried for 10 min. Afterward, phosphopeptides and sialylated glycopeptides were eluted with elution buffer (60 µl Ammonia solution (28%) in 940 µl H_2O, pH 11.3) for 15 min with constant shaking. Using small table centrifuge for about 1 minute the samples were centrifuged and the supernatant, containing phospho/sialylated glycopeptides, was passed through a C8 stage tip and lyophilized completely.

3.10.12 Enzymatic Deglycosylation

Samples containing sialylated glycopeptides enriched using TiO_2 were re-dissolved in 50 µl of 20 mM TEAB and 2 µl of 1U/µl PNGase F (Roche) and 0.5 µl of 1U Sialidase A. The enzymatic reaction was performed overnight at 37°C in a wet chamber [184].

3.10.3 SIMAC Purification of the Multi-Phosphorylated Peptides

The deglycosylated solution was acidified by adding 1 µl 10% TFA (v/v). The solution was further diluted with 200 µl 50% ACN/10% TFA (v/v) and the pH was adjusted to 1.6-1.8 with 10% TFA. IMAC beads (80 µl) were washed twice with 200 µl 50%ACN/0.1% TFA (v/v). IMAC beads were added to the peptides solution and incubated for 30 min at room temperature. Half of the supernatant "IMAC-FT" was transferred to a new low-binding tube and the remaining solution with IMAC beads was passed through a 200 µl GeLoader tip flat at the end to retain the IMAC beads with the help of a syringe to press the liquid through into the "IMAC-FT" eppendorf tube and pack the IMAC column. The IMAC beads in the GeLoader tip were washed with 50 µl 50%ACN/0.1% TFA, 70 µl 20% ACN/1% TFA and washes were collected in an eppendorf tube labeled "IMAC-FT". Multi-phosphorylated peptides were eluted, using 80 µl of ammonia elution buffer, directly down in a p200 stage tip with Poros R3 material (1-2 cm) and the eluate was acidified with 8 µl of 100% formic acid or 2 µl 10% TFA prior to R3 purification. Multi-phosphorylated peptides were purified on the R3 column, washed with 60 µl 0.1% TFA, eluted with 60 µl 60% ACN/0.1% TFA and vacuum dried [142, 183] (Fig.14).

3.10.4 Second TiO2 Purification of the Mono-Phosphorylated Peptides

The SIMAC-FT was vacuum dried and resuspended in 200 µl of 70% ACN/2% TFA. The same amount of TiO_2 was added to the solution as in the first TiO_2 incubation. Incubation for the second TiO_2 was carried out twice for 15 min at room temperature at constant shaking. The flow-through, containing all the deglycosylated peptides, was saved. The TiO_2 beads were pooled using 100 µl 50% ACN/0.1% TFA and vacuum dried for 10 min. The mono-phosphopeptides were eluted using ammonia elution buffer on a shaker for 15 min. The solution was spun for 1 min and passed over a C8 stage tip to recover the liquid directly down in a p200 stage tip with R3 material. The eluate was acidified with 8 µl of 100% formic acid or 2 µl 10% TFA prior to R3 purification. Mono-phosphorylated peptides were purified on the R3 column, washed with 60 µl 0.1% TFA, eluted with 60 µl 60% ACN/0.1% TFA and vacuum dried (Fig.14).

3.11 Sample Desalting

Samples were desalted using self-made microcolumns packed with either Poros R2 or R3 reversed-phase resin depending on the type of protein sample. R2 was used for unmodified samples and R3 for phospho/glyco samples. A mixture of both or sequential of R2 and R3 was used in case of uncertainty of the sample modification. Microcolumns were prepared by stamping out a small plug of C8 extraction disk and placed in the constricted end of the P200 tip. The reversed-phase resin was re-suspended in 100% ACN and packed by applying air pressure with the help of a syringe in the tip where the C8 stopped the leakage of the resin material. The vacuum dried samples were re-suspended in 100 µl of 0.1% TFA. The microcolumns were equilibrated with 60 µl of 0.1% TFA, samples were loaded onto the microcolumns, washed with 0.1% TFA and peptides were eluted with 60% ACN/0.1% TFA (v/v) and lyophilized. Mono-phosphorylated, deglycosylated (Sialo from second TiO_2 FT), and deglycosylated (from glycopeptides enrichment) peptides were desalted with Poros R3 reversed-phase resin repeated twice sequentially while non-phosphorylated peptides were desalted with Poros R2 and R3 reversed-phase resin sequentially in a way that all the peptides went through the R2 column and the flow-through went directly onto the R3 microcolumn [185].

3.12 HILIC fractionation of Mono-phosphorylated and non-phosphorylated peptides

HILIC fractionation of the mono-phosphorylated and non-phosphorylated was performed as described [186]. The lyophilized peptides were reconstituted in 90% ACN/0.1% TFA and 40 µl of the sample was injected onto an in-house packed TSK gel Amide-80 HILIC 320 um x 170 mm capillary HPLC column using an Agilent 1200 HPLC system. For the elution of peptides a gradient from 90% ACN/0.1% TFA to 60% ACN/0.1% TFA over 35 min at flow rate of 6 µl/min was used. Fractions were collected automatically in a microwell plate at 1 min intervals after UV detection at 210 nm and pooled in accordance with the UV detection. The fractions were dried down in speed vacuum.

3.13 Nano-Liquid Chromatography Tandem Mass Spectrometry (nano-LC-MS)

The samples were analyzed by a Proxeon EASY-nLC system (Thermo Fisher Scientific, Odense, Denmark), coupled with mass spectrometry LTQ-Orbitrap Velos (ThermoScientific). The peptides were loaded onto an 18cm homemade reversed-phase

capillary column (75 um inner diameter) packed with ReproSil-Pur C18 AQ 3µm material (Dr. Maisch, Ammerbuch Entringen, Germany) in buffer-A (0.1% formic acid). Peptides were eluted using 110-180 min gradients from 0-34% Buffer-B (95% ACN/0.1% formic acid) at 250 nl/min. The peptides were directly eluted into a LTQ-Orbitrap Velos mass spectrometer (MS). The MS method was set up in a data-dependent acquisition (DDA) mode. A full MS scan was performed in the mass area of 400-1200 m/z in the Orbitrap using a resolution of 30,000 FWHM (400 m/z) and the target value of $1x10^6$ ions. For each full scan the seven most intense ions (> 2^+ charge states) were selected for higher energy collision dissociation (HCD) using a resolution of 7,500. The settings for the HCD were as following: threshold for the ion selection was 20000, the target value of ions used for HCD was 300 ms, activation time was 0.1 ms, isolation window was 2 m/z, and normalized collision energy was 36.

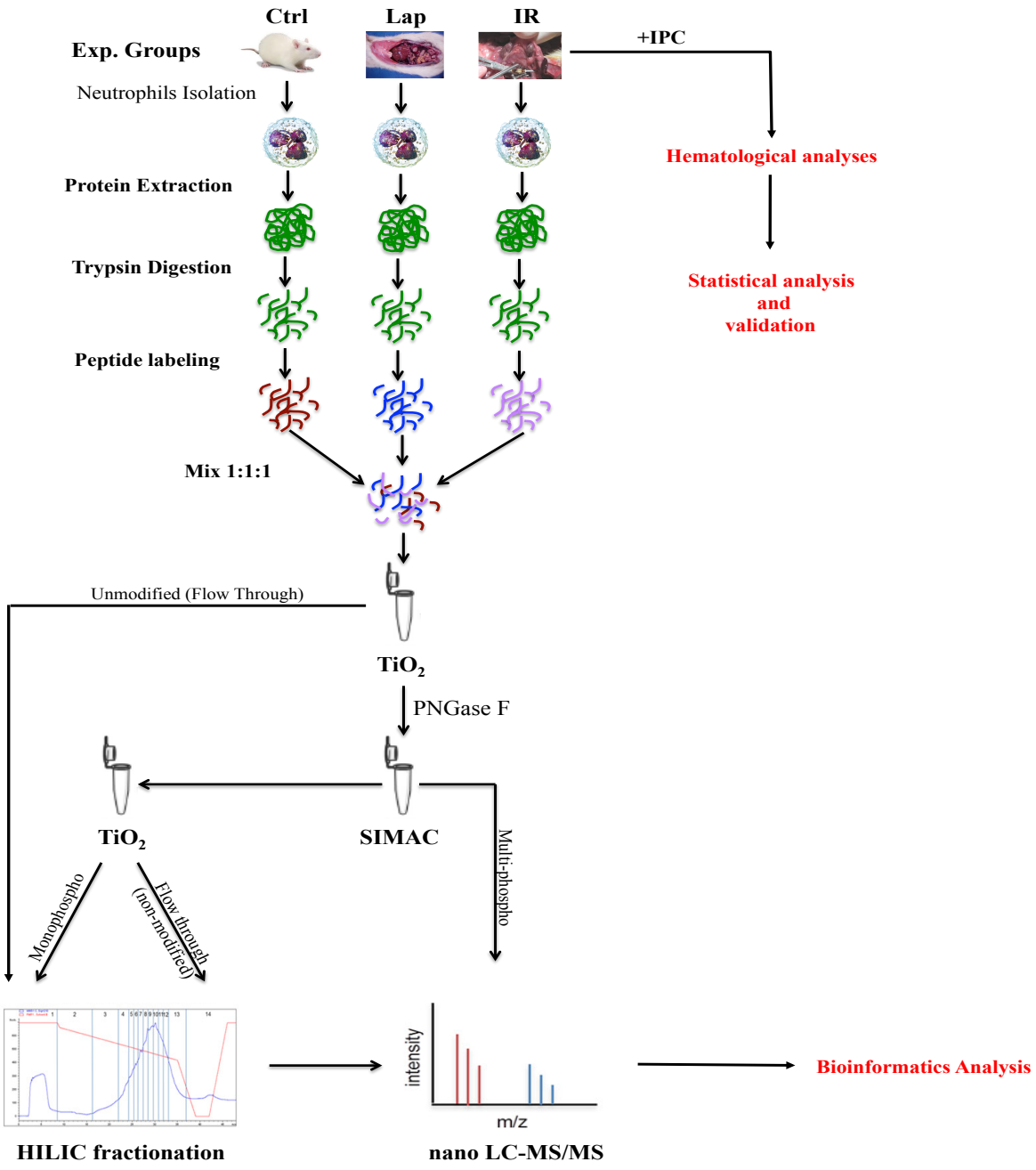

Figure 13 Schematic presentation of experimental procedure. IPC group (ischemic preconditioning) only for hematological analysis. Neutrophils isolation by Ficoll density gradient method from Ctrl (control), Lap (laparotomy) and IR (ischemia/reperfusion) groups followed by protein extraction by using FASP SDS protocol. Overnight trypsin digestion 1:50 trypsin to protein ratio. iTRAQ labeling 114 for Ctrl, 115 for Lap and 116 for IR. Mono- and multi-phosphopeptides enrichment using TiSH (TiO_2 SIMAC HILIC fractionation). LTQ Orbitrap MS analysis fallowed by bioinformatics tools.

3.14 Database Searching and Bioinformatics

Raw files were processed using Proteome Discoverer version 1.4.0.288 (Thermo Fisher Scientific). Tandem MS/MS spectra were converted to .mgf files and searched against the UniProt rodent's database using Mascot (v2.3.2, Matrix Science, London, UK). Database searches were performed with the following parameters: precursor mass tolerance 10 ppm, fragment (MS/MS) mass tolerance 0.05 Da, up to two missed cleavages and trypsin as digestion enzyme. Variable modifications included: oxidation (M) and deamidation (NQ); for phosphopeptides we included also phosphorylation (serine, threonine, tyrosine). The Carbamidomethylation on cystein residue was applied as a fixed modification. Results were filtered for 1% false discovery rate (FDR) using Percolator as validator [187]. We applied further filters for the analysis of phosphopeptides by excluding all phosphopeptides with phosphoRS 3.0 probability lower than 95%. Obtained ratios (115/114 and 116/114) were log2 transformed and normalized by the average value for each of the two datasets (115/114 and 116/114). Statistical validation for significantly regulated peptides or proteins was assessed by using a one tail one sample t-test (confidence <5%).

Another more sophisticated statistical approach for more detailed analysis was performed with statistical package R software. The data for non-modified fractions and phosphopeptides fractions consists of five biological replicates. The iTRAQ intensities values for each fraction were log-transformed and median-normalized. One peptide measurement was allowed by choosing "mean" instead of "median" in RRollup function of DanteR package for the multiple measurements of the same peptide [188]. The non-modified peptides values were converted into protein quantitation (RRollup, mean) with a minimum of three peptides per protein. Statistically significant regulations require more sophisticated tools than just application of the standard t-test. Limma [189] and rank products [190] provide sufficient power to deal with low replicate numbers and additional missing values [191]. Both statistical tests were carried out on all phosphopeptides and protein ratios against label 114 and corrected for multiple testing. [192]. From both statistical tests all the phosphopeptides and proteins with q-value below 0.05 (5% FDR) were considered regulated.

For the cluster analysis, we calculated the mean over all 5 replicated values for each condition. Phosphopeptides and proteins were merged into one data set. Fuzzy c-means clustering [193, 194] was applied after determining the value of the fuzzifier and obtaining the number of clusters according to Schwämmle (2010) [195]. A standard principal component analysis (PCA) was performed by using R package to check the variability between different conditions and similarity among the biological replicates of the same group.

ProteinCenter (Thermo Scientific, Waltham, USA) was used to interpret the results at protein level, e.g, statistical GO Slim classification with 5% False discovery rate (FDR) and number of transmembrane domains. For enzyme activity prediction and classification (Enzyme Commission (EC) numbers) Blast2GO software was used (http://www.blast2go.com/b2ghome) [196] with default parameters for prediction of enzymatic activity of the proteins. For KEGG pathways analysis WebGestalt [197] was used with default parameters and the overlap between uploaded data set and pathway data set was checked by using graph visualization option of EnrichNet [198]. STRING v9.1 [199] was used to check protein-protein interactions of the overlap proteins/proteins identified in a pathway (Fig.14). Phosphorylation in the regulating domains of kinases and phosphatases were checked manually in NCBI (http://www.ncbi.nlm.nih.gov/).

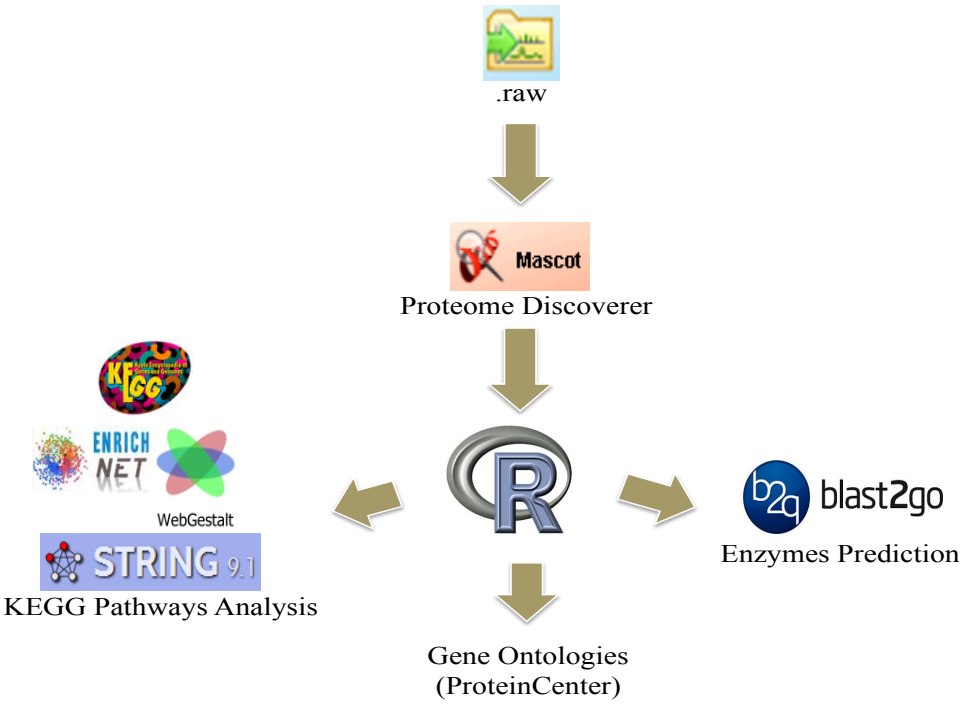

Figure 14 The raw files searched against Mascot database by using Proteome Discoverer.

RESULTS & DISCUSSION

Hematological Analysis
Results & Discussion

4 Results and Discussion of Hematological Analysis

All surgical groups (SL, IR and IPC) produced a remarkably smaller ($p<0.001$) amount of lymphocytes than the control group (Fig. 15-A). Among the surgical groups, IR showed a decrease in lymphocyte counts when compared with the LAP group; however, an increase was noted in IPC, compared with IR ($p<0.05$). Lymphocyte loss and dysfunction are well known in animal models of both SIRS and sepsis [200]. Preventing lymphocyte dysfunction, specifically preventing lymphocyte apoptosis following sepsis, has been shown to improve survival after sepsis [201]. IPC prevented lymphocyte loss, compared with the IR group in this study. The hematological parameters of the control, sham laparotomy, ischemia/reperfusion and ischemic preconditioning groups are summarized in table 1.

White blood cell counts (WBCs) showed a significant increase in both the IR and the IPC group, compared with the control group ($p<0.01$) (Fig. 15-B). Postoperative leukocytosis represents a normal physiologic response to surgery [202]. However, an augmentation in WBC counts has been viewed as a predictor of ischemic stroke [203].

A significant increase ($p<0.001$) in the granulocyte count was observed in the LAP, IR and IPC groups compared with controls. There was an increase in the IR group compared with the LAP group ($p<0.01$), and IPC promoted an important reduction ($p<0.05$) compared with the IR group, almost approaching the LAP level (Fig. 15-C). This increase was due to the marked elevation of leukocyte activation, as previously described in myocardial ischemia and reperfusion in dogs [204]. The increased number of granulocytes after ischemic strokes caused tissue damage, as these cells are implicated in the early responses of the hemostatic and inflammatory processes [205]. Studies have revealed that intestinal ischemia is characterized by the production of cytokines [206] and the sequestration of polymorphonuclear neutrophils (PMNs) into the ischemically damaged tissue. The complement system also contributes to the attraction of neutrophils to ischemically damaged areas [207] by releasing myeloperoxidase (MPO) and other proinflammatory mediators, further contributing to IR-induced tissue damage [208].

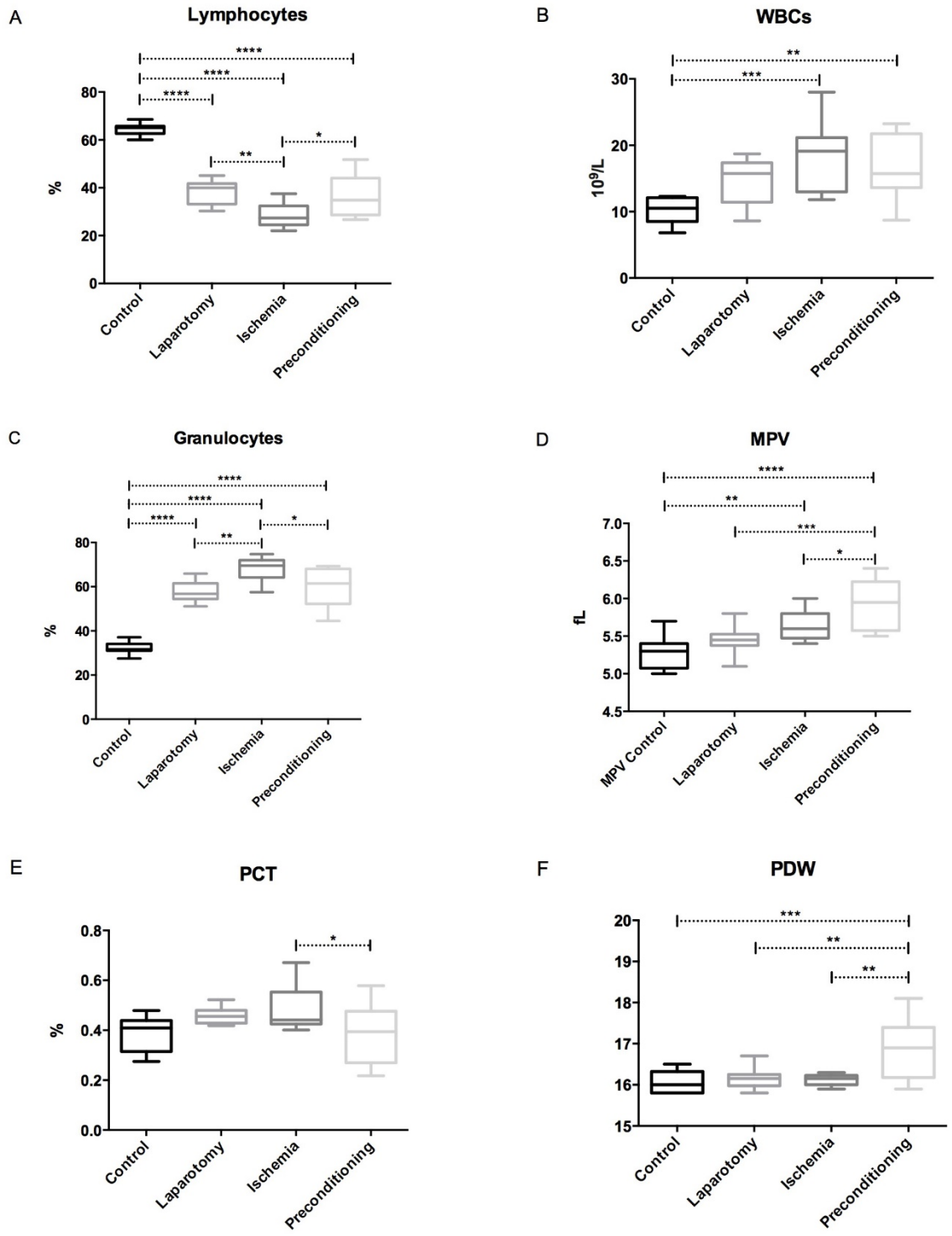

Figure 15 Distribution of the hematimetric parameters in the four experimental groups.

(A) Lymphocyte count, (B) White Blood Cell counts (C) Granulocyte counts, (D) Mean Platelet Volume, (E) Plateletcrit and (F) Platelet distribution. (***P < 0.001; **P < 0.001 to 0.01; *P < 0.01 to 0.

Table 1 Haematological analyses, expressed as mean ± standard deviation, median and range (min. - max.) of (Wistar Rat) control, laparotomy, intestinal ischemia/reperfusion and ischemic preconditioning.

Parameters	Control group			Laparotomy group			Ischemia/Reperfusion group			Preconditioning group		
	Mean ± std dev	Median	Range Min - Max	Mean ± std dev	Median	Range Min - Max	Mean ± std dev	Median	Range Min - Max	Mean ± std dev	Median	Range Min - Max
WBC (10^9/L)	10.27 ± 2.04	10.85	6.8 - 12.3	14.71 ± 3.4	15.75	8.6 - 18.7	18.13 ± 5.16	19.1	11.8 - 15.75	16.39 ± 4.67	15.7	8.7 - 23.2
Lymphocytes (10^9/L)	6.79 ± 1.59	7.2	4.1 - 8.8	5.6 ± 1.42	5.3	3.5 - 7.7	5.65 ± 1.28	5.65	3.7 - 8.8	5.61 ± 2.24	5.05	3.9 - 11.6
Monocytes (10^9/L)	0.31 ± 0.07	0.3	0.2 - 0.4	0.6 ± 0.28	0.5	0.3 - 1.2	0.71 ± 0.29	0.6	0.4 - 0.6	0.57 ± 0.19	0.6	0.3 - 0.8
Granulocytes (10^9/L)	3.17 ± 0.59	3.1	2.3 - 3.9	8.51 ± 2.11	9.15	4.7 - 10.7	13.36 ± 6.31	12.85	5 - 9.15	10.21 ± 3.7	9.85	4.5 - 17.6
Lymphocytes (%)	64.76 ± 2.96	65.1	60 - 70.8	38.26 ± 4.98	39.95	30.3 - 45.1	28.47 ± 5.23	27.35	22 - 70.8	36.33 ± 8.19	34.85	26.7 - 51.8
Monocytes (%)	3.25 ± 0.36	3.1	2.9 - 3.9	3.68 ± 0.6	3.6	2.9 - 4.7	3.36 ± 0.28	3.35	3 - 3.9	3.81 ± 0.43	3.85	3.2 - 4.7
Granulocytes (%)	32.1 ± 2.86	31.65	26.2 - 37.1	57.63 ± 4.61	56.75	51.1 - 65.9	67.87 ± 5.74	69.5	57.5 - 57.63	59.89 ± 8.25	61.45	44.5 - 69.3
RBC (10^{12}/L)	6.528 ± 0.55	6.58	5.49 - 7.52	7.38 ± 0.72	7.65	6.1 - 8.3	7.66 ± 0.52	7.665	6.88 - 7.65	7.32 ± 1.38	7.63	4.62 - 9.58
HGB (g/L)	128 ± 6.94	126.5	120 - 142	138.5 ± 12.03	138.5	120 - 156	143.3 ± 7.69	144	134 - 142	141 ± 20.02	147.5	107 - 167
HCT (%)	40.83 ± 1.86	40.45	38.8 - 44.4	44.63 ± 3.63	44.95	38.7 - 49.8	47.07 ± 2.61	46.85	43.3 - 44.95	45.14 ± 6.31	47.65	34.2 - 54.2
MCV (fL)	61.39 ± 2.46	61.1	57.2 - 65.1	60.41 ± 1.95	59.95	58 - 63.7	61.57 ± 2.34	61.2	58.2 - 65.1	60.8 ± 2.39	60.75	56.6 - 64.7
MCH (pg)	19.16 ± 0.75	19.15	17.6 - 20.3	18.6 ± 0.67	18.6	17.8 - 19.7	18.7 ± 0.8	18.8	17.5 - 20.3	18.98 ± 0.73	19.05	17.4 - 20.1
MCHC (g/L)	312.8 ± 4.61	312.5	307 - 320	308.7 ± 5.89	308.5	301 - 320	304.1 ± 5.36	302.5	297 - 320	312.7 ± 7.12	313.5	303 - 325
RDW (%)	11.46 ± 0.72	11.2	10.7 - 12.7	11.96 ± 0.65	11.95	10.5 - 12.9	12.52 ± 1.35	12.15	11 - 12.7	12.87 ± 1.32	12.7	11.5 - 15.2
PLT (10^9/L)	746.6 ± 148.32	785.5	529 - 943	837.3 ± 92.71	828	679 - 1024	867.2 ± 154.25	800.5	734 - 943	653.1 ± 248.34	665	341 - 1135
MPV (fL)	5.3 ± 0.2	5.3	5 - 5.7	5.45 ± 0.18	5.45	5.1 - 5.8	5.64 ± 0.2	5.6	5.4 - 5.7	5.93 ± 0.33	5.95	5.5 - 6.4
PDW	16.1 ± 0.24	16.05	15.8 - 16.5	16.15 ± 0.26	16.15	15.8 - 16.7	16.13 ± 0.13	16.15	15.9 - 16.5	16.86 ± 0.68	16.9	15.9 - 18.1
PCT (%)	0.3946 ± 0.08	0.412	0.275 - 0.49	0.46 ± 0.03	0.456	0.418 - 0.52	0.49 ± 0.09	0.441	0.401 - 0.49	0.3763 ± 0.12	0.3945	0.218 - 0.578

The monocytes, red blood cells (RBCs), hemoglobin (HGB), mean corpuscular volume (MCV) and mean corpuscular hemoglobin (MCH) was not influenced significantly in any experimental group. Only the MCHC level showed some changes among the groups. Except for the MCHC values, these results are similar to those of a study on a canine model investigating limb IR, with or without cooling [209]. The hematocrit (HCT) was increased ($p<0.05$) in the ischemia/reperfusion group, compared with the control (Fig. 16-A, supplementary). Dehydration during surgery or fluid sequestration due to edema can result into a higher hematocrit level than normal [210]. This increase was more prominent in the IR group and showed no significant difference in any other group. The mean corpuscular hemoglobin concentration (MCHC) was decreased in the IR group in comparison with the controls, while there was an increase ($p<0.05$) in the MCHC value in the IPC, compared with the IR, returning the MCHC value to a normal level (Fig. 16-B, supplementary). A decrease in this parameter may be associated with fluid loss from emesis, bowel edema and loss of absorptive capacity [210]. This reflects that IPC is able to reduce the influence of IR in hydro-electrolytic homeostasis.

The red cell deviation width (RDW) was higher ($p<0.05$) in the IPC group, compared with the controls; no other group showed a significant difference (Fig. 16-C, supplementary). Elevated RDW levels have been suggested as a marker and independent predictor of various cardiovascular diseases, including acute and chronic arterial diseases [211].

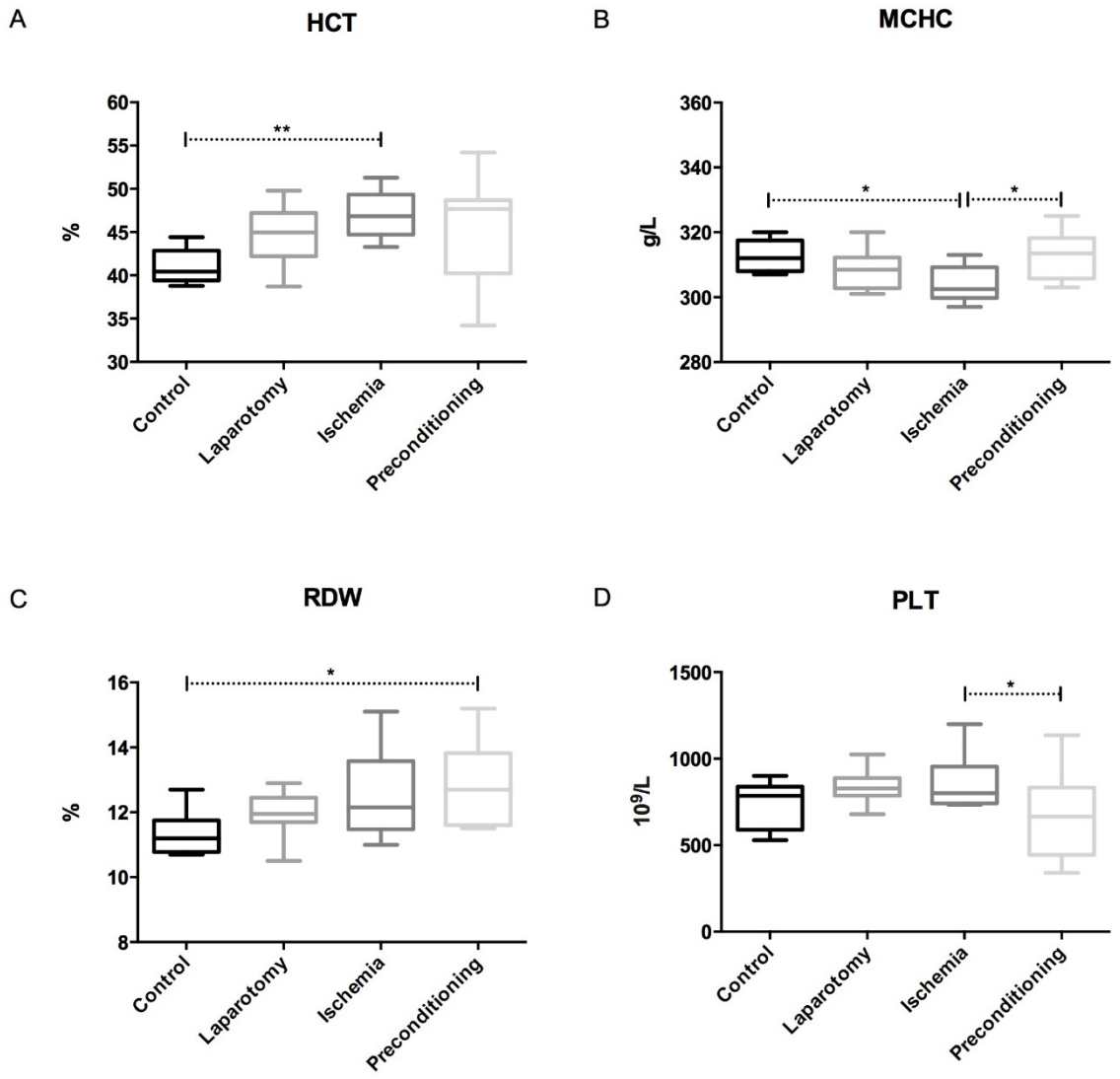

Figure 16 supplementary. Distribution of hematimetric parameters in the four experimental groups.

(A) Hematocrit count, (B) Mean corpuscular haemoglobin concentration, (C) Red cell distribution width, (D) Platelet count. (**P < 0.001 to 0.01; *P < 0.01 to 0.05).

The platelets showed significant variation between the ischemia/reperfusion and preconditioning groups. The platelet counts were higher ($p<0.05$) in the IR group than in the IPC group (Fig- 16-D, supplementary). Studies have shown that platelets also participate in ischemic strokes [212] and IR-mediated tissue damage [213]. However, the

role of platelets in the progression of tissue damage after IR injury is not clear. A recent study showed that platelet-deficient mice showed significant reductions in the damage to their villi in response to IR, compared with mice with normal platelet counts [214]. The mean platelet volume (MPV) here showed a significantly increased value in the IR ($p<0.01$) and IPC ($p<0.001$) groups, compared with the control and laparotomy groups. In preconditioned rats, the MPV was higher than in the ischemia/reperfusion rats ($p<0.05$) (Fig. 2-D). The MPV was higher when there was some destruction of the platelets in cases of inflammatory bowel disease [215]. Another study stated that MPV was not associated with stroke severity or functional outcomes [216]. Platelet distribution widths (PDWs) were significantly higher in IPC rats compared with controls ($p<0.001$) and in IPC rats, compared with LAP and IR rats ($p<0.01$). The activation of the platelets leads to morphologic changes, including pseudopodia formation and the development of spherical shape. Platelets with an increased number and size of pseudopodia differ in size, possibly affecting the platelet distribution width**.** PDW seems to be affected in a different pattern than MPV, as is clear in Fig. 15-D and Fig. 15-F. Only ischemia/reperfusion and preconditioning had a significant difference regarding their plateletcrit (PCT) levels, while the rest of the groups did not show any significance differences. The plateletcrit (PCT) was lower ($p<0.05$) in the IPC group than in the IR group (Fig. 15-E).

CONCLUSION.

The results presented in this work show significant differences in the hematimetric parameters among all of the conditions evaluated. The most remarkable parameters are those related to leukocytes and platelets; some of these, including the lymphocyte and granulocyte counts and the granulocytes/lymphocytes ratios, suggest that IPC attenuates the effect of the IR in the circulating blood cells. Our work provides data to aid the better understanding of hematological responses in the body after IR and IPC. Some of the parameters described here can be further validated as predictive markers for ischemia and may lay the basis for further studies aiming to reduce the tissue injury resulting from ischemia/reperfusion.

Proteomics Analysis

Results & Discussion

5.1 Identification of proteins by mass spectrometry

Rat neutrophils were isolated from the three biological groups (Control, Laparotomy and Ischemia) and proteins were extracted, digested and peptides were purified. The purified peptides were labeled with iTRAQ and analyzed by Orbitrap Velos Mass Spectrometry and a total of 2924 proteins were identified.

A statistical analysis (as described in materials & methods) showed that 393 and 653 proteins were regulated in laparotomy and ischemia groups as compared to the control respectively. Both laparotomy and ischemia have 198 regulated proteins in common (Fig.17, Table. 2)

Figure 17 Common and exclusive regulated proteins in laparotomy (Lap) and intestinal ischemia reperfusion (IR) groups.

Table 2 Number and percentage of all regulated proteins in LAP and IR group.

Set	Count	%
A	653	77
B	393	46.3
A-B	455	53.6
B-A	195	22.9
A∩B	198	23.3
A+B	848	100

Further analysis of proteins regulation showed that 190 proteins were up and 203 were down regulated in laparotomy whereas 367 proteins were up and 286 were down regulated in ischemia groups, whereas 2531 and 2271 proteins showed no regulation at all (Fig. 18). A 4-way Venn diagram was made to have a clear picture of all the regulated neutrophils proteins in both groups (Fig.19). The Venn diagram shows the unique and overlapping proteins expressed in neutrophils. Of the 190 up regulated proteins in laparotomy 87 are the unique proteins that are exclusively up regulated in neutrophils after laparotomy while the remaining 98 are the overlapping proteins that are also up regulated in neutrophil after intestinal ischemia and 5 proteins are down regulated during ischemia but up regulated in laparotomy. Of the 203 down regulated proteins during laparotomy in neutrophils 108 are unique proteins that are only down regulated in laparotomy whereas 8 proteins that are down regulated after laparotomy but up shows up regulation in ischemia. 87 proteins showed down regulation both in laparotomy and ischemia. The neutrophils after intestinal ischemia showed up and down regulation of 261 and 194 unique proteins in ischemia group respectively.

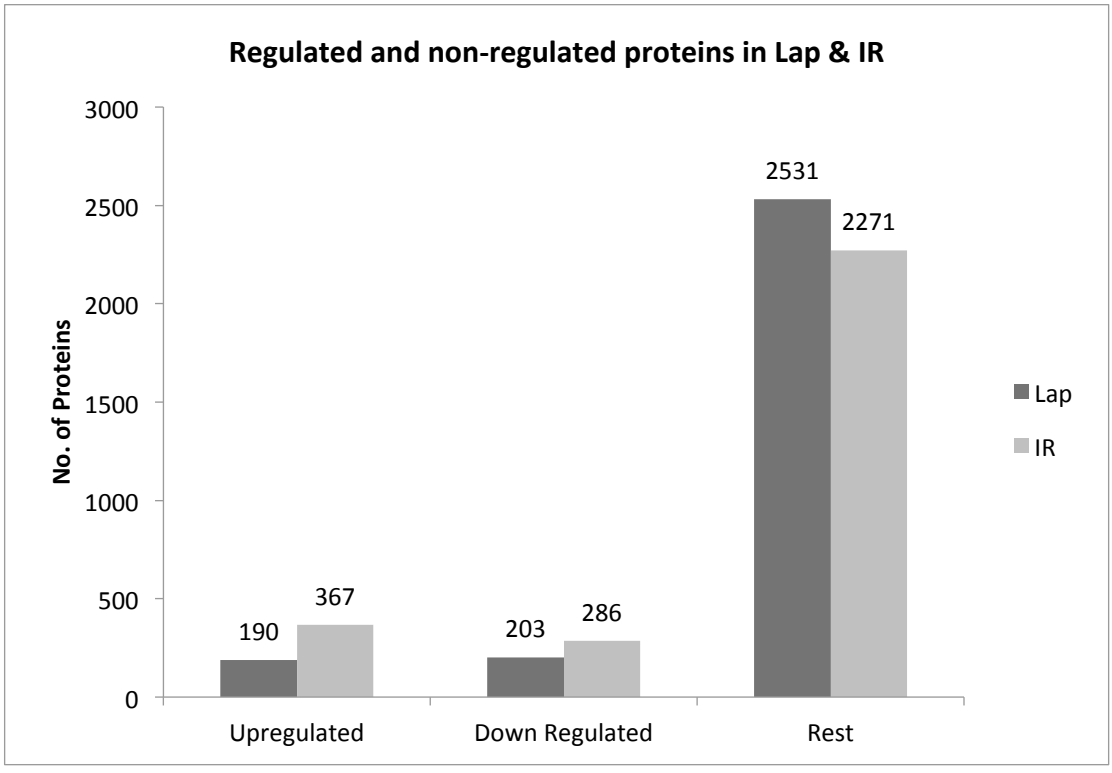

Figure 18 Number of Regulated and non-regulated proteins in LAP and IR groups.

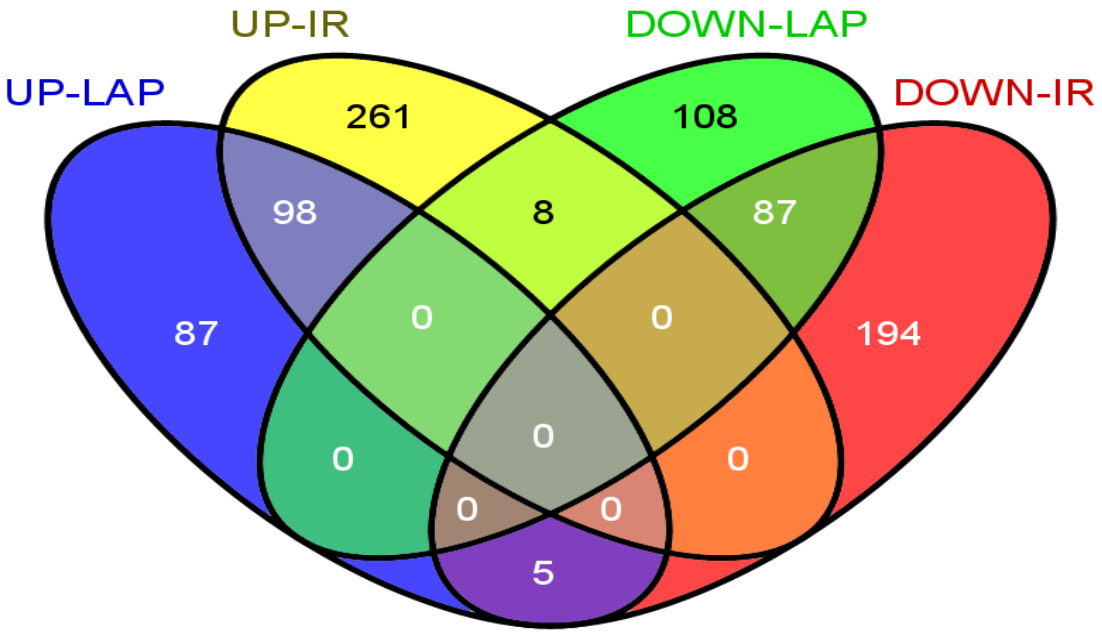

Figure 19 A 4-way Venn diagram illustrating unique and overlapping up and down regulated proteins in neutrophil after laparotomy and intestinal ischemia/reperfusion.

5.2 Statistical analysis of data with R package

We also analyzed the data with R software as described in materials and methods. The results obtained from both the different statistical approaches were almost similar but we proceeded for further analysis based on results by using the statistical package R for the reasons mentioned in material and methods. Five clusters with different abundance profiles were obtained (Fig. 20). Cluster 1 shows down regulation in both laparotomy and ischemia group making 20% (542 proteins) of the total regulated proteins whereas both cluster 2 and 5 shows up regulation in both laparotomy and ischemia making 19% (517 proteins) and 18% (464 proteins) of the total regulated proteins respectively. Cluster 3 making 28% (743 proteins) was down regulated only in laparotomy and cluster 4 making 15% (407 proteins) was slightly up in laparotomy but with down regulation in ischemia (Fig. 21).

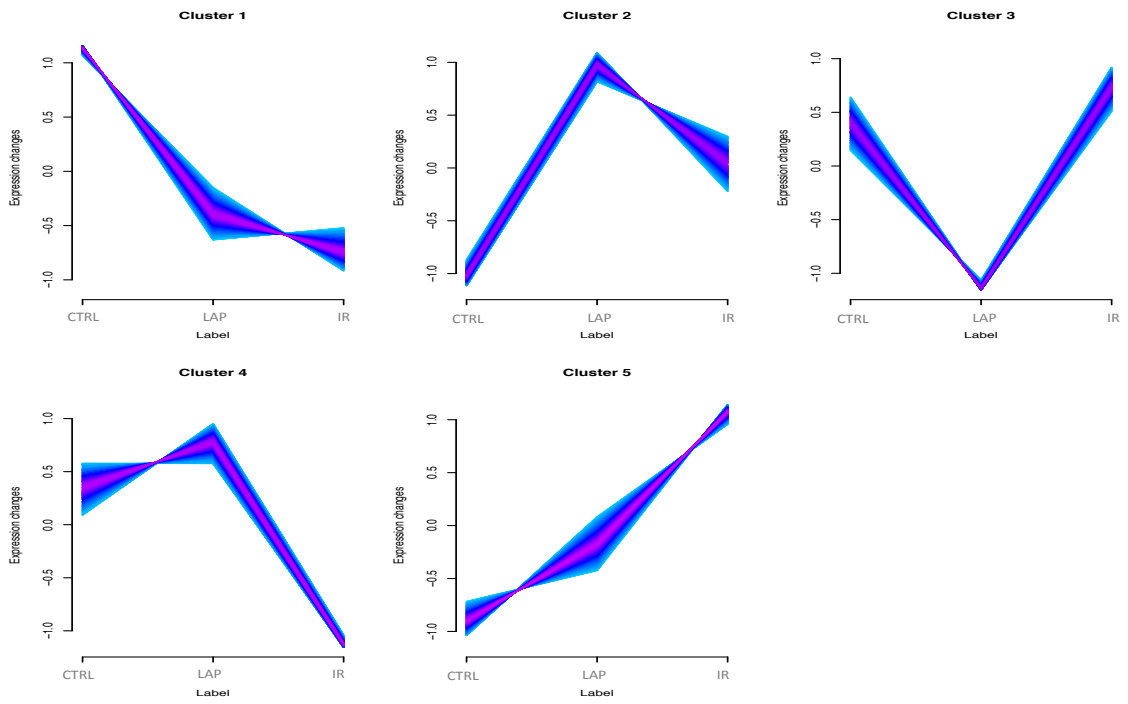

Figure 20 Expression profile of regulated proteins and phosphopeptides after laparotomy and Ischemia reperfusion in neutrophils. Control (114), Laparotomy (115), and Ischemia reperfusion (117).

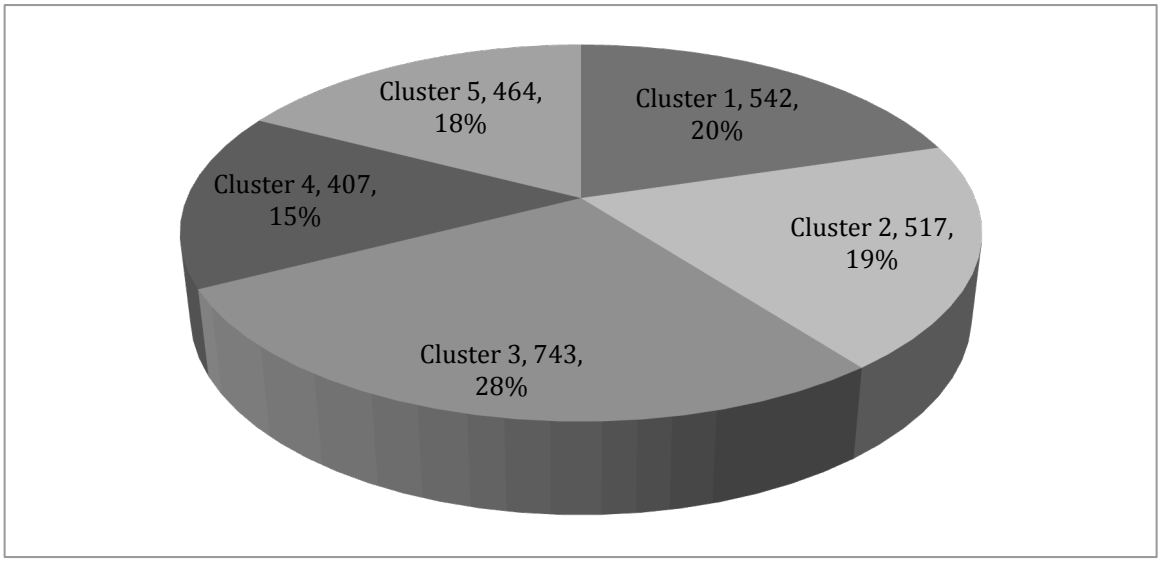

Figure 21 Regulated Proteins distribution among the five clusters in neutrophils.

5.3 Principal Component Analysis (PCA):

A standard principal component analysis (PCA) was performed to check the variability between different conditions and similarity among the biological replicates of the same group. All the proteins and peptides were taken for PCA analysis but the algorithm (prcomp function in R) only used the proteins and peptides that were quantified in all conditions and all biological replicates at the same time. The PCA plot, the so-called score plot, in Fig. 22 shows that although there is variability between the replicates they are clearly grouped in non-overlapping conditions that means a relatively good reproducibility in each condition. It roughly simplifies the whole data column into one data point.

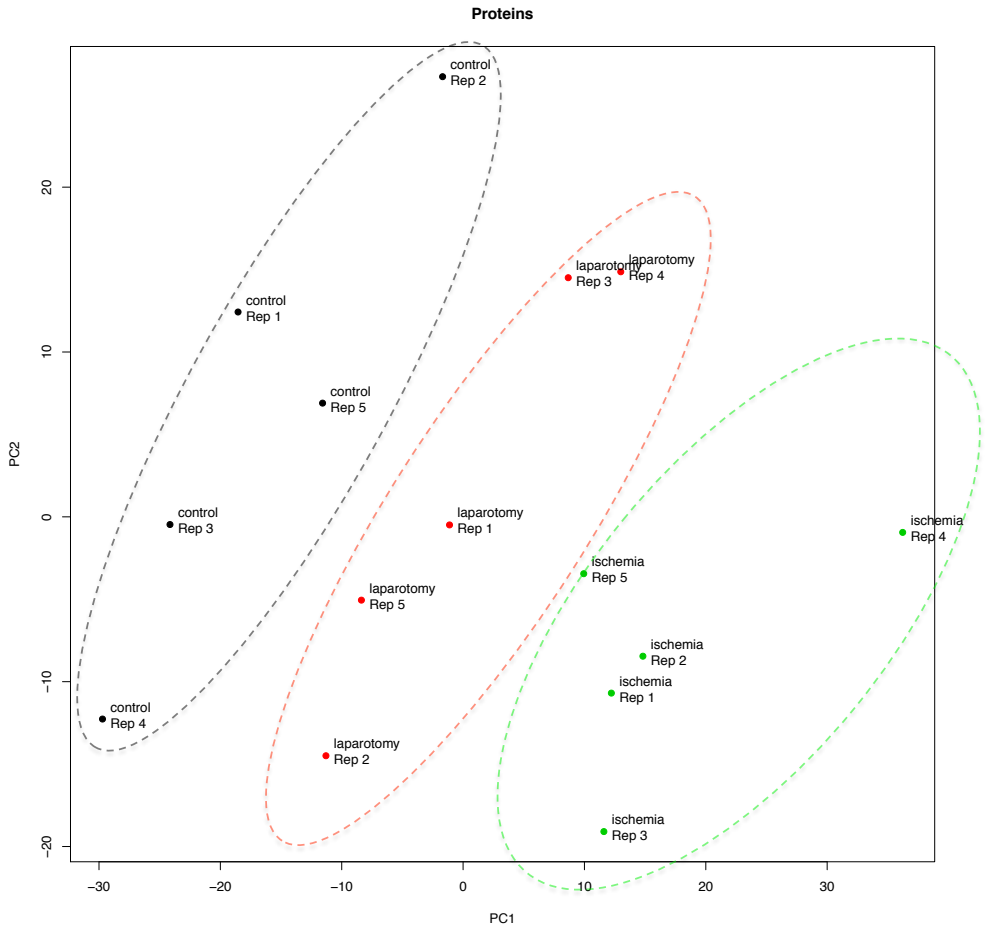

Figure 22 Principal component analysis (PCA).PCA analysis of all the proteins identified in all the five biological replicates in control (black), laparotomy (red) and ischemia reperfusion (green).

5.4 Phosphoproteome of rat neutrophil

Protein phosphorylation is a very common post-translation modification that takes place during signal transduction. Eukaryotic cells rely extensively on protein phosphorylation for their basic cellular processes, including metabolism, motility, differentiation, growth, division, organelle trafficking, membrane transport, immunity, muscle contraction, learning and memory [217, 218]. By combining the data from non-modified peptides and the modified phosphopeptides, we identified in total 3816 proteins. A total of 2231 non-phosphorylated unique proteins were identified and 892 unique phosphorylated proteins whereas 693 phosphorylated proteins were identified in both total and phosphoproteome making in total 1585 phosphorylated proteins as shown in the two way Venn diagram (fig. 23-E). Our analysis showed 41.5% of protein phosphorylation of the total neutrophil proteome identified in this study. Mass spectrometric analysis of the total phospho-proteome of rat neutrophil revealed the efficacy of the enrichment method that we used. We got 90% of the phosphorylated peptides that contained 95% of mono-, and 5% of di-phosphorylated peptides where as 10% were non-phosphorylated peptides (Fig. 23-A). We identified 4894 phosphosites in 4453 phosphopeptides for 1585 proteins Fig. 23-F. For signal transduction cascades, the eukaryotic cells depend on the phosphorylation of hydroxyl group on the side chain of serine (S), threonine (T) and tyrosine (Y) [219, 220]. Different studies have reported different ratios of S/T/Y phosphorylation in different cell lines. Macek et al, 2007 reported a ratio of 70:20:10 for S/T/Y in Bacillus subtilis [221] and the same group found 86:12:2 in human cell culture [222]. It has furthermore been estimated that the relative abundances of phosphoserine, -threonine, and -tyrosine in the human proteome are 90%, 10%, and 0.05%, respectively [223]. Phosphoproteomics analysis of hela cells from Matthias Mann lab showed almost the same ratio 86.4:11.8:1.8 for S/T/Y phosphorylation like [222]. The phosphosites analysis of phosphoproteome of rat neutrophils in the current work revealed a ratio of 87: 12:1 (S/T/Y) as in pie chart from fig. 23-B, similar to the phosphoproteomics analysis performed by Lundby *et al,* 2011 on 14 different rat organs and tissues where they found 88.1:11.4:1.5 ratio [224]. Our relative abundance of S/T/Y phosphorylation in regulated proteins Fig. 23-C showed 76:21:3 proportion that seems to be close to 79:17:2 of S/T/Y phosphorylation recently studied in human embryonic differentiation into neural stem cells [185]. In a cluster-wise

comparison, as shown in Fig. 23-G, of regulated proteins and peptides having regulated phosphorylation shows that more regulated proteins were present in cluster 3 whereas more phosphopeptides behaved like cluster 5, 2, and 4. We found 844 phosphopeptides from 277 proteins were grouped in cluster 5, 726 phosphopeptides from 288 proteins in cluster 2, while 605 phosphopeptides from 280 proteins were grouped in cluster 4. Cluster 1 combined 551 phosphopeptides from 252 proteins and cluster 3 gathered 542 phosphopeptides from 257 proteins. We identified 3268 peptides having regulated phosphorylation for 602 proteins.

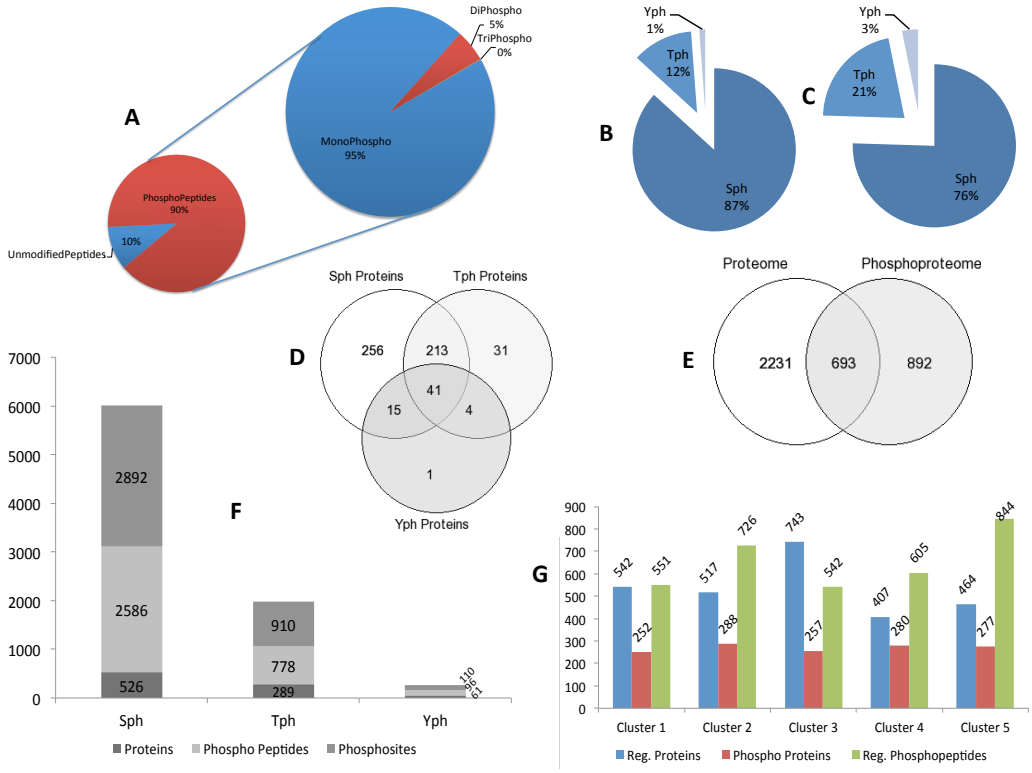

Figure 23 Phosphoproteome of rat neutrophil.

A, Significance of phospho enrichment & number of phosphosites per peptide. B, Distribution of phosphosites identified in total dataset. C, Distribution of phosphosites identified in regulated dataset. D, Overlap between serine, threonine and tyrosine phosphorylated proteins. E, Overlap between proteome and phosphoproteome. F, Number of phosphosites and phosphopeptides in phosphoproteins. G, Clusterwise

distribution of phosphorylated proteins, regulated proteins, and regulated phosphorylated peptides.

5.5 GO *Slim* analysis of total and regulated proteins of rat neutrophils

5.5.1 Cellular Component

Analysis of the Gene ontology (GO) from ProteinCenter of regulated proteins according to their Cellular Component is shown in fig. 24, 25. There is great variety among the regulated proteins from all the five clusters in their cellular localization. In cluster 1, (Fig. 24, 25-A) most of the regulated proteins belong to ribosome, cytoplasm and cytosol of the neutrophil. In cluster 2, (fig. 24, 25-B) most of the proteins showed enrichment from cytoskeleton, cytosol and extracellular component of neutrophil.

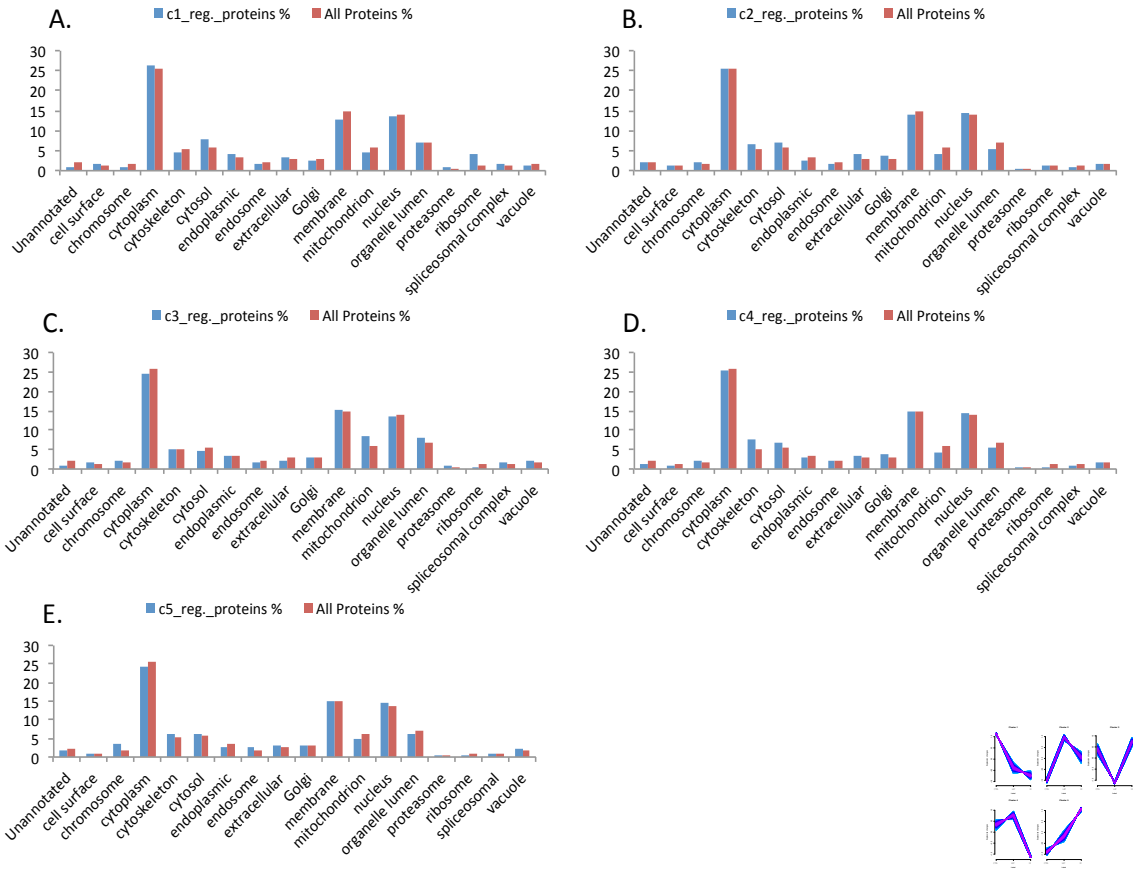

Figure 24 Bar chat of GO slim terms of cellular component of total and all regulated neutrophil proteins of (A) Cluster 1, (B) Cluster 2, (C) Cluster 3, (D) Cluster 4 (E) Cluster 5.

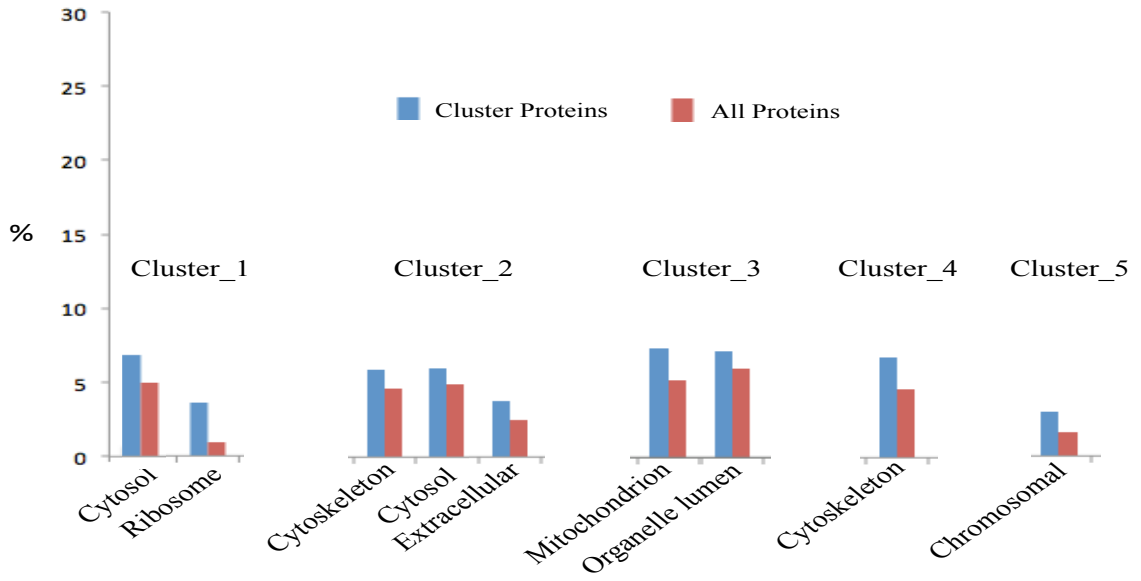

Figure 25 GO slim terms of more abundant cellular component of total and all regulated neutrophil proteins of (A) Cluster 1, (B) Cluster 2, (C) Cluster 3, (D) Cluster 4 (E) Cluster 5.

Proteins from Mitochondria and organelle lumen of neutrophils show enrichment in cluster 3 (fjg. 24, 25-C). In cluster 4 most of the enriched regulated proteins are part of cytoskeleton (Fig. 24, 25-D). Whereas in case of cluster 5, most abundant proteins were found in chromosome of neutrophil (Fig. 24, 25-E).

Neutrophils are highly motile cells and cytoskeleton plays a very important role in their motility. The cytoskeleton is a complex network of three cytosolic fibers namely microfilaments, intermediate filaments and microtubules. Studies have shown that actin fibers participate in neutrophil motility and also in the regulation of receptor affinity, apoptosis, cell cycle and signaling to the nucleus [225, 226]. Actin in cytoplasm, membrane and phagosome skeleton play very essential roles in neutrophil chemotaxis, trans-endothelial migration (TEM) and phagocytosis [227]. The cytoskeleton of the neutrophil is a very important part of the cell, which is still poorly characterized. Xu, P., *et al* has analyzed the sub-proteome of the neutrophil cytoskeleton of the cytosol, phagosome membrane and plasma membrane. Using 2DE and MALDI-TOF-MS they identified 138 proteins with few new proteins and the majority of these proteins were enzymes related to the energy metabolism [228]. Pattern of regulation from clusters 1, 2

and 4 shows down regulation of cytosolic and cytoskeletal proteins. The increased motility and chemotactic response of IR neutrophils might correlates with their down regulated cytoskeleton proteins compared to that of control and LAP.

The mitochondrion is the first site of damage in ischemia. During ischemia, the anaerobic metabolism produces a decrease in cell pH by accumulating hydrogen ions, and then the Na^+/H^+ exchanger excretes excess hydrogen ions, resulting into large influx of sodium ions [32]. Cellular ATP gets depleted which inactivates ATPases, reduces active Ca^{2+} efflux, and limits the re-uptake of calcium by the endoplasmic reticulum, thereby producing calcium overload in the cell. As a result the mitochondrial permeability transition (MPT) pore opens, that further disrupts ATP production by interrupting the mitochondrial membrane potential. The magnitude of blood flow and the duration of ischemia affect the degree of tissue injury [33]. Mitochondrial proteins show enrichment only in cluster 3, which is down regulated only in laparotomy and shows no difference in ischemia to control (Fig. 24-C).

5.5.2 Biological Processes

GO Slim terms of Biological Process of regulated proteins from all clusters are shown in fig.-26. Most regulated Proteins of cluster 1 are involved in metabolic processes (Fig 26-A, 27). Whereas proteins of cluster 2 are participating in cell organization and biogenesis (Fig 26-B, 27).

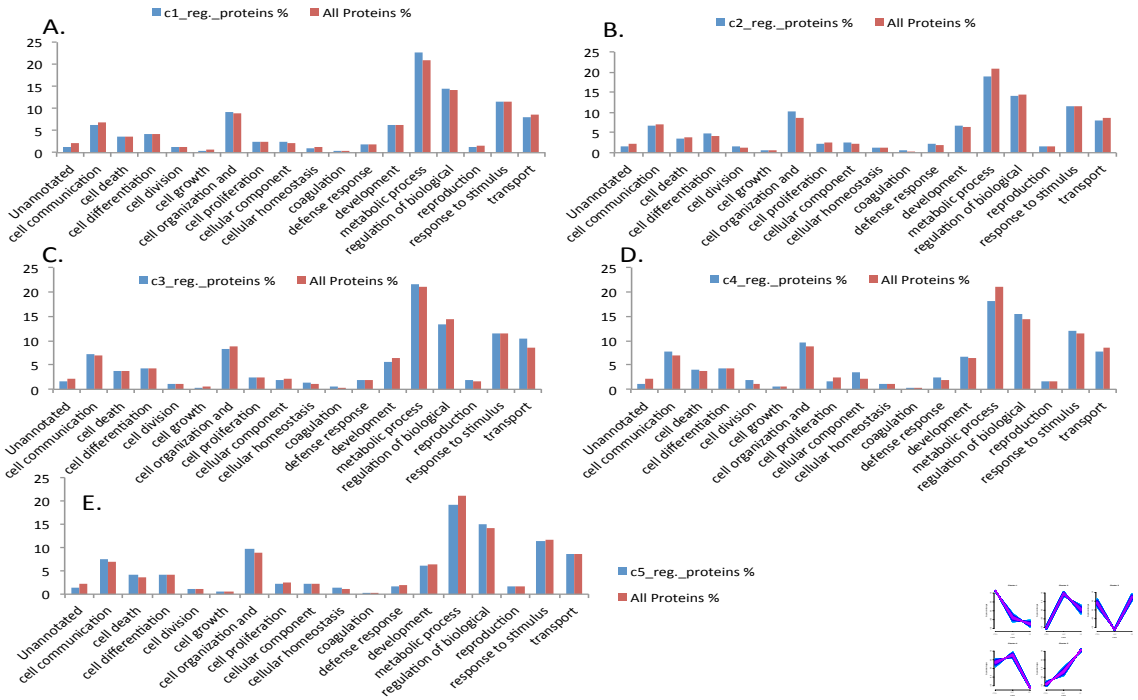

Figure 26 GO Slim terms of Biological Process of total and all regulated neutrophil proteins of (A) cluster 1, (B) Cluster 2, (C) Cluster 3, (D) Cluster 4 (E) Cluster 5.

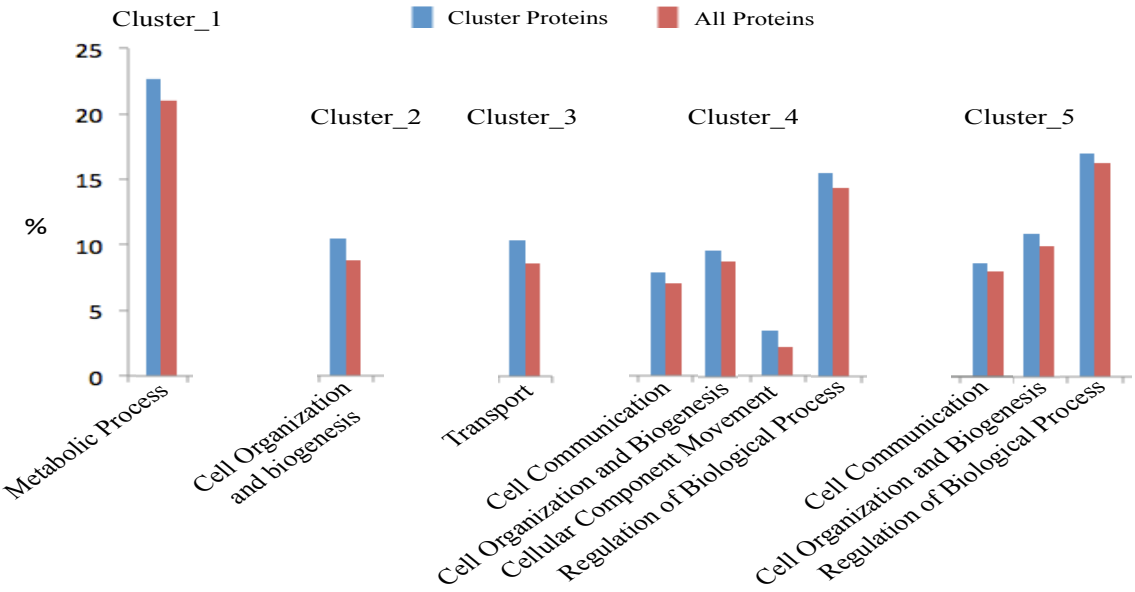

Figure 27GO Slim terms of more abundant Biological Process of total and all regulated neutrophil proteins of all clusters.

Proteins from cluster 3 are involved in transport (Fig 26-C, 27). Proteins from cluster 4 are participating in cell organization, cellular component motility, cell communication and regulation of biological processes (Fig 26-D, 27). Whereas most proteins from cluster 5 are playing role in cell organization, communication and regulation of biological processes (Fig 26-E, 27).

5.5.3 Molecular Function

GO Slim terms of molecular function of proteins of cluster 1 show enrichment for ribosome and cytoplasm (fig. 28-A, 29). These proteins are involved in RNA and nucleotide binding along with structural molecular activity. Proteins from cluster 2 are involved in protein binding and metal ion binding (Fig 28-B, 29).

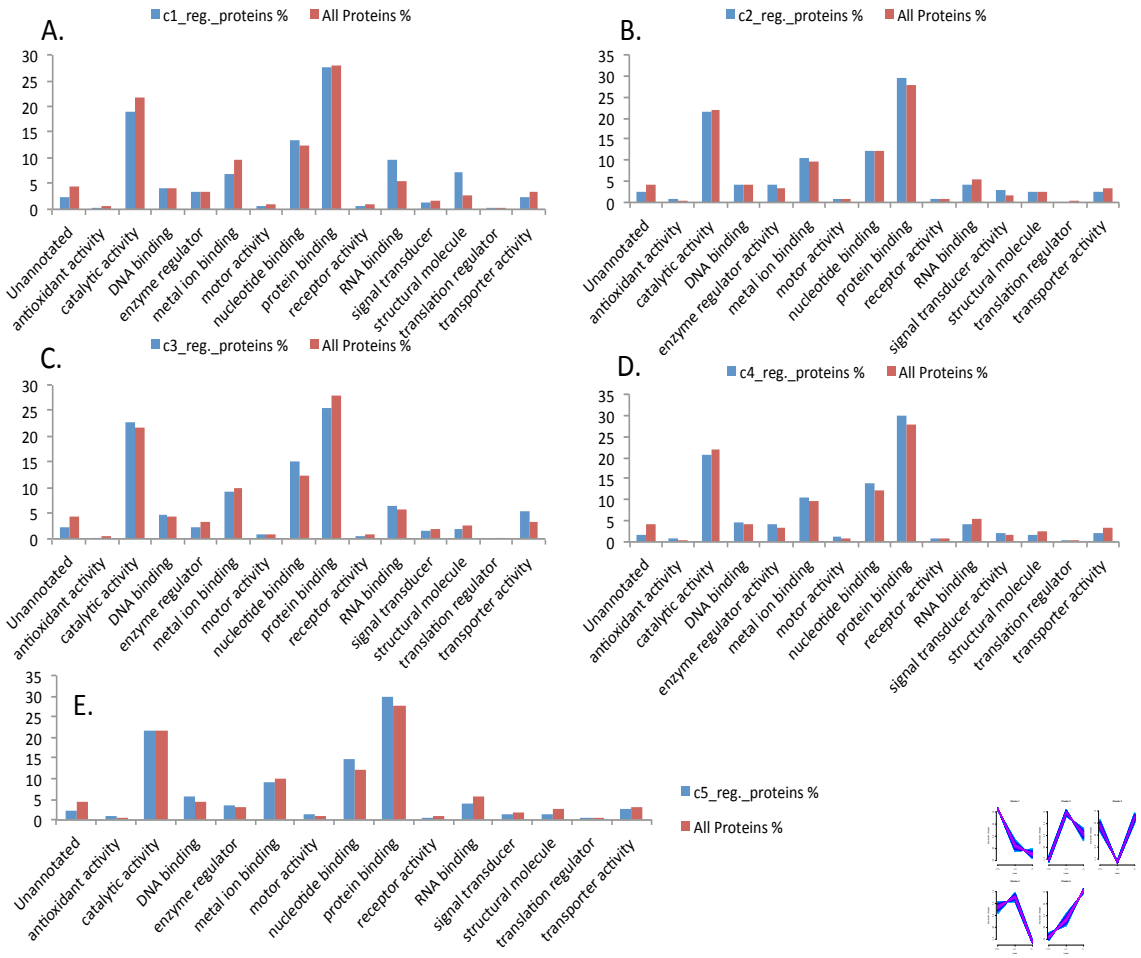

Figure 28 GO Slim terms of Molecular functions of total and all regulated neutrophil proteins of (A) cluster 1, (B) Cluster 2, (C) Cluster 3, (D) Cluster 4 (E) Cluster 5.

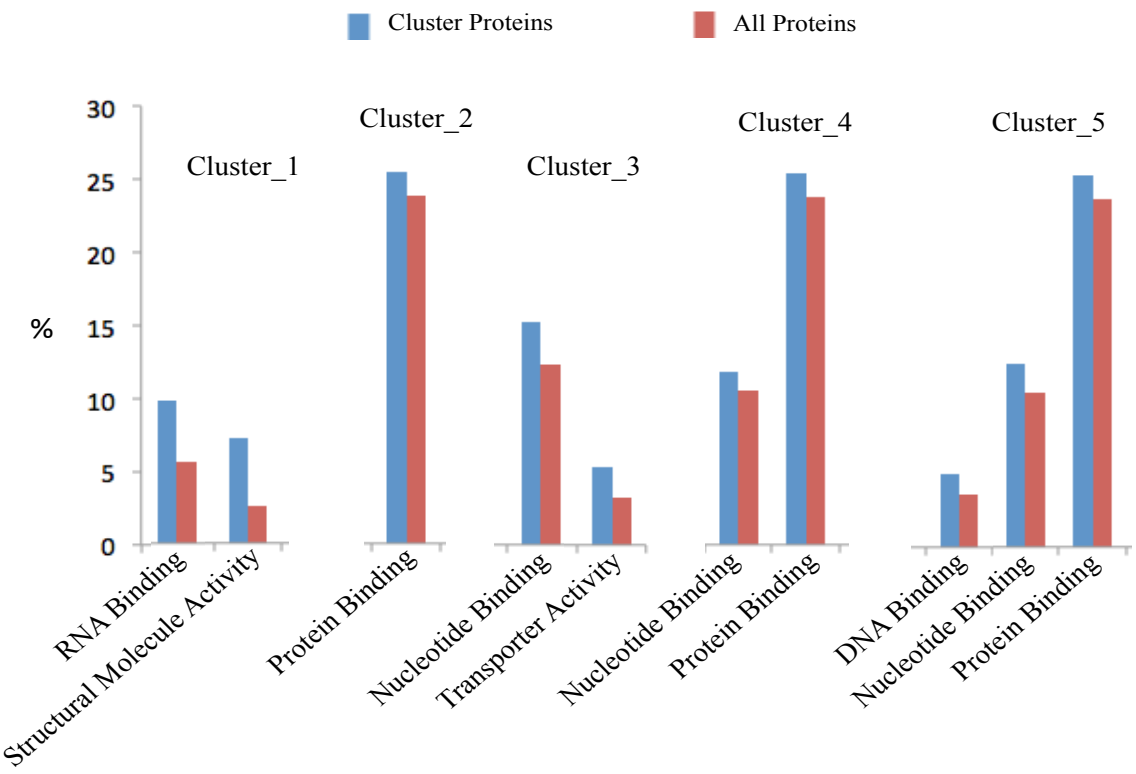

Figure 29 GO Slim terms of more abundant proteins for Molecular functions for all clusters.

Proteins from cluster 3 showed nucleotide binding and transporter activity (Fig 28-C, 29). Proteins of Cluster 4 and cluster 5 are involved in protein, nucleotide and RNA and DNA binding. It is clear from the five clusters that most of the regulated proteins are involved in binding to DNA, RNA and proteins, in other words transcription and translation of the proteins (Fig 228-D, E, 29).

5.6 Predicted Enzyme activity for the total rat neutrophil proteome

Using Blast2GO, as mentioned in materials and methods, the enzyme activity prediction for the rat neutrophil proteome was carried out. A pie chart of predicted enzymes of the whole regulated neutrophil proteome shows that most of the regulated enzymes are from Transferases (EC:2), Hydrolases (EC:3) and oxidoreductases (EC:1) respectively (Fig.30).

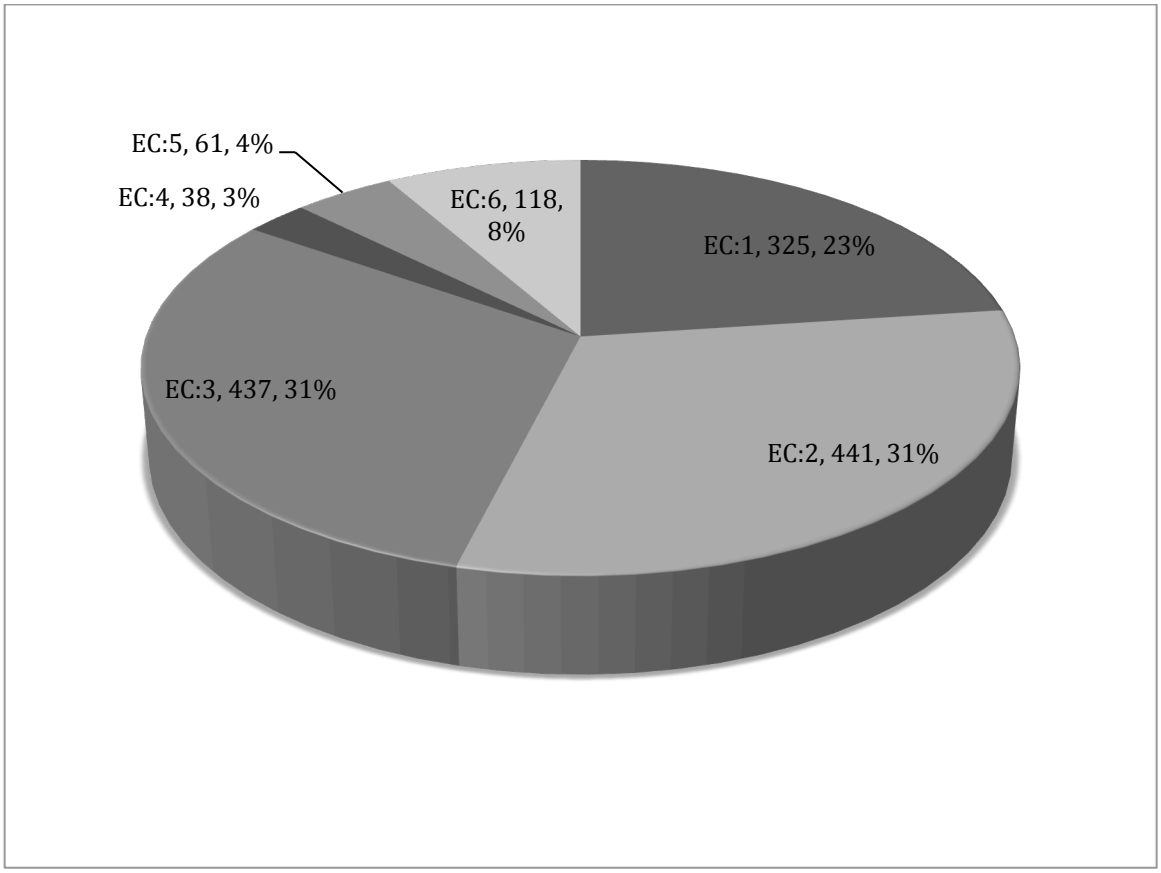

Figure 30 Enzyme prediction of total rat neutrophil proteome. Proteins sequence similarity based enzyme function prediction of total identified rat neutrophil proteome.

5.6.1 Enzyme function prediction for cluster 1

Isomerases (EC: 5) and ligases (EC: 6) are regulated enzymes enriched in cluster 1 as compared to total proteins identified (Fig. 31). It means that isomerases and ligases are down regulated in Laparotomy and IR group as compared to control. Details of the predicted down regulated enzymes from EC: 5 and EC: 6 are given in tables 3 and 4. Table 3 shows that the most down regulated enzymes among isomerases in IR group are peptidylprolyl isomerase (EC: 5.2.1.8) and protein disulfide-isomerase (PDI) (EC: 5.3.4.1).

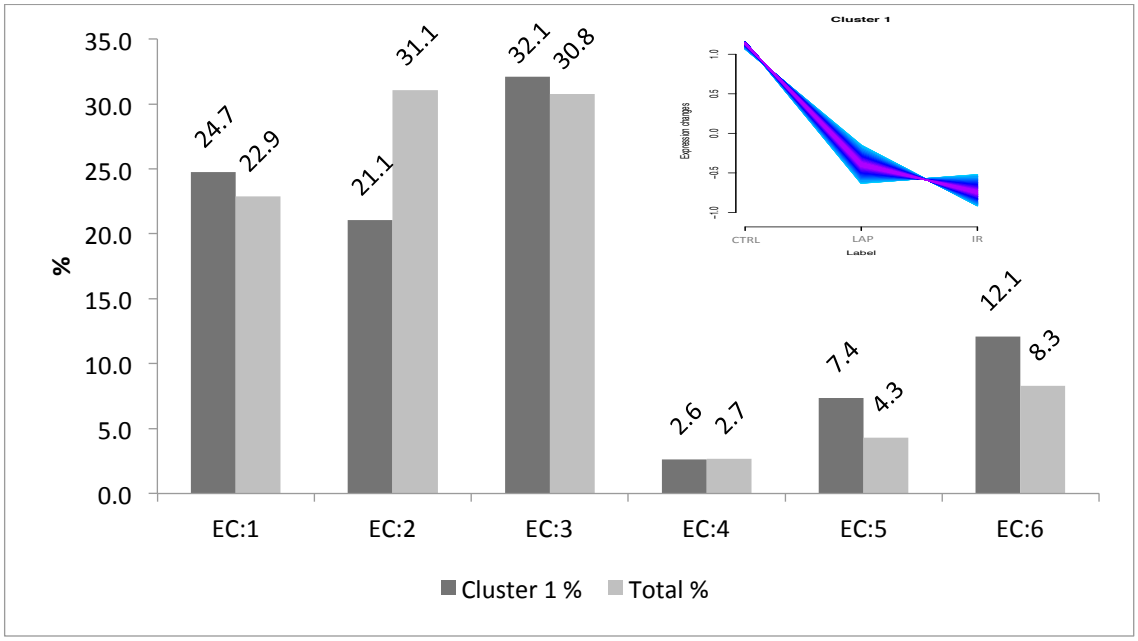

Figure 31 Enzyme prediction of cluster 1 proteins. Proteins sequence similarity based enzyme function prediction by B2GO of cluster 1 identified proteins.

Peptidylprolyl isomerase/cyclophilins (CyPs) are involved in cis/trans interconversion of proline peptide bonds and facilitate protein folding [229]. It was shown in Rheumatoid arthritis (RA) patients that CyPA affected IL-8 directed chemotaxis in neutrophils [230].

Protein disulfide-isomerase (PDI) is mainly located in the endoplasmic reticulum (ER) and is involved in folding of newly synthesized proteins (rearrangement of disulfide bonds, reductions or isomerization) [231] . Another study shows its role in ROS production because it was co-immunoprecipitated with NADPH oxidase subunits at the membrane p22phox as well as p47phox and p67phox in the cytosol of human neutrophils [232]. Recently, in vivo study using fluorescence intravital microscopy in mice found that PDI is involved in neutrophil adhesion (by interacting with αMβ2 integrin in lipid rafts) and crawling in TNF-α induced vascular inflammation. They suggested extracellular PDI as a novel therapeutic target to prevent neutrophil sequestration [233].

Phenylpyruvate tautomerase/ Macrophage migration inhibitory factor (MIF) (EC 5.3.2.1) is a cytokine with catalytic properties. The mature neutrophils from blood and tissue constitutively express MIF as a cytosolic protein not associated with azurophil granules.

Apoptotic neutrophils release active MIF after stimulation by TNF in a caspase-dependent manner [234].

Prostaglandin-E synthase (PGES) (EC: 5.3.99.3) is the final enzyme in the production of PGE2. PGE2 is a lipid mediator and basically is involved in many processes, such as gastrointestinal and renal functions, vascular homeostasis, bone remodeling, fever induction, pregnancy, and acute inflammation. Three isoforms of PGES are known cytosolic PGES (cPGES) [235, 236], microsomal PGES-1 (mPGES-1) [235], and mPGES-2 [237]. Proinflammatory cytokines IL-1β, TNF-α, and LPS, up regulate the expression of mPGES-1[238]. Mosca et al. showed that neutrophils are the readymade source of cellular mPGES-1[239].

Table 3 shows that most of the predicted down regulated ligases in cluster 1. According to their role in neutrophils, nothing has been reported in literature before. Some of these enzymes are involved in *de novo* synthesis of arginine and nucleotides and others are involved in the transfer of different amino acids to their cognate tRNAs as described below.

Aspartate tRNA ligase (EC: 6.1.1.12) [240]. Glycine tRNA ligase (EC:6.1.1.14) [241], proline tRNA ligase (EC:6.1.1.15) [242], glutamate tRNA ligase (EC:6.1.1.17) [243], Phenylalanine tRNA ligase (EC:6.1.1.20) [244] and Leucine tRNA ligase (EC:6.1.1.4) [245] catalyze attachment of their respective amino acids to their cognate tRNA and this reaction needs first activation of the amino acid by ATP to be used by the tRNA ligases.

Ubiquitin protein ligase (EC: 6.3.2.19) covalently attaches to the substrate, which is mediated by the action of an E1 activating enzyme, an E2 conjugase and an E3 ligase [246]. E3s can bind with E2 through RING finger, U box, or HECT domain and by F box, SOCS box, and DDB1 or BTB domain to the substrate [247, 248]. We are reporting, first time, the down regulation of these ligases in neutrophils that could lead to decrease in the biosynthesis of these amino acids. The effect on activated neutrophils is not clearly described in the literature.

Carbamoyl-phosphate synthase (EC: 6.3.4.16) participates in formation of carbamyl-phosphate from ammonia. It also starts both the urea cycle and synthesis of arginine and pyrimidines [249].

Formate tetrahydrofolate ligase (Fhs) (EC: 6.3.4.3) catalyses the formation of 10-formyl-tetrahydrofolate which is used directly in purine biosynthesis and formylation of Met-tRNA in Porphyromonas gingivalis (Gram-negative bacterium) [250]. Adenylosuccinate synthetase (EC: 6.3.4.4) that catalyzes the formation of adenylosuccinate from l-aspartate and IMP whereas hydrolysis of GTP also take place during this reaction, which is the first reaction in *de novo* synthesis of AMP [251]. Argininosuccinate synthase (EC: 6.3.4.5) is involved in de novo biosynthetic pathway for arginine and converts citrulline to arginine that is catalyzed by two argininosuccinate synthase and argininosuccinate lyase. First argininosuccinate synthase produces argininosuccinate as a result of condensation of citrulline and aspartate and later Argininosuccinate lyase then splits argininosuccinate to produce fumarate and arginine. Argininosuccinate synthase also play important role during synthesis of urea, nitric oxide, polyamine and creatine [252]. Phosphoribosyl formyl glycin amidine (FGAM) synthetase (EC 6.3.5.3) catalyzes one of the steps in *de novo* purine synthesis pathway. This enzyme catalyzes 5′-phosphoribosylformylglycinamide (FGAR) to FGAM in the presence of glutamine and ATP [253]. Carbamoyl-phosphate synthase (glutamine-hydrolysing) catalyzes formation of carbamoyl phosphate from L-glutamine in an intermediate in the biosynthesis of arginine and the pyrimidine nucleotides [253]. RNA ligase (EC: 6.5.1.3) transfer 5'-phosphate to the 3'-hydroxy terminus of RNA and as a result linear RNA changes to a circular form [254].

Table 3 Predicted isomerase function of cluster 1.

Acc	Gene	PD Description	Enzyme Codes
Q6DGG0	Ppid	Peptidyl-prolyl cis-trans isomerase D	EC:5.2.1.8
P45878	Fkbp2	Peptidyl-prolyl cis-trans isomerase FKBP2	EC:5.2.1.8
P10111	Ppia	Peptidyl-prolyl cis-trans isomerase A	EC:5.2.1.8
P17742	Ppia	Peptidyl-prolyl cis-trans isomerase A	EC:5.2.1.8
P30904	Mif	Macrophage migration inhibitory factor	EC:5.3.2.1
P30904	Mif	Macrophage migration inhibitory factor	EC:5.3.3.12
P38659	Pdia4	Protein disulfide-isomerase A4	EC:5.3.4.1
Q6IUU3	Qsox1	Sulfhydryl oxidase 1	EC:5.3.4.1
O54890	Itgb3	Integrin beta-3	EC:5.3.4.1
Q8BND5	Qsox1	Sulfhydryl oxidase 1	EC:5.3.4.1
P08011	Mgst1	Microsomal glutathione S-transferase 1	EC:5.3.99.3
Q7TSV4	Pgm2	Phosphoglucomutase-2	EC:5.4.2.2
Q7TSV4	Pgm2	Phosphoglucomutase-2	EC:5.4.2.2
Q9Z2M7	Pmm2	Phosphomannomutase 2	EC:5.4.2.2

Table 4 Predicted ligase function of cluster 1

Acc	Gene	PD Description	Enzyme Codes
P15178	Dars	Aspartate--tRNA ligase, cytoplasmic	EC:6.1.1.12
Q5I0G4	Gars	Glycine--tRNA ligase (Fragment)	EC:6.1.1.14
Q8CGC7	Eprs	proline--tRNA ligase	EC:6.1.1.15
Q8CGC7	Eprs	glutamate tRNA ligase	EC:6.1.1.17
Q505J8	Farsa	Phenylalanine--tRNA ligase	EC:6.1.1.20
Q8BMJ2	Lars	Leucine--tRNA ligase, cytoplasmic	EC:6.1.1.4
Q9CZY3	Ube2v1	Ubiquitin-conjugating enzyme E2 variant 1	EC:6.3.2.19
P83940	Tceb1	Transcription elongation factor B polypeptide 1	EC:6.3.2.19
B5DF89	Cul3	Cullin-3	EC:6.3.2.19
F1LP64	Trip12	E3 ubiquitin-protein ligase TRIP12	EC:6.3.2.19
Q2TL32	Ubr4	E3 ubiquitin-protein ligase UBR4	EC:6.3.2.19
O88738	Birc6	Baculoviral IAP repeat-containing protein 6	EC:6.3.2.19
P07632	Sod1	Superoxide dismutase (Cu-Zn)	EC:6.3.2.19
P48004	Psma7	Proteasome subunit alpha type-7	EC:6.3.2.2
Q62636	Rap1b	Ras-related protein Rap-1b	EC:6.3.4.16
P63321	Rala	Ras-related protein Ral-A	EC:6.3.4.16
P27653	Mthfd1	formate—tetrahydrofolate ligase	EC:6.3.4.3
P46664	Adss	Adenylosuccinate synthetase isozyme 2	EC:6.3.4.4
P09034	Ass1	Argininosuccinate synthase	EC:6.3.4.5
Q5SUR0	Pfas	Phosphoribosylformylglycinamidine synthase	EC:6.3.5.3
P63321	Rala	Ras-related protein Ral-A	EC:6.3.5.5
Q62636	Rap1b	Ras-related protein Rap-1b	EC:6.3.5.5
Q99LF4	Rtcb	tRNA-splicing ligase RtcB homolog	EC:6.5.1.3

5.6.2 Enzyme prediction of clusters 2 and 3

Predicted regulated enzymes of the cluster 2 present transferases (EC: 2), hydrolases (EC:3), and isomerases (EC:5) as enriched, while those for cluster 3 are oxidoreductases (EC:1), Hydrolases (EC:3) and Lyases (EC:4) . A bar chart comparison between total and regulated enzymes of clusters 2 and 3 show that there are no marked changes in enzymes regulation of both the clusters Fig. 32, 33.

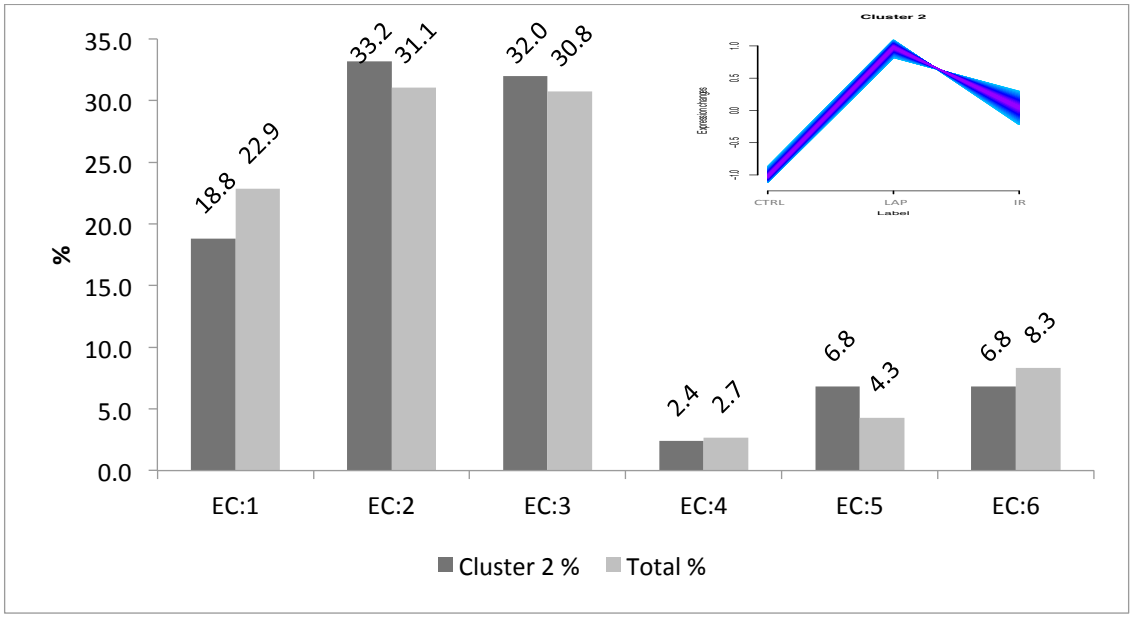

Figure 32 Enzyme prediction of cluster 2 proteins. Proteins sequence similarity based enzyme function prediction by B2GO of cluster 2 identified proteins.

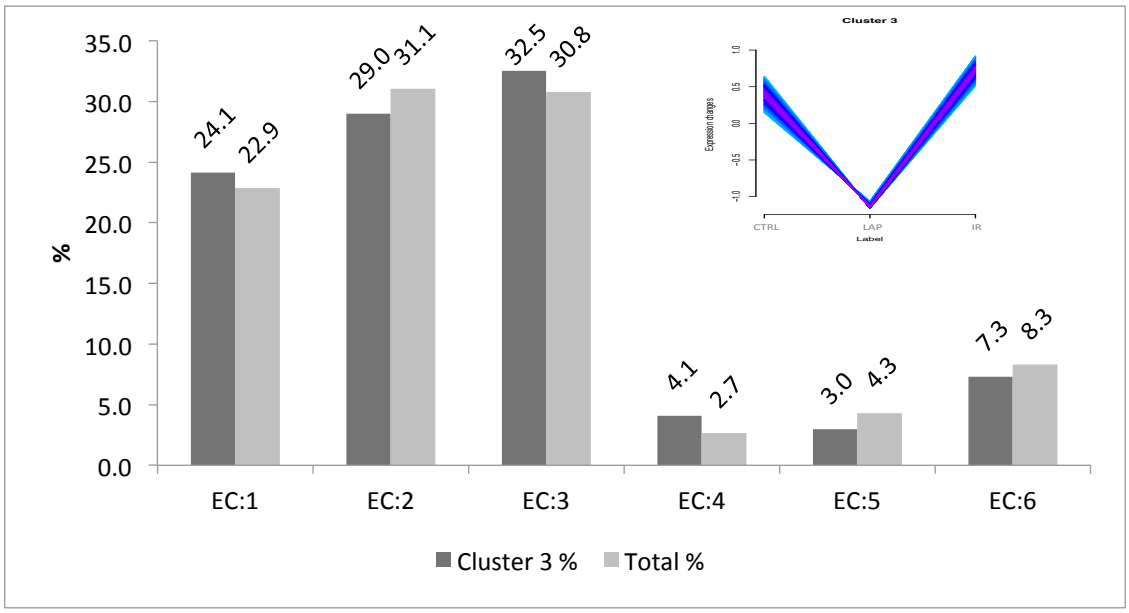

Figure 33 Enzyme prediction of cluster 3 proteins. Proteins sequence similarity based enzyme function prediction by B2GO of cluster 3 identified proteins.

5.6.3 Enzyme function prediction of cluster 4

The bar chart of predicted regulated enzymes of cluster 4 shows that (Fig.34) there is marked enrichment of Transferases (EC:2), increased in Laparotomy whereas clear down regulation has been observed in IR group. Detail of these regulated predicted enzymes is given in table 5.

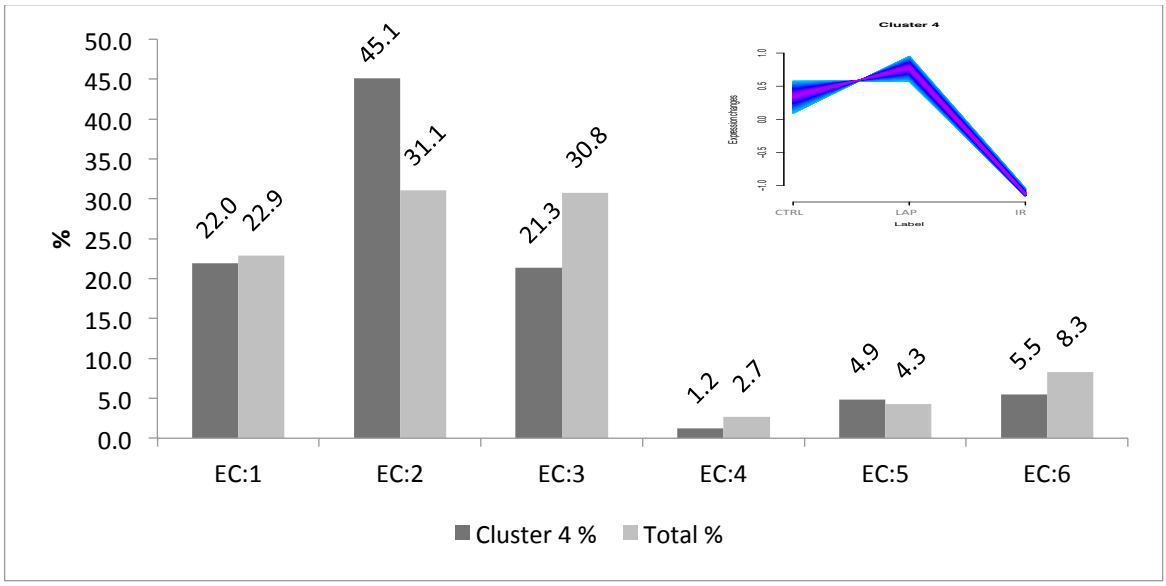

Figure 34 Enzyme function prediction of cluster 4 proteins. Proteins sequence similarity based enzyme function prediction by B2GO of cluster 4 identified proteins.

Phosphatidylinositol 4 phosphate 5 kinase (PIP5K) (EC: 2.7.1.149) enzyme catalyzes phosphorylation of phosphatidylinositol 4-phosphate (PtdIns4P) to produce phosphatidylinositol 4, 5-bisphosphate [255] which is also an important second messenger [256]. Three isoforms of PIP5K are well known such as α, β, and γ. PIP5Kα have many roles including regulation of neuronal microtubules depolymerization [257], suppression of phagocytosis [258], interaction with diacylglycerol kinase ζ (DGKζ), resulting in the the formation of PtdIns (4,5)P2 [259]. Both Ser/Thr and Tyr phosphorylation activate PIP5Kβ especially during oxidative stress [260] and is involved in directional movement and polarity of the neutrophil [261, 262].

NAD+ protein-arginine ADP-ribosyl transferase (ARTs) (EC: 2.4.2.31) is involved in the transfer of ADP-ribose from NAD to proteins. It is also produced by epithelial cells lining the human airway, where it can modify human neutrophil peptides (HNP-1),

altering its function. This alteration in neutrophil HNP-1 by ART1 is an important activity in inflammation and diseases. Here we have, for the first time, reported regulation of ARTs during IR in neutrophils [263].

Hexokinases (EC 2.7.1.2) catalyze the phosphorylation of glucose to glucose 6-phosphate (1st step of glycolysis) [264]. There are four isozymes present in mammal i-e HK1, HK2, HK3, and HK4. Hexokinase-3 (HK3) is present in all tissues in low amount whereas lung, kidney, and liver have moderate to high amount [265]. Particularly in granulcocytes, 70%-80% of total activity is provided by HK3 and remaining by HK1 [266]. Recently a study shown that HK3 was significantly down-regulated in primary Acute promyelocytic leukemia (APL) that impaired neutrophil differentiation of APL cells and finally promoted cell death of APL cells [267].

Protein-tyrosine kinases (EC: 2.7.10) including Src, Syk, and Tec play very important roles in signal transduction pathways regulating neutrophil activation and recruitment to inflammatory sites [268]. Protein-tyrosine kinases are first over expressed in laparotomy and then down regulated in IR group. Bruton tyrosine kinase (BTK) belongs to the Tec family of non-receptor tyrosine kinases. Recently it was shown that BTK-deficient neutrophils were impaired in maturation and function. This condition was found associated with inefficient development of granules as well as the expression of granule proteins, myeloperoxidase, neutrophilic granule protein, gelatinase and neutrophil elastase [269].

Serine/threonine protein kinases (EC: 2.7.11) are the most regulated of all the predicted enzymes in cluster 4. Most of these enzymes are not well annotated with respect to their role in neutrophils. One of the regulated serine/threonine protein kinases is PAK2 in this cluster. In neutrophils, p21-activated kinase (PAK2) can be stimulated by number of chemokines [270, 271]. Pak 2 can also be activated or auto phosphorylated on binding with activated GTP-bound Rac or Cdc42 [272]. Many studies showed that Paks are involved in a variety of cellular events such as rapid cytoskeletal responses, transcriptional events and the development of malignancy [273]. MAP kinase-activated protein kinase 2 (MAPKAPK 2), a Ser/thr kinase, has been shown to be phosphorylated and activated by MAP kinases (rapidly stimulated by mitogens, cytokines, and stresses)

both in vivo and in vitro. MAPKAP kinase 2 is involved in neutrophil activation [274, 275]. Surprisingly, it is down regulated in cluster 4 in IR group. Activation of Calcium/calmodulin-dependent protein kinase (EC: 2.7.11.17) (CaMKs) inhibits neutrophil maturation [276]. Mitogen-activated protein kinase (EC 2.7.11.24) includes Erk, jnk and p38. They participate in inflammation, apoptosis and migration whereas p38 regulates both in vitro and in vivo neutrophil chemotaxis [277].

5.6.4 Enzyme function prediction of Cluster 5

Figure 35 shows that the regulated enzymes in cluster 5 are enriched for oxidoreductases (EC: 1) when compared to the total regulated enzymes. Proteins in cluster 5 are up regulated in laparotomy and are also more abundant in the IR group. Details for these predicted enzymes are given in table 6.

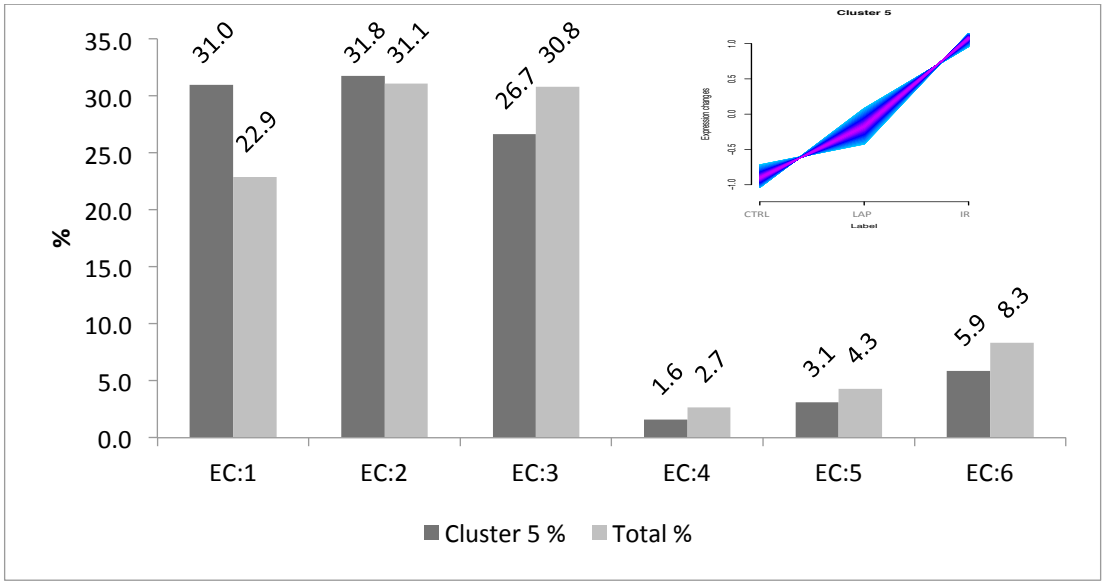

Figure 35 Enzyme prediction of cluster 5 proteins. Proteins sequence similarity based enzyme function prediction by B2GO of cluster 5 identified proteins.

Aldose reductase (AR) (EC: 1.1.1.21), which is a rate-limiting enzyme in polyol pathway 3, is a key player in myocardial ischemic injury and an increase in AR has been observed in the heart during ischemia that results into MTP opening [278, 279]. In addition, AR has been shown to mediate IRI in both diabetic and nondiabetic animals and results into microvascular dysfuntion [279, 280]. Inhibition of AR prevented the production of inflammatory cytokines and cardiac dysfunction induced by LPS in mice [281]. fMLP

Table 5 Predicted transferase function of cluster 4.

Acc	Gene	PD Description	Enzyme Codes
Q9Z0T0	Tpmt	Thiopurine S-methyltransferase	EC:2.1.1.67
P40142	Tkt	Transketolase	EC:2.2.1.1
P0C1Q3	P0C1Q4	P0C1Q5	P0C1Q6
P63005	Pafah1b1	Platelet-activating factor acetylhydrolase IB subunit alpha	EC:2.3.1.149
P0C1Q3	Lpcat2	Lysophosphatidylcholine acyltransferase 2	EC:2.3.1.23
P0C1Q3	Lpcat2	Lysophosphatidylcholine acyltransferase 2	EC:2.3.1.51
P0C1Q3	Lpcat2	Lysophosphatidylcholine acyltransferase 2	EC:2.3.1.63
P0C1Q3	Lpcat2	Lysophosphatidylcholine acyltransferase 2	EC:2.3.1.67
Q9CYK2	Qpct	Glutaminyl-peptide cyclotransferase	EC:2.3.2.5
A2RRU1	Gys1	Glycogen [250] synthase, muscle	EC:2.4.1.11
Q64633	Ugt1a7c	UDP-glucuronosyltransferase 1-7	EC:2.4.1.17
Q5RJQ4	Sirt2	NAD-dependent protein deacetylase sirtuin-2	EC:2.4.2.30
P84084	Arf5	ADP-ribosylation factor 5	EC:2.4.2.31
P61750	Arf4	ADP-ribosylation factor 4	EC:2.4.2.31
P04905	Gstm1	Glutathione S-transferase Mu 1	EC:2.5.1.18
P20291	Alox5ap	Arachidonate 5-lipoxygenase-activating protein	EC:2.5.1.18
Q9R0I8	Pip4k2a	Phosphatidylinositol 5-phosphate 4-kinase type-2 alpha	EC:2.7.1.149
O88370	Pip4k2c	Phosphatidylinositol 5-phosphate 4-kinase type-2 gamma	EC:2.7.1.149
P27926	Hk3	Hexokinase-3	EC:2.7.1.2
Q1HCL7	Nadk2	NAD kinase 2, mitochondrial	EC:2.7.1.23
P27926	Hk3	Hexokinase-3	EC:2.7.1.2
P11980	Pkm	Pyruvate kinase PKM	EC:2.7.1.40
Q9R0I8	Pip4k2a	Phosphatidylinositol 5-phosphate 4-kinase type-2 alpha	EC:2.7.1.68
O88370	Pip4k2c	Phosphatidylinositol 5-phosphate 4-kinase type-2 gamma	EC:2.7.1.68
P27926	Hk3	Hexokinase-3	EC:2.7.1.2
Q9Z0P5	Twf2	Twinfilin-2	EC:2.7.10
P35991	Btk	Tyrosine-protein kinase BTK	EC:2.7.10
P31938	Map2k1	Dual specificity mitogen-activated protein kinase kinase 1	EC:2.7.10
P36506	Map2k2	Dual specificity mitogen-activated protein kinase kinase 2	EC:2.7.10
P50545	Hck	Tyrosine-protein kinase HCK	EC:2.7.10
P50545	Hck	Tyrosine-protein kinase HCK	EC:2.7.10.2
Q9JI11	Stk4	Serine/threonine-protein kinase 4	EC:2.7.11
P19139	Csnk2a1	Casein kinase II subunit alpha	EC:2.7.11
Q9CQR6	Ppp6c	Serine/threonine-protein phosphatase 6 catalytic subunit	EC:2.7.11
P18654	Rps6ka3	Ribosomal protein S6 kinase alpha-3	EC:2.7.11
Q9WUT3	Rps6ka2	Ribosomal protein S6 kinase alpha-2	EC:2.7.11
Q63644	Rock1	Rho-associated protein kinase 1	EC:2.7.11
Q4G050	Mknk1	MAP kinase-interacting serine/threonine-protein kinase 1	EC:2.7.11
O54833	Csnk2a2	Casein kinase II subunit alpha	EC:2.7.11
Q63184	Eif2ak2	Interferon-induced, double-stranded RNA-activated protein kinase	EC:2.7.11
Q53UA7	Taok3	Serine/threonine-protein kinase TAO3	EC:2.7.11
Q99J45	Nrbp1	Nuclear receptor-binding protein	EC:2.7.11
P80386	Prkab1	5'-AMP-activated protein kinase subunit beta-1	EC:2.7.11
Q8K1R7	Nek9	Serine/threonine-protein kinase Nek9	EC:2.7.11
P18265	Gsk3a	Glycogen synthase kinase-3 alpha	EC:2.7.11
P47197	Akt2	RAC-beta serine/threonine-protein kinase	EC:2.7.11
P27926	Hk3	Hexokinase-3	EC:2.7.11.2
Q64303	Pak2	Serine/threonine-protein kinase PAK 2	EC:2.7.11
P31938	Map2k1	Dual specificity mitogen-activated protein kinase kinase 1	EC:2.7.11
P49138	Mapkapk2	MAP kinase-activated protein kinase 2	EC:2.7.11
Q9WTY9	Mapk13	Mitogen-activated protein kinase 13	EC:2.7.11

Continues Table-5: Predicted transferase function of cluster 4

Q66H84	Mapkapk3	MAP kinase-activated protein kinase 3	EC:2.7.11
P36506	Map2k2	Dual specificity mitogen-activated protein kinase kinase 2	EC:2.7.11
Q64303	Pak2	Serine/threonine-protein kinase PAK 2	EC:2.7.11.11
Q91VJ4	Stk38	Serine/threonine-protein kinase 38	EC:2.7.11.11
P09215	Prkcd	Protein kinase C delta type	EC:2.7.11.13
Q91VJ4	Stk38	Serine/threonine-protein kinase 38	EC:2.7.11.13
Q64303	Pak2	Serine/threonine-protein kinase PAK 2	EC:2.7.11.13
Q9JI11	Stk4	Serine/threonine-protein kinase 4	EC:2.7.11.13
P26817	Adrbk1	Beta-adrenergic receptor kinase 1	EC:2.7.11.14
P26817	Adrbk1	Beta-adrenergic receptor kinase 1	EC:2.7.11.15
P26817	Adrbk1	Beta-adrenergic receptor kinase 1	EC:2.7.11.16
P62204	Calm1	Calmodulin	EC:2.7.11.17
P49138	Mapkapk2	MAP kinase-activated protein kinase 2	EC:2.7.11.17
Q66H84	Mapkapk3	MAP kinase-activated protein kinase 3	EC:2.7.11.17
P11730	Camk2g	Calcium/calmodulin-dependent protein kinase type II subunit gamma	EC:2.7.11.17
P31938	Map2k1	Dual specificity mitogen-activated protein kinase kinase 1	EC:2.7.11.24
Q9WTY9	Mapk13	Mitogen-activated protein kinase 13	EC:2.7.11.24
P36506	Map2k2	Dual specificity mitogen-activated protein kinase kinase 2	EC:2.7.11.24
Q64303	Pak2	Serine/threonine-protein kinase PAK 2	EC:2.7.11.25
P97930	Dtymk	Thymidylate kinase	EC:2.7.4.4
P97930	Dtymk	Thymidylate kinase	EC:2.7.4.9
Q91ZJ5	Ugp2	UTP--glucose-1-phosphate uridylyltransferase	EC:2.7.7.9
O35156	UGP2	UTP--glucose-1-phosphate uridylyltransferase	EC:2.7.7.9

induced CD11b up-regulation as well as superoxide generation is completely prevented by AR inhibition. A study investigating the role of AR in mediating ALI showed that AR is required for neutrophils to respond for chemokines released by ECs after TNF-α stimulation. AR also affects CD11b up-regulation, neutrophil shape changes, and neutrophil adhesion to ECs [282]. Our data also suggested the increase production of AR in neutrophil during IRI.

Proteomic analysis of rat intestinal mucosa after ischemic preconditioning in IRI model identified 10 proteins using 2DE in combination with MALDI-TOF-MS and these proteins were involved in anti-oxidation, apoptosis inhibition and energy metabolism. This study also revealed up-regulation of aldehyde dehydrogenase and aldose reductase in IPC group [152]. Another study used 2-DE combined with MALDI-MS to analyze proteome of intestinal mucosa subjected to I/R injury in the absence or presence of IPC pretreatment in rats. A total of 16 proteins were deferentially expressed which belonged to cellular energy metabolism, anti-oxidation and anti-apoptosis of which aldose reductase, which removes ROS, was significantly down regulated in IR and up regulated

in IPC [153]. From these studies and our analysis it seems interesting that during IR aldose reductase is up regulated in the neutrophil and myocardium but down regulated in the intestinal mucosa.

Lactate dehydrogenase (LDH) (EC: 1.1.1.27) is a well-known nonspecific marker of cell injury and necrosis in cardiac, hepatic, muscular and renal tissue, in a variety of infections, lymphomas, hemolysis and delayed graft function [283]. Lactate dehydrogenase (LDH) is released from azurophil granules when neutrophils undergo necrosis [284].

6-Phosphogluconate dehydrogenase (6PGDH) (EC 1.1.1.44), which converts 6 - phosphogluconate into ribose 5-phosphate (second step of PPP) with the release of a second molecule of NADPH. 6PGDH was found associated with the neutrophil oxidase complex [285] and recently it was found to regulate phagocyte NADPH oxidase activity in neutrophils [286].

Myeloperoxidase (MPO) (EC: 1.11.1.7) is abundantly produced and released from azurophilic granules in neutrophil [287]. It catalyzes the formation of hypochlorous acid (HOCl), an oxidant having bactericidal activity *in vitro* [288]. In addition MPO-H2O2-chloride system subsequently produces chlorine, chloramines, hydroxyl radicals, singlet oxygen, and ozone which on release to outside of the cell may attack normal tissue and thus contribute to the pathogenesis of disease [289]. Another study demonstrated that the binding of MPO to CD11b/CD18 integrins results into PMN activation in a mechanism independent of MPO catalytic activity [290].

Arachidonate 5-lipoxygenase (EC: 1.13.11.34) and Arachidonate 15-lipoxygenase 15-LO (EC: 1.13.11.33) catalyzes the insertion of molecular oxygen into arachidonic acid at carbon 5 and 15. The enzymes can also oxygenate other polyenoic free fatty acids as well as a variety of phospholipids [291]. Immunocytochemical localization of 15-LO failed to prove the expression of 15-LO in neutrophils [292] and here we are, for the first time reporting over expression of these lipooxygenases during IRI in neutrophil.

Prostaglandin endoperoxide synthase (EC: 1.14.99.1) also known as cyclooxygenase (COX), which converts Archidonic acid (AA) to Prostaglandin G2 (PGG2) and a PGG2

reduction to Prostaglandin H2 (PGH2) which is a common precursor for all prostanoids [293]. Neutrophils can synthesize prostanoids in response to various types of stimulation [294, 295]. In moncytes, COX-2 expression for prostanoid synthesis needs activation of p38MAPK [296]. Whereas in neutrophils both ERK and p38MAPK pathways are involved in LPS-induced COX-2 expression and prostaglandin E(2) PGE2 production although IL-10 and IL-4 can inhibit neutrophil prostanoid synthesis by down-regulating the activation of p38MAPK [297].

Superoxide dismutase (SOD) (EC: 1.15.1.1) is involved in the regulation of neutrophil apoptosis and can lead to neutrophil mediated tissue injury during inflammation [298]. Recently it was found that extracellular superoxide dismutase impairs neutrophil function and inhibits its innate immune response thus leading to impaired bacterial clearance [299].

Xanthine oxidase, (XO), (EC 1.17.3.2) is an important enzyme having a role in the catabolism of purines. In mammals endothelial xanthine dehydrogenase (XDH) (EC: 1.17.1.4) can be converted to XO either reversibly or irreversibly [300]. The hypoxic stress also initiates conversion of XDH to XO. Molecular O_2 re-enters into tissues during the reperfusion of the Intestine, where it reacts with hypoxanthine and XO to produce a variety of oxygen free radicals superoxide anion (O^-_2), hydrogen peroxide (H_2O_2) and nitric oxides [301]. Activated neutrophils also convert XDH to XO in ECs, by secreting elastase in close proximity to the ECs [302]. Here we are reporting for the first time the presence and consistent increase in XDH and XO abundance in neutrophils after ischemia and reperfusion.

Glyceraldehyde-3-phosphate dehydrogenase, (GAPDH), (EC:.2.1.12) is a glycolytic enzyme whereas mammalian GAPDH also has diverse functions including membrane fusion, microtubule bundling, phosphotransferase activity, nuclear RNA export, DNA replication, and DNA repair. Moreover, it also takes part in apoptosis, age-related neurodegenerative diseases, prostate cancer, and viral pathogenesis [303]. It has been proved that it is involved in up to 25% of the total Ca^{2+} dependent cytosolic neutrophil degranulation [304].

Retinal dehydrogenase, (RALDH), (EC 1.2.1.36) converts vitamin A to retinoic acid (RA) in dendritic cells (DCs) and stromal cells in gut and induces gut homing of T cells [305] like Foxp3 producing regulatory T cells [306], and IgA expressing B cells [307], as well as suppressing the differentiation of Th17 cells [308]. Here we report for the first time an increased expression of RALDH in neutrophils after intestinal ischemia and reperfusion.

NADPH dehydrogenase, (quinone), (EC: 1.6.5.2) also known as NAD(P)H quinone oxidoreductase 1 (NQO1) is a flavoprotein that catalyzes the metabolic reduction of quinones [309]. Higher level of NQO1 has been observed in tumor tissues compared with normal ones [310] such as non–small cell lung cancer, colon cancer, breast cancer, ovarian cancer, and melanoma [310, 311]. Also higher NQO1 amounts have been found in liver, lung, colon, and breast tumors of human patients [312]. Here we are reporting for the first time a higher expression of NQO1 in neutrophils after ischemia and reperfusion.

Glutathione reductase, (Gsr), (EC: 1.8.1.7) catalyzes the regeneration of glutathione from glutathione disulfide utilizing NADPH where Glutathione is a major antioxidant, essential for the removal of H_2O_2 from the cytosol of granulocytes and leukocytes [313, 314]. Recently, Gsr has been found to facilitate host defense by sustaining phagocytic oxidative burst and promoting the development of neutrophil extracellular traps (NET) in mice [315].

NADPH-dependent thioredoxin reductases (TrxR) 1 (EC: 1.8.1.9) is involved in denitrosylation of proteins in cytosol [316]. Thom, S.R., et al. showed recently that TrxR is also involved in cytoskeletal control in neutrophils through association with Focal Adhesion Kinase (FAK) [317].

Table 6 Predicted oxidoreductase function of cluster 5.

Acc	Gene	PD Description	Enzyme Codes
P07943	Akr1b1	Aldose reductase	EC:1.1.1.112
P07943	Akr1b1	Aldose reductase	EC:1.1.1.149
P22985	Xdh	Xanthine dehydrogenase/oxidase	EC:1.1.1.158
O70351	Hsd17b10	3-hydroxyacyl-CoA dehydrogenase type-2	EC:1.1.1.159
O70351	Hsd17b10	3-hydroxyacyl-CoA dehydrogenase type-2	EC:1.1.1.178
O70351	Hsd17b10	3-hydroxyacyl-CoA dehydrogenase type-2	EC:1.1.1.201
P07943	Akr1b1	Aldose reductase	EC:1.1.1.21
O70351	Hsd17b10	3-hydroxyacyl-CoA dehydrogenase type-2	EC:1.1.1.239
P04642	Ldha	L-lactate dehydrogenase A chain	EC:1.1.1.27
P19629	Ldhc	L-lactate dehydrogenase C chain	EC:1.1.1.27
Q811X6	Cryl1	Lambda-crystallin homolog	EC:1.1.1.35
O70351	Hsd17b10	3-hydroxyacyl-CoA dehydrogenase type-2	EC:1.1.1.35
O70351	Hsd17b10	3-hydroxyacyl-CoA dehydrogenase type-2	EC:1.1.1.36
Q99KE1	Me2	NAD-dependent malic enzyme, mitochondrial	EC:1.1.1.38
Q99KE1	Me2	NAD-dependent malic enzyme, mitochondrial	EC:1.1.1.39
P85968	Pgd	6-phosphogluconate dehydrogenase, decarboxylating	EC:1.1.1.43
P85968	Pgd	6-phosphogluconate dehydrogenase, decarboxylating	EC:1.1.1.44
O70351	Hsd17b10	3-hydroxyacyl-CoA dehydrogenase type-2	EC:1.1.1.51
O70351	Hsd17b10	3-hydroxyacyl-CoA dehydrogenase type-2	EC:1.1.1.62
P85968	Pgd	6-phosphogluconate dehydrogenase, decarboxylating	EC:1.1.1.95
Q3MID2	Cyp4f3	Leukotriene-B(4) omega-hydroxylase 2	EC:1.1.4.1
P11247	Mpo	Myeloperoxidase	EC:1.11.1.7
P49290	Epx	Eosinophil peroxidase	EC:1.11.1.7
P00406	Mtco2	Cytochrome c oxidase subunit 2	EC:1.11.1.7
Q63189	Prg2	Bone marrow proteoglycan	EC:1.11.1.7
P04041	Gpx1	Glutathione peroxidase 1	EC:1.11.1.9
Q02759	Alox15	Arachidonate 15-lipoxygenase	EC:1.13.11.33
P48999	Alox5	Arachidonate 5-lipoxygenase	EC:1.13.11.34
P00406	Mtco2	Cytochrome c oxidase subunit 2	EC:1.13.11
P48999	Alox5	Arachidonate 5-lipoxygenase	EC:1.13.11.34
Q02759	Alox15	Arachidonate 15-lipoxygenase	EC:1.13.11.33
Q02759	Alox15	Arachidonate 15-lipoxygenase	EC:1.13.11.33
P48999	Alox5	Arachidonate 5-lipoxygenase	EC:1.13.11.34
Q02759	Alox15	Arachidonate 15-lipoxygenase	EC:1.13.11.33
P48999	Alox5	Arachidonate 5-lipoxygenase	EC:1.13.11.34
P48999	Alox5	Arachidonate 5-lipoxygenase	EC:1.13.11.34
Q02759	Alox15	Arachidonate 15-lipoxygenase	EC:1.13.11.33
P00388	Por	NADPH--cytochrome P450 reductase	EC:1.14.12.17
Q99MS7	Ehbp1l1	EH domain-binding protein 1-like protein 1	EC:1.14.13
Q3MID2	Cyp4f3	Leukotriene-B(4) omega-hydroxylase 2	EC:1.14.13
P00388	Por	NADPH--cytochrome P450 reductase	EC:1.14.13
Q3MID2	Cyp4f3	Leukotriene-B(4) omega-hydroxylase 2	EC:1.14.13.30
Q3MID2	Cyp4f3	Leukotriene-B(4) omega-hydroxylase 2	EC:1.14.14.1
Q3MID2	Cyp4f3	Leukotriene-B(4) omega-hydroxylase 2	EC:1.14.15.3
P00406	Mtco2	Cytochrome c oxidase subunit 2	EC:1.14.99.1
P05982	Nqo1	NAD(P)H dehydrogenase 1	EC:1.15.1.1
Q4V8K1	Steap4	Metalloreductase STEAP4	EC:1.16.1

Continue Table 6 Predicted oxidoreductase function of cluster 5.

Q4V8K1	Steap4	Metalloreductase STEAP4	EC:1.16.1.7
Q4V8K1	Steap4	Metalloreductase STEAP4	EC:1.16.1.9
P09528	Fth1	Ferritin heavy chain	EC:1.16.3.1
P22985	Xdh	Xanthine dehydrogenase/oxidase	EC:1.17.1.4
P22985	Xdh	Xanthine dehydrogenase/oxidase	EC:1.17.3.2
P07943	Akr1b1	Aldose reductase	EC:1.2
P11884	Aldh2	Aldehyde dehydrogenase, mitochondrial	EC:1.2.1
Q4KYY3	GAPDH	Glyceraldehyde-3-phosphate dehydrogenase	EC:1.2.1.12
Q9Z2I8	Suclg2	Succinyl-CoA ligase subunit beta, mitochondrial	EC:1.2.1.24
P11884	Aldh2	Aldehyde dehydrogenase, mitochondrial	EC:1.2.1.3
P11884	Aldh2	Aldehyde dehydrogenase, mitochondrial	EC:1.2.1.36
P07943	Akr1b1	Aldose reductase	EC:1.2.1.36
Q5XI42	Aldh3b1	Aldehyde dehydrogenase family 3 member B1	EC:1.2.1.5
P11884	Aldh2	Aldehyde dehydrogenase, mitochondrial	EC:1.2.1.5
O08984	Lbr	Lamin-B receptor	EC:1.3.1.70
P11348	Qdpr	Dihydropteridine reductase	EC:1.5.1.34
Q63189	Prg2	Bone marrow proteoglycan	EC:1.5.5.1
P00388	Por	NADPH--cytochrome P450 reductase	EC:1.6.2.2
P05982	Nqo1	NAD(P)H dehydrogenase [quinone] 1	EC:1.6.2.2
P00388	Por	NADPH--cytochrome P450 reductase	EC:1.6.2.4
O70145	Ncf2	Neutrophil cytosol factor 2	EC:1.6.3
P05982	Nqo1	NAD(P)H dehydrogenase [quinone] 1	EC:1.6.5.10
P05982	Nqo1	NAD(P)H dehydrogenase [quinone] 1	EC:1.6.5.2
Q9DCZ1	Gmpr	GMP reductase 1	EC:1.7.1.7
P70619	Gsr	Glutathione reductase (Fragment)	EC:1.8.1.7
P47791	Gsr	Glutathione reductase, mitochondrial	EC:1.8.1.7
O89049	Txnrd1	Thioredoxin reductase 1, cytoplasmic	EC:1.8.1.9
Q9ESH6	Glrx	Glutaredoxin-1	EC:1.8.4.2
P00406	Mtco2	Cytochrome c oxidase subunit 2	EC:1.9.3.1
P00388	Por	NADPH--cytochrome P450 reductase	EC:1.9.99.1
P32577	Csk	Tyrosine-protein kinase CSK	EC:1.97.1
P09528	Fth1	Ferritin heavy chain	EC:1.97.1

5.7 KEGG Pathway Analysis of Rat Neutrophil Proteome

The Kyoto Encyclopedia of Genes and Genomes (KEGG) is used as a reference knowledge base for understanding signal transduction, cellular process and biological pathways [318]. Uniprot accession numbers were mapped to gene symbols by protein center. Gene symbols from all the differentially abundant proteins from the five clusters were mapped with the genome from KEEG pathways using the online databases WebGestalt and enrichnet [197, 198]. Most of the pathways showed significant results in different clusters so we analyzed and discussed those common pathways together. The reason for the presence of these pathways in different set of clusters is that as most of the databases including WebGestalt and enrichnet use Gene symbols instead of UniProt Accessions that resulted into assignment of different proteins to same genes that lead to duplication of genes. If we removed these duplicate genes from all the five clusters then almost 200 genes would be deleted along with a decrease in the level of significance and overlapping genes with not much change in pathway assignment. So we removed the duplicates from pathways of interest rather than to remove from all the clusters. In table. 7, overlap genes are genes in the uploaded gene set and also found in the reference genes in the category. Ratio is the ratio of enrichment; raw P-value is the P value from hypergeometric test and p value adjusted by multiple test adjustment.

Table 7 Predicted KEGG pathways for all clusters.

PathwayName	Overlap Gene	Cluster No.	Reference Genes	Ratio	Raw P-value	Adjusted P-value
Ribosome	57	1	122	44.41	8.98E-80	1.11E-77
Spliceosome	28	1	135	19.72	4.74E-28	2.94E-26
Metabolic pathways	49	1	1169	3.98	3.16E-16	1.31E-14
Protein processing in endoplasmic reticulum	20	1	164	11.59	1.12E-15	3.47E-14
RNA transport	19	1	156	11.58	5.96E-15	1.48E-13
Phagosome	18	1	185	9.25	1.54E-12	3.18E-11
Proteasome	10	1	49	19.4	8.60E-11	1.52E-09
Neurotrophin signaling pathway	12	1	129	8.84	1.38E-08	2.14E-07
Focal adhesion	13	1	186	6.64	1.05E-07	1.45E-06
Lysosome	10	1	124	7.67	8.46E-07	9.54E-06
Regulation of actin cytoskeleton	24	2	208	11.53	1.78E-18	2.06E-16
Fc gamma R-mediated phagocytosis	17	2	91	18.67	4.37E-17	2.53E-15
Neurotrophin signaling pathway	18	2	129	13.94	1.15E-15	4.45E-14
Oocyte meiosis	17	2	115	14.77	2.67E-15	6.19E-14
Leukocyte transendothelial migration	17	2	114	14.9	2.29E-15	6.19E-14
Protein processing in endoplasmic reticulum	19	2	164	11.58	6.17E-15	1.19E-13
Long-term potentiation	14	2	69	20.27	7.74E-15	1.28E-13
Chemokine signaling pathway	18	2	178	10.1	3.45E-13	5.00E-12
Metabolic pathways	42	2	1169	3.59	1.38E-12	1.78E-11
Cell cycle	15	2	124	12.09	2.37E-12	2.75E-11
Metabolic pathways	109	3	1169	6.5	2.28E-55	3.58E-53
Spliceosome	36	3	135	18.59	3.41E-35	2.68E-33
Huntington's disease	41	3	218	13.11	2.87E-33	1.50E-31
Parkinson's disease	34	3	164	14.45	2.71E-29	1.06E-27
Oxidative phosphorylation	30	3	156	13.41	5.65E-25	1.77E-23
Proteasome	20	3	49	28.45	1.95E-24	5.10E-23
Citrate cycle (TCA cycle)	17	3	30	39.5	3.77E-24	8.46E-23
Alzheimer's disease	31	3	212	10.19	4.95E-22	9.71E-21
Protein processing in endoplasmic reticulum	26	3	164	11.05	1.34E-19	2.34E-18
Lysosome	22	3	124	12.37	7.00E-18	1.10E-16
Neurotrophin signaling pathway	22	4	129	21.85	3.75E-23	4.57E-21
Regulation of actin cytoskeleton	25	4	208	15.4	3.06E-22	1.87E-20
Long-term potentiation	16	4	69	29.71	1.77E-19	7.20E-18
Oocyte meiosis	17	4	115	18.94	4.39E-17	1.34E-15
Insulin signaling pathway	17	4	131	16.62	4.21E-16	1.03E-14
Metabolic pathways	41	4	1169	4.49	1.40E-15	2.85E-14
Fc gamma R-mediated phagocytosis	12	4	91	16.89	7.71E-12	1.18E-10
Leukocyte transendothelial migration	13	4	114	14.61	6.83E-12	1.18E-10
Chemokine signaling pathway	15	4	178	10.8	1.36E-11	1.84E-10
Glioma	10	4	62	20.66	5.55E-11	6.41E-10
Metabolic pathways	51	5	1169	4.77	3.39E-20	4.24E-18
Vasopressin-regulated water reabsorption	11	5	44	27.35	1.91E-13	1.19E-11
Chemokine signaling pathway	16	5	178	9.83	1.12E-11	4.67E-10
Systemic lupus erythematosus	14	5	132	11.6	2.35E-11	7.34E-10
Fc gamma R-mediated phagocytosis	12	5	91	14.43	4.77E-11	1.19E-09
Endocytosis	16	5	230	7.61	5.16E-10	1.08E-08
Regulation of actin cytoskeleton	15	5	208	7.89	1.09E-09	1.95E-08
Glycolysis / Gluconeogenesis	10	5	78	14.03	2.64E-09	4.03E-08
Neurotrophin signaling pathway	12	5	129	10.18	2.90E-09	4.03E-08
Oocyte meiosis	11	5	115	10.46	9.90E-09	1.24E-07

5.7.1 Ribosomal Pathway:

From table 6 it is clear that the most significant and important pathway encountered from WebGestalt database is the ribosomal pathway with an adjusted *P-value* of 1.11e-77 and 57 overlapping proteins from our dataset that are present in the pathway (Fig. 36, 37).

Ribosomal proteins are fundamental components in the cellular metabolism and ribosome synthesis is critical for cell growth and development. The ribosomal (r-) proteins are responsible for the correct folding and cleavage of rRNA as well as for subunit assembly [1]. The eukaryotic ribosome consist of two subunits a large (60S) and a small (40S) subunit. The large subunit contains three RNAs and 46 proteins and the small subunit is composed of one RNA and 33 proteins. Ribosomal proteins have some extra ribosomal activities including catalytic functions replication, transcription, RNA processing, DNA repair, and even inflammation (in monocytes) but these functions for each ribosomal protein are not yet clear [319-321]. During normal conditions, equal amounts of rRNA and ribosomal proteins are synthesized in a cell while altered conditions also alter the levels of ribosomal proteins synthesis [322]. As during neuronal differentiation of human embryonic carcinoma cells, proteins of the large subunit such as L3, L7, L8, L10, L23a, L27a, L36a, and L39 showed decreased expression exhibited a constant down regulation, along with some proteins from small subunit (S2, S3, S3a, S4X, S6, S9, S12, S13, S16, S19, S20, S23, and S27a).

Whereas a L11, L32, S8, and S11 were constant initially or up regulated and then down regulated later like L6, L15, L17, L31, and S27y [323]. This independent alteration in ribosomal protein synthesis suggests that these proteins have some roles other than protein synthesis. For example, P0 and S3 have shown endonuclease activity so might have role in DNA repair [324, 325] and L7 can also act as co-regulator of the vitamin D receptor [326]. L7 in Jurkat T-lymphoma cells [327] , S20 in the human leukemic cell line CEM C7 [328], and S3a in tumor cell [329] have a role in apoptosis.

RP S19 oligomers act as chemoattractant for migrating monocytes/macrophages to apoptotic cells via the C5aR [330]. RP S19 oligomers have dual role on the C5aR of phagocytic leucocytes; it induces an agonist-induced effect on the monocyte C5aR but an antagonist-induced effect on the neutrophil C5aR [331]. C5a causes chemotactic

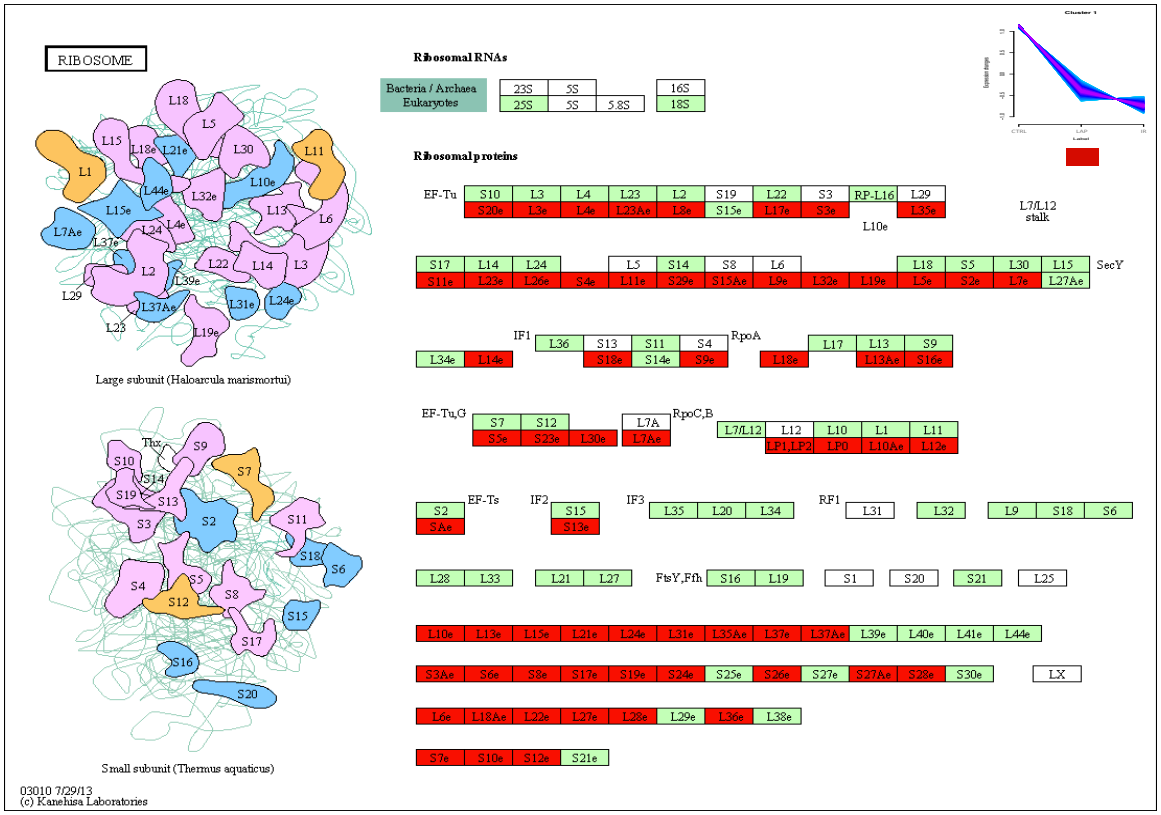

Figure 36 The enriched ribosome pathway of the differentially abundant proteins (DAPs) from cluster 1. The down-regulated overlapped proteins are highlighted in red.

migration and secretion via the C5aR-mediated classical ERK1/2 pathway. RP S19 oligomers inhibit neutrophil C5aR mediated chemotactic pathways however the mechanism is not known [332, 333]. Here we are reporting for the first time the down regulation of 57 ribosomal proteins in neutrophils after laparotomy and intestinal ischemia/reperfusion (Figure 36). RPS19 is also among the down-regulated proteins, which may be involved in the up regulation of C5aR mediated chemotaxis in neutrophil after IR.

Overall connectivity of identified proteins in cluster 1 was determined using the online database STRING. For more conformation about the interaction we have also analyzed these ribosomal proteins in STRING and results (Fig.38) showed highly strong connection between these proteins.

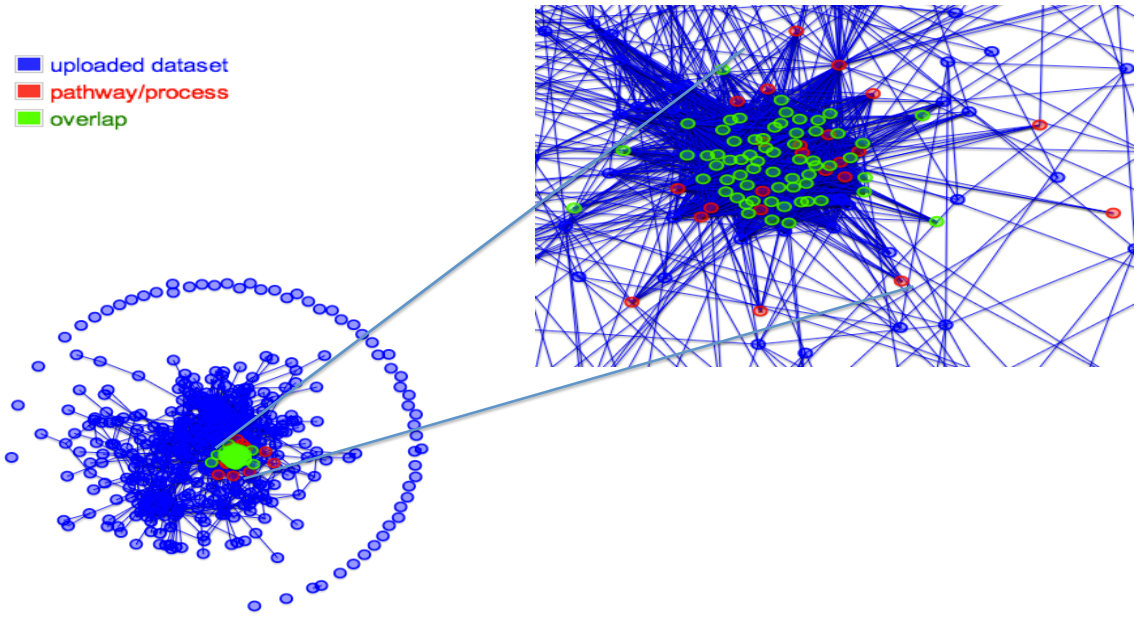

Figure 37 Computer graph visualization of the enrichnet of the dataset from cluster 1 overlap (green) is shown for the regulation of the ribosomal pathway.

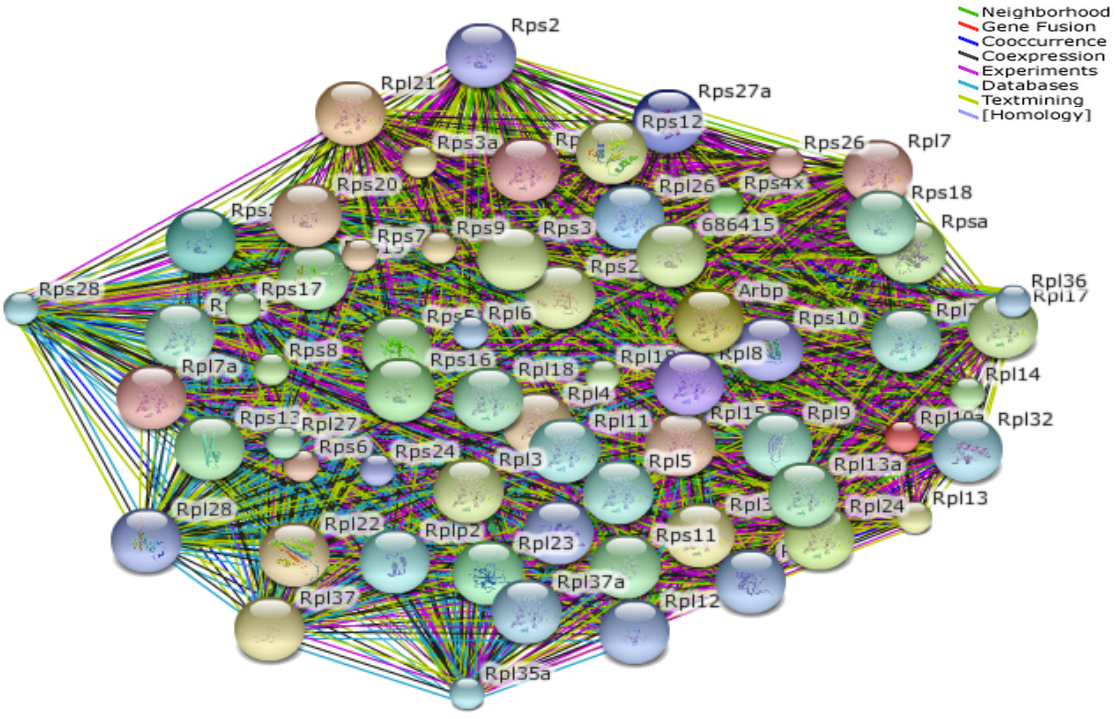

Figure 38 Interaction network of proteins from cluster 1 identified in ribosomal KEGG pathway.

5.7.2 Regulation of Actin Cytoskeleton Pathway

Regulation of Actin Cytoskeleton Pathway shows common proteins from cluster 2, 4 and 5 with *P-values,* P=2.06e-16 and 24 overlapping protein, P=1.87e-20 and 25 overlapping proteins and P=1.95e-08 with 15 overlapping proteins respectively. The *P-values* of this pathway for each cluster are significant so we did a comparison of all three clusters with different colors for each cluster as shown in fig.39. Most of the proteins are up regulated (Gold and Yellow) and some are down regulated (red) in this pathway.

Normal circulating neutrophils are non-polarized. Once a chemoattractant binds to its cell-surface receptor, activation of the cytoskeletal machinery takes place after cytoplasmic signal transductions leading to formation of lamellar filamentous actin or F-actin (front) and the uropod rich in actomyosin filaments (back) (polarization). Neutrophils can align their front-back polarity with the chemoattractant gradient and start directional migration [334]. Studies have shown association between PI-3 kinase activity and activation of a family of small GTP-binding proteins, Ras and of a Ras subfamily including Rho, Rac, and CDC-42 which are important regulators of motility and cell shape [335]. The Arp2/3 complex localizes to regions of active actin polymerization in neutrophils and is involved in multiple pathways from signal to actin assembly [336]. Regulation of Actin Cytoskeleton Pathway analysis of our data showed that most of these proteins including Rho, Rac, Rac, ARP2/3 among others are present in the data. They are up regulated in neutrophils during IR as compared to control leading to enhanced motility, locomotion and chemotaxis (Fig.39).

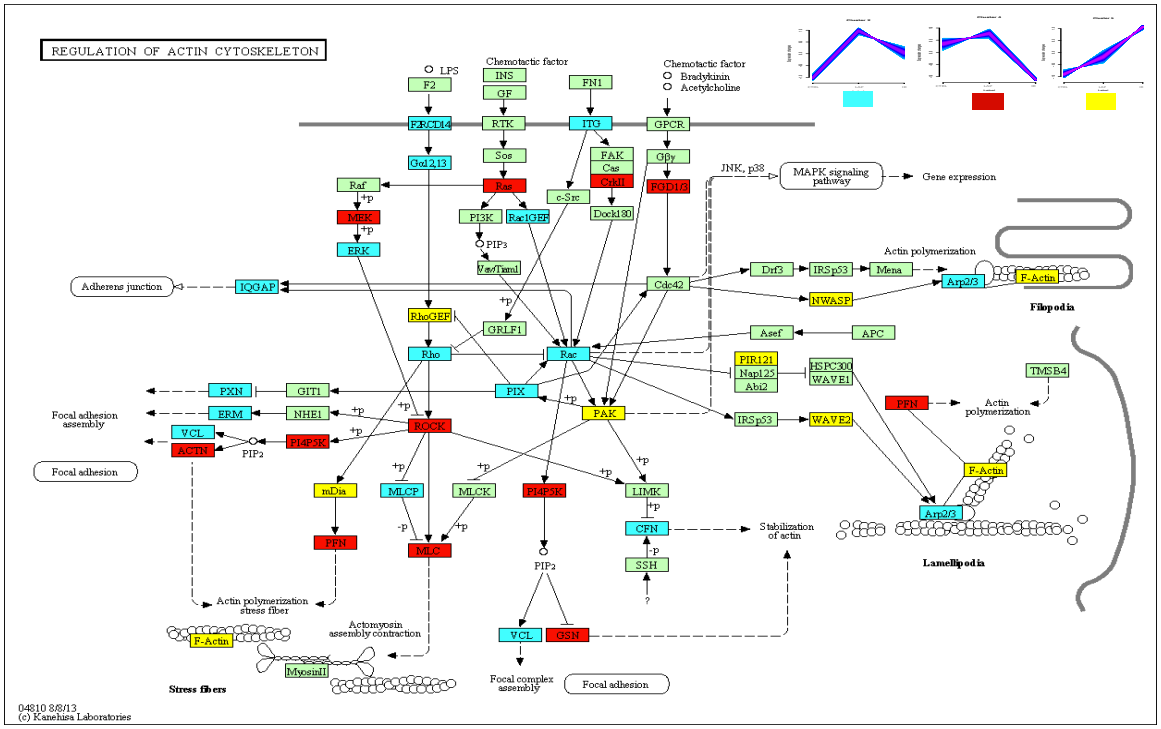

Figure 39 The enriched regulation of actin cytoskeleton pathway of the differentially abundant proteins (DAPs) from clusters 2, 4 and 5. Cyan (cluster 2) and yellow (cluster 5) show up regulation, red (cluster 4) down regulation and green not found in our dataset.

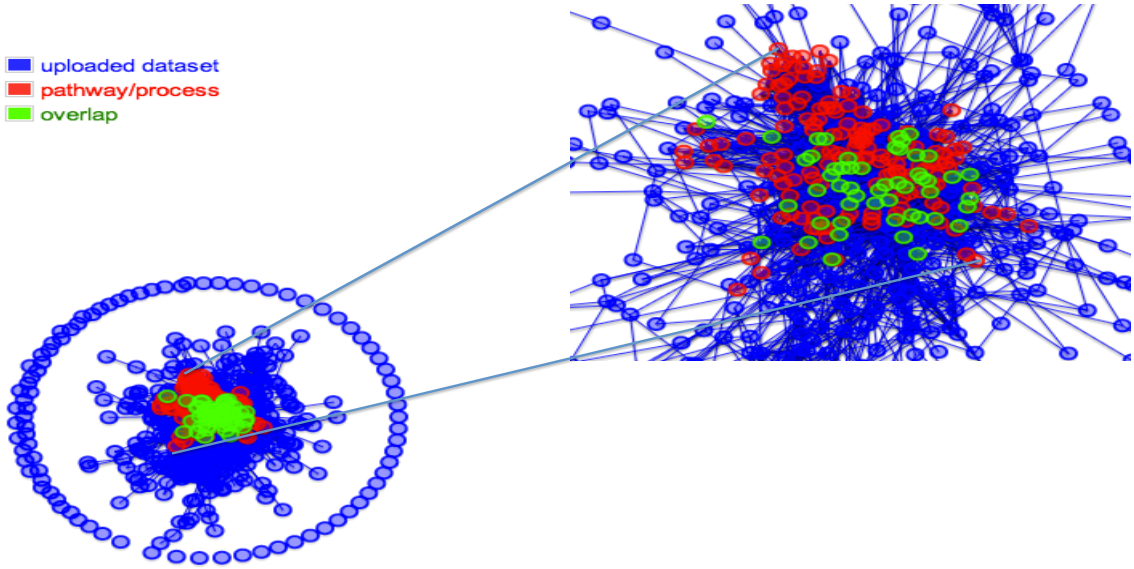

Figure 40 Computer graph visualization from enrichnet.org of uploaded dataset for clusters 2, 4 and 5 overlap (green) is shown for regulation of actin cytoskeleton pathway.

Computer graph visualization from enrichnet.org of uploaded dataset from cluster 2, 4 and 5, overlap is shown for regulation of actin cytoskeleton pathway in fig.40. Overlapping genes are shown in green. For the overlapping proteins, a STRING based protein-protein interaction analysis was performed to find out the interactions among the proteins (Fig. 41).

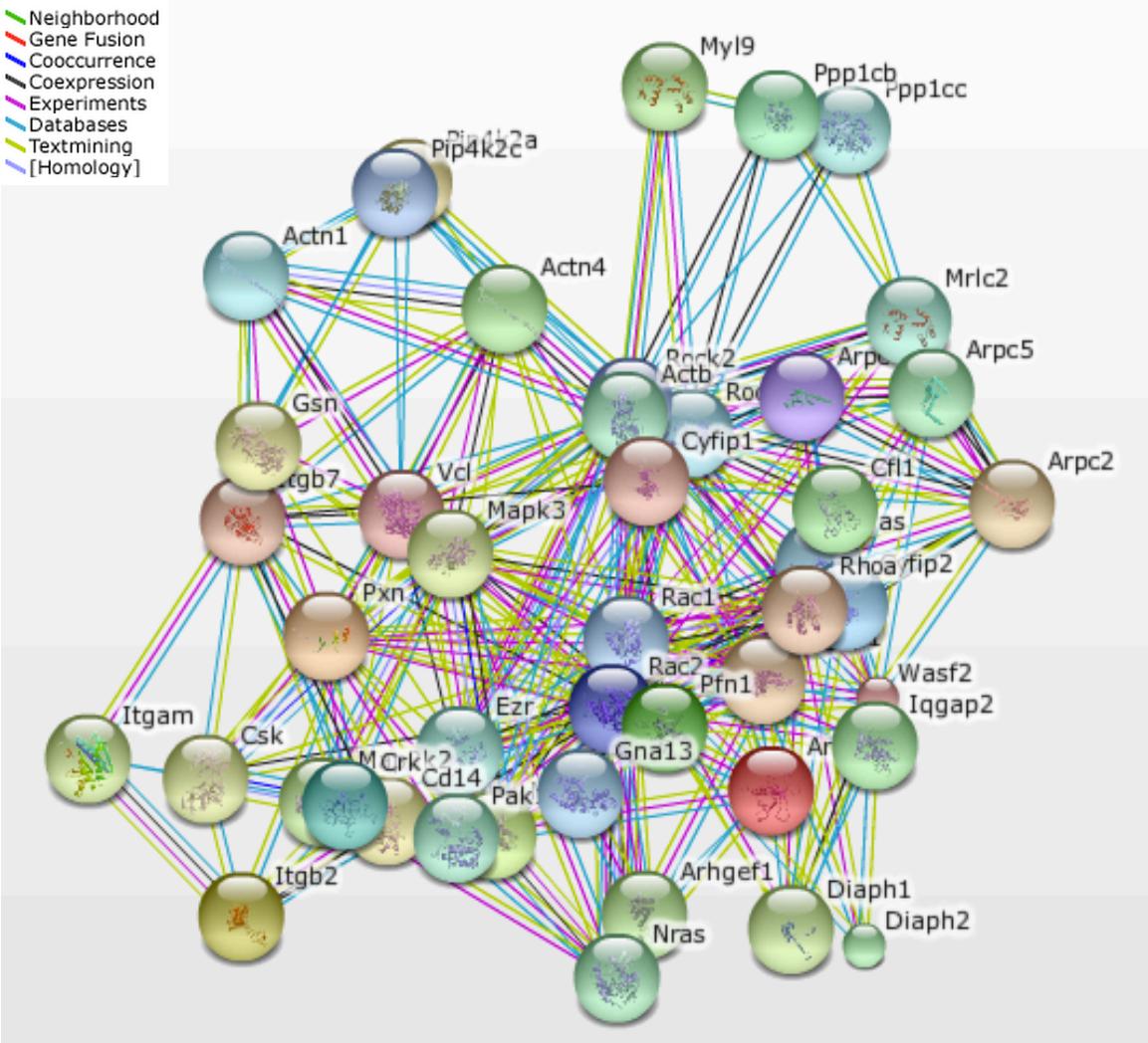

Figure 41 Interaction network of proteins from cluster 2, 4 and 5 identified in regulation of actin cytoskeleton KEGG pathway.

Figure 41 obtained from STRING for the protein-protein interactions of the 46 proteins encountered during Actin cytoskeleton regulation pathway shows highly interconnected sub-networks.

5.7.3 Fc gamma R-mediated phagocytosis pathway:

Table 7 shows that the other interesting pathway predicted by WebGestalt is Fc gamma R-mediated phagocytosis pathway with *P-value* P=2.53e-15 and 17 overlapping proteins, P=1.18e-10 and 12 overlapping proteins and P=1.19e-09 with 12 overlapping proteins from clusters 2, 4 and 5 respectively fig. 42. The up regulated proteins include Src, Syk, SPHK, WASP, PLC, ERK1/2, c PKC, p47phox, Arp2/3, Rac, PAG3, PAK1, WASP, WAVE and cofilin (yellow and golden) and few down regulated proteins such as PKC, gelsolin, VASP, CrkII (red). Computer graph visualization from enrichnet of uploaded dataset from these clusters shows overlapping proteins (green) for Fc gamma R-mediated phagocytosis pathway in fig. 38. Blue are the total uploaded proteins dataset from clusters and red are the non-overlapping proteins of this pathway.

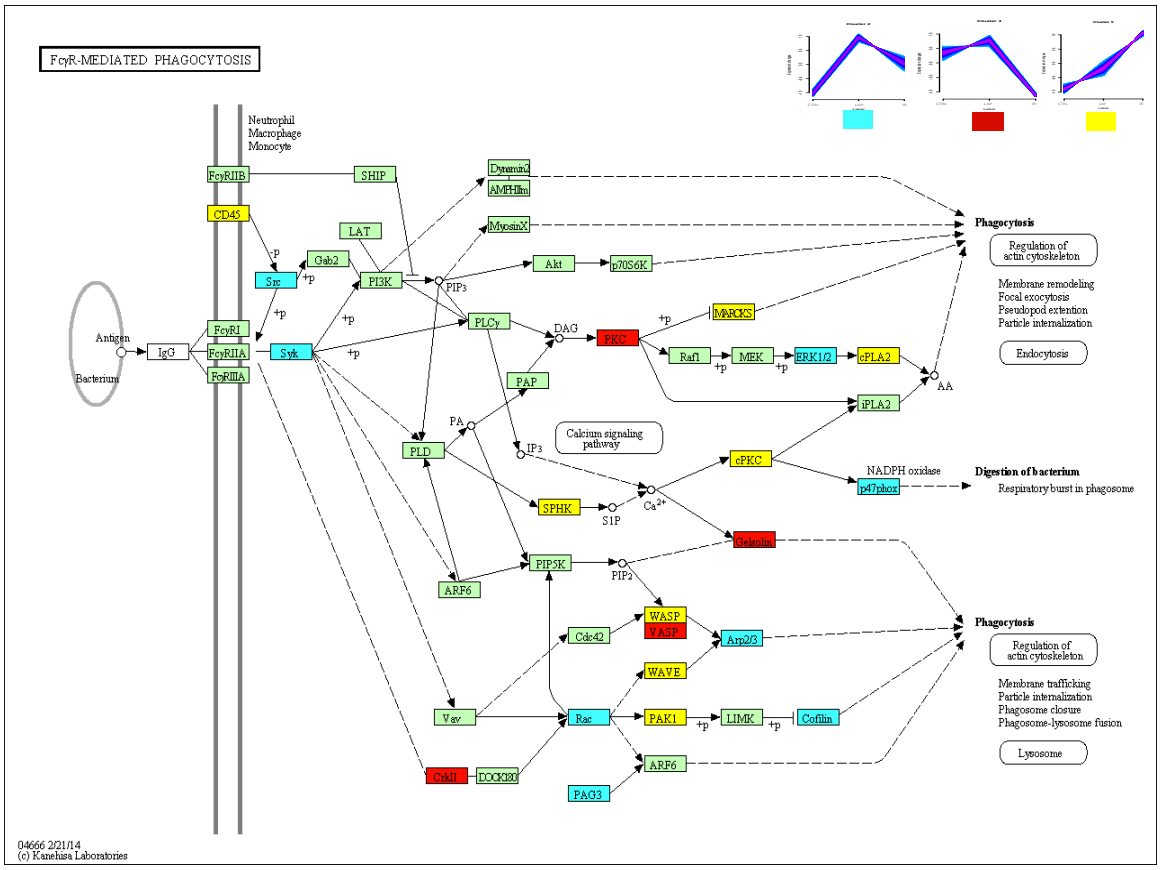

Figure 42 The enriched Fc gamma R-mediated phagocytosis pathway for the differentially expressed proteins (DEPs) from cluster 2, 4 and 5. Cyan (cluster 2) and yellow (cluster 5) are up regulated and red (cluster 4) down regulated.

As a result of Interaction of FcR with their Ig ligands in leukocyte initiates a number of responses including phagocytosis, antibody-dependent cell-mediated cytotoxicity (ADCC), release of pro-inflammatory mediators and cytokines production [337, 338]. Phosphorylation of specific tyrosine residues within immunoreceptor tyrosine-based activation motifs (ITAMs) takes place after receptor and ligand clustering [339] and Src tyrosine-kinase family enzymes are involved in initial ITAM phosphorylation [340]. Syk is a tyrosine kinase, very important player of this pathway as in neutrophils, its inhibition repel phagocytosis of IgG coated particles [341]. But the exact role of Syk in this process remains unclear. Some studies show its role in the formation of the actin filament cup during FcRγ-mediated phagocytosis [341, 342].

PLCγ (phospholipase) produces IP3 and diacylglycerol (DAG) from PI-4, 5 bisphosphate [PI(4,5)P2]. This leads to IP3, that mediates calcium release and DAG dependent activation of several PKC isoforms. Inhibition of PLCγ resulted into impaired phagocytosis in macrophages and PLCγ havs been found accumulated at the phagocytic cup [343].

ERK activation occurs after translocation of PKC and Raf-1 to the plasma membrane [344]. Raf-1 then activates MAPK kinase (MEK), and MEK activation directly leads to ERK activation which mediates activation of nuclear factors, such as Elk and nuclear factor-B, important for cytokine production [345]. Rac is also important participant in this process as its inhibition in macrophages leads to complete inhibition of actin assembly and internalization of IgG coated particles [346].

PAG3 (GTPase activating protein for ARF6) have been found accumulated with ARF6 and F-actin at phagocytic cups [347]. Cofilin and gelsolin are of the several actin-binding molecules taking part in this phagocytosis through regulation of actin dynamics by various mechanisms [348]. Arp2/3 complex was also found accumulated in phagosomes and is required for particle ingestion by receptor [349]. Wiskott-Aldrich syndrome protein (WASP) binds directly to Cdc42 and Rac in a GTP-dependent manner [350] and is actively recruited to the phagocytic cup during IgG mediated phagocytosis (Fig. 42) [351].

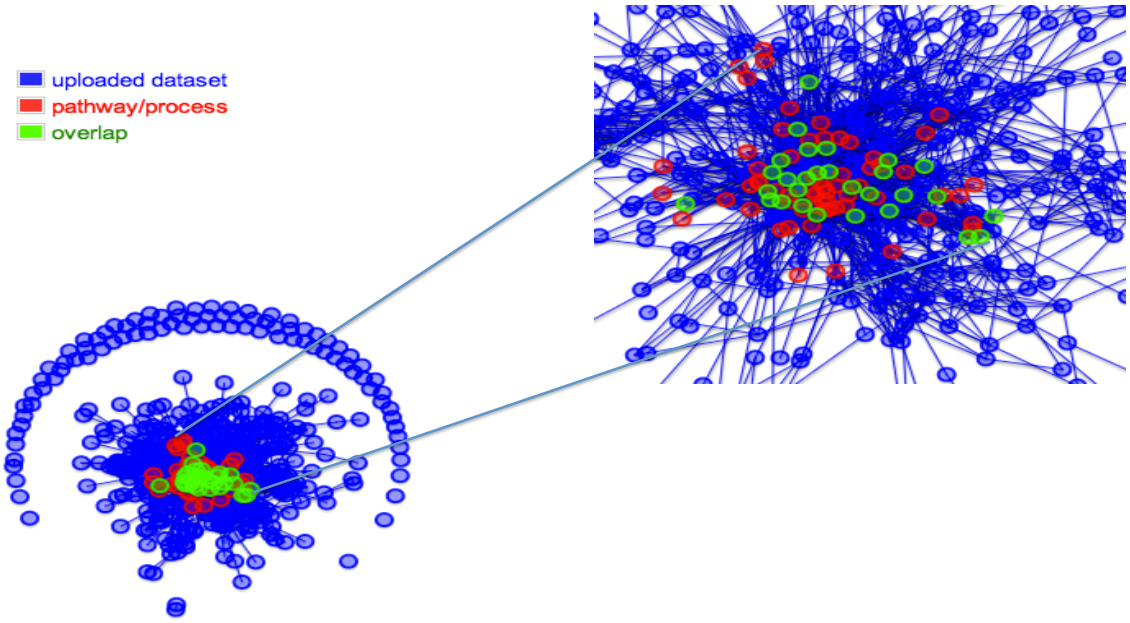

Figure 43 Computer graph visualization from enrichnet of uploaded dataset from cluster 2, 4 and 5 overlap (green) is shown for Fc gamma R-mediated phagocytosis pathway.

Proteins encountered in Fc gamma R-mediated phagocytosis pathway were analyzed by STRING for protein-protein interactions, which show strong binding interactions fig. 44.

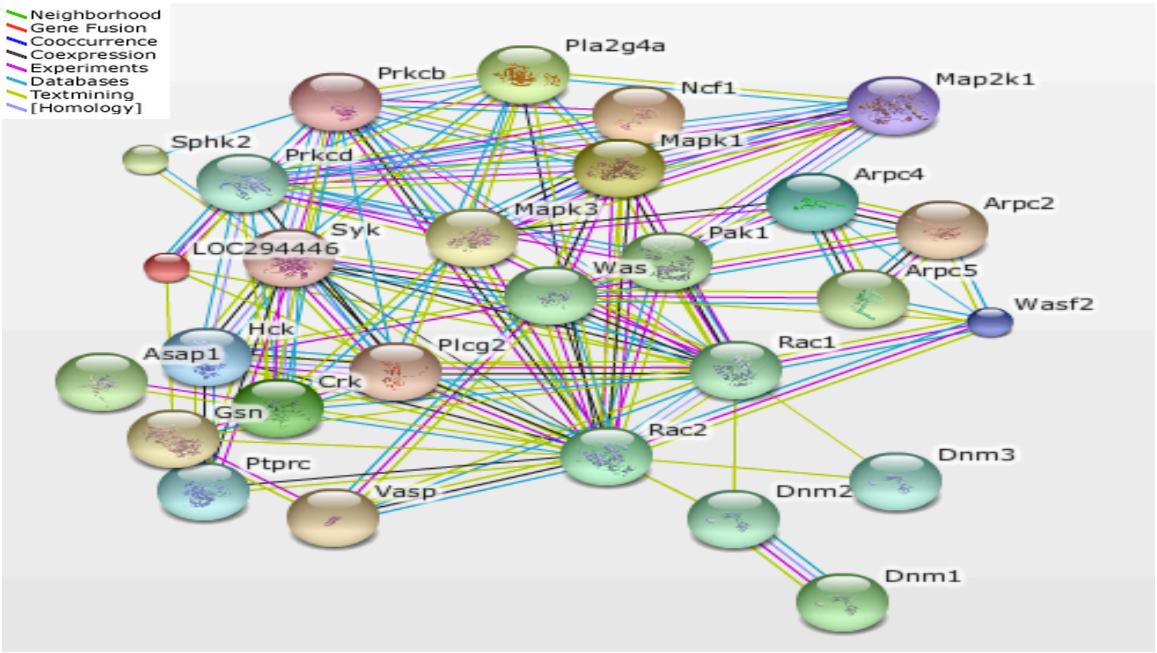

Figure 44 STRING network analysis of proteins from Fc gamma R-mediated phagocytosis pathway from cluster 2, 4 and 5.

5.7.4 Chemokine Signaling Pathway:

The next common, significant, interesting and relevant pathway present in the table 7 is the chemokine signaling pathway. The *P-values* and overlapping proteins for cluster 2, 4 and 5 are P=5.00e-12 and 18, P=1.84e-10 and 15, and 4.67e-10 and 16 respectively. The up regulated (yellow and golden) and down regulated proteins (red) from this pathway are shown in Fig. 45.

Neutrophils migrate toward the source of chemoattractants like formylated peptides, C5a, leukotriene B4, and chemokines such as IL-8 [352] and after binding to its surface receptor, a number of cytoplasmic events occurs which activates the cytoskeletal machinery [353]. Ligand binding results in conformational change in the receptor resulting in the exchange of GDP to GTP on the alpha subunit. This induces the release of the α subunit from the βγ subunit pair [354]. The α and βγ subunits are then free to interact with downstream effectors [355]. Rac GTPases regulate different functions in neutrophils including cytoskeletal structure, gene expression, and reactive oxygen species (ROS) production [356, 357]. P-Rex1, a guanine-nucleotide exchange factor (GEF) for Rac [358] is supposed to link GPCRs and PI3Kγ to Rac-dependent neutrophil responses. Another study proved the involvement of P-Rex1 in GPCR-dependent Rac2 activation and ROS formation in neutrophils, as well as neutrophil recruitment to inflammatory sites and chemotaxis, but not in degranulation [359]. P21-activated kinases (PAKs) are serine/threonine kinases which have been identified as targets of Rac and Cdc42 and affect actin cytoskeleton [360]. Both G-protein-coupled chemoattractant receptors and Fc receptors regulate PAK activity in human leukocytes [361]. PAK1 has been also co-localized with polymerized actin in the leading lamellae and phagocytic cups of stimulated human neutrophils, consistent with a role for PAK in modulating leukocyte responsiveness to physiological stimuli [362]. Paxillin localizes in cultured cells primarily to sites of focal adhesions, which are structural links between the extra cellular matrix (ECM) and actin cytoskeleton and are also important sites of signal transduction. Importantly, focal adhesion proteins including paxillin also serve as a point of convergence for signals resulting from stimulation of various classes of growth factor receptor [363]. Computer graph visualization (Fig. 46) was performed to see the overlap proteins of uploaded dataset and the pathway dataset. The STRING analysis of the

overlapped dataset was analyzed for the protein-protein interactions that showed very good interactions (Fig. 47).

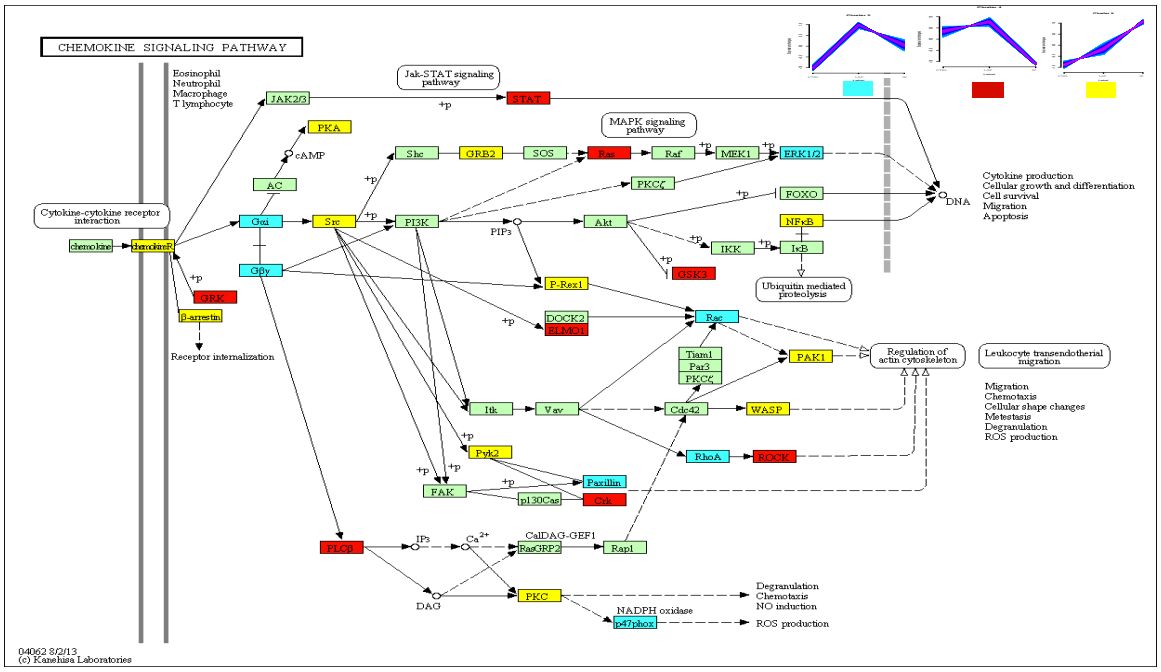

Figure 45 The enriched chemokine-signaling pathway of the differentially expressed proteins (DEPs) from cluster 2, 4 and 5. Cyan- (cluster 2) and yellow (cluster 5) are up regulated and red (cluster 4) down regulated.

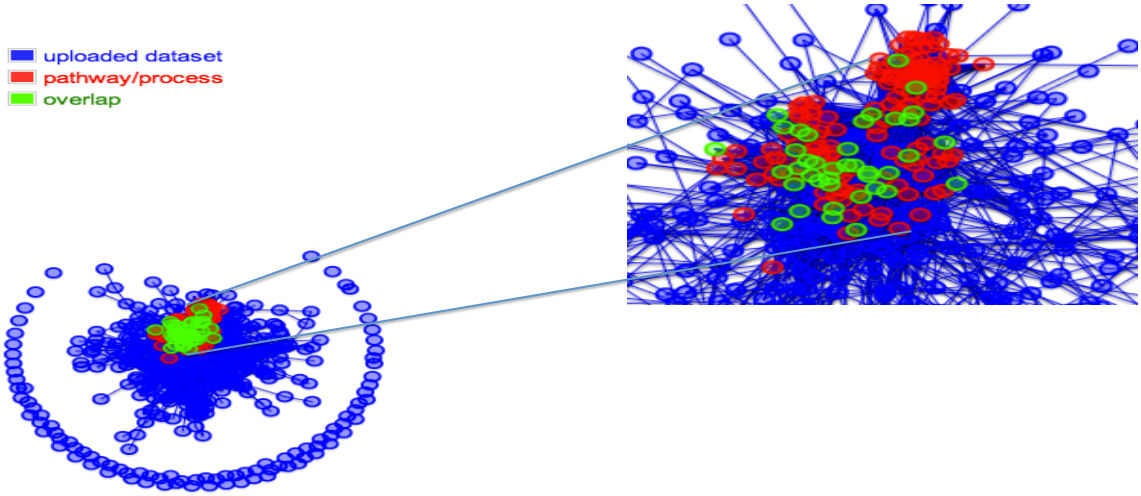

Figure 46 Computer graph visualization from enrichnet of uploaded dataset from cluster 2, 4 and 5 and overlapping genes in green for chemokine signaling pathway.

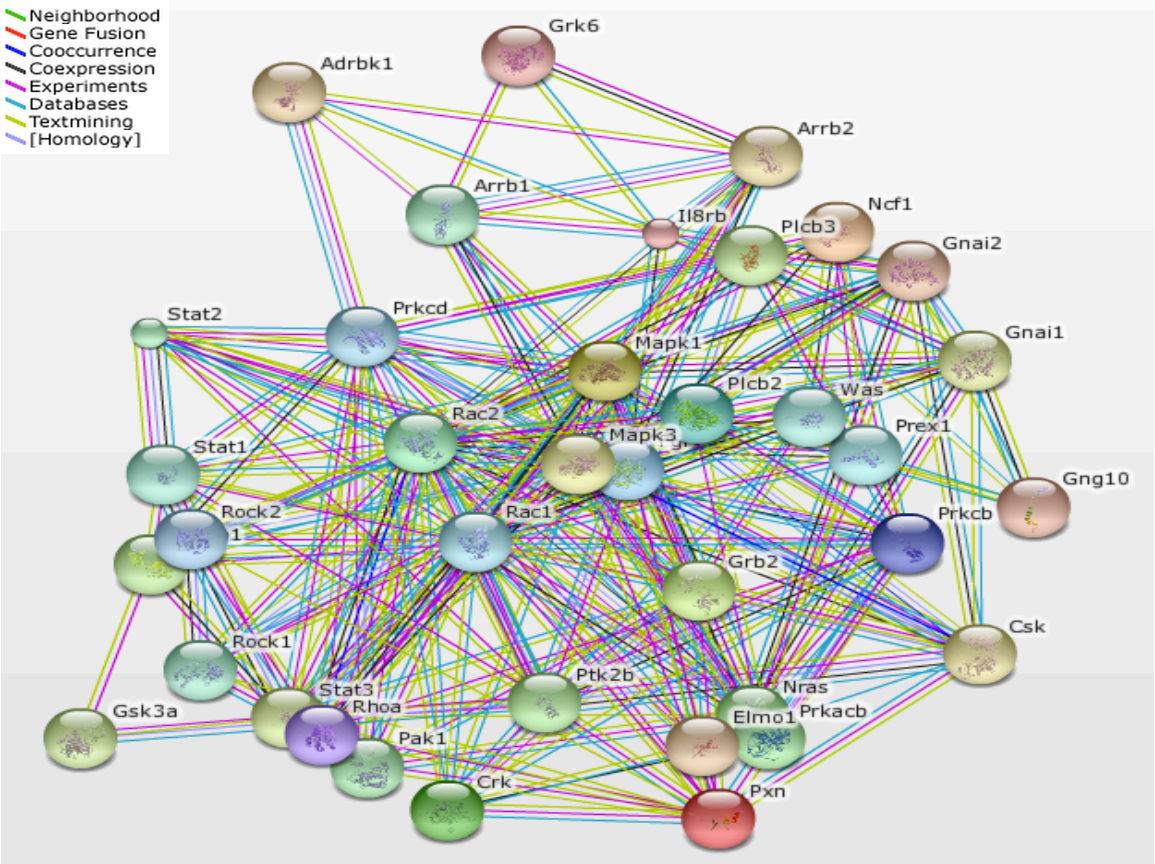

Figure 47 STRING network for proteins from Fc gamma R-mediated phagocytosis pathway from cluster 2, 4 and 5.

5.7.5 Pathways from Cluster 3

The most significant group of pathways encountered in cluster 3 comprehends metabolic pathways in neutrophil with *P-value* P=3.58e-53 and 109 overlapping proteins. Computer graph visualization from enrichnet of uploaded dataset from cluster 3 and overlapping proteins (green) from metabolic pathways is shown in fig. 48. These proteins belong to energy metabolism, carbohydrates and lipid metabolism, also including nucleotide and amino acid metabolism and secondary metabolism. STRING analysis showed high interactions among the proteins from such metabolic pathways Fig. 49.

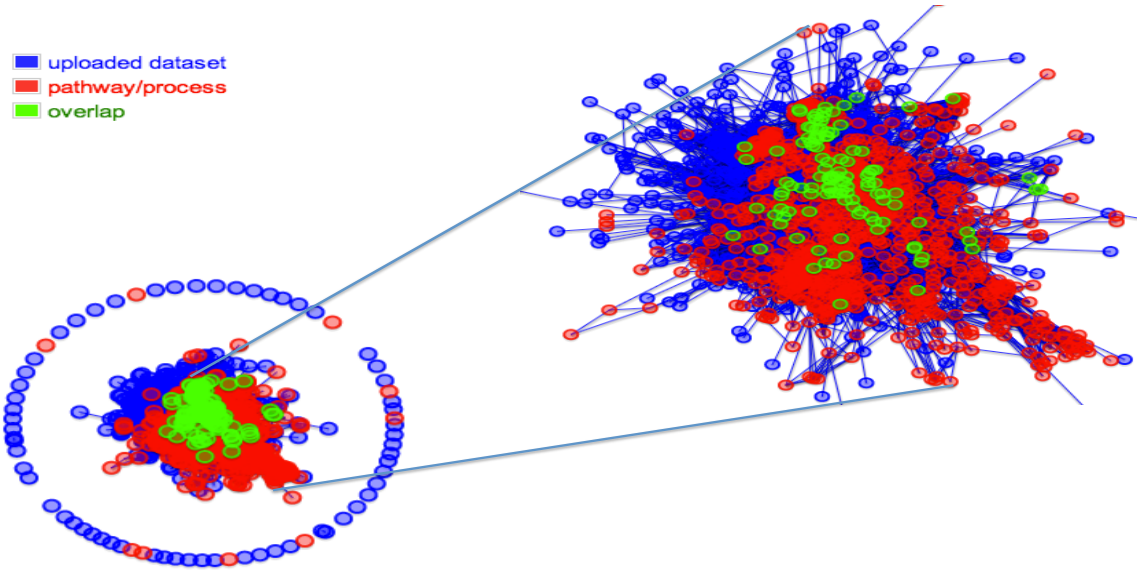

Figure 48 Computer graph visualization from enrichnet of uploaded dataset from cluster 3.

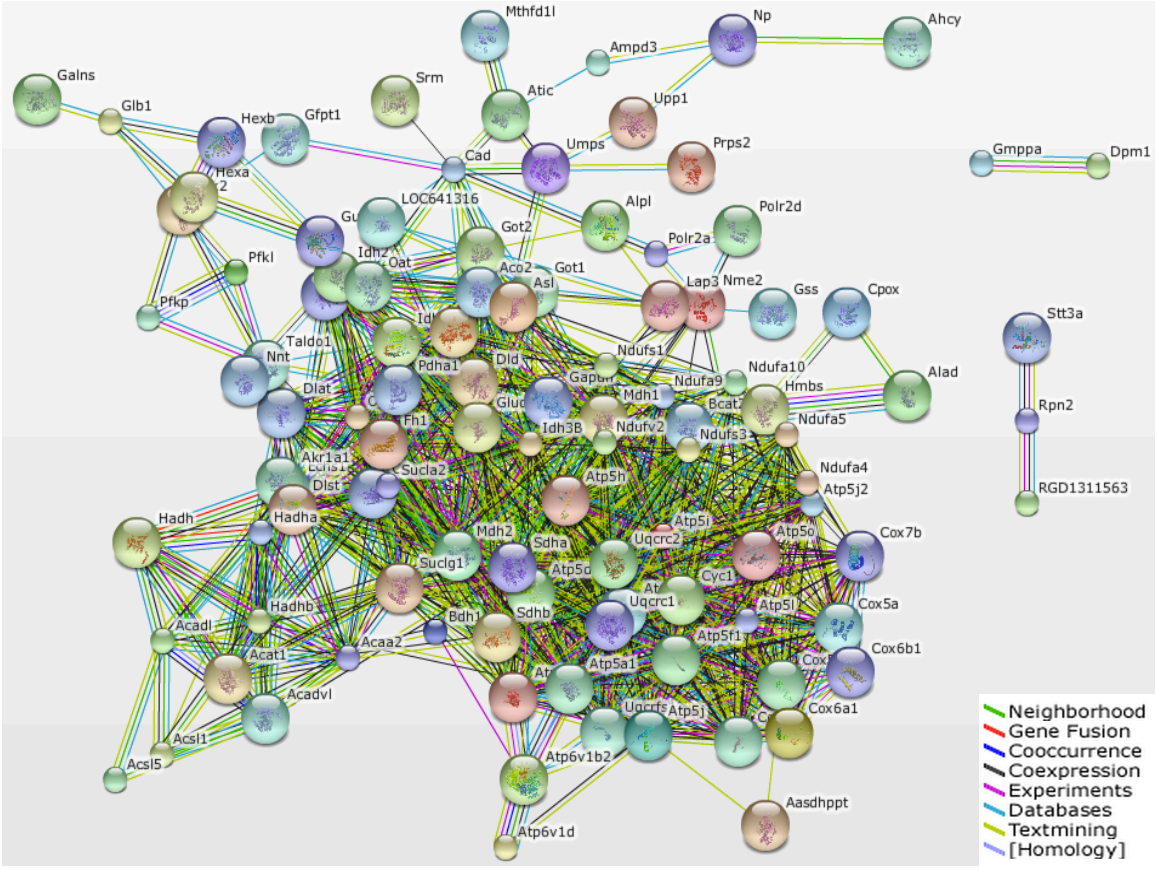

Figure 49 STRING network analysis of proteins from metabolic pathways from cluster 3.

Other significant and important pathway predicted for the cluster 3 proteins is the oxidative phosphorylation having *P-value* P=1.77e-23 with 30 overlapping proteins as shown in fig. 50.

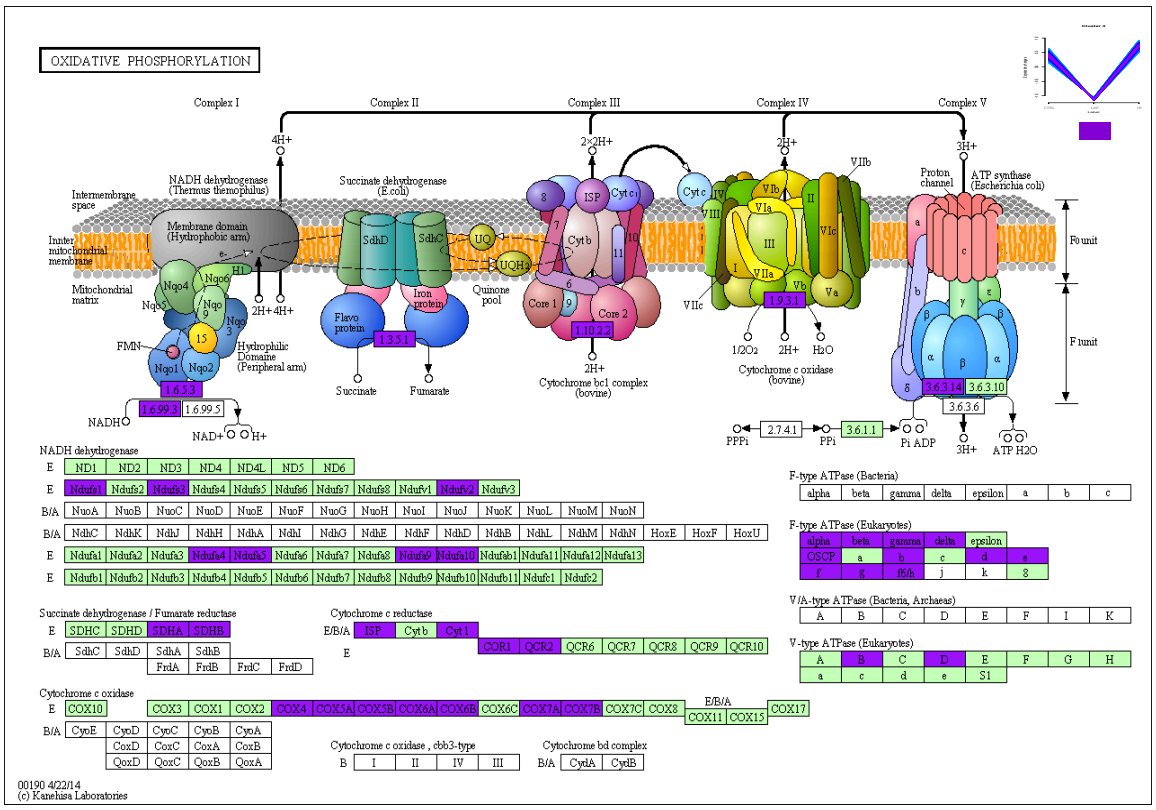

Figure 50 The enriched Oxidative Phosphorylation pathway for differentially abundant proteins (DAPs) from cluster 3. The purple highlighted show the overlapping proteins.

It was believed that mature neutrophils possess no or only a few mitochondria, having no role in cellular function [364], proved by electron microscopy [365], and with very low rate of mitochondrial respiration in the neutrophil [366]. Later, specific fluorescent dyes were used and mitochondria were identified as a tubular network [365, 367]. Furthermore, clusters of mitochondria were shown in neutrophils undergoing spontaneous or induced apoptosis, to which the pro-apoptotic Bax protein was located [367-369]. In case of ischemia and reperfusion injury, the loss of mitochondrial membrane potential and integrity along with the decrease in mitochondrial activity has been noticed [201, 370].

The importance of mitochondria in the regulation of neutrophil pro-inflammatory functions is not clear, although alteration of cell shape and chemotaxis occurs as a result of a decrease in the mitochondrial membrane potential [365]. Activated (and some inactive) immune cells prefer to utilize glycolysis, as it is 100-times faster than oxidative phosphorylation for macromolecule synthesis and proliferation [371]. Glycolysis provides energy for chemotaxis but there is little knowledge about the regulatory role of glycolysis under normal and pathological conditions in neutrophils [364]. Studies show that neutrophils do not depend on oxidative phosphorylation and surprisingly glycolysis is not increased on inhibition of mitochondrial ATP synthase [372]. Our data also showed down regulation of oxidative phosphorylation during LAP and up regulation in IR group to almost the same level of the control group. The role of these pathways during these pathalogical conditions is not clear from the literature. We found glycolysis pathway to be upregulated with *P-value* P=4.03e-08 and 10 overlapping proteins (Table 7) that might be used by neutrophil for rapid enery production rather than oxidative phosphorylation which is down regulated in cluster 3.

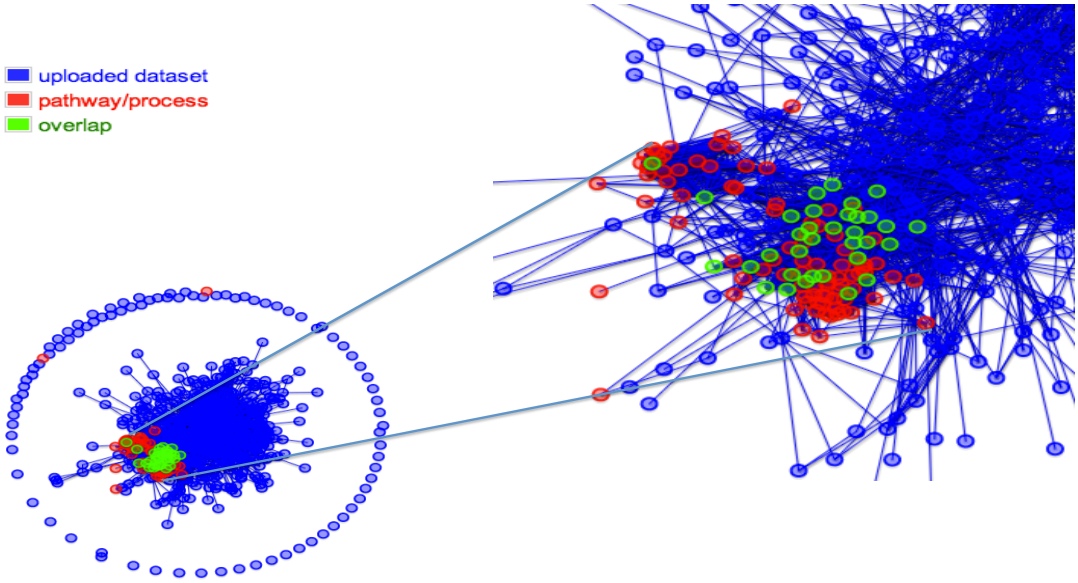

Figure 51 Computer graph visualization from enrichnet of uploaded dataset from cluster 3 and over lapping proteins (green) for oxidative phosphoryalation pathway.

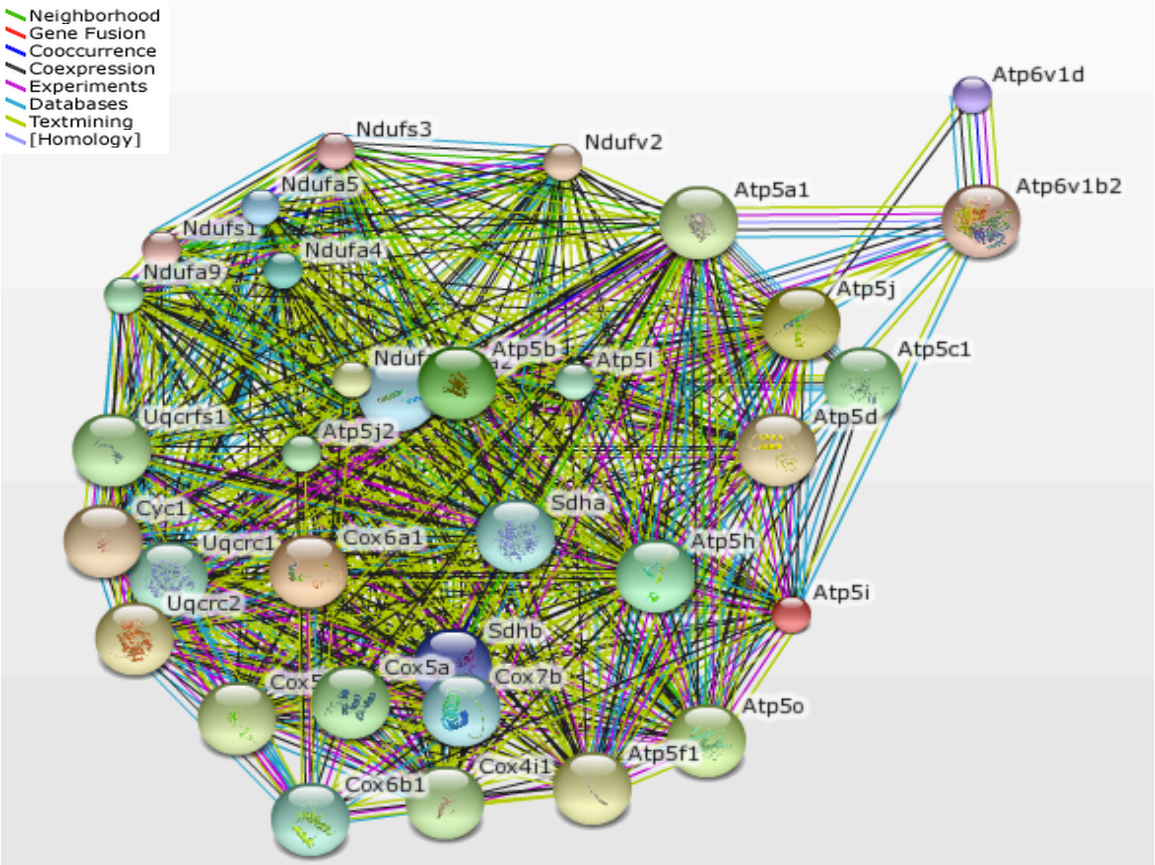

Figure 52 STRING network analysis for proteins from Oxidative Phosphorylation pathway of cluster 3.

Computer graph visualization analysis was performed for oxidative phosphorylation pathway by using enrichnet (Fig. 51). STRING analysis of the overlapped proteins of oxidative phosphorylation pathway shows high protein-protein interactions (Fig. 52).

5.8 Kinases and Phosphatases

Protein phosphorylation, an essential post-translational modification, affects most cellular activities including signal transduction, gene expression, cell cycle progression, immunity, learning and memory and other biological functions [124, 217, 218]. It is a reversible reaction that is catalyzed by protein kinases by transferring the γ-phosphate from ATP to Ser, Thr and Tyr residues whereas phosphatases act in reverse fashion to kinases (Fig. 53-A). Protein kinases have broad importance in signal transduction, are among the largest families of eukaryotes genes, making up to about 2% of the genome and have been extensively studied [218, 373, 374]. The human genome contains about

518 putative protein kinases [375-377], which can be divided into two families: 428 serine/threonine (Ser/Thr) kinases (PSKs) and 90 tyrosine (Tyr) kinases (PTKs). There are about 107 putative protein Tyr phosphatases (PTPs) and very few, about 30, protein Ser/Thr phosphatases (PSPs) [378, 379]. In this study we identified 188 phosphorylation sites in 84 proteins with term kinases making 2% and 107 phosphorylation sites in 50 proteins with term phosphatases making 1% of the total identified rat neutrophil proteome that significantly changed their regulation in control, laparotomy and ischemia (Fig. 53-B).

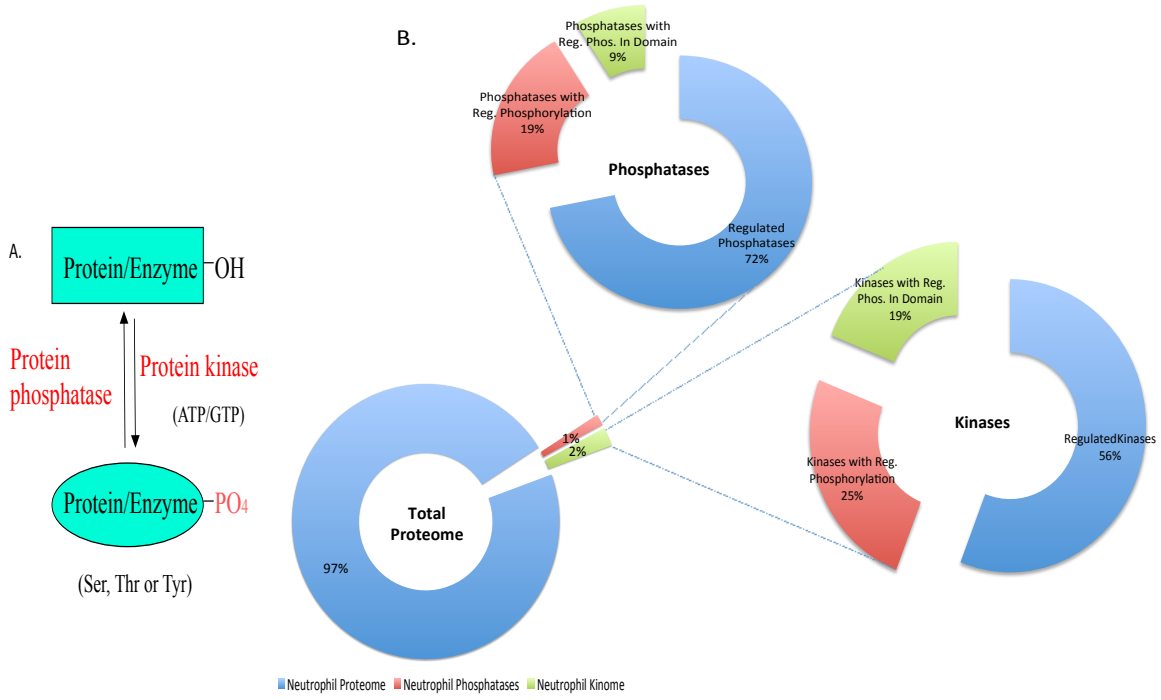

Figure 53 A shows protein phosphorylation and de-phosphorylation by protein kinase and phosphatase respectively. Fig. B. shows distribution of regulated kinases and phosphatases with and without regulation of phosphorylation in domains identified in total rat neutrophils.

5.8.1 Phosphorylated Kinases in Neutrophil

In the total neutrophil proteome 84 proteins were found with the term "Kinase", which also showed regulation. In these 84 proteins 47 were only regulated, 21 showed regulation in phosphorylation in addition to abundance but these phosphorylations were not encountered in the regulatory domain regions whereas only 16 showed regulation in

abundance, regulation in phosphorylation and these phosphorylations were encountered in domains. Of the 2% of the kinases that are only regulated make 56%, kinases that showed regulation in their phosphorylation make 25% and those whose phosphorylation in addition to expression was found in domain make 19% of the total identified kinases (Fig. 53-B). Kinases with cluster-wise expression, number of phosphorylated peptides and their domains having significant change in the phosphorylation are given in table 8.

5.8.1.1 Serine/threonine-protein kinase, MARK2, (O08679)

The serine/threonine-protein kinase, MARK2, (O08679) was up regulated (Cluster 2) and also its phosphorylation was up regulated (Cluster 5) at S562 and interestingly this phosphorylation was in APC basic domain that interacts with microtubules. MARK2 has a single trans-membrane domain and is involved in regulating the stability of microtubule, the Wnt signaling pathway, and plays a role in vesicular trafficking [380-388]. The role of microtubule in neutrophil polarity and migration has already been known in zebrafish [389] whereas Wnt signaling pathway regulates transendothelial migration in monocytes [390]. STE20-like serine/threonine-protein kinase, slk, (O08815) showed progressive up regulation in laparotomy and further in ischemia groups as compared to control (Cluster 5), and we found phosphorylation on Ser residues S372, S780, S778 and S77.

Table 8 Phosphorylated Kinases with regulated expression after laparotomy and ischemia.

UNIPROT	No. of regulated phosphopeptides	Cluster	GENE Official symbol	TM	Description	Length	Enzyme Codes	Domain containing the phosphopeptide
O08679	1	2	Mark2	1	serine/threonine-protein kinase MARK2	722	EC:2.7.11.26; EC:2.7.11	APC basic domain.
O08815	4	5	Slk	1	STE20-like serine/threonine-protein kinase	1206	2.7.11.1	AAA ATPase containing von Willebrand factor type A (vWA) domain; RecF/RecN/SMC N terminal domain.
P09215	12	4	Prkcd	1	protein kinase C delta type	673	EC:2.7.11.13	STKc_nPKC_delta, Catalytic domain of the Protein Serine/Threonine Kinase, Novel Protein Kinase C delta; active site on conserved domain STKc_nPKC_delta; substrate binding site on conserved domain STKc_nPKC_delta; activation loop (A-loop) on conserved domain STKc_nPKC_delta; protein kinase A catalytic subunit; S_TK_X, Extension to Ser/Thr-type protein kinases; Pkinase_C domain; Protein kinase C terminal domain.
P11980	1	2	Pkm	0	pyruvate kinase PKM	531	EC:2.7.1.40	Pyruvate kinase (PK); domain interface.
P16879	2	3	Fes	0	tyrosine-protein kinase Fes/Fps	822	EC:2.7.10.2; EC:1.97.1	PTKc_Fes, Catalytic domain of the Protein Tyrosine Kinase, Fes; activation loop (A-loop) on conserved domain PTKc_Fes; active site on conserved domain PTKc_Fes; substrate binding site on conserved domain PTKc_Fes.
P18654	5	1	Rps6ka3	2	ribosomal protein S6 kinase alpha-3	740	EC:2.7.11	STKc_RSK_N[cd05582]; turn motif phosphorylation site on conserved domain STKc_RSK_N.
P26817	2	4	Adrbk1	0	beta-adrenergic receptor kinase 1	689	EC:2.7.11.16; EC:2.7.11.14; EC:2.7.11.15	G Protein-Coupled Receptor Kinase 2 subgroup pleckstrin homology (PH) domain.
P35991	5	4	Btk	0	tyrosine-protein kinase BTK	659	EC:2.7.10.2	
P36506	2	3	Map2k2	0	dual specificity mitogen-activated protein kinase kinase 2	400	EC:2.7.11.24; EC:2.7.11; EC:2.7.10	
P47811	3	2	Mapk14	1	mitogen-activated protein kinase 14 isoform 1	360	EC:2.7.11.24	Active site, substrate binding site, active loop (A-loop); KIM docking site; Catalytic domain of the Serine/Threonine Kinase, p38alpha Mitogen-Activated Protein Kinase ;Serine/Threonine Kinases (STKs), p38alpha subfamily, catalytic (c) domain.
P50545	6	2	Hck	2	tyrosine-protein kinase HCK	524	EC:2.7.10.2; EC:2.7.10	Hydrophobic binding pocket; autoinhibitory site; SH2_Src_HCK; active site; substrate binding site; active loop (A-loop); PTKc_Src_like domain; Pkinase_Tyr; STYKc; SPS1; PLN00034.
P54645	8	5	Prkaa1	1	5'-AMP-activated protein kinase catalytic subunit alpha-1	559	EC:2.7.11	AMPKA1_C, C-terminal regulatory domain of 5'-AMP-activated protein kinase (AMPK) alpha 1 catalytic subunit; AMPKA_C_like superfamily; beta/gamma subunit interface on conserved domain AMPKA1_C.
P67871	1	1	Csnk2b	0	casein kinase II subunit beta	215	EC:3.4.21; EC:2.7.11	
P68404	1	5	Prkcb	1	Protein kinase C beta type	671	EC:2.7.11	STKc_cPKC_beta; turn motif phosphorylation site.
P70600	5	5	Ptk2b	1	protein-tyrosine kinase 2-beta	1009	EC:2.7.10	
P81799	1	2	Nagk	0	N-acetyl-D-glucosamine kinase	343	EC:2.7.1.59; EC:2.7.1.60	Neucleotide binding site; NBD_sugar-kinase_HSP70_actin domain; BcrAD_BadFG; COG2971.
P97820	1	2	Map4k4	1	Mitogen-activated protein kinase kinase kinase kinase 4	1233	EC:2.7.11	
Q53UA7	5	4	Taok3	0	serine/threonine-protein kinase TAO3	898	EC:2.7.11	
Q5S006	1	3	Lrrk2	3	leucine-rich repeat serine/threonine-protein kinase 2	2527	EC:2.7.11	
Q5XIS9	2	2	Prkd2	1	serine/threonine-protein kinase D2	875	EC:2.7.11.13	
Q63433	10	3	Pkn1	0	serine/threonine-protein kinase N1	946	EC:2.7.11; EC:2.7.11.13	Catalytic domain of the Protein Serine/Threonine Kinase, Protein Kinase N ; Serine/Threonine Kinases (STKs), Protein Kinase N (PKN) subfamily, catalytic (c) domain.
Q63531	4	1	Rps6ka1	2	ribosomal protein S6 kinase alpha-1	735	EC:2.7.11	SPS1 Domain; STKc_RSK_N Domain; hydrophobic motif (HM) on conserved domain STKc_RSK_N; Protein kinase C terminal domain; protein kinase A catalytic subunit; turn motif phosphorylation site on conserved domain STKc_RSK_N.

Continue

Q64725	5	2	Syk	0	tyrosine-protein kinase SYK	629	EC:2.7.10.2; EC:2.7.10.1; EC:2.7.10	
Q6P6U0	17	5	Fgr	0	tyrosine-protein kinase Fgr	517	EC:2.7.10	PTKc_Src_like, Catalytic domain of Src kinase-like Protein Tyrosine Kinases; Protein Tyrosine Kinase (PTK) family; active site on conserved domain PTKc_Src_like; substrate binding site on conserved domain PTKc_Src_like; activation loop (A-loop) on conserved domain PTKc_Src_like; SH3/SH2 domain interface on conserved domain PTKc_Src_like; SH2_Src_Fgr, Src homology 2 (SH2) domain; SH2 domain; hydrophobic binding pocket on conserved domain SH2_Src_Fgr; autoinhibitory site on conserved domain SH2_Src_Fgr; phosphotyrosine binding pocket on conserved domain SH2_Src_Fgr.
Q6P9R2	5	5	Oxsr1	2	serine/threonine-protein kinase OSR1	527	EC:2.7.11	SPS1.
Q8K1R7	4	4	Nek9	2	serine/threonine-protein kinase Nek9	984	EC:2.7.11	
Q91XS8	3	5	Stk17b	1	serine/threonine-protein kinase 17B	371	EC:2.7.11.18; EC:2.7.11.17	
Q9JI11	3	4	Stk4	0	serine/threonine-protein kinase 4	487	EC:2.7.11; EC:2.7.11.13	
Q9JIH7	10	2	Wnk1	0	serine/threonine-protein kinase WNK1 isoform 3	2126	EC:2.7.11	
Q9WUT3	3	3	Rps6ka2	2	ribosomal protein S6 kinase alpha-2	733	EC:2.7.11	STKc_RSK_N, N-terminal catalytic domain of the Protein Serine/Threonine Kinase.
Q9Z277	2	5	Baz1b	2	tyrosine-protein kinase BAZ1B	1479	EC:2.7.10.2; EC:2.3.1.48	

Phosphorylation on S372 and S780 showed down phospho-regulation in Laparotomy (Cluster 3), whereas S778 and S776 showed down regulation in ischemia only (Cluster 4). It has one transmembrane domain and recently SLK-mediated phosphorylation of paxillin has been shown to be required for focal adhesion turnover and cell migration [391]. We found paxillin up regulated (Cluster 2) with 22 different phospho sites. Slk exacerbates apoptosis and may regulate cell survival during injury or repair [392]. Other studies have also shown the apoptotic role of slk after its expression during *in vitro* ischemia-reperfusion injury [393-395].

5.8.1.2 Protein kinase C delta type, prkcd, (P09215)

Protein kinase C delta type, prkcd, (P09215) is an AGC kinase of serine-threonine specific protein kinase C (PKC) family with a single trans-membrane domain. Prkcd was down regulated in ischemia as compared to control and laparotomy (Cluster 4) and we found 12 phosphosites with regulated phosphorylation on prkcd protein. Blake et al, 1999, have shown that Src promotes PKC delta degradation by phosphorylating it at Tyr311 residue [396] and our studies support their analysis as we also found prkcd downregulated and phosphorylated at Y311. It would also be interesting to mention that

we found Src kinase-associated phosphoprotein 2 (Q920G0) up regulated (Cluster 2) in our studies with 14 phosphosites showing its role in prkcd phosphorylation at Y311 to cause its degradation. We found down regulation in phosphorylation at Ser504, Thr505 and Thr509 residues, which were in the active site, substrate binding site and activation loop (A-loop) of the STKc_nPKC_delta Domain. We also found Ser643, Ser662 phosphosites down regulated (Cluster 1) and Ser645 up regulated (Cluster 5) at the C-terminal Domain of PKC.

5.8.1.3 Pyruvate kinase, pkm, (P11980)

Pyruvate kinase, pkm, (P11980) catalyzes a phosphate group transfer from phosphoenolpyruvate (PEP) to ADP resulting in an ATP and a pyruvate molecule. In our study we found an increase in pkm expression profile (Cluster 2) and also an increase in phosphorylation at Ser437 (Cluster 5) and interestingly this phosphorylation was in PK_C domain. Oehler et al, 2000, have reported an increased expression of pkm in PMNs from polytrauma patients [397] and our results are in accordance with that as we can see that pkm expression is higher in laparotomy group that is a surgical trauma and a little down in ischemia but higher in both as compared to the control group. Further they suggested that the increased expression of pkm in neutrophils of polytrauma patients results in a higher pentose phosphate pathway (PPP) for higher NADPH production that is involved in reactive oxygen species (ROS) production in the neutrophils when exposed to appropriate stimuli [398].

5.8.1.4 Tyrosine-protein kinase Fes/Fps, fes, (P16879)

Tyrosine-protein kinase Fes/Fps, fes, (P16879) was down regulated in the laparotomy group (Cluster 3) and we found two phosphosites with down regulation in phosphorylation at Thr412 and Tyr713 (Cluster 1). The down regulation at Tyr713 was in PTKc_Fes, Catalytic domain of the Protein Tyrosine Kinase, Fes; activation loop (A-loop) on conserved domain PTKc_Fes, active site on conserved domain PTKc_Fes and substrate binding site on conserved domain PTKc_Fes. Directional movements and recruitment of neutrophils are extremely important in innate immunity. Parsons et al, 2007, have shown that Fps/Fes kinase regulates leucocytes recruitment and extravasation during inflammation and they found high leucocytes adherence to venules, high

transendothelial migration in fps/fes-knockout mice [399]. Another recent study from the same group also supports this previous study that fer kinase restricts neutrophil chemotaxis in direction of chemoattractants where they observed enhanced chemotaxis in kinase-inactivating mutation (FerDR/DR) mice neutrophil toward the end target chemotactic peptide (WKYMVm) and C5a compared to the wild type [400]. Both of these studies support our analysis and suggest fps/fes as an inhibitory kinase for leucocytes and neutrophils chemotaxis towards chemoattractants.

5.8.1.5 Ribosomal protein S6 kinase alpha-3, Rps6ka3/RSK2, (P18654)

Ribosomal protein S6 kinase alpha-3, Rps6ka3/RSK2, (P18654) an AGC kinase of the RSK family, with two transmembrane domains, undergoes phosphorylation resulting in activation of transcription factors (e.g., cyclic AMP response element-binding protein (CREB), inhibitor of κBα/nuclear factor-κB, c-fos) [401-403]. It has been investigated in neutrophils that RSK2 phosphorylates and causes glycogen synthase kinase 3 inactivation, an event that improves neutrophils survival [404, 405]. Our analysis shows down regulation of RSK2 (Cluster 1) and 5 phosphosites were found. The phosphorylation at Thr365 residue showed up regulation that was found in STKc_RSK_N domain and phosphorylation at Ser369 was down regulated (Cluster 4) that was encountered in "turn motif phosphorylation site" of the STKc_RSK_N domain. The Ser369 phosphorylation has already been shown for the activation of RSK2 [406] and we found down regulation in both RSK2 expression and Ser369 phosphorylation probably leading to glycogen synthase kinase 3 activation, that is involved in neutrophils survival [404, 405] and interestingly glycogen synthase kinase-3 alpha (P18265) was found up regulated (Cluster 2).

5.8.1.6 Beta-adrenergic receptor kinase 1, Adrbk1/GRK2, (P26817)

Beta-adrenergic receptor kinase 1, Adrbk1/GRK2, (P26817) is a ubiquitous protein kinase of GRK family that phosphorylates the beta-2 adrenergic receptor [407], can regulate chemotactic activity [408] and increases neutrophil mobilization if not fully expressed [409] . It has been demonstrated that activated neutrophils produce oxygen radicals during ischemia and reperfusion [410] and in vitro studies show the capability of inflammatory mediators like pro-inflammatory cytokines and oxygen radicals to reduce

GRK2 protein [411, 412]. Its expression was down regulated (Cluster 4) with two phosphosites at Ser666 and Ser670 in PH_GRK2_subgroup. So probably this low expression of GRK2 was because of high oxygen radicals production by the neutrophils during ischemia, facilitating their migration.

5.8.1.7 Tyrosine-protein kinase, BTK/BPK, (P35991)

Tyrosine-protein kinase, BTK/BPK, (P35991) is a tyrosine kinase of the Tec-family kinases that are expressed in blood cells like monocytes, macrophages, B cells and neutrophils [413]. During ischemia it was down regulated (Cluster 4) with 5 phosphosites including Ser180. It is clear from the literature that PKCβ mediated phosphorylation at Ser180 causes down regulation of btk resulting in sequestration of btk in the cytoplasm [414]. Our results support down regulation of btk but Ser180 phosphorylation was found down regulated (Cluster 1) showing phosphorylation regulation of another candidate amino acid for btk down regulation in neutrophils. In human neutrophils btk negatively regulates stimulation induced apoptosis and ROS production [415].

5.8.1.8 Dual specificity mitogen-activated protein kinase kinase 2, Map2k2/MEK2, (P36506)

It has been reported that MEK2, a member of the STE7 kinase family, is phosphorylated and activated by upstream serine/threonine kinases like MEK and Raf kinase and MEK2 phosphorylates and activates ERK2 [416]. MEK2 was down regulated (Cluster 3) in laparotomy and during ischemia its expression was not changed. Two phosphosites Ser393 and Thr394 were encountered with down (Cluster 4) and up regulation (Cluster 2) respectively. There are different Anti-MEK2 Phospho T394 antibodies available in the market but there is no known function of significantly up regulation on Thr394 phosphorylation [417].

5.8.1.9 Mitogen-activated protein kinase 14 isoform 1, Mapk14/ P38A/P38MAPK, (P47811)

P38MAPK belongs to the family of MAPKs with two transmembrane domains, and is activated by phosphorylation of Thr and Tyr residues. It was up regulated (Cluster 2) with three phosphosites, Thr180, Thr185 and Tyr182. All these phosphosites were found

in the active site, substrate binding site, active loop (A-loop), KIM docking site of the Catalytic domain of the Serine/Threonine Kinase, p38alpha Mitogen-Activated Protein Kinase (STKc_p38alpha_MAPK14). Phosphorylation on Thr185 was down regulated (Cluster 1) whereas the other two were up regulated (Cluster 2). This dual phosphorylation on Thr180 and Tyr182 is caused by the MAP2Ks MAP2K3/MKK3, MAP2K4/MKK4 and MAP2K6/MKK6 in response to environmental stress, growth factors or inflammatory cytokines and is important for the activation of the enzyme [418, 419]. Furthermore, it has also been demonstrated that phosphorylated p38MAPK at both residues Thr180 and Tyr182 has 10-20 fold more activity than its phosphorylation at Thr180 only, whereas p38MAPK phosphorylated at Tyr182 alone is inactive [419]. This phosphorylation pattern was not previously described as a response to IRI. Based on the localization of Thr185 in the important domain sites, the down regulation of Thr185 could be of importance for the activation of p38MAPK. Various studies have shown that pharmacological inhibition of p38MAPK attenuates different functions of neutrophils like adherence, chemotaxis and degranulation [420-422]. Moreover, some studies in neutrophils and others in general have shown the blockage of NADPH oxidase activity by inhibiting p38MAPK [420, 423-426].

5.8.1.10 Tyrosine-protein kinase, HCK, (P50545) and tyrosine-protein kinase, Fgr, (Q6P6U0)

Tyrosine-protein kinase, HCK, (P50545) and tyrosine-protein kinase, Fgr, (Q6P6U0) belong to the Scr family that is predominantly expressed in hematopoietic cell types. Both Hck and Fgr were found up regulated belonging to cluster 2 and 5 with six and nineteen phosphosites respectively. Hck showed down phosphorylation (Cluster 3) in laparotomy at Tyr207 that was in hydrophobic binding pocket and autoinhibitory site of SH2_Src_HCK domain. Phosphorylation at Tyr409, Thr410 and Ser460 was up regulated (Cluster 5). Tyr409 and Thr410 were found in the active site, substrate binding site, active loop (A-loop) and SH3/SH2 domain interface of the PTKc_Src_like domain whereas Ser460 phosphorylation was found in all like Tyr409 and Thr410 except the activation loop (A-loop). Phosphorylation at Tyr400 in Fgr was found up regulated (Cluster 2) that is inhibited by a prior phosphorylation at Tyr511 [427], which was not

found in our case. Hck and Fgr deficient mouse and human neutrophils result in the failure of respiratory burst activation and neutrophils migration in response to fMLP [428]. Two contradictory studies on fMLP stimulated but Hck and Fgr deficient mice neutrophils have been published stating the inability [421] and ability [429] of Hck and Fgr to activate p38MAPK. In neutrophils, the Hck enzyme has been shown to have important roles like regulation of actin-based chemotaxis and adhesion [430-432] and integrin and FcRγ-mediated phagocytosis as well [433, 434].

5.8.1.11 Protein kinase C beta type, Prkcb/pkcb, (P68404)

Pkcb is an AGC kinase of the PKC family. It has one transmembrane domain and showed up regulation (Cluster 5) with one phosphorylation at Thr642 that was encountered up regulated (Cluster 2) in the turn motif phosphorylation site of the STKc_cPKC_beta domain. It has been demonstrated that phosphorylation at Thr642 is very important for the enzymatic function of the PKC [435]. Zhang et al show that neutrophils require sustained increase in concentration of cytosolic Ca^{2+} for the production of superoxide because of the Ca^{2+} dependent activation of the protein kinase C (PKC) isoforms (PKCa and PKCb) [436] as these isoforms are very important to phosphorylate components of the NADPH oxidase [437, 438].

5.8.1.12 N-acetyl-D-glucosamine kinase, Nagk, (P81799)

Nagk, belongs to the sugar kinase/Hsp70/actin superfamily. It converts N-acetyl-D-glucosamine to N-acetyl-D-glucosamine-6-phosphate, converting ATP to ADP, [439]. In Addition, like ATPases, Nagk also converts ATP to ADP and up regulation of Nagk may contribute to energy loss [440]. Its expression was up regulated (Cluster 2) with one phosphosite Ser76 that showed down regulation (Cluster 4) in ischemia. This phosphorylation at Ser76 was found in the nucleotide-binding site of the NBD_sugar-kinase_HSP70_actin domain, which is nucleotide-Binding Domain of the sugar kinase/HSP70/actin superfamily. This phosphorylation on Ser76, which may have some role in Nagk regulation because of its localization, is not reported in the literature showing its role on the regulation of this enzyme although phosphorylation of Tyr205 was reported that may have a role in the activation of Nagk [439].

5.8.1.13 Serine/threonine-protein kinase N1, Pkn1/Prk1/Pak1, (Q63433)

Pkn1 is a member of protein kinase C superfamily of serine/threonine kinases which is one of the first identified effectors for RhoA-GTPase existing in an integral plasma membrane pool and a cytosolic/peripheral pool [441]. It was down regulated in laparotomy (Cluster 3). Total ten phosphosites were found for Pkn1 and two phosphosites showed up regulation (Cluster 5) at Thr918 and Ser920 and these were found in a turn motif phosphorylation site of the STKc_PKN domain, which is the catalytic domain of the Protein Serine/Threonine Kinase, Protein Kinase N. Another up regulation (Cluster 2) in phosphorylation on Ser377 was also encountered in our analysis that is involved in the facilitation of Pkn1 integration into the plasma membrane to function as a Rho effector [441].

5.8.1.14 Ribosomal protein S6 kinase alpha-1, Rps6ka1/Rsk1, (Q63531)

Rps6ka1 is an AGC kinase of the RSK family. It has two transmembrane domains and it showed down regulation (Cluster 1) with four phosphosites, one with down regulation (Cluster 1) Ser732 and the other three phosphosites Tyr359, Ser363 and Ser380 with up regulation (Cluster 2). All of the last three up regulated phosphorylations were found in STKc_RSK_N domain, which is the N-terminal catalytic domain of the Protein Serine/Threonine Kinase, 90kDa ribosomal protein S6 kinase. Ser363 phosphorylation was found in a turn motif phosphorylation site of the STKc_RSK_N domain whereas phosphorylation on Ser380 was found in a hydrophobic motif (HM) on the conserved domain STKc_RSK_N. Rps6ka1 can interact with transcription factors like CREB in neutrophils and G subunit of phosphatase 1 that regulates the glycogen synthase activation [442, 443].

5.8.1.15 Ribosomal protein S6 kinase alpha-2, Rps6ka2/Rsk3, (Q9WUT3)

Rps6ka2 is an AGC kinase of the RSK family. It has two transmembrane domains and it was down regulated in laparotomy (Cluster 3) and has three phosphosites Ser360 (Cluster 5), Ser377 (Cluster 2) and Ser716 (Cluster 1). Up regulation of the phosphorylation on Ser360 was found in a turn motif phosphorylation site and Ser377 was in a hydrophobic motif (HM) of the STKc_RSK_N domain, which is the N-terminal catalytic domain of

the Protein Serine/Threonine Kinase, 90kDa ribosomal protein S6 kinase. It has been found that under similar in vitro conditions RSK3 activity is not affected by RSK2 and also Rsk3 phosphorylates nuclear target proteins like c-fos and histones [444]. Both Rsk2 and Rsk3 have been found to be activated by Ngf and activate CREB by phosphorylating it at Ser133 in vitro [445] and in our data we did not find any phosphorylation at Ser133 on (P15337) Creb (cyclic AMP-responsive element-binding protein 1 isoform B) but we found other phosphorylated residues.

5.8.1.16 Serine/threonine-protein kinase, Oxsr1/Osr1, (Q6P9R2)

Oxsr1 is an oxidative-stress responsive 1 protein of the STE20 family. It has two transmembrane domains and was up regulated (Cluster 5) with three phosphosites Ser325 that was down regulated (Cluster 1) and Ser324 and Ser359, which were up regulated (Cluster 5). All these three phosphosites were found in SPS1, which is Serine/threonine protein kinase domain. The Osr1 is stimulated by Wnk1 [446] that was also found up regulated in our datasets with 10 phosphosites as mentioned before. Osr1 regulates Na^+/H^+ exchanger activity, which further participates in the cell volume regulation [447-449] and ROS production [446] as ROS production is paralleled by the generation of H^+ that inhibits NADPH oxidase, which generates ROS [450].

5.8.2 Phosphorylated Phosphatases in Neutrophil

In the neutrophil proteome we describe, 50 regulated proteins with term “phosphatase” were found. Among these 50 phosphatases, 13 showed regulation in their phosphorylation and the regulation in phosphosites for 4 phosphatases were found in domain regions. Of the 1% of the phosphatases that showed only regulation make 72%, those who showed regulation in phosphorylation make 19% and only 9% of phosphatases were encountered to have regulated phosphorylation in domain regions (Fig. 53-B). Phosphatases with cluster-wise expression, number of phosphorylated peptides and their domains having significant change in the phosphorylation are given in table 9.

5.8.2.1 Receptor-type tyrosine-protein phosphatase C isoform 4 precursor, Ptprc/CD45, (P04157)

CD45 is a receptor type protein tyrosine phosphatase with two transmembrane domains and commonly known as CD45 or LCA (Luekocyte common antigen). It was found up regulated (Cluster 5) with 18 phosphosites. Regulation in phosphorylation was found in Protein tyrosine phosphatase (PTPc) catalytic domain. CD45 plays a role in neutrophil adhesion, chemotaxis, phagocytosis, ROS production and bacterial killing [451]. The receptor-like protein tyrosine phosphatase (RPTPs) CD45 and CD148, have redundant roles in the SFK activity in B cells and macrophages in ITAM immune-receptor stimulation [452]. A study showed that both CD45 and CD 148 are essential for chemoattractant mediated chemotaxis in the neutrophil after *S. aureus* infection. CD45 positively while CD148 positively and negatively regulate GPCR function and proximal signals including Ca^{2+}, PI3K, and pERK activity. Moreover, CD45 and CD148 preferentially target different SFK members (Hck and Fgr versus Lyn, respectively) during regulation of GPCR pathways [451].

5.8.2.2 Tyrosine-protein phosphatase non-receptor type 6, Ptpn6/Shp-1, (P81718)

Ptpn6 has one transmembrane domain and was found up regulated (Cluster 2) with ten phosphosites. Phosphorylation on Ser12 was found up regulated in SH2_N-SH2_SHP_like, N-terminal Src homology 2 (N-SH2) domain found in SH2 domain Phosphatases (SHP) proteins. The Src homology domain 2 (SH2)-containing tyrosine phosphatase-1 (SHP-1) is found in the regulation of differentiation, proliferation, and activation of hematopoietic cells. SHP-1 is also involved in modulating apoptotic pathways in neutrophils. Low level of SHP-1 has been associated with increased neutrophil survival in vitro and mice deficient of SHP-1 developed severe neutrophilic inflammatory responses. In contrast, high expression has been noticed in neutropenic patients [453]. Recently Ptpn6 deletion in neutrophils and dendritic cell from moth eaten mice resulted in cutaneous inflammation (neutrophilic dermatoses) and severe autoimmunity, without inflammation respectively [454]. It has been also proposed that SHP1 binds to multiple kinases, such as Jak2, Jak3, TAK1, ERK1/2, p38, JNK, IL-1R-

associated kinase 1, and Lyn, through a novel phosphorylation-independent kinase tyrosyl inhibitory motif [455].

Table 9 Phosphorylated Phosphatases with regulated expression after laparotomy and ischemia.

UNIPROT	No. of regulated phosphopeptides	Cluster	GENE Official symbol	TM	Description	Length	Enzyme Codes	Domain containing the phosphopeptide
B2GV87	3	4	Ptpre	1	receptor-type tyrosine-protein phosphatase epsilon precursor	699	3.1.3.48	
P04157	18	5	Ptprc	2	receptor-type tyrosine-protein phosphatase C isoform 4 precursor	1273	EC:3.1.3.48	Protein tyrosine phosphatase (PTPc) catalytic domain
P20417	2	3	Ptpn1	0	tyrosine-protein phosphatase non-receptor type 1	432	-	
P81718	10	2	Ptpn6	1	tyrosine-protein phosphatase non-receptor type 6	613	EC:3.1.3.48	SH2_N-SH2_SHP_like[cd10340], N-terminal Src homology 2 (N-SH2) domain found in SH2 domain Phosphatases (SHP) proteins; SH2 domain; Src homology 2 domains
P97573	28	3	Inpp5d	0	phosphatidylinositol 3,4,5-trisphosphate 5-phosphatase 1	1190	EC:3.1.3; EC:3.1.3.56	PTZ00449, 104 kDa microneme/rhoptry antigen; Catalytic inositol polyphosphate 5-phosphatase (INPP5c) domain of SH2 domain; putative catalytic site; putative active site; putative MG binding site; putative PI/IP binding site
Q10728	29	4	Ppp1r12a	1	Protein phosphatase 1 regulatory subunit 12A	1032	EC:3.1.3.16	
Q5HZV9	2	2	Ppp1r7	0	protein phosphatase 1 regulatory subunit 7	360	-	
Q6PD03	4	3	Ppp2r5a	1	serine/threonine-protein phosphatase 2A 56 kDa regulatory subunit alpha isoform	486	-	
Q7TSI3	2	5	Ppp6r1	1	serine/threonine-protein phosphatase 6 regulatory subunit 1	856	-	CAF-1_p60_C, Chromatin assembly factor complex 1 subunit p60, C-terminal; PHA03247, large tegument protein UL36

Phosphatidylinositol 3,4,5-trisphosphate 5-phosphatase 1, Inpp5d/Ship, (P97573)

Inpp5d was found down regulated in laparotomy and with no change in ischemia (Cluster 3) with 28 regulated phosphorylation sites in PTZ00449, a 104 kDa microneme/rhoptry antigen; Catalytic inositol polyphosphate 5-phosphatase (INPP5c) domain of SH2 domain; putative catalytic site; putative active site; putative MG binding site and putative PI/IP binding site. SHIP1 (Inpp5d) SHIP converts phosphatidylinositol 3, 4, 5 triphosphate to phosphatidyl 3, 4 biphosphate and neutrophils deficient of SHIP1 showed impaired polarization and motility in vitro, suggesting its role in neutrophil motility [456]. Recently a study in zebra fish showed that SHIP phosphatases limit neutrophil motility by modulating PI3K signaling. Depletion of SHIP phosphatases led to increased

neutrophil 3D motility and neutrophil infiltration into wounds. Moreover, overexpression of the SHIP phosphatase domain in neutrophils impaired neutrophil 3D migration [457]. SHIP is a negative regulator in TLR2-induced neutrophil activation and in the development of related in vivo neutrophil-dependent inflammatory processes, such as acute lung injury [458].

Serine/threonine-protein phosphatase 6 regulatory subunit 1, Ppp6r1/Saps1, (Q7TSI3)

Ppp6r1 has one transmembrane domain and was found up regulated (Cluster 5) with two up regulated phosphosites on Ser531 and Ser817. Phosphorylation on Ser817 was up regulated (Cluster 5) and was found in CAF-1_p60_C, Chromatin assembly factor complex 1 subunit p60, C-terminal and PHA03247, large tegument protein UL36.

Protein phosphatase 6 (PP6) is the major T-loop phosphatase for Aurora A, which is an important mitotic kinase. Depletion of catalytic or regulatory subunits interferes with spindle formation and chromosome alignment and resulted into loss of PP6 function because of increased Aurora A activity. PP6 holoenzyme consist of PPP6C catalytic, SAPS1–3 regulatory, and ANKRD28–44 subunits and all of these are require for normal mitosis [459]. We are here first time reporting the presence of SAPS1 (Ppp6r1) regulatory subunit in neutrophil. Literature shows that it is not even reported in any immune cell before.

6 Summary of pathway results

Summarizing the results from pathways and enzymes analysis in the figure-54 shows that in case of ischemia and reperfusion signal for neutrophil activation came from the intestine/endothelial cells (ECs) in the form of chemokines and chemoattractants. As C5a and LTB4 are the potent chemoattractants and leads to up regulation of vascular adhesion molecules, ICAM-1, endothelial E-selectin, P-selectin, IL-8, MCP-1 [82, 83] and finally activate the chemokine signaling pathway. Most of the proteins of chemokine signaling pathway has been found up regulated after IR. We have also encountered down regulation of 57 ribosomal proteins and role of most of the proteins is not clear in neutrophil. However RP19 has antagonist-induced effect on the neutrophil C5aR and alters the chemotaxis of leukocytes by causing functional differences in the C5a receptor response. [333]. Neutrophils migrate toward the source of chemoattractants like formylated peptides, C5a, leukotriene B4, and chemokines such as IL-8 [352] and after binding to its surface receptor, a number of cytoplasmic events occur which activates the cytoskeletal machinery [353]. Proteins from cytoskeleton pathway are also found up regulated in neutrophil after IR. Activation of proteins belonging to this pathway further lead to enhanced motility, locomotion, chemotaxis, firm focal adhesion, trans-endothelial migration (TEM) through formation of lamellopodia and fillopodia. As a result of Interaction of FcR with their Ig ligands in leukocyte initiates a number of responses including phagocytosis, antibody-dependent cell-mediated cytotoxicity (ADCC), release of pro-inflammatory mediators and cytokines production [337, 338]. Lipoxygenases (5-LO and 15-LO) are involve in arachidonic acid (AA) metabolism leading to production of LTB4, which is another source of PMNs recruitment in ECs. After TEM degranulation, neutrophil releases cytokines and ROS inside the endothelium that not only results into recruitment of further PMNs but also causes endothelial damage. Energy require for neutrophil activation comes from metabolic pathways as 109 proteins have been found upregulated from metabolic pathways. We also found glycolysis pathway to be upregulated that might be used by neutrophil for rapid enery production rather than oxidative phosphorylation which is found down regulated. Activated immune cells prefer to utilize glycolysis, as it is 100-times faster than oxidative phosphorylation for macromolecule synthesis and proliferation [371]. However exact role of these metabolic

pathways is clear.

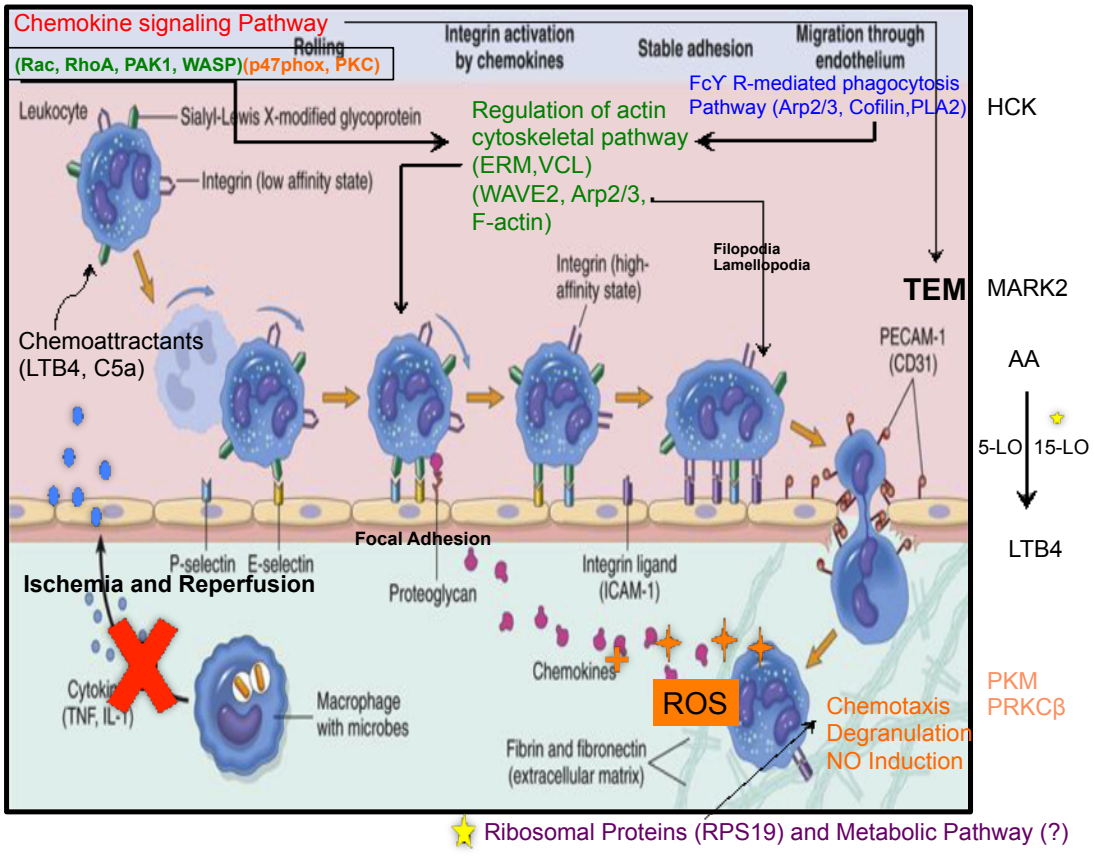

Figure 54 Summary of some important results and interaction between pathways.

7 Conclusion and Future perspectives:

In clinical conditions ischemia reperfusion injury is associated with high morbidity and mortality. The role of neutrophils in the pathogenesis of IRI is clear from the literature and we did not find any study showing the underlying mechanisms and different proteins expression or abundance in neutrophils in these surgical procedures. Our study illustrates the significance of comparative proteomic strategies applied to the neutrophil in different surgical groups. We report the most comprehensive proteomic coverage of the neutrophil up to date showing the adequacy and sensitivity of the equipment and methods used during this study. The applied tools and strategies discussed are appropriated for the high level identification of unmodified proteome and phosphoproteome in neutrophils and to better understand the molecular facets of neutrophil biology. Our results contradict and support existing results and can generate novel ideas and hypothesis. This study of the rat neutrophil proteome shows the regulation of some important enzymes from cluster analysis. Some of these are well known for their role in neutrophil while few of the enzymes were identified here for the first time in neutrophil and their role is poorly characterized. Important kinases and phosphatases have been identified along with their expression and phosphorylation regulation in different surgical groups and may be considered as future therapeutic targets in neutrophil biology.

This study opens new window to the better understanding of neutrophil proteome and provides database for the further studies. Validation of these enzymes can be very helpful in this regard and can further lead to the biomarker discovery.

We are reporting some interesting predicted events like Ribosomal Pathway, Regulation of Actin Cytoskeleton Pathway, Fc gamma R-mediated phagocytosis pathway, Chemokine Signaling Pathway, and Oxidative phosphorylation with regulation pattern.

As part of an ongoing research line from the laboratory LBQP-UnB, the analysis completed to date will be extended by the comprehensive study of the proteomics activated in different experimental conditions. Further examination of the other post-translation modifications like glycosilation and acetylation will provide more insights into the underlying signaling pathways and neutrophil biology.

The results presented in this work show significant differences in the hematimetric parameters among all of the conditions evaluated. The most remarkable parameters are those related to leukocytes and platelets; some of these, including the lymphocyte and granulocyte counts and the granulocytes/lymphocytes ratios, suggest that IPC attenuates the effect of the IR in the circulating blood cells. Our work provides data to aid the better understanding of hematological responses in the body after IR and IPC. Some of the parameters described here can be further validated as predictive markers for ischemia and may lay the basis for further studies aiming to reduce the tissue injury resulting from ischemia/reperfusion. From platelets count, platelet distribution width (PDW) and mean platelet volume (MPV) and plateletcrit (PCT) show the involvement of platelet activation in IR and IPC. As platelets role is not clear from the literature so proteomic analysis of platelets in similar model may be helpful to minimize the tissue injury by unveiling the potential candidate biomarkers, underlying pathways and overall mechanisms of tissue injury a long with the neutrophils.

PORTUGUESE VERSION

1. Introdução

1.1 Polimorfonucleares: Neutrófilos (PMNs)

Os neutrófilos são parte do sangue periférico e desempenham um papel importante na eliminação microrganismos, participando na resposta inflamatória sistêmica após sua ativação [1]. Assim que ocorre a invasão por patógenos, os neutrófilos são ativados e migram para local da lesão. Para controlar a infecção os neutrófilos disparam mecanismos de fagocitose e produzem radicais livres. Estas células podem ser ativadas por hipóxia, produtos microbianos e citocinas, e a completa ativação destas células resulta na produção de ânions superóxido, adesão endotelial e expressão de receptores de membrana [2]. O recrutamento de neutrófilos é um processo de múltiplos passos que exige três classes de receptores de adesão, incluindo as selectinas, integrinas e os receptores de adesão da superfamília das imunoglobulinas [3]. Estes passos são demonstrados na figura 1.

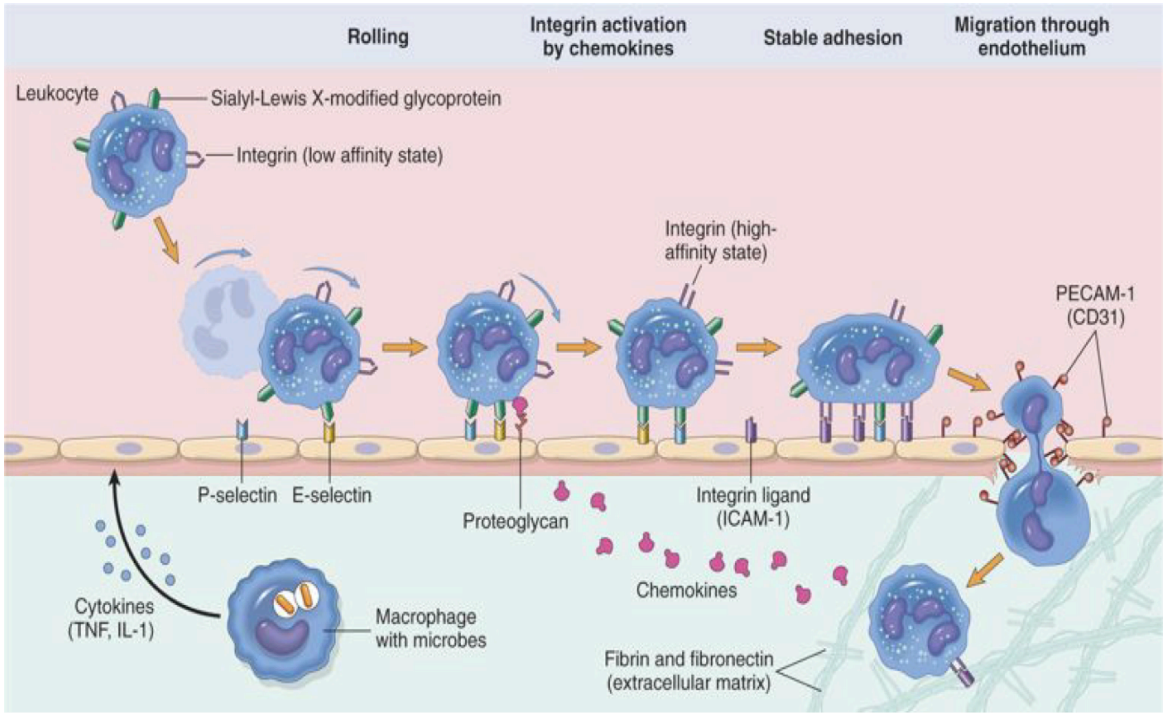

Figura 1 Recrutamento de neutrófilos para os locais de inflamação. Um processo passo a passo que envolve o rolamento de leucócitos, ativação e adesão ao endotélio, rolamento basal, transmigração através do endotélio direcionados pelos quimioatraentes que são liberados na sítio da lesão. Adaptado de [4].

1.1.1 Rolamento

Selectinas são glicoproteínas de adesão de superfície, como a L-selectina (em leucócitos), E-selectina (células endoteliais (EC)), e P-selectina (EC e plaquetas), que não só auxiliam no rolamento, como também contribuem no processo de adesão [5]. Os ligantes de neutrófilos para L-selectina são múltiplos determinantes de carboidratos sialilados, que estão ligados a moléculas similares a mucinas [5]. A ativação de receptores toll like (TLR-2) e do sistema complemento, produção de EROS e de trombina e uma alta concentração de cálcio intracelular, causam o aumento máximo da expressão de P-selectina endotelial de Weibel-Palade dentro de 10-20 min de reperfusão após isquemia. A interação da P-selectina com a glicoproteína ligante-1 da P-selectina (PSGL-1) expressa por neutrófilos resulta em uma fraca e reversível interação entre neutrófilos e endotélio, ou seja, a adesão seguida de rolamento[6, 7]. Em um modelo experimental de isquemia / reperfusão o bloqueio de L-selectina e /ou P-selectinas diminuiu tanto rolamento dos neutrófilos quanto adesão [8].

1.1.2 Firme adesão

Integrinas são proteínas heterodiméricas, contendo α-subunidades e β-subunidades que são expressas na superfície da célula. β2 integrinas são expressas em leucócitos e consistem em três α-subunidades distintas tais como CD11a, CD11b, e CD11c, que se ligam a uma β-subunidade comum, tal como CD18. A expressão relativa de α-subunidade difere de acordo com o estímulo, causando a adesão dos leucócitos e transmigração [9]. Moléculas de células endoteliais, tais como molécula de adesão intercelular (ICAM-1) agem como ligante para ambos CD11a / CD18 e CD11b / CD18; mas ICAM-2 apenas se liga com CD11a, resultando em forte adesão dos neutrófilos ao endotélio [10]. O aumento da adesão e migração de PMN para regiões pós capilares foi observado durante o estudo de um tecido que sofreu injúria por isquemia e reperfusão (IRI) [11]. Espécies reativas de oxigênio, fator de ativação plaquetária (PAF), a IL-1, Fator de necrose tumoral - α (TNF-α) e leucotrieno B4 (LTB4) liberados pelo endotélio e células do sistema imune após reperfusão provocam um aumento na expressão de β2 integrinas de neutrófilos a partir de grânulos intracelulares que resultam na firme adesão [12, 13].

1.1.3 Migração transendotelial /Diapedese

Moléculas de adesão plaquetária ao endotélio (PECAM-1) expressas sobre as bordas laterais das células endoteliais (CE) bem como em neutrófilos e estão envolvidas na transferência de neutrófilos para os tecidos, processo chamado como diapedese. O bloqueio de PECAM-1, conduz à inibição da diapedese, pois diminui a forte adesão entre neutrófilos e o endotélio [14]. Em outro estudo, o aumento da regulação de moléculas de adesão têm sido observadas após IRI, o que pode promover a diapedese de neutrófilos, contribuindo ainda mais para a disfunção muscular [15]. A interação entre CD11 / CD18-ICAM-1 e ROS também facilitam a diapedese e diminuem a expressão de caderina, e ao induzir a fosforilação de Caderina-vascular e catenina endoteliais , levando à soltura de junções intercelulares resultando na transmigração de neutrófilos [16, 17].

1.1.4 Quimiotaxia

Após a transmigração celular, as células se movem no sentido do aumento do gradiente de quimioatraentes, num processo conhecido como quimiotaxia [18]. Esses quimioatrativos para diferentes populações de leucócitos incluem os peptídios N-formilados produzidos por bactérias, tais como formil-Metionil-Leucil-Fenilalanina (fMLP), peptídios (por exemplo, C5a), e lípidos (por exemplo, leucotrieno-B4) [19]. Citocinas e quimiocinas, são uma nova família que inclui IL-8 [20], peptídio ativador de neutrófilos-2; relacionados ao oncogene de crescimento (GRO) -α, GRO-β e GRO-δ; e as proteínas inflamatórias de macrófagos MIP-2α e MIP-2β. Estas quimiocinas pertencem à família de CXC quimiocinas α/quimiocinas e são semelhantes em nível de estrutura. Outra família de quimiocinas é a CC quimiocinas β / quimiocinas, que inclui RANTES / CCL5 (regulada na ativação; expressa e secretada por células T normais); proteína quimioatrativa de monócitos-1, -2 e -3 (MCP-1/2/3) ; e proteínas inflamatórias de macrófagos, MIP-1α e MIP-1β [21].

Juntamente com a produção massiva de ROS, são liberadas proteases a partir dos grânulos de neutrófilos e metabólitos de ácido araquidónico (AA), tais como PAF e LTB4 que também estão envolvidos na lesão tecidual promovida por neutrófilos. PAF e LTB4 são potentes quimiocinas que estimulam a desgranulação dos neutrófilos [22].

1.2 Os grânulos de neutrófilos e Degranulação

Existem quatro tipos fundamentais de granulados em neutrófilos , como mostrado abaixo (Figura 2).

1.2.1 Grânulos azurófilos

Grânulos azurófilos ou grânulos primários são produzidos pela primeira vez durante a maturação dos neutrófilos, e contêm mieloperoxidase (MPO), que é uma enzima muito importante para o estresse oxidativo [23]. As defensinas, lisozima, proteína indutora da permeabilidade (BIP), e um número de serino proteases como: elastase de neutrófilos (NE), a proteinase 3 (PR3), e catepsina G (CG), também são armazenados nos grânulos primários [24].

1.2.2 Grânulos específicos (ou secundários)

Grânulos específicos contêm a glicoproteína lactoferrina e compostos anti-microbianos diferentes, que incluem a lipocalina associada a gelatinase de neutrófilos(NGAL), a proteína antimicrobiana catelicidina humana (hCAP-18), e a lisozima [23, 24].

1.2.3 As Gelatinases (grânulos terciários)

Os grânulos de gelatinase contêm alguns antimicrobianos, e armazenam metaloproteases, como gelatinase e leucolisina [25].

1.2.4 Vesículas secretórias:

Vesículas secretórias são ricas em albumina ligada à membrana, e armazenam moléculas necessárias à migração de neutrófilos [26].

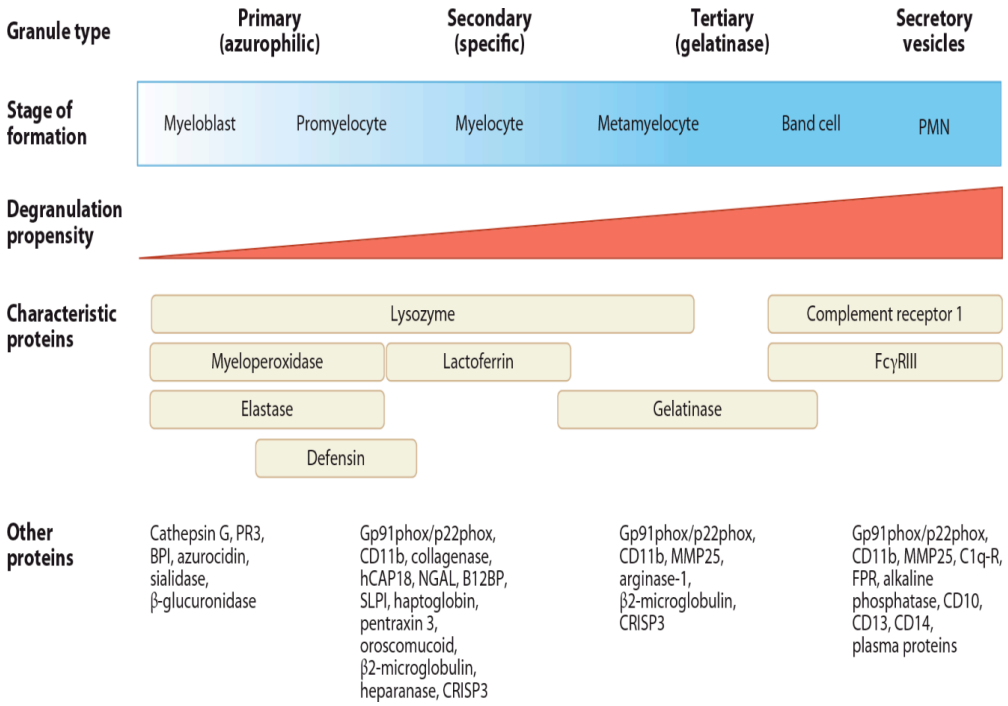

Figura 2 Os grânulos de neutrófilos e as suas proteínas características.

Os grânulos de neutrófilos transportam uma grande variedade de agentes antimicrobianos e moléculas de sinalização. Adaptado de [27].

1.2.5 Degranulação

A ativação de neutrófilos, provoca alteração da composição molecular de membrana dos grânulos resultando na mobilização dos mesmos, a fusão com a membrana plasmática ou fagossoma e a liberação do conteúdo para fora da célula. A ordem de mobilização é a primeira secreção de terciários, e depois de primários e secundários, sendo esta mobilização disparada pelos níveis de cálcio intra celular[28].

A mobilização de vesículas secretórias é necessária para a continuação da ativação dos neutrófilos, pois sua membrana contém as β2 integrinas, complemento e receptores de fMLP, bem como o receptor FcyRIII [25]; resultando na firme adesão dos neutrófilos ao endotélio e liberação dos grânulos de gelatinase, adicionando mobilizadores que liberam metaloproteases [29].

Depois do extravasamento, o estresse oxidativo se inicia com mobilização dos grânulos azurófilos e específicos que contêm flavocitocromo B558, um componente da maquinaria

de NADPH-oxidase. Como um resultado da montagem do complexo de NADPH-oxidase ocorre a produção de ROS tanto no interior do fagolisossoma e quanto fora da célula, criando um ambiente antimicrobiano [30].

1.3 Isquemia

A isquemia é o fornecimento insuficiente de sangue a um órgão, que conduz a uma disfunção celular e necrose. Ela ocorre principalmente no caso de trauma, choque, cirurgia ou transplante de órgãos [31].

1.3.1 Efeitos celulares da Isquemia

Uma Isquemia prolongada resulta numa variedade de alterações metabólicas celulares e ultra-estruturais (fig-3A). Durante a isquemia, o metabolismo anaeróbio produz uma diminuição no pH celular por acumulação de íons de hidrogênio e, em seguida, a bomba de Na^{+}/ H^{+} excreta os íons de hidrogênio em excesso, resultando em grande influxo de íons de sódio [32]. O ATP celular se esgota e inativa as ATPases, reduzindo efluxo ativo de Ca^{2+} e limitando a re-absorção de cálcio pelo retículo endoplasmático, produzindo assim, uma sobrecarga de cálcio na célula. Como um resultado de transição da permeabilidade mitocondrial (MPT) e de poros abertos, o que perturba ainda mais a produção de ATP, interrompendo o potencial de membrana mitocondrial. A magnitude do fluxo sanguíneo e duração do efeito isquemia influencia no grau de lesão tecidual [33] (fig-3A). O factor indutível de hipoxia 1 (HIF-1) induz o aumento na transcrição do fator de crescimento endotelial vascular (VEGF), que também desempenha um papel importante na angiogênese [34, 35].

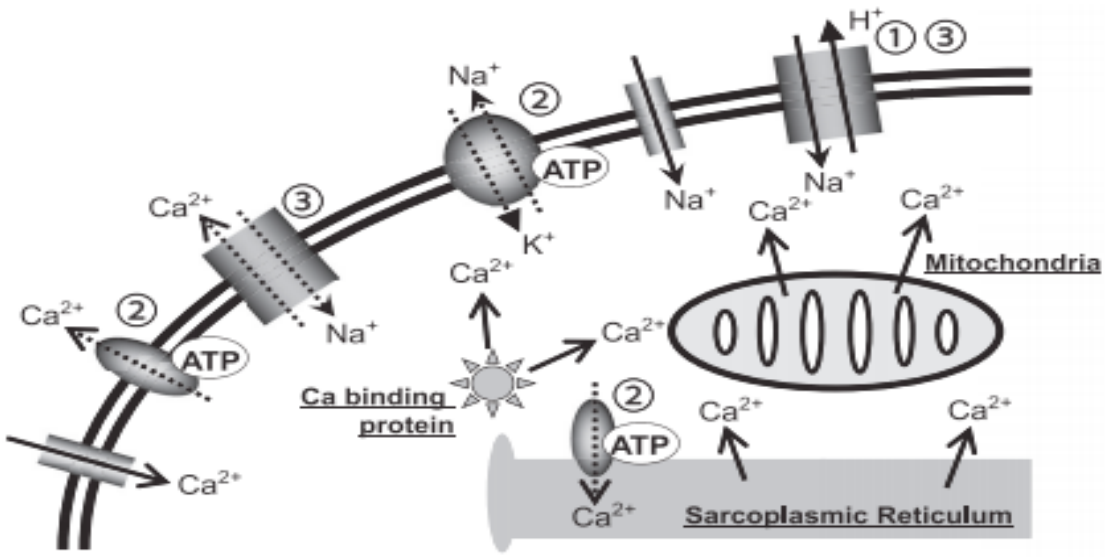

Figura 3 Efeitos da esquemia na célula.

Modificado de [32]. (1) A excreção de H +, devido a uma diminuição do pH, (2) desativação devida à perda de ATP, e (3) redução de Na + / Ca2 + devido à redução de pH extracelular e a acumulação de Na + intracelular.

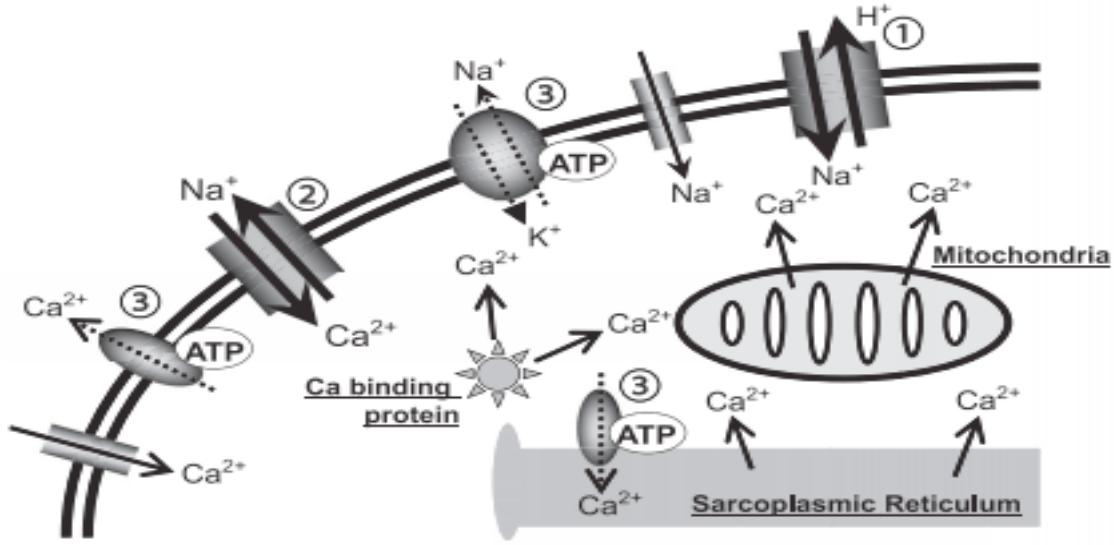

Figura 3-B: Efeito celular da reperfusão. Modificado de [32]. (1) A robusta excreção de H +, devido à pronta recuperação de pH extracelular, (2) "modo reverso" excreção de Na + acumulado e influxo de Ca2 +, por sua vez, e (3) re-excreção de Ca2 + seguido de recuperação da síntese de ATP.

1.4 Lesão isquêmica de reperfusão (IRI)

Reperfusão resulta na infiltração de neutrófilos ativados no local da lesão, contribuindo para a resposta inflamatória aguda [36]. O mecanismo subjacente a lesão de reperfusão é complexo, multi-fatorial (Fig-3B) e envolve:

1. A geração de espécies reativas de oxigênio (ROS) durante a re-introdução de oxigênio molecular,

2. Sobrecarga de cálcio,

3. Abertura de poros MPT,

4. Disfunção endotelial,

5. Acúmulo de hipoxantina,

6. A expressão de determinados produtos gênicos pró inflamatórios, tais como as moléculas de adesão dos leucócitos, citocinas,

7. Repressão de produtos de genes de proteção como constitutiva da óxido nítrico sintase, trombomodulina e agentes bioativos, isto é, a prostaciclina, óxido nítrico [37].

Vasoconstrição após a lesão por reperfusão ocorre como um resultado da diminuição da biodisponibilidade de mediadores endoteliais, que resultam em uma maior produção de moléculas de adesão e citocinas. Essas moléculas de adesão e citocinas recrutam células inflamatórias que libertam ainda mais mediadores inflamatórios, conduzindo a disfunção endotelial e maiores danos aos tecidos [38, 39].

1.5 Reperfusão Isquêmica Intestinal (IRI) e PMN

Intestino é o órgão mais sensível à IRI e é causada por várias condições clínicas, como isquemia mesentérica aguda, obstrução intestinal, hérnia encarcerada, o transplante de intestino delgado, enterocolite necrosante neonatal, trauma e choque. Tal fenômeno pode resultar em síndrome clínica grave, ou até mesmo a morte [40, 41]. Por exemplo, a isquemia mesentérica aguda (AMI) tem mortalidade de 60% a 80%, e a incidência está aumentando com o tempo, havendo dificuldade em se reconhecer a condição [42, 43].

IRI dos intestinos altera a absorção intestinal, resultando na baixa absorção de nutrientes, causando infarto do intestino, síndrome do intestino curto e até mesmo a morte [44]. A translocação bacteriana através da mucosa epitelial para locais extra-intestinais pode ocorrer após IRI que, posteriormente, pode induzir sepse, choque ou falência de múltipla de órgãos (MOF). A translocação bacteriana tem sido notada em 44% dos pacientes pediátricos após o transplante de intestino delgado [45, 46]. Similarmente a endotoxina lipopolissacarídeo (LPS), que é parte da membrana exterior de bactérias gram-negativas, liga-se a TLR4 e no final amplifica a produção de citocinas [47-49]. Espécies reativas de oxigênio, tais como peróxido de hidrogênio, superóxido, juntamente com citocinas levam ao desenvolvimento de síndrome da resposta inflamatória sistêmica (SIRS), que pode evoluir para falência de múltiplos órgãos (MOF) [50]. A infiltração pulmonar de neutrófilos, que é um processo bem estudado, contribui para o desenvolvimento da síndrome da angústia respiratória aguda (ARDS) e lesão pulmonar aguda (ALI) [51].

O intestino é composto de células lábeis que são sensíveis e facilmente feridas por isquemia e reperfusão [52]. A mucosa do intestino torna-se o local para a produção de várias proteínas de fase aguda [53], hormônios intestinais [54], citocinas [55], espécies reativas de oxigênio [11], o óxido nítrico [56], derivados do AA [57], e moléculas de adesão celular [58]. Respostas inflamatórias moleculares e celulares como a transcrição de fatores nucleares -κB (NF-κB) [59], a indução do fator de estimulação de colônias de granulócitos (G-CSF) e interleucina (IL) -6 influenciam recrutamento de neutrófilos para a região o muscular intestinal após ocorrer a IRI [55].

Diversos estudos comprovaram que PMNs estão envolvidos na fisiopatologia da IRI, onde a lesão de reperfusão intestinal é principalmente devido a interações de leucócitos e CE na mucosa do intestino transplantado [60]. O esgotamento dos PMNs do sangue antes da reperfusão mostrou diminuir IRI no intestino delgado humano [61]. Estudos com microscopia intra-vital em tecidos após eventos de IRI mostraram uma resposta inflamatória aguda devido ao aumento do efluxo de proteínas e de adesão de PMN em vênulas pós capilares [11]. Riaz et al. demonstraram que após o IRI do intestino do rato, tanto P- e E-selectinas aumentaram sua expressão. O bloqueio de P-selectina reduz o rolamento e adesão dos PMN, de modo a atenuar a lesão [62]. PMNs causam danos por

caminhos diferentes, como a secreção de enzimas proteolíticas de grânulos citoplasmáticos [63], a produção de radicais livres pela explosão respiratória [64], e danos à microcirculação e extensão da isquemia [65]. Estudos demonstraram que PMNs são a fonte inicial de radicais livres, em modelo de rato com IRI do intestino [66]. Esta lesão por reperfusão intestinal provoca não só resposta local inflamatória aguda, mas também lesões pulmonares notáveis, bem como alterações inflamatórias sistêmicas [67]. Estratégias farmacológicas, que reduziram a infiltração de neutrófilos também reduzir IRI [67, 68]. Apesar de inúmeras modalidades e substâncias que foram testadas para reduzir a mortalidade induzida por isquemia/reperfusão, nenhuma foi totalmente bem sucedida. Além disso, os mecanismos moleculares e vias subjacentes da IRI ainda são pouco conhecidos. Neutrófilos são muito importantes na IRI, e a participação dos neutrófilos neste processo ainda não é completamente conhecida. Para uma melhor compreensão dos mecanismos moleculares que ocorrem durante o IRI, é necessário uma maior compreensão da biologia dos neutrófilos. Isso será possível a partir do conhecimento do proteoma de neutrófilos.

1.6 Os mediadores e receptores de IRI

1.6.1 Leucotrienos (LT) B4

Leucotrieno (LT) B4 é um dos mediadores inflamatórios conhecido por ativar neutrófilos e induzir seu recrutamento em tecidos intestinais após a isquemia e reperfusão grave da artéria mesentérica superior. Em estudos farmacológicos com antagonista do receptor LTB4, não foi demonstrado nenhum efeito sobre os neutrófilos, portanto, receptor BLT desempenha um papel menor nas lesões locais, remotas e sistêmicas após IRI grave em ratos [69]. O LTB4 é produzido como um resultado do metabolismo do ácido araquidônico (AA). Ele é produzido por uma reação de catálise da 5-lipoxigenase e de leucotrieno A4 hidrolase [70] que se liga ao receptor acoplado à proteína G de BLT-1, promovendo a quimiotaxia dos neutrófilos [71, 72].

1.6.2 TNF-α

TNF-α é liberado durante a IRI e atua como mediador da cascata inflamatória. A diminuição do recrutamento dos neutrófilos e lesão de tecidos foi observada após a inibição do TNF-α [73]. TNF-α também induziu apoptose em neutrófilos [74]. Num

estudo de TNF-α e IL-1β a produção do mesmos foi associada com a resposta inflamatória mediada em parte pelo receptor Toll-like (TLR), na sinalização em modelos de IR. Esta inflamação pulmonar e intestinal era dependente de sinalização TLR / MyD88 sugerindo o envolvimento da cinase p38 e NF-kB [75].

1.6.3 Trombina

A trombina induz o rolamento e adesão de leucócitos após IR e antitrombina diminuiu acentuadamente a lesão pulmonar caracterizada pela diminuição do extravasamento, sequestro de leucócitos e atividade da MPO [76]. Trombina induz a via PAR1 através de receptores acoplados à proteína G, resultando na libertação de neutrófilos de rato induzida por citocina quimioatrativa-1 (CINC-1) (quimiocina) durante IR [77].

1.6.4 Canais de potássio (KATP)

Em células epiteliais do intestino delgado, os canais de K + fornecem a força motriz para o processo de transporte através da membrana plasmática, e estão envolvidos na regulação do volume celular. O ajuste fino de transporte de sal e água e de K + (homeostase) ocorre em células epiteliais do cólon, onde os canais de K + estão envolvidos nos processos de secreção e reabsorção [78].

Em estudos com bloqueadores de canais de potássio (KATP), foi mostrado a supressão na migração de neutrófilos e a quimiotaxia, durante as respostas inflamatórias agudas. Lesão local, remota e sistêmica foram impedidas após o tratamento com glibenclamida (bloqueador de canais KATP), sugerindo importante papel dos canais KATP na lesão intestinal em modelo de rato associada aos neutrófilos [79].

1.6.5 Sistema complemento

Sistema do complemento é um mediador conhecido que está envolvido na lesão por isquemia / reperfusão (I / R), que exerce os seus efeitos de várias maneiras. Por exemplo, o complexo de anafilatoxinas (C3a e C5a) e o complexo de ataque à membrana (C5b-9), induzem a expressão aumentada de ICAM-1, E-selectina endotelial, P-selectina, IL-8, MCP-1, e de ROS. Como resultado temos a atração e agregação de neutrófilos, quimiotaxia, atividade citotóxica, ocorrendo a liberação de ROS metabólitos e proteases [80, 81]. Além disso, a C5a é um quimioatraente potente para outras células do sistema imunológico e leva à produção aumentada de moléculas de adesão vascular [82]. O

receptor C5a (C5aR) em camundongos knockout, antes da oclusão SMA levou a proteção de lesão intestinal e diminui o seqüestro derivados do intestino neutrófilos pulmonar [83].

1.6.6 Receptores CXC 1 e 2 (CXCR1/2)

CXCR1 e CXCR2 pertencem à classe de receptores acoplados à proteína G (GPCR), atuando como receptores para C5a, LTB4, PAF, e fMLP [84]. O Bloqueio de CXCR1 e CXCR2 reduziu significativamente a infiltração de neutrófilos na lâmina jejuno, no parênquima pulmonar e no derrame vascular nas vias aéreas (proteína BAL), porém não teve nenhum efeito sobre a expressão de mieloperoxidase, IL-1, IL-6, GRO, MIP-2 e MMP-9 [85, 86].

1.6.7 Espécies reativas de oxigênio (ROS)

Espécies reativas de oxigênio como ânion superóxido (O2 •), peróxido de hidrogênio (H_2O_2) e radical hidroxila (OH•) pode provocar a oxidação de proteínas, DNA, fosfolipídios e outras estruturas biológicas. Durante a reperfusão, o PAF, o TNF-α, IL-6, IL-1β, GMCSF, C5a e a ROS auto estimulam as células endoteliais e a produção ROS em neutrófilos [87, 88]. As principais fontes de ROS em neutrófilos são NADPH-oxidase, xantina oxidase (XO), as mitocôndrias e o metabolismo do ácido araquidônico após a reperfusão [89, 90]. As ROS podem levar diretamente a danos estruturais, aumentar a abertura MTP, ativar o sistema imunológico e ECs, e induzir a apoptose [91].

1.7 Proteômica baseada em Espectrometria de Massas

1.7.1 Introdução à espectrometria de massas

O espectrômetro de massa é um instrumento que mede as razões entre massa-carga (m / z) de íons de modo a encontrar sua massa molecular. Um espectrômetro de massa típico consiste em uma fonte de íons, um analisador de massa e um detector. A fonte de íons cria os mesmos em fase gasosa a partir de diferentes analitos. O analisador de massa resolve os íons de acordo com a sua proporção de massa-carga (m / z). E, sequencialmente, o detector detecta os íons. Fig.4 é um esquema gráfico de um espectrômetro de massa.

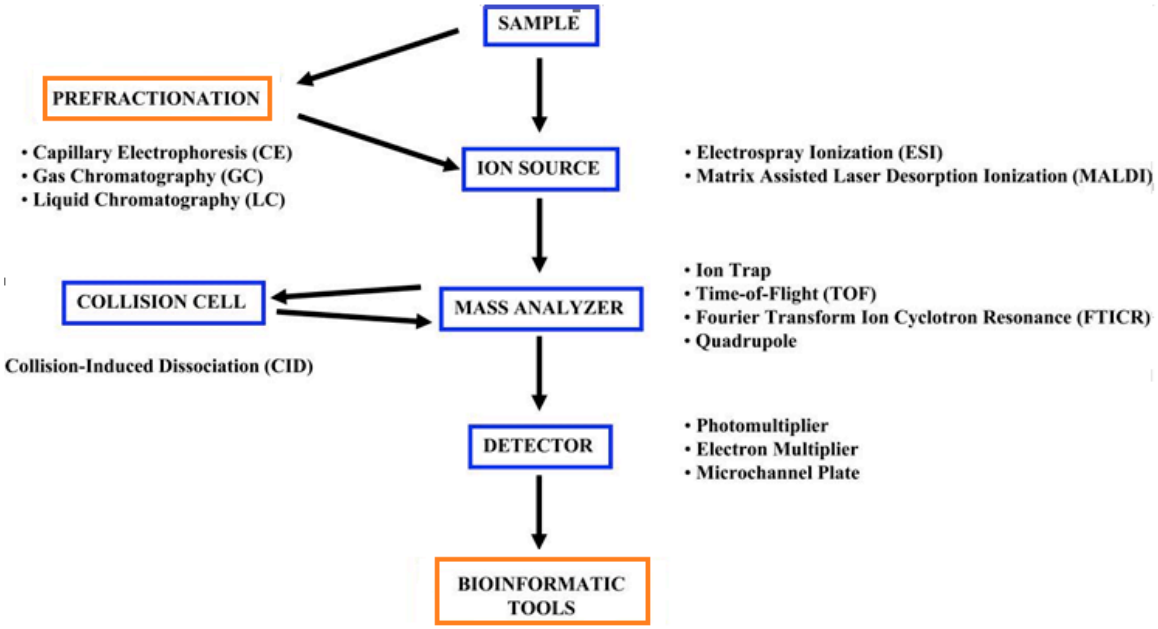

Figura 4 Esquema representativo de passos realizados em um espectrômetro de massas.

(caixas azuis) com algumas medidas relacionadas com a preparação da amostra e análise de dados (caixas de laranja). A maioria das caixas representam componentes de um espectrômetro de massa. As caixas nomeadas pré-fracionamento e amostra, representam passos executados para preparar a amostra para a espectrometria de massa. Ao lado das caixas são representados alguns dos tipos mais comuns de elementos de espectrometria de massa. Adaptado de [92].

1.7.1.1 Fonte de íons

Existem muitos métodos de ionização, incluindo ionização química (CI) e dessorção por plasma (PD), que foram introduzidas em 1966 e 1974 [93]. Mais tarde, por bombardeamento atômico rápido (FAB) [94], a espectrometria de massa de íons secundários em meio líquido (LSI-MS) [95], com ionização por eletrospray (ESI) (Fig.5-A) [96] e de matriz assistida por laser de ionização e dessorção (MALDI) (Fig.5-B) [97] foram desenvolvidos, sendo os dois últimos os métodos predominantes atualmente aplicados em proteômica. Na análise por MALDI, o analito é a primeiramente co-cristalizado a uma matriz. Depois disso, uma radiação laser é aplicada a esta mistura (matriz-analito) conduzindo à sublimação de matriz e do analito, e a matriz doa uma carga para o analito [98]. Os íons gerados a partir MALDI são na sua maioria isolados

carregadamente e acelerados por um campo eletrostático para o analisador. A principal desvantagem de MALDI é a reprodutibilidade inferior (diferente de tiro a tiro) devido à preparação da amostra e o seu depósito não homogêneo sobre a superfície da placa/sonda. No entanto, permite a ionização por MALDI dos analitos de massa molecular muito elevada; até 300,000 Da. ESI ioniza analitos em solução, onde a aplicação de um campo elétrico forte resulta na evaporação da solução de amostra para a fase gasosa de electrospray com gotículas altamente carregadas (ES). Enquanto as gotículas carregadas evaporam, o analito é ionizado e transferidos para a fase gasosa e MS lentes com carga oposta atraem estes íons. ESI tem a vantagem de produzir íons de cargas múltiplas a partir de grandes biomoléculas. Além disso, o acoplamento a um pré-fraccionamento de moléculas utilizando cromatografia líquida de alta eficiência (HPLC), com a ESI-MS tornou esta técnica altamente proficientes na análise de diferentes tamanhos de moléculas com diferentes polaridades, em uma amostra contendo uma mistura complexa[99].

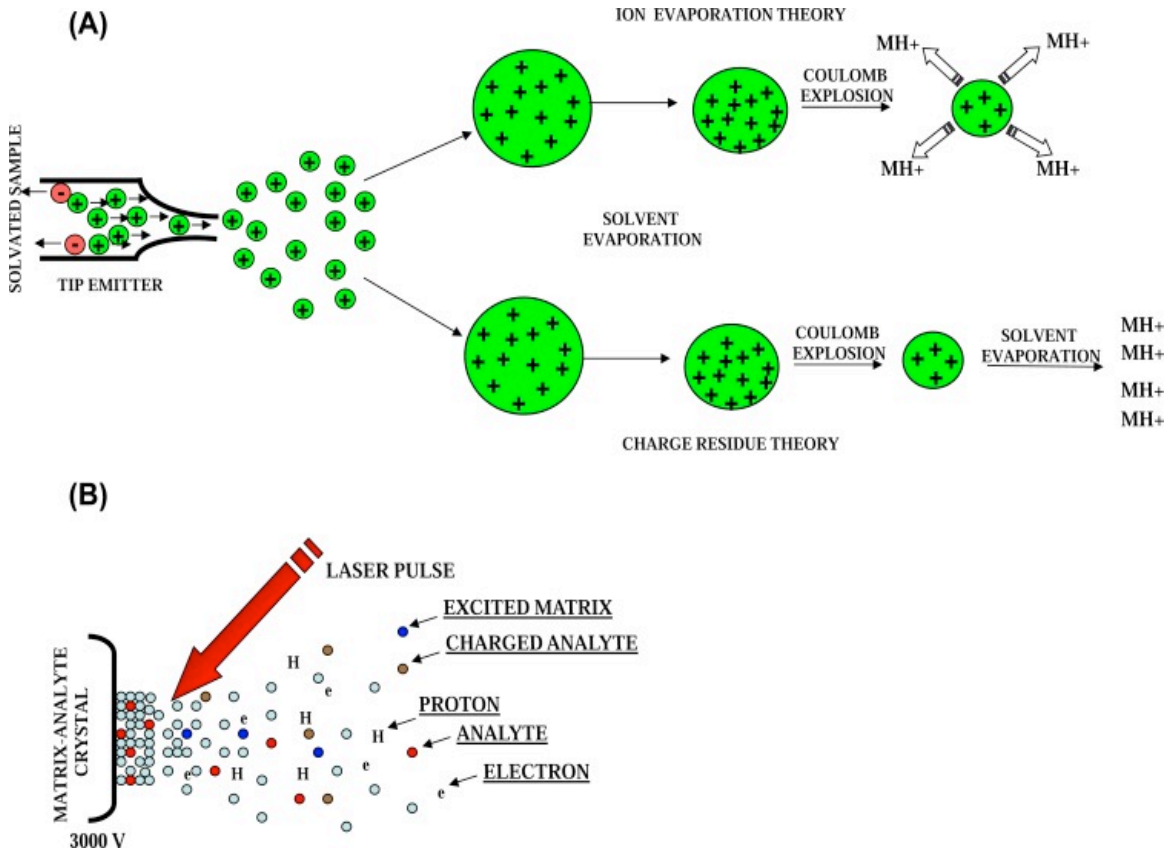

Figura 5 Técnicas de ionização por MS.

1.7.1.2 Analisador de massa

Um analisador de massa separa os íons de acordo com os seus valores de m / z. Existem diferentes princípios físicos utilizados para a separação de íons, em analisadores de tradicionais são feitas eletricamente (ou seja, utilizando pólos magnéticos) utilizando um campo magnético. Atualmente, analisadores de massa são compostos por um quadrupolo (Q), quadrupolo ion trap (QIT), time-of-flight (TOF), e transformada de Fourier de ressonância cyclotrone ion (FT-ICR); tipos de analisadores (Fig. 6).

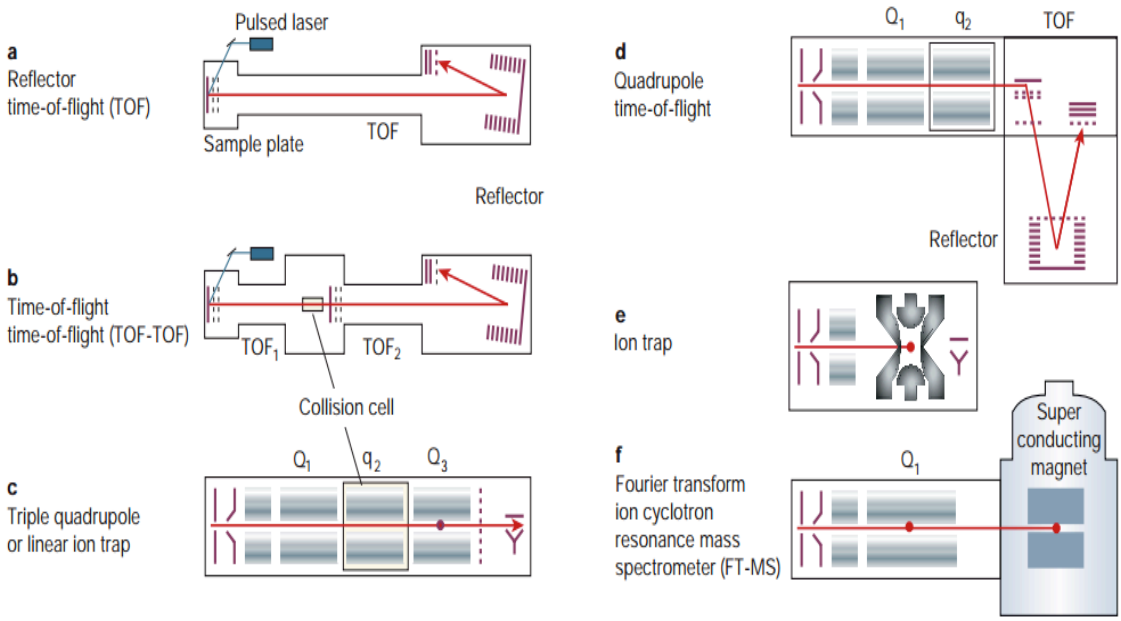

Figura 6 Espectrômetro de massa utilizada na pesquisa de proteoma.

Adaptado de [100]. (a) Instrumentos Tempo de vôo (TOF), (b) Instrumento TOF-TOF, (c) Espectrômetros de massa de quadrupolo, (d) instrumento Quadrupolo TOF, (e) O ion trap (tridimensional) e (f) instrumento FT-MS.

As características de um analisador de massa são determinados pela resolução (a eficiência de separação de íons, através da sua razão (m / z), a precisão de massa (confiança dos valores de m / z), faixas de massa, a aquisição e precisão de MS / MS (a capacidade de reproduzir uma medida da massa de um dado composto) incluindo a faixa dinâmica (a razão entre o mais abundante e o menos abundante detectados dentro de um único *scan*, para garantir precisão massa específico). A aquisição mais recente da família

FT / MS é o analisador Orbitrap, que é uma modificação da QIT, onde o Orbitrap trabalha com campos eletrostáticos estáticos, enquanto o QIT usa uma dinâmica de campo elétrico tipicamente oscilante em ~1 MHz. Espectrômetros de massa Orbitrap fundamentalmente se diferem da maioria dos espectrômetros de massa FT-ICR por causa de sua constituição no mecanismo de excitação por injeção [101]. Orbitraps tem uma elevada precisão de massa (1-2 ppm), um poder de resolução elevado (de 240.000 , e detecção de m/z de até 400), uma faixa dinâmica elevada (cerca de 5000) e de alta sensibilidade [102-104].

O tipo de instrumento aplicado em espectrometria de massa neste trabalho de pesquisa de doutorado foi um LTQ-Orbitrap Velos. Ele inclui uma fonte de íons por eletrospray (ESI), e duas armadilhas de íons LTQ. É possível ejetar os íons diretamente no analisador de massa Orbitrap ou na câmara de colisão (. Fig 8).

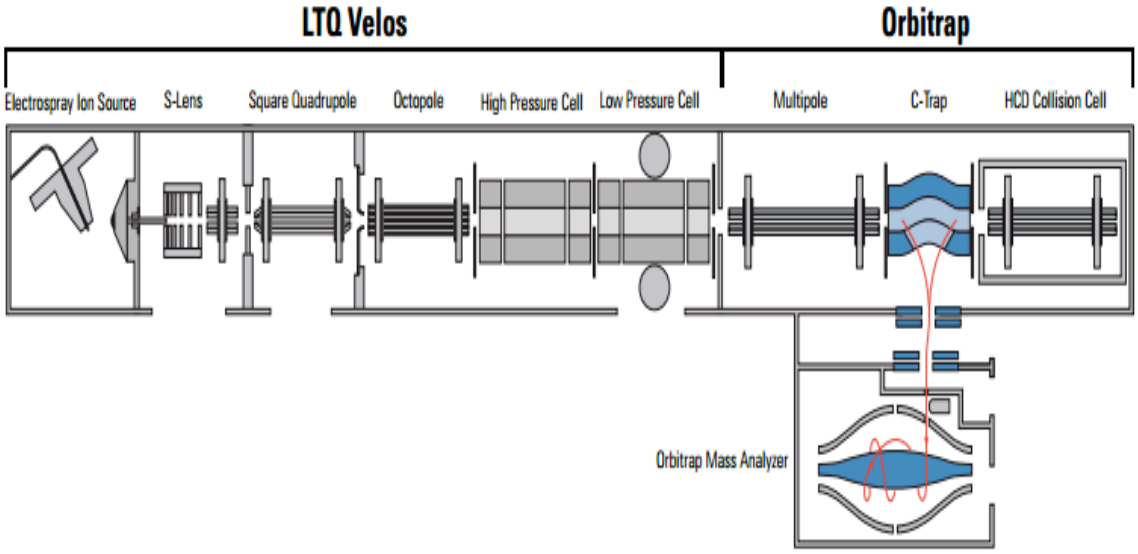

Figura 1 Visualização esquemática do LTQ Orbitrap Velos. Adaptado de [105].

1.7.1.3 Fragmentação de peptídeos

Para obter informações sobre a sequência de aminoácidos de um peptídeo a partir de uma proteína proteoliticamente digerida usando espectrometria de massa, o peptídeo precursor de íons tem de ser fragmentado em uma "escada" de íons consecutivamente em fragmentos de íons menores, cada um tendo perdido um aminoácido ou mais. A técnica

de fragmentação de peptídeos mais comum em MS, é a dissociação induzida por colisão (CID), leva os íons dos fragmentos em N e C-terminais resultando da clivagem de uma ligação C-N no esqueleto do peptídeo, produzindo então íons *y* e *b*, respectivamente (Fig. 8). Os outros tipos de métodos de fragmentação importantes na análise de peptídeos são a dissociação de captura de elétrons (ECD) e dissociação por transferência de elétrons (ETD), que produzem fragmentos N e C-terminais da cadeia principal entre o átomo de carbono alfa e o nitrogênio, gerando assim íons *c* e *z*, respectivamente [106, 107]. A fragmentação por ETD pode identificar modificações pós-traducionais CID-estáveis (PTMs). Com o uso do ETD, para estes peptídeos com PTMs, pode-se adicionar tanto a informação da sequência quanto da localização dos sítios de modificação. Outro método alternativo é a fragmentação que é um tipo de CID, porém sendo de alta energia de dissociação por colisão (HCD). O destaque do padrão de fragmentação do HCD é a maior energia de ativação e menor tempo de ativação em comparação com a tradicional CID em ion trap. Na fragmentação por HCD também são gerados fragmento de íons do tipo *b* e *y*. Embora a energia mais elevada para o HCD leva a uma predominância de íons de *y*; íons do tipo *b* podem ser ainda fragmentados a espécies menores de íons. Sem a restrição de corte baixa massa e com elevada precisão MS2 espectros de massa, HCD tem sido aplicado com sucesso para sequenciamento *de novo* de peptídeos, fornecendo uma série de íons mais informativa. Quanto aos estudos com PTMs, certos íons diagnósticos específicos para HCD podem ser reconhecidos para a identificação de PTMs. Fragmentação eficiente com detecção em uma larga faixa de m/z faz do HCD uma ferramenta poderosa para sequenciamento e quantificação de peptídeos marcados com *tags* do tipo iTRAQ . Em particular, a combinação de alta qualidade de exatidão de massa em espectros MS/MS, com a alta resolução e abundância de íons repórter do marcador iTRAQ é bem adequado para a identificação e quantificação simultânea de peptídeos em digestos de amostras complexas de proteína [108, 109].

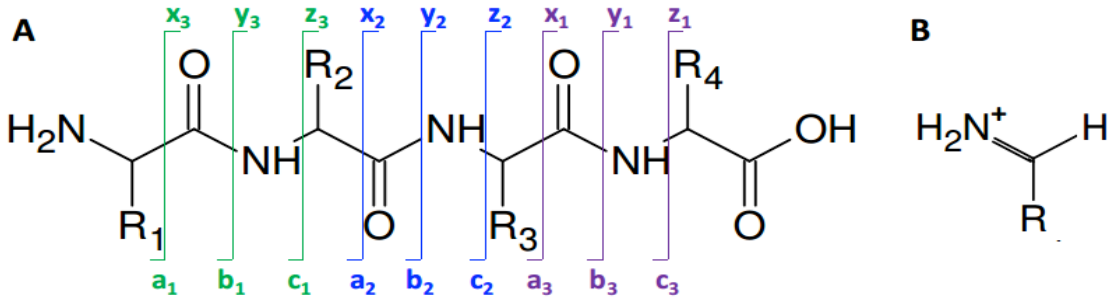

Figure 2 Nomenclatura de fragmentação de peptídoes Roepstorff-Fohlman-Biemann [107, 110].

A. A clivagem de um simples Cα-C, C-N, ou N-C α bond resulta em íons *a*, *b*, e *c*, respectivamente, quando a carga é retida da porção N-terminal; enquanto íons x,y ou z são produzidos, respectivamente, quando a carga é retida da porção C-terminal do fragmento. **B**. Dupla clivagem da estrutura, resultando em apenas um imônio, contendo uma única cadeia lateral.

1.8 Proteômica Quantitativa

Espectrometria de massa baseada em proteômica quantitativa é usada em pesquisas biológicas e clínicas, para a identificação de módulos funcionais e vias, ou até mesmo para a identificação de biomarcadores de doenças. Resultados quantitativos podem ser obtidos através da utilização de uma marcação com isótopos estáveis, ou através de métodos sem marcação (*Label free*)[104, 111]. As técnicas com marcação isotópica têm alta reprodutibilidade, enquanto técnicas *label-free* requerem sistemas de alta reprodutibilidade cromatográfica (LC- MS/MS) [112]. Vários métodos foram desenvolvidos baseados em marcação com isótopos pesados (2H, 13C, 15N e 18O), como a marcação com aminoácidos marcados com isótopos estáveis em cultura de células (SILAC) [113], Isótopos marcados com afinidade a uma *tag* (ICAT) [114] e *Tags* isobáricas para quantificação relativa e absoluta (iTRAQ) [115]. Em contraste com as marcações ICAT e SILAC onde duas ou três amostras são comparadas, a marcação com iTRAQ de quatro a oito amostras são marcadas e analisadas e quantificadas simultaneamente [115, 116]. Ao analisar a combinação de múltiplas amostras e uma única corrida, reduz-se o tempo de uso do equipamento das análises, e da variação entre

diferentes corridas de LC/MS, aumentando a acurácia dos resultados. Estudos comparativos para diferentes marcações isotópicas, incluindo eletroforese diferencial em gel (DIGE), ICAT, e iTRAQ mostraram que iTRAQ é mais sensível do que ICAT [117]. A técnica com a marcação por iTRAQ possibilita alto rendimento para análises de proteômica quantitativa, produzindo um grande conjunto de dados [115, 116, 118].

1.8.1 Marcações isobáricas para quantificação relativa e absoluta (iTRAQ)

Quantificação relativa e absoluta pode ser realizada com iTRAQ, porém para quantificação absoluta são necessários padrões internos de referência [115, 116].

1.8.2 A química do reagente iTRAQ™

O reagente iTRAQ™ é uma *tag* isobárica que pode marcar a maioria dos peptídeos e proteínas, uma vez que o mesmo reage com aminas primárias da porção amino terminais, incluindo o N-terminal e o grupo ε-amino da cadeia lateral das lisinas. Cada *tag* contém um único grupo repórter, um grupo de peptídeo reativo, e um grupo de balanço neutro, estes em conjunto mantém uma massa total of 145Da (Figura 9). Durante a fragmentação peptídica no evento de MS/MS, os grupos repórter iTRAQ™ se separaram das *tags* isobáricas e produzir íons distinguíveis com m/z 114, 115, 116 e 117. Desse modo, as intensidades relativas dos íons repórter forneceram a abundância relativa de cada peptídeo para cada uma das amostras. Esta fragmentação MS/MS de iTRAQ™ ligaado aos peptídeos também produz fortes sinais dos íons y e b, favorecendo uma identificação com maior confiabilidade [119].

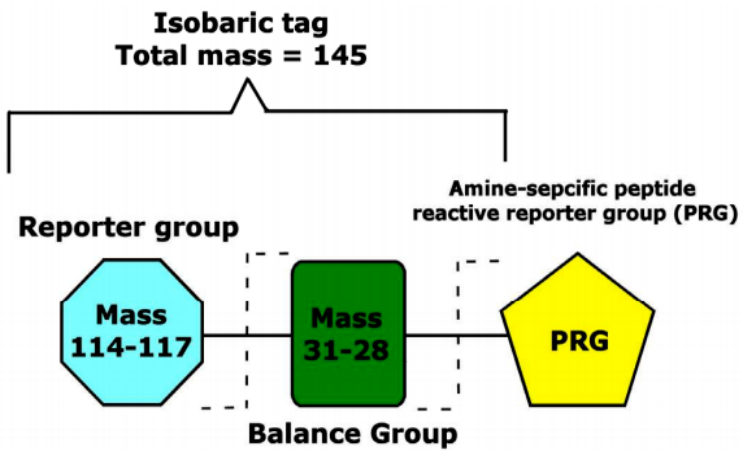

Figura 9 Estrutura do reagent iTRAQTM. Adaptado de [120].

1.8.3 Fluxograma de trabalho do reagente iTRAQ™

As amostras são reduzidas, alquiladas e depois digeridas com a enzima tripsina. O conjunto de peptídeos obtidos depois da digestão são então marcadas com uma das quatro *tags* de iTRAQ™. Em seguida, os peptídeos marcados são reunidos em uma única alíquota, separados por cromatografia líquida (LC), e as frações obtidas ao fim do processo são analisados por Espectrometria de Massas (Figura 10).

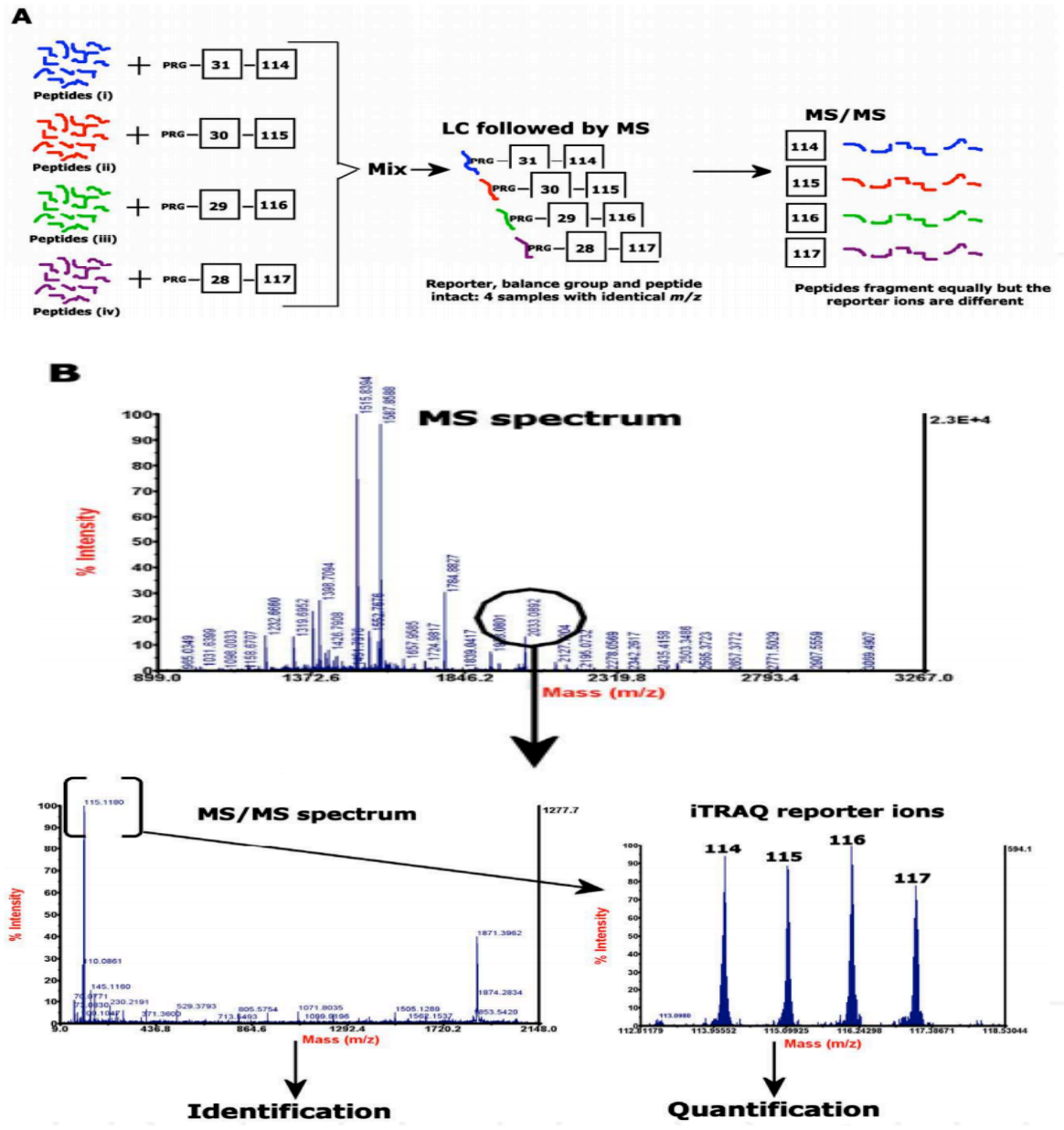

Figura 10 Um esquema geral e exemplo de dados para um experimento iTRAQ 4-Plex. Adaptado de [120].

A quantificação por iTRAQ^{TM} pode ser realizada com base no LTQ-Orbitrap e incluem a dissociação Q pulsada (PQD) [121] e de dissociação de maior energia na C-trap (HCD) [122]. A quantificação com iTRAQ^{TM} é mais sensível e precisa para um proteoma total, podendo ser feito usando o método fragmentação HCD em complemento a técnica de fragmentação CID [123].

1.9 Fosfoproteômica

A fosforilação de proteínas é uma modificação pós-traducional essencial, afeta a maioria das atividades celulares incluindo a transdução do sinal, a expressão de genes, a progressão do ciclo celular e outras funções biológicas [124]. Enzimas dedicadas à fosforilação de proteínas estão entre a maior classe de enzimas de PTM (modificação pós traducional). Essa superfamília de proteínas cinases foi denominado o kinome, com mais de 500 membros do kinome humano. As proteína cinases catalisam a transferência de um grupo fosfato a partir de um composto orgânico de alta energia, tais como a adenosina trifosfato (ATP) para a cadeia lateral de serina, treonina, tirosina ou histidina resíduos de aminoácidos das proteínas de mamíferos. Cinases são conhecidas por englobar 1,7% dos genes humanos [125, 126]. Além disso, estima-se que a abundância relativa de fosfoserina, treonina, e tirosina no proteoma humana são 90%, 10%, e 0,05%, respectivamente [127]. Por hidrólise da ligação covalente fosfodiéster, libertando assim o ortofosfato, as fosfatases catalisam a remoção enzimática destes grupos fosfato a partir de proteínas, devolvendo-nas ao seu estado não fosforilado [128]. A fosforilação afeta a estrutura da proteína, alterando a carga e a hidrofobicidade da cadeia lateral do aminoácido. Aminoácidos carregados positivamente ou negativamente, em estreita proximidade com o resíduo fosforilado serão repelidos ou atraídos, respectivamente, e a porção de fosforil, além disso, vai introduzir uma região muito hidrófilica e polar na proteína afetada. Deste modo, podem ser induzidas alterações conformacionais, que afetarão as propriedades da proteína [129].

A análise de fosfopeptídeos é um desafio para espectrometria de massa por várias razões [130]:

1. A alta atividade da fosfatases requerem uma preparação sensível amostra, evitando a perda das proteínas modificadas;

2. A fosforilação é uma PTM lábil, que pode ser perdido durante o processo de fragmentação MS/MS;

3. A fragmentação de um peptídeo incompleto complica a localização correta do sítio de fosforilação;

4. A baixa estequiometria dos fosfopeptídeos implica no uso de estratégias de enriquecimento, que têm suas limitações (veja a próxima seção);

5. Alguns dos peptídeos multi fosforilados exibem menos intensidades de íons, em comparação com os peptídeos menos fosforilados pela análise convencional por RPLC-MS/MS [131, 132];

6. O fosfoproteoma é dinâmico e complexo. Atualmente, prevê-se que mais de 100,000 sítios de fosforilação estão presentes em proteínas de mamíferos, distribuído numa vasta faixa dinâmica [133]. No entanto, estudos de grande escala atingem atualmente mais de 20.000 sítios utilizando técnicas de enriquecimento para fosfopeptídeos e LC-MS. Diferentes estratégias de fracionamento de amostra e enriquecimento para fosfopeptídeos podem então resolver o problema da baixa estequiometria dos fosfopeptídeos.

1.9.1 Enriquecimento de PTM-específicas

Existem vários métodos de enriquecimento de PTM-específicas para proteínas e peptídeos, incluindo cromatografia de afinidade para PTM-específicas ou imunoprecipitação com anticorpos específicos da PTM. Fosfoproteínas podem ser purificadas por meio de resinas de afinidade específica para a PTM [134] ou anticorpos que reconhecem resíduos de aminoácidos fosforilados [135]. A digestão subsequente da proteína e análise por LC-MS/MS dos peptídeos fornecerá a localização dos sítios de fosforilação nas proteínas recuperadas. No entanto, esta técnica é mais útil para enriquecer peptídeos, antes da análise por MS da PTM, o que pode melhorar a sensibilidade e especificidade da análise. A Cromatografia por afinidade com metal imobilizado (IMAC), [136], ou colunas de TiO_2 [137] são utilizados para enriquecer os peptídeos com PTM antes da análise por MS/MS. Métodos de cromatografia de troca de cátions e aniôns também são úteis para reduzir a complexidade da amostra de peptídeos, incluindo fosfopeptídeos. As combinações destes métodos revelaram milhares de sítios

de fosforilação em proteínas de diferentes espécies. A técnica IMAC mostrou maior sensibilidade para peptídeos multi-fosforilados, sendo assim, a troca por cromatografia de fase reversa antes IMAC tem sido usado com um alto risco de perda destes peptídeos fosforilados [138, 139].

1.9.1.1 Cromatografia de afinidade com dióxido de titânio TiO2:

TiO_2 é uma resina que pode criar uma interação iônica com os grupos fosfato das biomoléculas, que ao ser misturado a amostra ou usado em microcolunas, se liga aos peptídeos que apresentam fosforilações. O procedimento de lavagem elimina todos os peptídeos não que estão vinculados a resina; na etapa seguinte, a de eluição quebra-se a ligação entre a modificação e a resina, criando-se uma mistura de peptídeos eluídos contendo uma fração altamente enriquecida de fosfopeptídeos. Esta abordagem, comparada a outros métodos, é mais barata, mais rápido e mais reprodutível, sendo também compatível MS devido a composição dos tampões utilizados para a eluição. Em relação à aplicação de TiO2 para enriquecimento de fosfopeptídeos, em primeiro lugar a razão entre a quantidade de titânio e a concentração de peptídeos deve ser otimizada a fim de alcançar a mais alta eficiência de enriquecimento [140]. Nesta estratégia de enriquecimento, o valor de pH do tampão de eluição deve ser ácido para permitir que os resíduos dos peptídeos ácidos tornem-se neutros, enquanto, os grupos fosfo permanecem carregados negativamente. Vários estudos têm sido feitos para alcançar a maior seletividade de enriquecimento, comparando diferentes tampões de eluição, os quais permitem as condições ácidas [141].

1.9.1.2 Eluição sequencial por IMAC (SIMAC)

SIMAC (Figura 12) É um método de enriquecimento para fosfopeptídeos combinando MOAC (Cromatografia de afinidade por óxidos metálicos) e IMAC [142]. Ele separa ambos, tanto multi quanto mono-fosforilados, onde, as primeiras condições ácidas são usados para eluir peptídeos monofosforilado a partir do material IMAC, enquanto a eluição subsequente baseia-se na recuperação de peptídeos multifosforilados, estes que normalmente não são facilmente detectados. Individualmente peptídeos fosforilados, são eluídos da ligação TiO2-MOAC. Finalmente, as duas alíquotas contendo peptídeos distintos podem agora ser analisados separadamente, utilizando parâmetros de

espectrometria de massa que são otimizados para cada tipo de amostra [143]. No método de enriquecimento TiO2 os peptídeos não fosforilados são eluídos na primeiro etapa, sendo esta alíquota chamada de *flow-through* [143].

O método SIMAC resulta em uma maior identificação de fosfopeptídeos do que a própria MOAC, ampliando assim o espectro de identificação para fosfopeptídeos[142]. A eluição sequencial é uma outra vantagem, uma vez que tem uma maior quantidade de frações com uma menor complexidade, aumentando a probabilidade de ionização e de identificação dos fosfopeptídeos por MS [144]. Em geral o fluxograma de trabalho de SIMAC é apresentado da seguinte forma, como mostrado na figura abaixo (figura11):

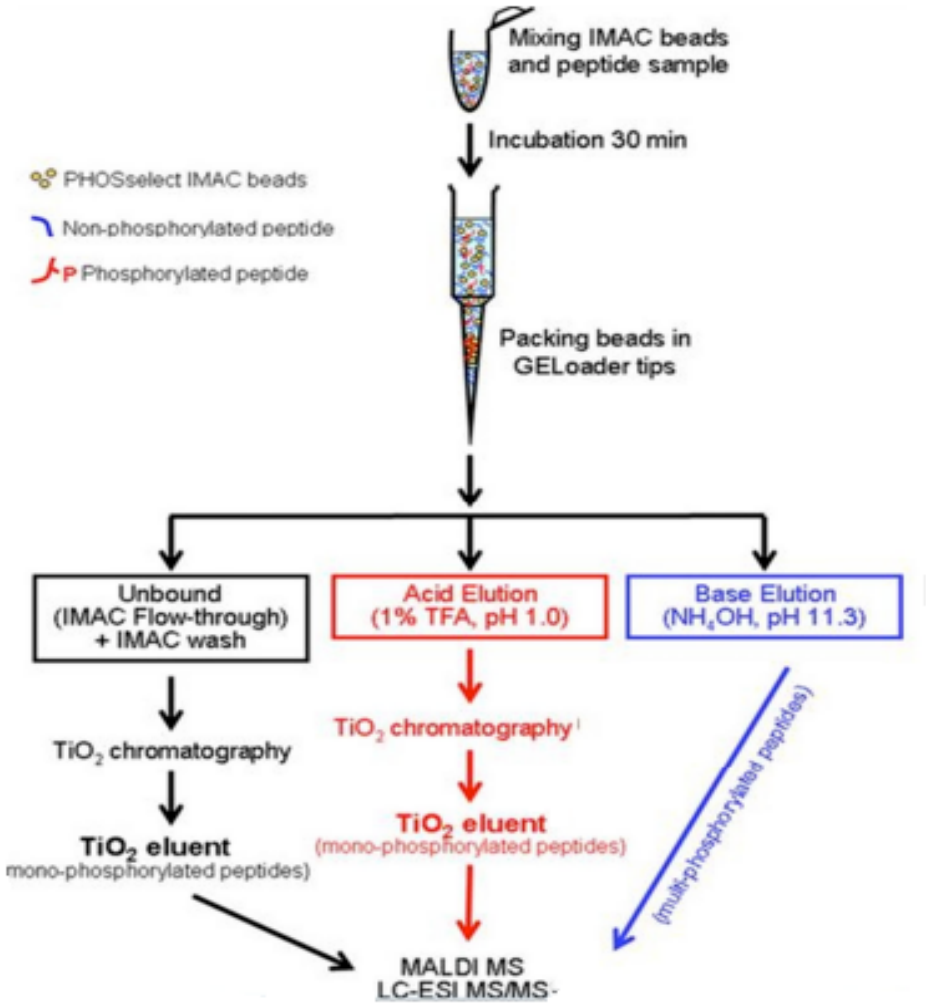

Figure 3 Fluxograma geral de SIMAC

Adaptado de[142].

1.10 Proteômica em neutrófilos

Existe uma necessidade de se identificar a expressão das proteínas que compõem uma célula, pois nem todos os genes são traduzidos em proteínas, isso se confirma também em neutrófilos, onde a correlação entre mRNA e expressão de proteínas é inconsistente . Existem alguns estudos proteômicos bem limitadas para neutrófilos, particularmente explicando o efeito da resposta inflamatória no proteoma de neutrófilos [77].

A primeira análise global com proteínas de neutrófilos de rato foi feita por eletroforese em gel bidimensional (2DE) e MS apresentando 52 proteínas identificadas [145]. Mais tarde, 250 proteínas foram identificadas através de uma combinação de 1DE seguido por ESI-MS / MS a partir de neutrófilos bovinos. As proteínas identificadas nestes trabalhos pertenciam ao metabolismo celular, motilidade celular, resposta imune, síntese de proteínas, a sinalização celular e tráfico de membrana [146].

Análise proteômica de grânulos de gelatinase, grânulos específicos e azurofílicos feita por 2DE e MALDI-TOF identificou 87 proteínas, incluindo uma proteína integral de membrana. Embora a capacidade de detecção de 2DE ainda fosse muito limitada, proporcionou a identificação de uma abundância diferencial de actina associada a todos os grânulos [147]. Foram identificadas 247 proteínas identificados a partir de grânulos azurofilicos de neutrófilos humanos, sendo estas proteínas componentes do citoesqueleto, proteínas de fusão estrutural, e de lipid rafts de membrana analisadas por 10% SDS-PAGE e de LC-MS / MS [148]. Um estudo similar identificou um total de 23 proteínas de plasma de membrana utilizando eletroforese em gel gradiente e MALDI-MS ou por MALDI-MS/MS; onde Nove das proteínas pertencentes ao citoesqueleto eram comuns a um estudo anterior de grânulos azurofílicos de neutrófilos humanos grânulos e lipd rafts [149]. Fessler et al. [150] identificou 1200 proteínas a partir de neutrófilos após a exposição ao lipopolissacárido (LPS) durante 4 h, o que resultou em 50% de aumento na expressão de 100proteínas, e 50% de diminuição na expressão de proteínas de outras 100. Usando 2DE seguido por MALDI-TOF-MS, foram identificados substratos de MMP2 e MMP9 de BAL de ratos. Estes substratos incluem Ym1, S100A8, S100A9 e, corroborando uma atividade quimiotática [151]. A análise Proteômica da mucosa intestinal em modelo ratos após pré-condicionamento isquêmico (IRI) identificou 10

proteínas utilizando 2DE em combinação com MALDI-TOF-MS e estas proteínas estavam envolvidas em mecanismos anti oxidativos, na inibição de apoptose e do metabolismo energético. Este estudo também revelaram o aumento na abundância da aldeído-desidrogenase e redutase de aldose no grupo IPC [152]. Um estudo semelhante utilizado 2-DE combinado com MALDI-MS para analisar o proteoma da mucosa intestinal de ratos submetidos a I / R de lesão, na ausência ou na presença de pré-tratamento em ratos IPC. Um total de 16 proteínas foram diferencialmente expressos, e estas pertenciam ao metabolismo energético celular, anti-oxidativo e anti-apoptótico, dentre elas a Aldose redutase que remove as ROS, foi significativamente regulada para diminuição na abundância em IR e aumento no IPC [153].

Nosso grupo vem trabalhando com abordagem proteômica para a identificação e caracterização de um conjunto de proteínas em neutrófilos. A fim de obter uma visão mais abrangente do perfil de proteínas em neutrófilos humanos ativados pelo PAF, fMLP e PMA. As técnicas de 2DE e MS com amostras de neutrófilos humanos foi realizada com 22 identificações de proteínas [154]. A comparação do proteoma de neutrófilos de indivíduos normais comparados aos de indivíduos politraumatizados em gel 2DE revelou 114 spots proteicos com abundancia diferencial, sendo aumentada em 27 e diminuída em 87 em condições de trauma [155].

1.10.1 Fosforilação de proteínas em neutrófilos

Oito substratos de MAPKAPK2 (uma cinase a juzante na via de MAPK p38) foram identificadas pela combinação *in vitro* de fosforilação ^{32}P-ortofosfato ligados a lisados de neutrófilos, usando eletroforese unidimensional SDS-PAGE, e a identificação de peptídeos por MALDI-TOF/MS. Um destes substratos, 14-3-3ζ foi encontrado fosforilado na Ser-58, e esta fosforilação regula 14-3-3ζ a dimerização e ligação a Raf-1 [156]. Uma análise semelhante identificou a subunidade p16-Arc do complexo Arp2/3 como substrato MAPKAPK2. As consequências funcionais dessa fosforilação ainda não são conhecidos, mas podem explicar a participação da MAPK p38 em funções celulares dependentes da actina [157]. Outra abordagem semelhante para identificar a proteína de ligação de cálcio relacionados com a proteína mielóide-14 (MRP-14) como um alvo para

a de fosforilação de p38 MAPK em neutrófilos estimulados com fMLP, sugerindo um papel da MRP-14 na estimulação da exocitose[158].

O regulador RhoGTPase, a proteína LyGDI, foi identificado por 2DE, imunotransferência e MS/MS e foi encontrado para ser tirosina fosforilada durante a aceleração por fibronectina mediadas pelo TNF-α na apoptose neutrófilos. A fosforilação foi seguida por um aumento da caspase-3 mediando a clivagem de LyGDI, esta clivagem foi uma sinalização para apoptose mediada por TNF-α [74]. Pacquelet et al. [159] utilizou-se análise de neutrófilos lisados por SDS-PAGE de LC-MS /MS para descobrir se a interleucina cinase 1 de associada ao receptor-4 (IRAK-4) é a juzante de TLR-4 e de serina e treonina que foram fosforiladas em $p47^{phox}$ (um componente do complexo NADPH-oxidase) diretamente por IRAK-4, que resulta em aumento da atividade da NADPH-oxidase.

Usando coloração em gel específica para fosfoproteínas (Pro-Q Diamond), mudanças na expressão de L-plastina, meosina, cofilina e proteínas stathmin foram encontrados devido a sua fosforilação ou desfosforilação [160]. Foi confirmado por MS / MS que $p47^{phox}$, é fosforilada na Ser345 por proteínas extracelulares reguladas uma proteína de sinalização quinase-1/2 (ERK1 / 2) em resposta a GM-CSF, e por p38 MAPK em resposta ao TNF-α. Esta fosforilação seletiva é um ponto de convergência para a sinalização MAPK que prepara a explosão respiratória [161]. A combinação de IMAC com ESI-MS/MS para análise de grânulos específicos isolados de neutrófilos humanos não estimuladas ou estimuladas fMLP resultou na identificação de 31 e 49 fosfopeptídeos, respectivamente. Um peptídeo que continha duas fosfoserinas foi identificado como Slp homolog lacking C2 domains b (Slac2-b) composto de um motivo conhecido de fosforilação de p38 MAPK, que está envolvido na ativação de exocitose de grânulos em neutrófilos humanos [162, 163].

De nossas observações na literatura, o mecanismo molecular pelo qual neutrófilos provocam lesão tecidual na IRI não é claro. A pesquisa proteômica tem sido feita para uma melhor compreensão da biologia dos neutrófilos no passado, mas ainda não há estudo disponível em análise proteômica de neutrófilos após isquemia e reperfusão intestinal em ratos. Para uma compreensão mais profunda das proteínas de neutrófilos

que participam das vias moleculares envolvidas na IRI buscamos realizar uma abordagem de proteômica quantitativa com iTRAQ e fosfo-Proteômica em um modelo de rato com isquemia e reperfusão intestinal.

1.11 Análise hematológica

Lesão isquêmica é resultante da interrupção do fluxo de sangue, danificando os tecidos ativos; lesão isquêmica de reperfusão (IRI) ocorre após a restauração do fluxo sanguíneo, levando à lesão tecidual adicional [164]. Parques e Granger [165], em 1986, relataram que a reperfusão nesses processos é mais prejudicial do que somente a isquemia isoladamente. O dano tecidual causado pela isquemia e reperfusão no intestino está associado a altas taxas de morbidade e mortalidade em pacientes cirúrgicos. A IRI ocorre durante a cirurgia corretiva de aneurisma de aorta abdominal, choque hemorrágico, hérnias estranguladas, enterocolite necrotizante neonatal, circulação extracorpórea e transplante de órgãos [166]. Entre os órgãos internos, o mais sensível à IRI é o intestino [164]. Lesão intestinal por IR pode levar a danos na mucosa intestinal e a liberação de vários mediadores inflamatórios, potencialmente resultando no desenvolvimento de Síndrome da Resposta Inflamatória Sistêmica (SIRS), podendo levar a falencia múltipla de órgãos (MOF), lesões pulmonares, especialmente aguda (LPA) [50, 51, 155, 167]. A isquemia e reperfusão provoca alterações sistêmicas e locais na hemodinâmica, função endotelial, na microcirculação, no equilíbrio de fluidos e na homeostase metabólica, e ao mesmo tempo induz o complemento e vias inflamatórias [154, 168-173]. Numa tentativa de atenuar este dano, várias modalidades de tratamento têm sido aplicadas em diferentes modelos animais de IRI, como hipotermia, antioxidantes, o pré-condicionamento isquêmico (IPC), modulação de mediadores inflamatórios e moléculas de adesão. Entre eles, o pré-condicionamento isquêmico parece ser uma estratégia mais promissora contra o dano de reperfusão, à medida que aumenta a tolerância do intestino contra o dano causado por isquemia, seguido de reperfusão [174-176].

O sangue é um componente do sistema de fluidos do corpo dos vertebrados, que pode ser facilmente acessado e analisado para verificar seu estado fisiológico [177]. Todos os componentes de células do sangue, como eritrócitos, leucócitos e trombócitos se originam a partir de células-tronco que são encontradas na medula óssea, que se

diferenciam em consequência de reguladores como as poietinas [178, 179]. O objetivo do presente estudo foi obter um conhecimento básico da hematologia após IRI e IPC em ratos, pois não há nenhum estudo disponível na literatura. Os parâmetros hematológicos aqui analisados incluem a determinação da contagem total de eritrócitos (RBC), contagem total de glóbulos brancos (WBC), hematócrito (HCT), hemoglobina (Hb), índices de eritrócitos (VCM, HCM, CHCM), e contagem diferencial células brancas do sangue. Neste estudo prospectivo avaliamos a significância dos parâmetros de sangue de rotina após a isquemia intestinal e pré-condicionamento em ratos, que podem ajudar no diagnóstico precoce do IRI e na compreensão de como IPC afeta os componentes do sangue.

5 Resultados

5.1 Identificação de proteínas por espectrometria de massa

Neutrófilos de ratos foram isolados a partir de três grupos biológicos (Controle, Laparatomia, Isquemia/reperfusão) e as proteínas foram extraídas, clivadas e os peptídeos foram purificados e marcados (iTRAQ). Após análise por espectrometria de massa (Orbitrap Velos), um total de 2.924 proteínas foram identificadas.

A análise estatística (conforme descrita em materiais e métodos) mostrou que 393 proteínas foram diferencialmente abundantes no grupo Laparatomia, enquanto e 653 o foram no grupo Isquemia/reperfusão, comparados com os respectivos controles. Ambos os grupos possuem 198 proteínas em comum (Fig.17, Tabela 2).

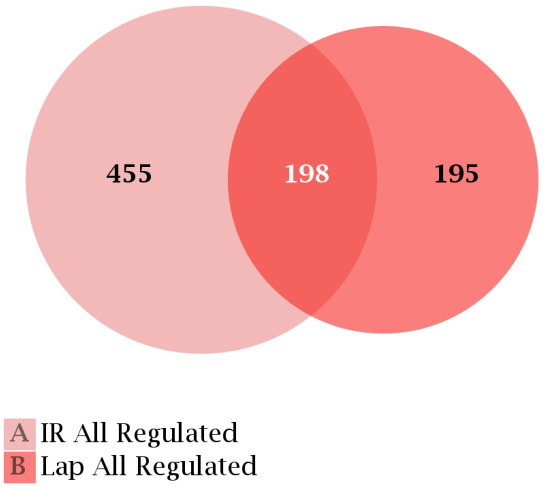

Figura 17 - Diagrama com a quantidade de proteínas diferencialmente abundantes comuns e exclusivas dos grupos laparotomia (Lap) e isquemia reperfusão intestinal (IR).

Tabela 2 - Quantidade e percentual de proteínas diferencialmente abundantes nos grupos LAP (grupo A) e IR (conjunto B)

Conjunto	Quantidade	%
A	653	77
B	393	46.3
A-B	455	53.6
B-A	195	22.9
A∩B	198	23.3
A+B	848	100

A análise subsequente dessas proteínas mostrou que 190 tiveram a abundância aumentada, 203 diminuídas, e 2531 não tiveram abundância diferencial significativa no grupo laparotomia; enquanto 367 tiveram a abundância aumentada, 286 diminuída e 2271 não tiverem abundância diferencial no grupo isquemia (Fig. 18). Um diagrama de Venn com quatro grupos (Fig. 19) foi elaborado para deixar mais clara a distribuição das proteínas extraídas dos neutrófilos.

O diagrama permite verificar a única intersecção nos grupos protéicos desses neutrófilos: das 190 proteínas com abundância aumentada no grupo laparatomia, 87 tiveram a abundância aumantada exclusivamente em neutrófilos após laparotomia enquanto as 98 restantes representam a intersecção, pois têm abundância aumentada em neutrófilos após isquemia intestinal e após laparotomia. Além disso, há 5 proteínas com abundância reduzida após isquemia mas apresentam abundância aumentada no grupo laparotomia.

Das 203 proteínas de neutrófilos com abundância diminuída durante laparotomia, 108 apresentaram abundância diminuída apenas neste grupo, enquanto 8 proteínas apresentaram abundância diminuída após laparotomia mas estão com abundância aumentada no grupo isquemia. E ainda, 87 proteínas mostraram-se com abundância

diminuída em ambos os grupos laparotomia e isquemia. Os neutrófilos após isquemia intestinal mostraram-se com 261 proteínas com abundância aumentada e 194 proteínas com abundância diminuída .

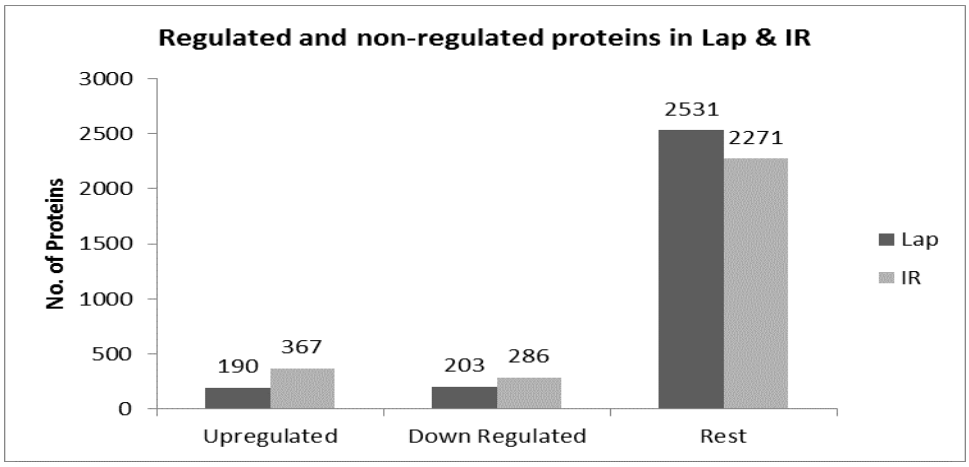

Figura 48 Quantidade de proteínas com e sem abundância diferencial nos grupos LAP e IR.

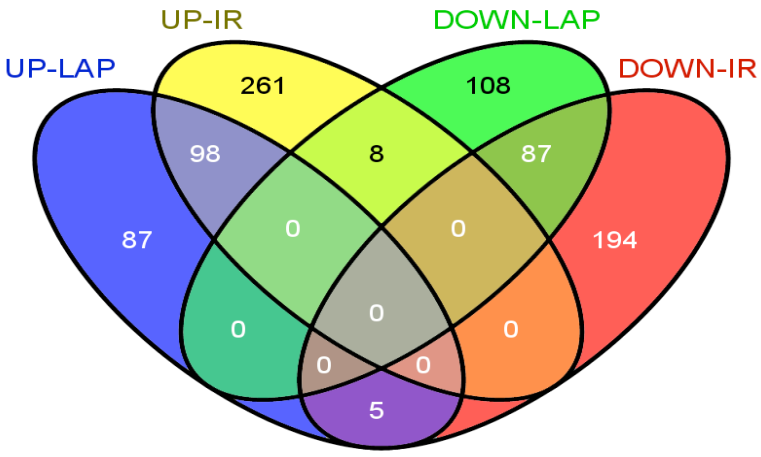

Figura 19- Um diagrama de Venn de 4 grupos ilustrando as intersecções e exclusividades nos subgrupos de abundância aumentada e abundância diminuída de proteínas de neutrófilos após laparotomia e isquemia-reperfusão intestinal.

5.2 Análise estatística com R

Foram usadas duas abordagens estatísticas diferentes na análise inicial, cujos resultados foram quase similares. As análises estatísticas seguintes foram baseadas nos dados obtidos com o pacote estatístico R devido aos motivos expostos em material e métodos. Cinco *clusters* com diferentes perfis foram obtidos (Fig. 20). O *cluster* 1 mostra abundância proteica diminuída tanto no grupo laparotomia quanto no grupo isquemia, perfazendo 20% (542 proteínass) do total de proteínas com abundância diferencial. Os *clusters* 2 e 5 mostraram abundância aumentada em ambos os grupos laparotomia e isquemia, com 19% (517 proteínas) e 18% (464 proteínas), do total de proteínas com abundância diferencial, respectivamente. O *cluster* 3 aponta que 28% (743 proteínas) foram encontradas com abundância diminuída apenas no grupo laparotomia e o *cluster* 4 sugere que 15% (407 proteínas) teve discreto aumento de abundância no grupo laparotomia mas com abundância diminuída no grupo isquemia (Fig. 21).

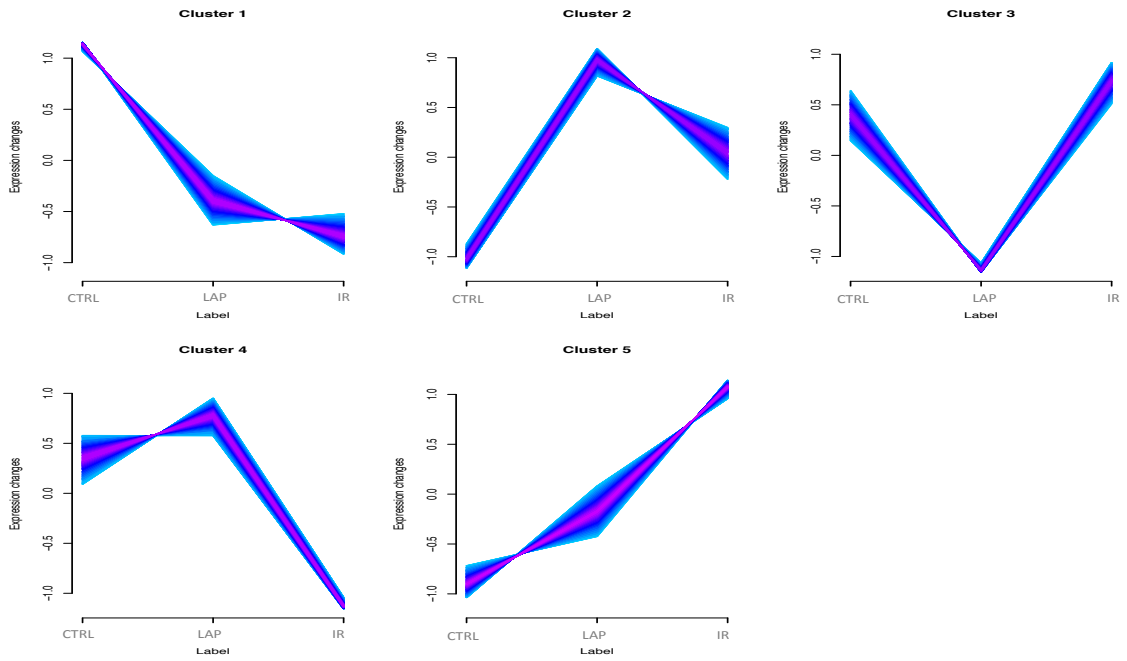

Figura 20 Perfil de abundância diferencial de proteínas e fosfopeptídeos após laparotmia e isquemia-reperfusão em neutrófilos. Controle (114), Laparotomia (115), e Isquemia-reperfusão (117).

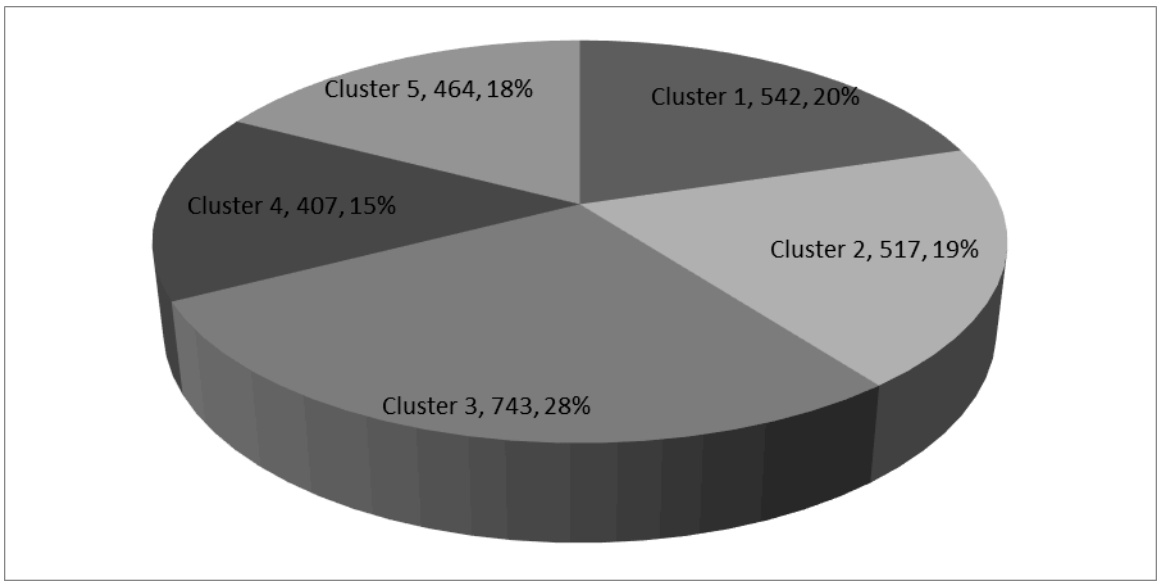

Figura 21 Proteínas de neutrófilos com abundância diferencial distribuídas em cinco clusters.

5.3 Análise dos Componentes Principais (ACP):

Uma análise dos components principais (ACP) padrão foi calculada para verificar a variabilidade entre diferentes condições e a similaridade entre as replicatas biológicas do mesmo grupo. Todas as proteínas e peptídeos foram submetidos à ACP, mas o algoritmo completo (com função prcomp no R) foi usado apenas nos casos em que as proteínas e peptídeos foram quantificados em todas as condições e em todas as replicatas biológicas simultaneamente. O gráfico gerado pela ACP, o chamado *score plot* (Fig. 22) mostra que, embora haja variabilidade entre as replicatas, elas podem ser claramente agrupadas em conjuntos sem intersecções, o que significa uma boa reprodutibilidade em cada condição experimental. Numa comparação grosseira, toda uma coluna de dados poderia ser exemplificada por ponto de dados.

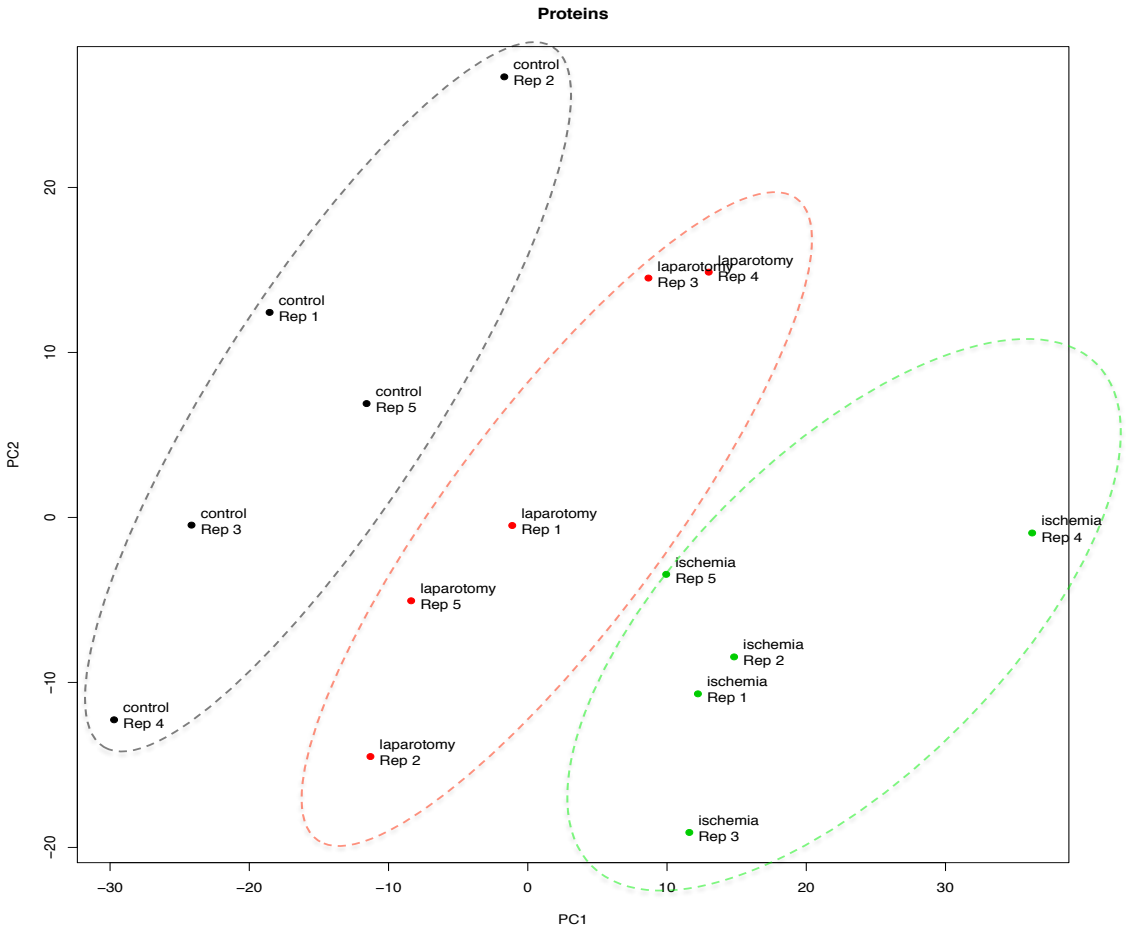

Figura 22 Análise dos components principais (ACP). ACP de todas as proteínas identificadas em todas as cinco replicatas biológicas nos respectivos grupos controle (preto), laparatomia (vermelho) e isquemia-reperfusão (verde).

5.4 Fosfoproteoma de neutrófilos de ratos

Fosforilação proteica é uma modificação pós-traducional muito comum que ocorre durante a transdução de sinal. Células eucarióticas dependem em grande medida desse processo para funções básicas, incluindo metabolismo, mobilidade, diferenciação, crescimento, divisão, descolamento de organelas, transporte em membranas; bem como para funções fisiológicas, tais como imunidade, contração muscular, aprendizado e memória [217, 218].

Combinando-se os dados de peptídeos não modificados com aqueles fosforilados foram identificadas 3.816 proteínas. Aquelas exclusivamente não-fosforiladas foram 2.231 e as

proteínas exclusivamente fosforiladas foram 892. Um grupo de 693 proteínas fosforiladas foram encontradas também no grupo geral, perfazendo um total de 1.585 proteínas fosforiladas conforme mostrado no diagrama de Venn (Fig. 23-E). Nossa análise mostrou 41.5% de fosforilação do proteoma total de neutrófilos identificado neste estudo.

A análise espectrométrica de massa do fosfoproteoma total de neutrófilos de ratos revelou a eficiência do método de enriquecimento utilizado. Foram obtidos 10% de peptídeos não fosforilados e 90% de peptídeos fosforilados, sendo 95% monofosforilados e 5% difosforilados (Fig. 23-A).

Foram ainda identificados 4.894 sítios de fosforilação em 4.453 fosfopeptídeos de 1.585 proteínas (Fig. 23-F). Para a cascata de transdução de sinal, as células eucarióticas dependem da fosforilação do grupo hidroxila na cadeila lateral de serina (S), treonina (T) e tirosina (Y) [219, 220]. Diferentes estudos relataram taxas variadas de fosforilação de S/T/Y em algumas linhagens celulares. No ano de 2.007, Macek *et al* publicou uma taxa de 70:20:10 (S/T/Y) para *Bacillus subtilis* [221] e o mesmo grupo encontrou uma taxa de 86:12:2 (S/T/Y) em cultura de células humanas [222].

Mais tarde foi estimado que as quantidades relativas de fosfoserina, fosfotreonina e fosfotirosina no proteoma humano são 90%, 10%, e 0.05% respectivamente [223]. A análise fosfoproteômica de células Hela do laboratório Matthias Mann mostrou quase a mesma relação: 86,4: 11,8: 1.8 (S/T/Y) [222].

A análise dos sítios de fosforilação do fosfoproteoma de neutrófilos de ratos neste trabalho revelou uma taxa de 87: 12: 1 (S/T/Y, Fig. 23-B), semelhante à análise fosfoproteômica realizada por Lundby *et al,* que descreveu no ano de 2.011, para 14 diferentes órgãos e tecidos de ratos, a taxa de 88.1: 11.4: 1.5 [224].

Com relação às proteínas que tiveram abundância diferencial nos grupos aqui pesquisados, as quantidades relativas de fosforilação S/T/Y mostradas na Fig. 23-C seguem a proporção 76:21:3, que parecem estar próximas à proporção 79:17:2 (S/T/Y) de fosforilação recentemente descrita na diferenciação de células humanas embrionárias para células-tronco neurais [185].

Destaque-se agora outra forma de analisar, subjacente aos *clusters* descritos anteriormente, conforme mostrado na Fig. 23-G: das proteínas com abundância diferencial e dos peptídeos com fosforilação diferencial, o *cluster 3* possui maior quantidade de proteínas diferencialmente abundantes, enquanto o padrão de distribuição associado aos fosfopeptídeos são mais semelhantes nos *clusters* 5, 2, e 4.

Foram encontrados 844 fosfopeptídeos de 277 proteínas agrupadas no *cluster 5*; 726 fosfopeptídelos de 288 proteínas no *cluster 2*; enquanto 605 fosfopeptídelos de 280 proteínas foram agrupadas no *cluster 4*. O *cluster 1* reuniu 551 fosfopeptídelos de 252 proteínas e o *cluster 3* acumulou 542 fosfopeptídelos de 257 proteínas. Foram identificados 3.268 peptídeos com fosforilação diferencial para 602 proteínas.

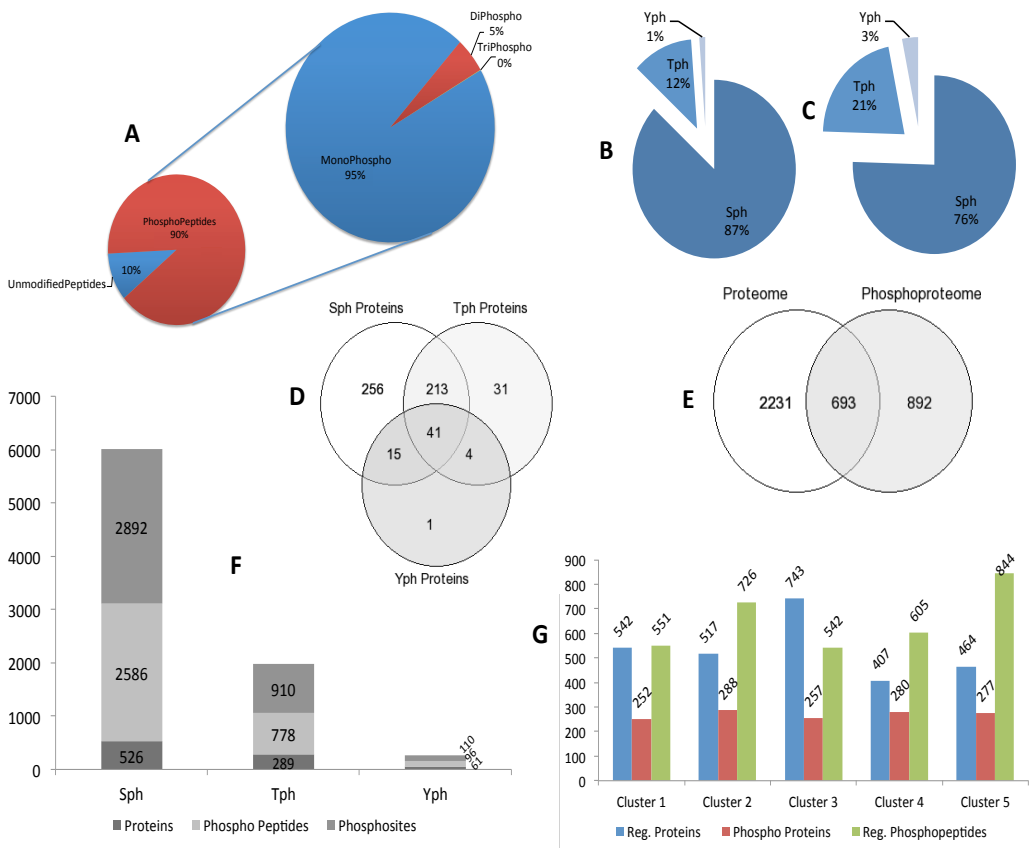

Figura 23 Fosfoproteoma de neutrófilos de ratos.

A, Importância do método de enriquecimento na identificação do fosfoproteoma e quantidade de sítios de fosforilação por peptídeo. B, Distribuição dos sítios de fosforilação no conjunto total dos dados. C, Distribuição dos sítios de fosforilação identificados no conjunto de dados com abundância diferencial. D, Intersecção entre os conjuntos de proteínas com fosforilação de serina, treonina e tirosina. E, Intersecção entre os conjuntos de proteoma e fosfoproteoma. F, Quantidade de sítios de fosforilação e fosfopeptídeos em fosfoproteínas. G, Distribuição, baseada nos *clusters,* de proteínas fosforiladas, proteínas com abundância diferencial, e peptídeos com fosforilação diferencial.

5.5 Análise GO Slim das proteínas totais e diferencialmente abundantes em neutrófilos de ratos

5.5.1 Componente celular

A análise de ontologia genética (GO) utilizando o programa Proteína Center para as proteínas diferencialmente abundantes, de acordo do os componenetes celulares é mostrada nas Fig. 24 e 25. Há grande variedade entre as proteínas diferencialmente abundantes em todos os cinco *clusters* e suas localizações celulares. No *cluster* 1 (Fig. 24, 25-A) a maioria das proteínas diferencialmente abundantes pertencem a ribossomo, citoplasma e citosol dos neutrófilos. No *cluster* 2 (Fig. 24, 25-B) a maior parte das proteínas mostrou origem no citoesqueleto, citosol e componenete extracelular dos neutrófilos.

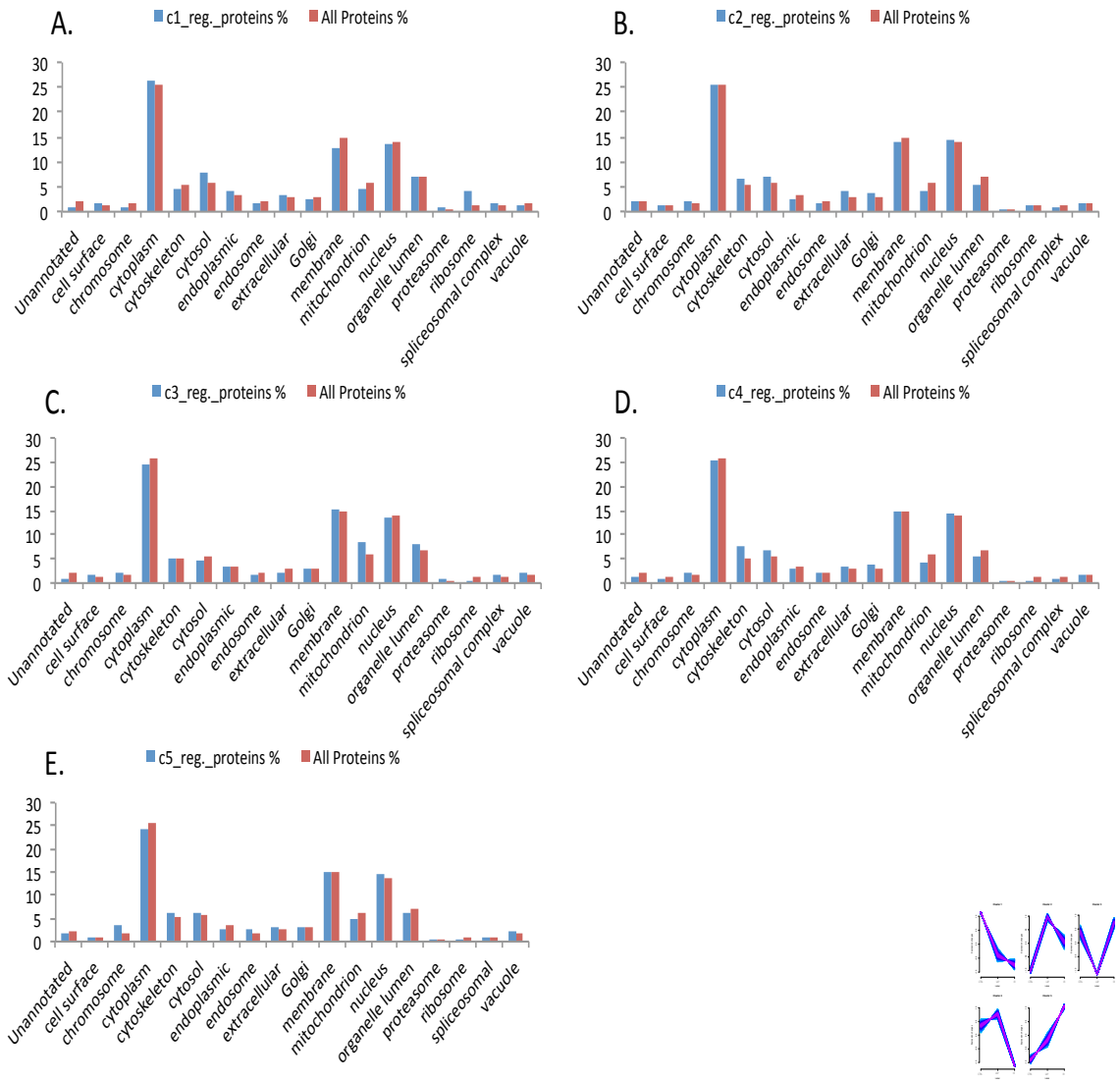

Figura 24 Gráfico de barras do GO reduzido para components celulares a partir das proteínas totais de neutrófilos e daquelas diferencialmente abundantes de acordo com (A) Cluster 1, (B) Cluster 2, (C) Cluster 3, (D) Cluster 4 (E) Cluster 5.

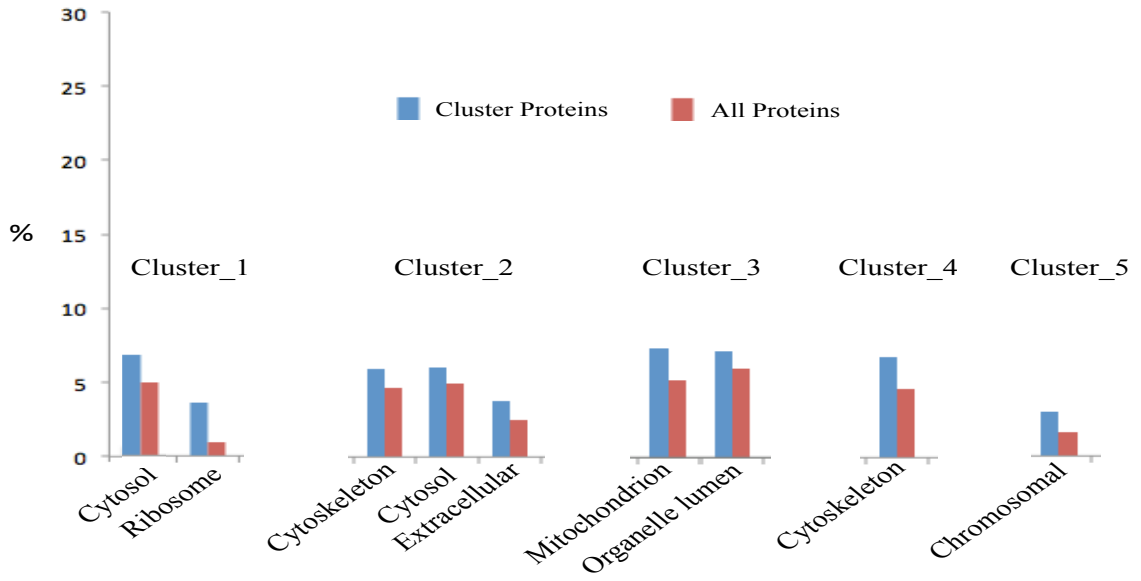

Figura 25 Análise GO dirigida para os componentes celulares que mais contêm as proteínas totais e diferencialmente abundantes no (A) Cluster 1, (B) Cluster 2, (C) Cluster 3, (D) Cluster 4 e (E) Cluster 5.

Proteínas mitocondriais e do interior de outras organelas estão muito presentes no *cluster* 3 (Fig. 24, 25-C). No *cluster* 4 a maior parte de proteínas diferencialmente abundantes são do citoesqueleto (Fig. 24, 25-D). Enquanto no caso do *cluster* 5, as proteínas mais abundantes foram encontradas em cromossomos de neutrófilos (Fig. 24, 25-E).

Neutrófilos possuem alta mobilidade e o citoesqueleto desempenha um papel muito importante nesse quesito. O citoesqueleto é uma rede complexa de três classes estruturais chamadas microfilamentos, filamentos intermediários e microtúbulos. Estudos mostram que cadeias de actina participam da motilidade neutrofílica e também regulam receptores de afinidade, apoptose, ciclo celular e sinalização para o núcleo [225, 226].

Actina citoplasmática, membrana e citoesqueleto ligado ao fagossomo possuem papel essencial na quimiotaxia de neutrófilos, na transmigração endotelial (TEM) e na fagocitose [227]. O citoesqueleto em neutrófilos é parte muito importante e ainda está pobremente caracterizado. Xu, P., *et al* analisaram o subproteoma de citoesqueleto citossólico de neutrófilo e membranas plasmática e de fagossomos. Por meio de 2DE e

MALDI-TOF-MS identificaram 138 proteínas (algumas novas), sendo a maioria relacionada a enzimas do metabolismo energético [228].

O padrão de regulação dos *clusters* 1, 2 e 4 mostra abundância diminuída de proteínas citosólicas e do exoesqueleto. O aumento da mobilidade e da resposta quimiotáctica dos neutrófilos do grupo IR podem estar relacionados com essa abundância diminuída de proteínas do citoesqueleto comparada com os grupos controle e LAP.

A mitocôndria é o primeiro sítio de lesão na isquemia. Durante a isquemia o metabolismo anaerobico produz uma queda no pH celular devido a acumulação de íons hidrogênio, e então a bomba de Na^+/H^+ elimina o excesso de H^+, resultando em grande influxo de Na+ [32]. A queda no ATP celular e relativa desativação de ATPases reduzem o influxo ativo de Ca^{2+} e limitam a reabsorção de cálcio pelo retículo endoplasmático, produzindo assim a sobrecarga de cálcio intralelular. Como resultado ocorre a abertura dos poros na mitocôndria (mitochondrial permeability transition - MPT), que afeta mais ainda a produção de ATP por afetar o potencial de membrana mitocondrial.

A magnitude do fluxo sanguíneo e a duração da isquemia afetam o grau de lesão tecidual [33]. Proteínas mitocondriais se mostram enriquecidas somente no *cluster 3*, que por sua vez mostra abundância diminuída somente no grupo laparatomia e não mostra diferenças no grupo isquemia e controle. (Fig. 24-C).

5.5.2 Processos biológicos

A análise GO referente a processos biológicos é mostrada na Fig. 26. A maior parte das proteínas com abundância diferencial do *cluster 1* está relacionada a processos metabólicos (Fig. 26-A, 27); enquanto aquelas do *cluster 2* participam da organização celular e biogênese (Fig. 26-B, 27).

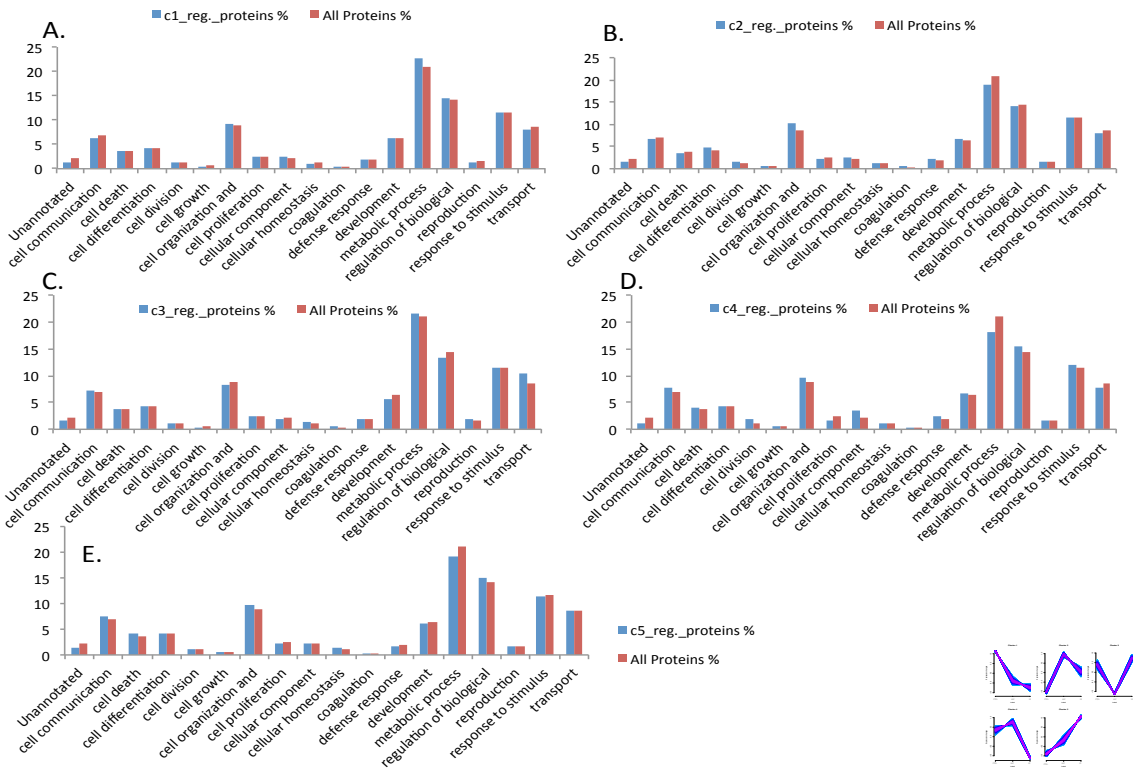

Figura 26 - Análise GO relativa a processos biológicos das proteínas totais de neutrófilos e das proteínas com abundância diferencial nos (A) cluster 1, (B) Cluster 2, (C) Cluster 3, (D) Cluster 4 e (E) Cluster 5.

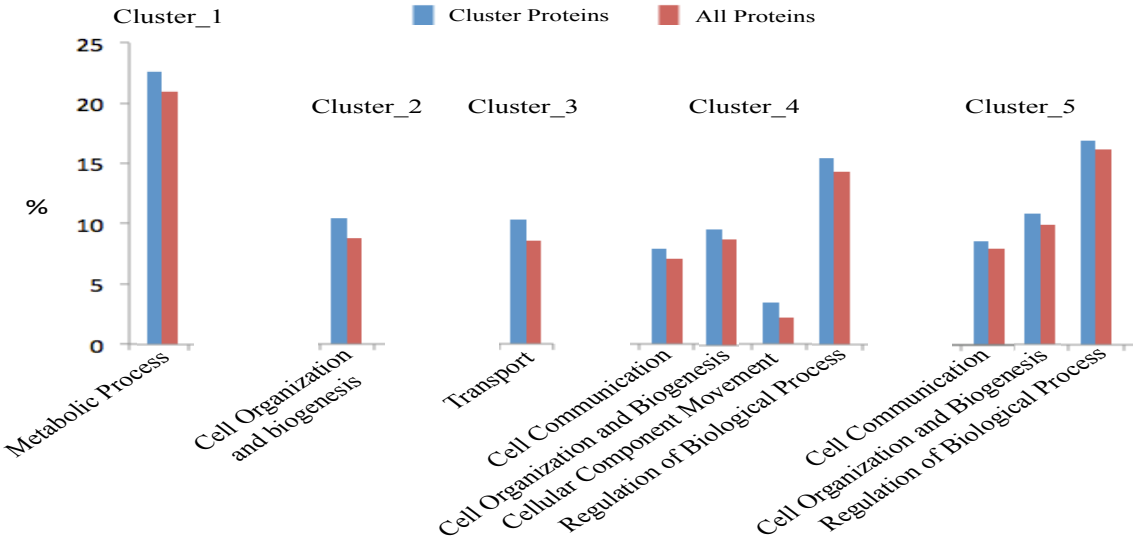

Figura 27 – Análise GO dos processos biológicos mais frequentes relacionados às proteínas totais e diferencialmente abundantes em neutrófilos e em cada cluster.

Proteínas do *cluster 3* estão relacionadas a transporte (Fig 26-C, 27). Proteínas do *cluster 4* participam da organização celular, componentes da motilidade, comunicação e regulação de processos biológicos (Fig 26-D, 27); enquanto a maior parte das proteínas do *cluster 5* participam da organização celular, comunicação e regulação de processos biológicos (Fig. 26-E, 27).

5.5.3 Função molecular

Análise *GO Slim* de termos da função molecular das proteínas do *cluster 1* mostra aumento relacionado aos ribossomos e citoplasma (Fig. 28-A, 29). Essas proteínas estão envolvidas com RNA e ligação nucleotídica dentro da atividade molecular estrutural. Proteínas do *cluster 2* estão relacionadas à função de ligação protéica e ligação com íons metálicos (Fig 28-B, 29).

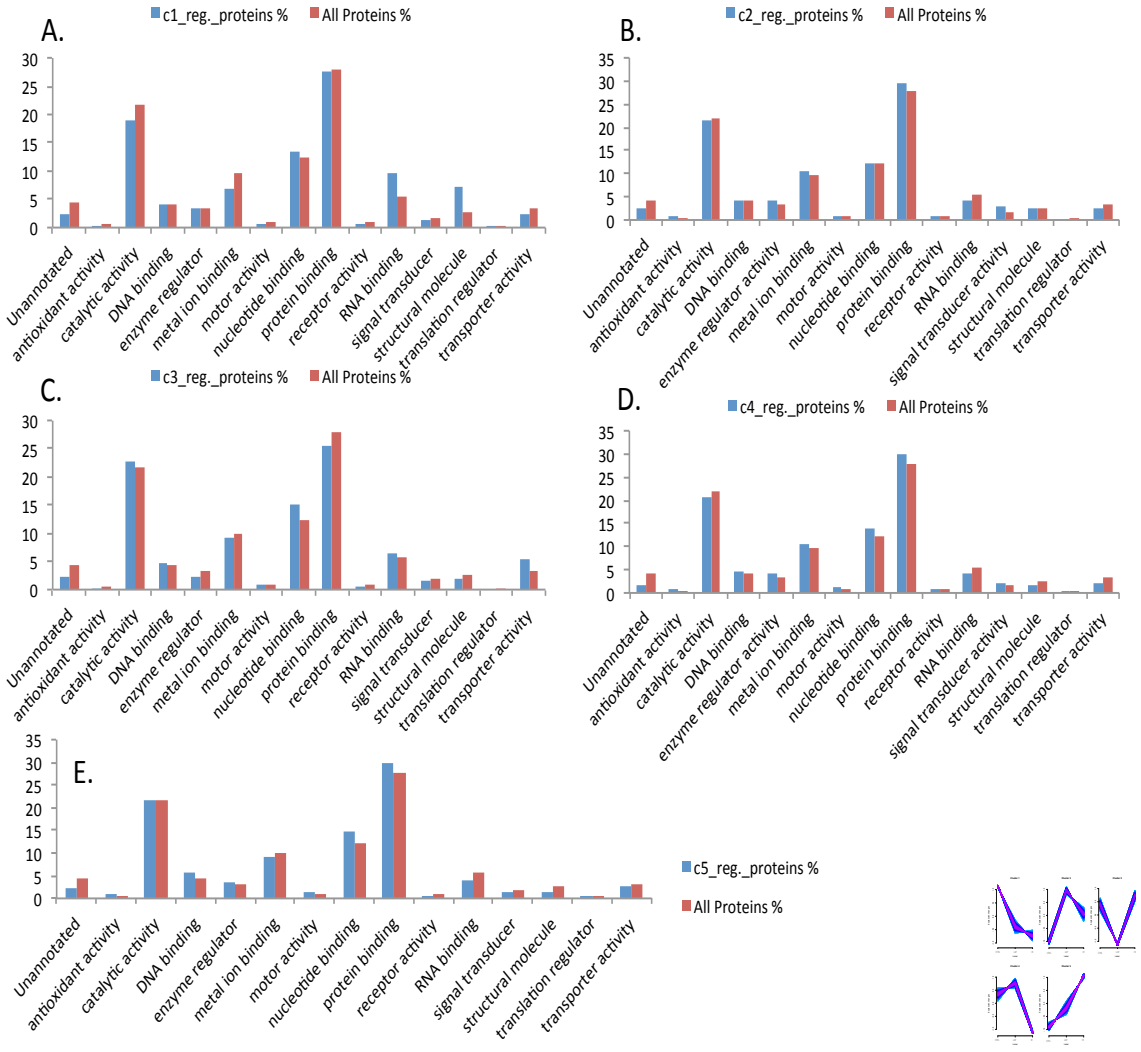

Figura 28 - Análise GO das funções moleculares das proteínas totais e diferencialmente abundantes de neutrófilos nos (A) cluster 1, (B) Cluster 2, (C) Cluster 3, (D) Cluster 4 e (E) Cluster 5.

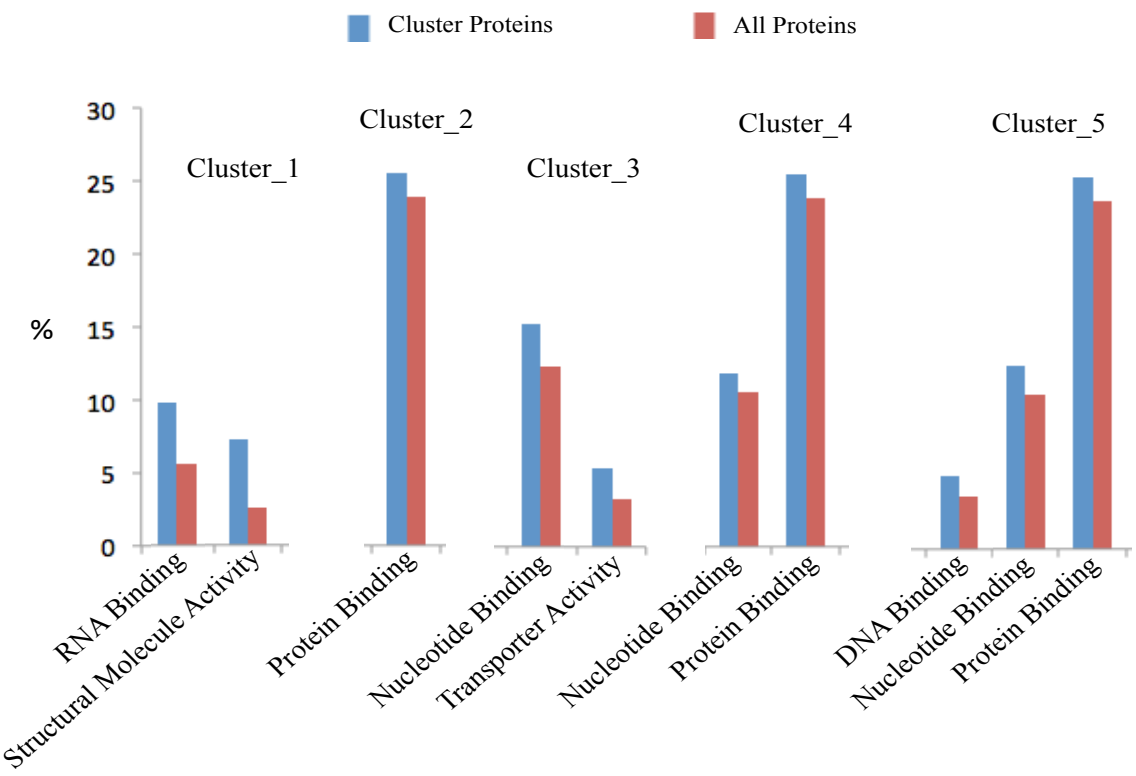

Figura 29 – Análise GO das proteínas mais abundantes relacionadas a termos de função molecular de todos os clusters.

As proteínas do *cluster 3* mostram-se relacionadas à ligação nucleotídica e atividade transportadora (Fig. 28-C, 29), enquanto proteínas do *cluster 4* e *cluster 5* estão envolvidas na ligação com outras proteínas, RNA e DNA. Está claro que dentre os cinco *clusters,* as proteínas diferencialmente abundantes em maioria estão relacionadas à função de ligação intermolecular (proteínas, DNA, RNA). Em outras palavras, transcrição e tradução (Fig. 228-D, E, 29).

5.6 Atividade enzimática prevista para o proteoma total de neutrófilos de ratos

Usando a ferramenta Blast2GO, conforme já mencionado nos Materias e Métodos, a Predição de atividade enzimática para o proteoma total de neutrófilos de ratos foi executada. Um gráfico em fatias das enzimas preditas do proteoma total regulado de neutrófilo de ratos mostra que a maior parte das enzimas reguladas são do grupo de Transferases (EC:2), Hidrolases (EC:3) e Oxiredutases (EC:1), respectivamente (Fig 30).

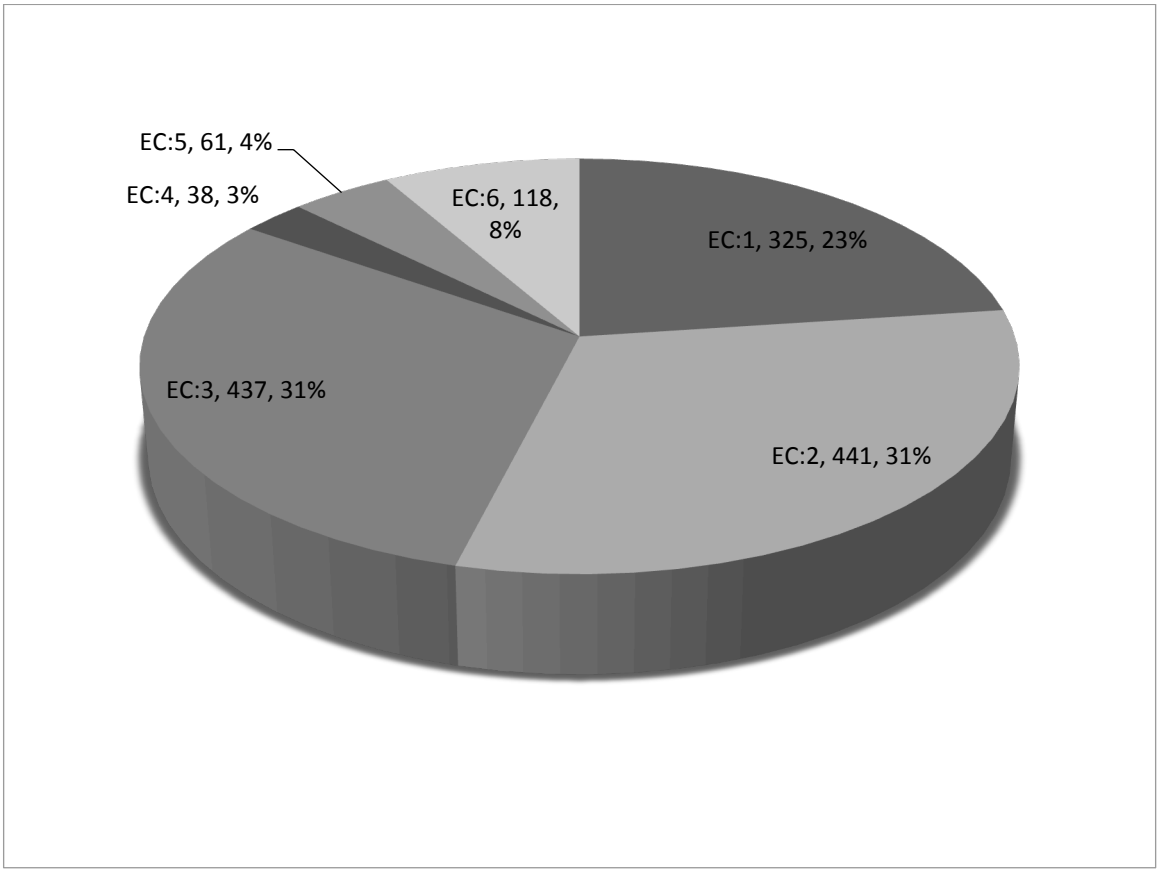

Figura 30 Predição enzimática do proteoma total de neutrófilos de ratos. Predição de atividade enzimática do proteoma total de ratos baseada em similaridade de sequência das proteínas.

5.6.1 Predição de atividade enzimática para o *cluster* 1

Isomerases (EC:5) e ligases (EC:6) são enzimas reguladas enriquecidas no *cluster* 1 quando comparadas ao total de proteínas identificadas (Fig31). Isso significa que isomerases e ligases são suprimidas nos grupos Laparotomia e IR, quando comparados ao controle. Detalhes das enzimas suprimidas preditas para EC:5 e EC:6 são dados nas tabelas 3 e 4. A tabela 3 mostra que a maior parte das enzimas isomerases suprimidas no grupo IR são isomerase peptidilprolil (EC:5.2.1.8) e proteína disulfil-isomerase (PDI) (EC:5.3.4.1).

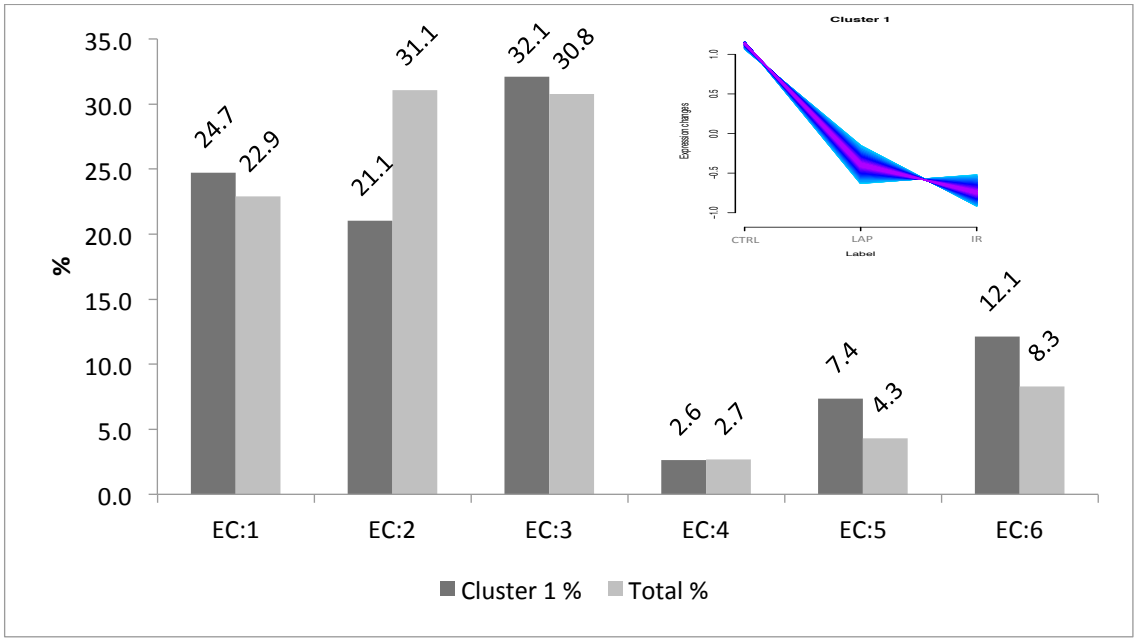

Figura 31 Predição enzimática das proteínas do cluster 1. Predição por B2GO de atividade enzimática das proteínas identificadas no *cluster* 1 baseada em similaridade de sequência das proteínas.

Peptidilpropil isomerase/ciclofilinas (CyPs) são envolvidas na interconversão cis/trans de ligações prolina em peptídeos e facilitam o dobramento de proteínas [229]. Foi demonstrado em pacientes com Artrite Reumatóide (AR) que CyPs afetou a quimiotaxia mediada por IL8 em neutrófilos [230].

A proteína disulfil-isomerase (PDI) está localizada pincipalmente no retículo endoplasmático (ER) e é envolvida no dobramento de proteínas recém-sintetizadas (rearranjo de ligações disulfídicas, redução de isomerizações) [231]. Outro estudo demonstra o seu papel na produção de ROS por conta de sua co-imunoprecipitação com subunidades NADPH oxidase como p22phox de membrana e p47phox e p67phox de citoplasma de neutrófilos humanos [232]. Recentemente, um estudo in vivo usando microscopia de fluorescência intravital em ratos demonstrou que a PDI está envolvida na adesão de neutrófilos (por meio de interação com aMb2 integrina em lipid rafts) e no rolamento em condições inflamatórias mediadas por TNF-a. Eles sugerem que a PDI extracelular como alvo terapêutico novo para prevenir sequestro de neutrófilos [233].

Tautomerase fenilpiruvato/fator inibidor da migração de macrófagos (MIF) (EC5.3.2.1) é uma citocina com propriedades catalíticas. Neutrófilos maduros do sangue ou tecidos consistentemente expressam MIF como uma proteína citossólica não associada a grânulos azurofílicos. Neutrófilos apoptóticos secretam MIF na forma ativa após estimulação por TNF, por uma mecanismo dependente de caspases [234].

Prostaglandina E sintetase (PGES) (EC: 5.3.99.3) é a enzima final na produção de PGE2. PGE2 é um mediador lipídico e é parte fundamental de vários processos, como função gastrointestinal e renal, homeostasia vascular, remodelamento ósseo, indução de febre, gravidez e inflamação aguda. Três isoformas de PGES são conhecidas, sendo as PGES citosólicas (cPGES) [235,236], PGES-1 microssomais (mPGES-1) [235] e mPGES-2 [237]. As citocinas pró-inflamatórias IL-1b, TNF-x e LPS elevam a expressão de mPGES-1 [238]. Mosca et al. Demonstraram que os neutrófilos são fonte de mPGES-1 celular [239].

A Tabela 3 mostra a maioria das ligases de supressão prevista no *cluster* 1. Nada foi previamente reportado na literatura com relação ao seus papéis em neutrófilos. Algumas dessas enzimas estão envolvidas na síntese de novo de arginina e nucleotídeos, sendo outras envolvidas na transferência de diferentes aminoácidos para o seu RNA transportador, conforme descrito abaixo.

Aspartato tRNA ligase (EC 6.1.1.12) [240], Glicina tRNA ligase (EC 6.1.1.14) [241], Prolina tRNA ligase (EC 6.1.1.15) [242], Glutamato tRNA ligase (EC 6.1.1.17) [243], Fenilalanina tRNA ligase (EC 6.1.1.20) [244] e Leucina tRNA ligase (EC 6.1.1.4) [245] catalisam a ligação desses respectivos aminoácidos ao seu respective tRNA e essa reação necessita da ativação anterior do aminoácido por ATP para o seu uso pelas tRNA ligases.

Proteína ubiquitina ligase (EC 6.3.2.19) se liga de forma covalente ao substrato através da mediação de uma enzima ativadora E1, uma conjugasse E2 e uma ligase E3 [246]. As E3 podem se ligar com E2 através de domínios RING Finger, U Box ou HECT e ao substrato por meio de domínios F Box, SOCS Box e DDB1 ou BTB [247, 248]. Nós estamos reportando, pela primeira vez, a inibição dessas ligases em neutrófilos, que pode

levar à diminuição da biossíntese desses aminoácidos. Esse efeito em neutrófilos ativos não é claramente descrito na literatura.

Carbamoil-fosfato sintase (EC 6.3.4.16) participa da formação de carbamoil-fosfato a partir de amônia. Ela também inicia tanto o ciclo da ureia quanto a síntese de arginina e pirimidinas [249].

Formil tetrahidrofolato ligase (Fhs) (EC 6.3.4.3) catalisa a formação de 10-formil-tetrahidrofolato que é usado diretamente na biossíntese de purina e na formilação de Met-tRNA em Porphyromonas gingivalis (bactéria gram-negativa) [250].

Adenilsuccinato sintetase (EC 6.3.4.4) catalisa a formação de adenilsuccinato à partir de 1-aspartato e IMP, sendo que a hidrólise de GTP também acontece durante essa reação, que é a primeira reação na síntese de novo de AMP [251].

Argininosuccinato sintetase (EC 6.3.4.5) é envolvida na via de biossíntese de novo de arginina e age na conversão de citrulina em arginina, que é catalisada por argininosuccinato sintase e argininosuccinato liase. Primeiramente a argininosuccinato sintase produz argininosuccinato por meio da condensação de citrulina e aspartato e posteriormente a argininosuccinato liase quebra argininosuccinato para produzir fumarato e arginina. Argininosuccinato sintase também tem papel importante durante a síntese de ureia, óxido nítrico, poliamina e creatina [252]. Fosforibosil formil glicinamida (FGAM) sintetase (EC 6.3.5.3) catalisa um dos passos na via de síntese de novo de purina. Essa enzima catalisa a conversão de 5'-fosforibosilformilglicinamida (FGAR) em FGAM na presença de glutamina e ATP [253]. Carbamoil-fosfato sintase (hidrolizante de glutamina) catalisa a conversão de carbamoil fosfato à partir de L-glutamina, em um intermediário na biossíntese de nucleotídeos de arginina e pirimidina [253]. RNA ligase (EC 6.5.1.3) transfere o 5'-fosfato para a porção 3'-hidroxi-terminal do RNA e como resultado o RNA linear assume sua forma circular [254].

Tabela 3 Enzimas do cluster 1 com funções preditas de isomerases .

Acc	Gene	PD Description	Enzyme Codes
Q6DGG0	Ppid	Peptidyl-prolyl cis-trans isomerase D	EC:5.2.1.8
P45878	Fkbp2	Peptidyl-prolyl cis-trans isomerase FKBP2	EC:5.2.1.8
P10111	Ppia	Peptidyl-prolyl cis-trans isomerase A	EC:5.2.1.8
P17742	Ppia	Peptidyl-prolyl cis-trans isomerase A	EC:5.2.1.8
P30904	Mif	Macrophage migration inhibitory factor	EC:5.3.2.1
P30904	Mif	Macrophage migration inhibitory factor	EC:5.3.3.12
P38659	Pdia4	Protein disulfide-isomerase A4	EC:5.3.4.1
Q6IUU3	Qsox1	Sulfhydryl oxidase 1	EC:5.3.4.1
O54890	Itgb3	Integrin beta-3	EC:5.3.4.1
Q8BND5	Qsox1	Sulfhydryl oxidase 1	EC:5.3.4.1
P08011	Mgst1	Microsomal glutathione S-transferase 1	EC:5.3.99.3
Q7TSV4	Pgm2	Phosphoglucomutase-2	EC:5.4.2.2
Q7TSV4	Pgm2	Phosphoglucomutase-2	EC:5.4.2.2
Q9Z2M7	Pmm2	Phosphomannomutase 2	EC:5.4.2.2

Tabela 4 Enzimas do cluster 1 com funções preditas de ligase

Acc	Gene	PD Description	Enzyme Codes
P15178	Dars	Aspartate--tRNA ligase, cytoplasmic	EC:6.1.1.12
Q5I0G4	Gars	Glycine--tRNA ligase (Fragment)	EC:6.1.1.14
Q8CGC7	Eprs	proline--tRNA ligase	EC:6.1.1.15
Q8CGC7	Eprs	glutamate tRNA ligase	EC:6.1.1.17
Q505J8	Farsa	Phenylalanine--tRNA ligase	EC:6.1.1.20
Q8BMJ2	Lars	Leucine--tRNA ligase, cytoplasmic	EC:6.1.1.4
Q9CZY3	Ube2v1	Ubiquitin-conjugating enzyme E2 variant 1	EC:6.3.2.19
P83940	Tceb1	Transcription elongation factor B polypeptide 1	EC:6.3.2.19
B5DF89	Cul3	Cullin-3	EC:6.3.2.19
F1LP64	Trip12	E3 ubiquitin-protein ligase TRIP12	EC:6.3.2.19
Q2TL32	Ubr4	E3 ubiquitin-protein ligase UBR4	EC:6.3.2.19
O88738	Birc6	Baculoviral IAP repeat-containing protein 6	EC:6.3.2.19
P07632	Sod1	Superoxide dismutase (Cu-Zn)	EC:6.3.2.19
P48004	Psma7	Proteasome subunit alpha type-7	EC:6.3.2.2
Q62636	Rap1b	Ras-related protein Rap-1b	EC:6.3.4.16
P63321	Rala	Ras-related protein Ral-A	EC:6.3.4.16
P27653	Mthfd1	formate—tetrahydrofolate ligase	EC:6.3.4.3
P46664	Adss	Adenylosuccinate synthetase isozyme 2	EC:6.3.4.4
P09034	Ass1	Argininosuccinate synthase	EC:6.3.4.5
Q5SUR0	Pfas	Phosphoribosylformylglycinamidine synthase	EC:6.3.5.3
P63321	Rala	Ras-related protein Ral-A	EC:6.3.5.5
Q62636	Rap1b	Ras-related protein Rap-1b	EC:6.3.5.5
Q99LF4	Rtcb	tRNA-splicing ligase RtcB homolog	EC:6.5.1.3

5.6.2 Predição de atividade enzimática para os *cluster*s 2 e 3

A regulação predita de enzimas para o *cluster* 2 inclui transferases (EC 2), hidrolases (EC 3) e isomerases (EC 5) como enriquecidas, enquanto no *cluster* 3 as enriquecidas são oxiredutases (EC 1), hidrolases (EC 3) e liases (EC 4). Um gráfico de barras comparando o total e as enzimas reguladas nos *cluster*s 2 e 3 mostra que não há mudanças marcantes na regulação enzimática nos dois *cluster*s. Fig 32, 33.

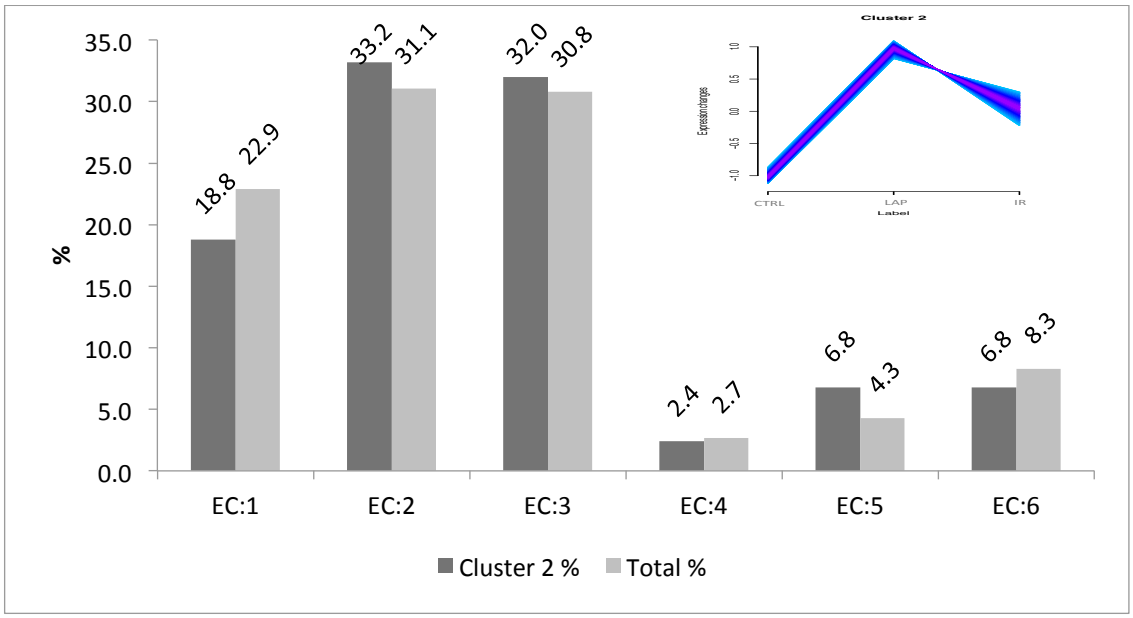

Figura 32. Predição enzimática das proteínas do cluster 2. Predição de atividade enzimática baseada em similaridade de sequência de proteínas por B2GO das proteínas identificadas do *cluster* 2.

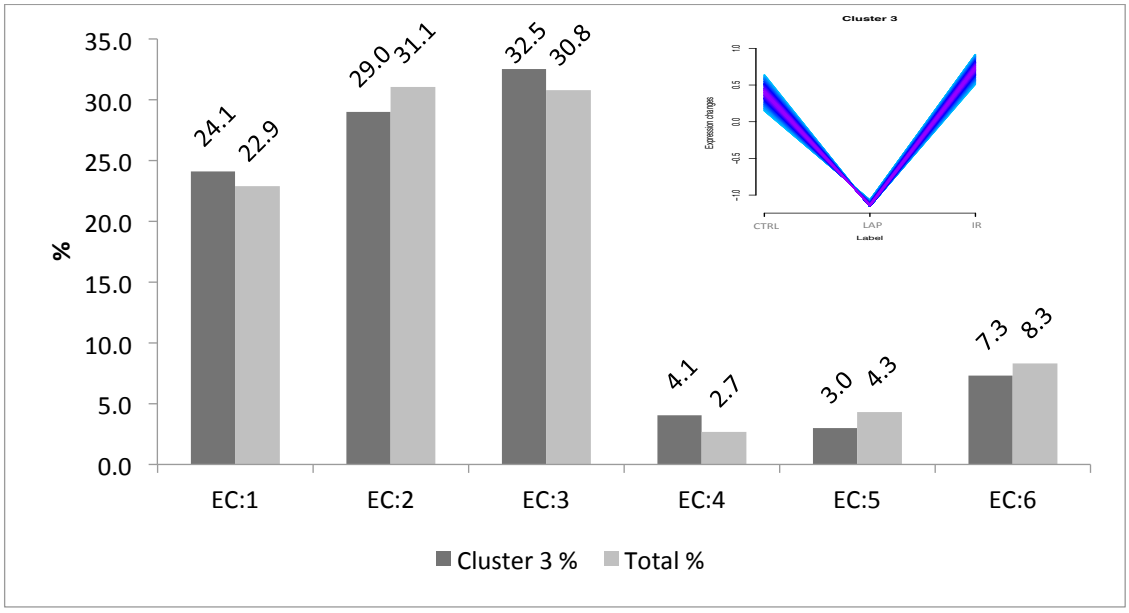

Figura 33. Predição enzimática das proteínas do cluster 3. Predição de atividade enzimática baseada em similaridade de sequência de proteínas por B2GO das proteínas identificadas do *cluster* 3.

5.6.3 Predição de atividade enzimática para o *cluster* 4

O gráfico de barras da Predição das enzimas reguladas do *cluster* 4 (Fig 34) mostra que há marcante enriquecimento de transferases (EC 2), aumentadas no grupo Laparotomia, enquanto há clara supressão no grupo IR. Detalhes dessas enzimas reguladas preditas são dados na tabela 5.

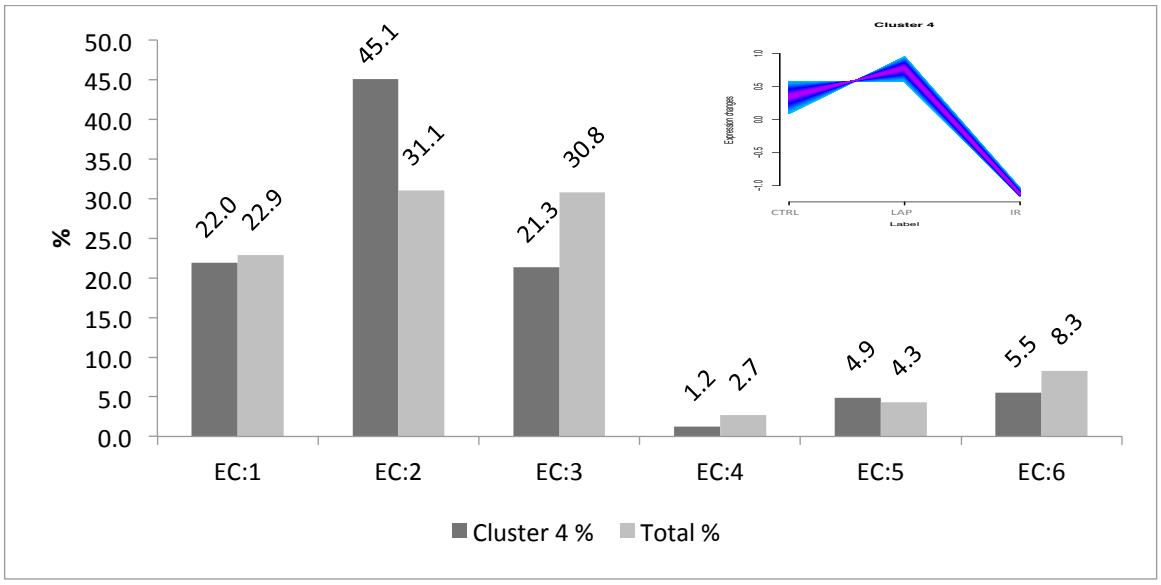

Figura 34 Predição enzimática das proteína do cluster 4. Predição de atividade enzimática baseada em similaridade de sequência de proteínas por B2GO das proteínas identificadas do *cluster* 4.

A enzima fosfatidilinositol 4 fosfato 5 cinase (PIP5K) (EC 2.7.1.149) catalisa a fosforilação de fosfatidilinositol 4-fosfato (PtdIms4P) para produzir fosfatidilinositol 4, 5-bifosfato [255], que é também um importante segundo mensageiro [256]. Três isoformas de PIP5K são bem conhecidas, como a, b e y. A PIP5Ka tem diversos papéis, incluindo a regulação da despolimerização de microtúbulos neuronais [257], a supressão da fagocitose [258], a interação de diacilglicerol cinase g (DGKg), resultando na formação de PtdIns (4,5) P2 [259]. Tanto a fosforilação de Ser/Thr quanto de Tyr ativam PIP5Kb, especialmente durante estresse oxidativo [260], além de ser envolvida na determinação da direção do movimento e na polarização de neutrófilos [261, 262].

NAD+ proteína-arginina ADP-ribosil transferase (ARTs) (EC 2.4.2.31) é envolvida na transferência de ADP-ribose de NAD para proteínas. Ela também é produzida por células epiteliais que revestem as vias aéreas de humanos, onde pode promover a modificação de peptídeos de neutrófilos humanos (HNP-1), alterando sua função. Essa alteração no HNP-1 de neutrófilos por ART1 é uma atividade importante em situações inflamatórias e outras doenças. Aqui nós demonstramos, pela primeira vez, a modulação de ARTs durante IR em neutrófilos [263].

Hexocinases (EC 2.7.1.2) catalisam a fosforilação de glicose em glicose 6-fosfato (primeira etapa da glicólise) [264]. Existem quatro isozimas presentes nos mamíferos, i.e. HK1, HK2, HK3 e HK4. A hexocinase 3 (HK3) está presente em baixas quantidades em todos os tecidos, enquanto os pulmões, rins e fígado as têm em quantidades moderadas a altas. [265]. Particularmente em granulócitos, 70-80% da atividade dessa família é dada pela HK3 e o restante pela HK1 [266]. Recentemente um estudo mostrou que a HK3 era significativamente suprimida em casos de Leucemia Promielocítica Aguda (APL) primária onde a diferenciação neutrofílica era prejudicada em células APL e que eventualmente causava a morte de células APL [267].

Proteínas tirosina cinases (EC 2.7.10) incluindo Src, Syk e Tec têm um papel muito importante em vias de transdução de sinal que regulam ativação e recrutamento de neutrófilos para o sítio de inflamação [268]. Proteínas tirosina cinases têm sua abundância primeiramente intensificada no grupo Laparotomia e posteriormente são suprimidas no grupo IR. A Tirosina Cinase Bruton (BTK) pertence à família Tec de tirosina cinases não receptoras. Recentemente foi demonstrado que neutrófilos BTK-deficientes tinham sua maturação e função prejudicadas. Essa condição foi encontrada associada ao desenvolvimento ineficiente de grânulos, assim como à expressão de proteínas de grânulos, tais como mieloperoxidase, proteína de grânulo neutrofílico, gelatinase e elastase de neutrófilos [269].

Proteínas cinase de serina/treonina (EC 2.7.11) são as mais reguladas de todas as enzimas preditas do *cluster* 4. A maior parte dessas enzimas não são bem anotadas na literatura em relação ao seu papel em neutrófilos. Uma das proteínas cinases de serina/treonina reguladas nesse grupo é a PAK2. Em neutrófilos, a cinase ativada por p21 (PAK2) pode ser estimulada por diversas quimiocinas (2770, 271]. A PAK2 também pode ser ativada ou sofrer auto-fosforilação quando ligada à Rac Ligada a GTP ativada ou Cdc42 [272]. Muitos estudos demonstraram que PAKs são envolvidas numa variedade de eventos celulares, como nas respostas rápidas de citoesqueleto, em eventos transcricionais e no desenvolvimento de malignidade [273]. Proteína cinase 2 ativada por MAP (MAPKAPK2), uma cinase Ser/thr, foi demonstrada como sendo fosforilada e ativada por MAP cinases (rapidamente estimuladas por mitógenos, citocinas e estresse) tanto in vivo quanto in vitro. A MAPKAP2 é envolvida na ativação de neutrófilos [274, 275]. De forma surpreendente, ela se encontra suprimida no *cluster* 4 da condição IR. A ativação da proteína cinase dependente de cálcio/calmodulina (EC 2.7.11.17) (CaMKs) inibe a maturação de neutrófilos [276]. A proteína cinase ativada por mitose (EC 2.7.11.24) inclui Erk, jnk e p38. Elas participam na inflamação, apoptose e migração, enquanto a p38 regula a quimiotaxia de neutrófilos tanto in vivo quanto in vitro [277].

Tabela 5 Enzimas do cluster 4 com função predita de transferase

Acc	Gene	PD Description	Enzyme Codes
Q9Z0T0	Tpmt	Thiopurine S-methyltransferase	EC:2.1.1.67
P40142	Tkt	Transketolase	EC:2.2.1.1
P0C1Q3	P0C1Q4	P0C1Q5	P0C1Q6
P63005	Pafah1b1	Platelet-activating factor acetylhydrolase IB subunit alpha	EC:2.3.1.149
P0C1Q3	Lpcat2	Lysophosphatidylcholine acyltransferase 2	EC:2.3.1.23
P0C1Q3	Lpcat2	Lysophosphatidylcholine acyltransferase 2	EC:2.3.1.51
P0C1Q3	Lpcat2	Lysophosphatidylcholine acyltransferase 2	EC:2.3.1.63
P0C1Q3	Lpcat2	Lysophosphatidylcholine acyltransferase 2	EC:2.3.1.67
Q9CYK2	Qpct	Glutaminyl-peptide cyclotransferase	EC:2.3.2.5
A2RRU1	Gys1	Glycogen [250] synthase, muscle	EC:2.4.1.11
Q64633	Ugt1a7c	UDP-glucuronosyltransferase 1-7	EC:2.4.1.17
Q5RJQ4	Sirt2	NAD-dependent protein deacetylase sirtuin-2	EC:2.4.2.30
P84084	Arf5	ADP-ribosylation factor 5	EC:2.4.2.31
P61750	Arf4	ADP-ribosylation factor 4	EC:2.4.2.31
P04905	Gstm1	Glutathione S-transferase Mu 1	EC:2.5.1.18
P20291	Alox5ap	Arachidonate 5-lipoxygenase-activating protein	EC:2.5.1.18
Q9R0I8	Pip4k2a	Phosphatidylinositol 5-phosphate 4-kinase type-2 alpha	EC:2.7.1.149
O88370	Pip4k2c	Phosphatidylinositol 5-phosphate 4-kinase type-2 gamma	EC:2.7.1.149
P27926	Hk3	Hexokinase-3	EC:2.7.1.2
Q1HCL7	Nadk2	NAD kinase 2, mitochondrial	EC:2.7.1.23
P27926	Hk3	Hexokinase-3	EC:2.7.1.2
P11980	Pkm	Pyruvate kinase PKM	EC:2.7.1.40
Q9R0I8	Pip4k2a	Phosphatidylinositol 5-phosphate 4-kinase type-2 alpha	EC:2.7.1.68
O88370	Pip4k2c	Phosphatidylinositol 5-phosphate 4-kinase type-2 gamma	EC:2.7.1.68
P27926	Hk3	Hexokinase-3	EC:2.7.1.2
Q9Z0P5	Twf2	Twinfilin-2	EC:2.7.10
P35991	Btk	Tyrosine-protein kinase BTK	EC:2.7.10
P31938	Map2k1	Dual specificity mitogen-activated protein kinase kinase 1	EC:2.7.10
P36506	Map2k2	Dual specificity mitogen-activated protein kinase kinase 2	EC:2.7.10
P50545	Hck	Tyrosine-protein kinase HCK	EC:2.7.10
P50545	Hck	Tyrosine-protein kinase HCK	EC:2.7.10.2
Q9JI11	Stk4	Serine/threonine-protein kinase 4	EC:2.7.11
P19139	Csnk2a1	Casein kinase II subunit alpha	EC:2.7.11
Q9CQR6	Ppp6c	Serine/threonine-protein phosphatase 6 catalytic subunit	EC:2.7.11
P18654	Rps6ka3	Ribosomal protein S6 kinase alpha-3	EC:2.7.11
Q9WUT3	Rps6ka2	Ribosomal protein S6 kinase alpha-2	EC:2.7.11
Q63644	Rock1	Rho-associated protein kinase 1	EC:2.7.11
Q4G050	Mknk1	MAP kinase-interacting serine/threonine-protein kinase 1	EC:2.7.11
O54833	Csnk2a2	Casein kinase II subunit alpha	EC:2.7.11
Q63184	Eif2ak2	Interferon-induced, double-stranded RNA-activated protein kinase	EC:2.7.11
Q53UA7	Taok3	Serine/threonine-protein kinase TAO3	EC:2.7.11
Q99J45	Nrbp1	Nuclear receptor-binding protein	EC:2.7.11
P80386	Prkab1	5'-AMP-activated protein kinase subunit beta-1	EC:2.7.11
Q8K1R7	Nek9	Serine/threonine-protein kinase Nek9	EC:2.7.11
P18265	Gsk3a	Glycogen synthase kinase-3 alpha	EC:2.7.11
P47197	Akt2	RAC-beta serine/threonine-protein kinase	EC:2.7.11
P27926	Hk3	Hexokinase-3	EC:2.7.11.2
Q64303	Pak2	Serine/threonine-protein kinase PAK 2	EC:2.7.11
P31938	Map2k1	Dual specificity mitogen-activated protein kinase kinase 1	EC:2.7.11
P49138	Mapkapk2	MAP kinase-activated protein kinase 2	EC:2.7.11
Q9WTY9	Mapk13	Mitogen-activated protein kinase 13	EC:2.7.11

Tabela 5 Enzimas do cluster 4 com função predita de transferase

Q66H84	Mapkapk3	MAP kinase-activated protein kinase 3	EC:2.7.11
P36506	Map2k2	Dual specificity mitogen-activated protein kinase kinase 2	EC:2.7.11
Q64303	Pak2	Serine/threonine-protein kinase PAK 2	EC:2.7.11.11
Q91VJ4	Stk38	Serine/threonine-protein kinase 38	EC:2.7.11.11
P09215	Prkcd	Protein kinase C delta type	EC:2.7.11.13
Q91VJ4	Stk38	Serine/threonine-protein kinase 38	EC:2.7.11.13
Q64303	Pak2	Serine/threonine-protein kinase PAK 2	EC:2.7.11.13
Q9JI11	Stk4	Serine/threonine-protein kinase 4	EC:2.7.11.13
P26817	Adrbk1	Beta-adrenergic receptor kinase 1	EC:2.7.11.14
P26817	Adrbk1	Beta-adrenergic receptor kinase 1	EC:2.7.11.15
P26817	Adrbk1	Beta-adrenergic receptor kinase 1	EC:2.7.11.16
P62204	Calm1	Calmodulin	EC:2.7.11.17
P49138	Mapkapk2	MAP kinase-activated protein kinase 2	EC:2.7.11.17
Q66H84	Mapkapk3	MAP kinase-activated protein kinase 3	EC:2.7.11.17
P11730	Camk2g	Calcium/calmodulin-dependent protein kinase type II subunit gamma	EC:2.7.11.17
P31938	Map2k1	Dual specificity mitogen-activated protein kinase kinase 1	EC:2.7.11.24
Q9WTY9	Mapk13	Mitogen-activated protein kinase 13	EC:2.7.11.24
P36506	Map2k2	Dual specificity mitogen-activated protein kinase kinase 2	EC:2.7.11.24
Q64303	Pak2	Serine/threonine-protein kinase PAK 2	EC:2.7.11.25
P97930	Dtymk	Thymidylate kinase	EC:2.7.4.4
P97930	Dtymk	Thymidylate kinase	EC:2.7.4.9
Q91ZJ5	Ugp2	UTP--glucose-1-phosphate uridylyltransferase	EC:2.7.7.9
O35156	UGP2	UTP--glucose-1-phosphate uridylyltransferase	EC:2.7.7.9

5.6.4 Predição de atividade enzimática para o *cluster* 5

A figura 35 mostra que as enzimas reguladas no *cluster* 5 são enriquecidas para oxiredutases (EC1) quando comparadas ao total de enzimas reguladas. Proteínas do *cluster* 5 encontram-se estimuladas na condição Laparotomia e também são mais abundantes na condição IR. Detalhes dessas enzimas preditas são dados na tabela 6.

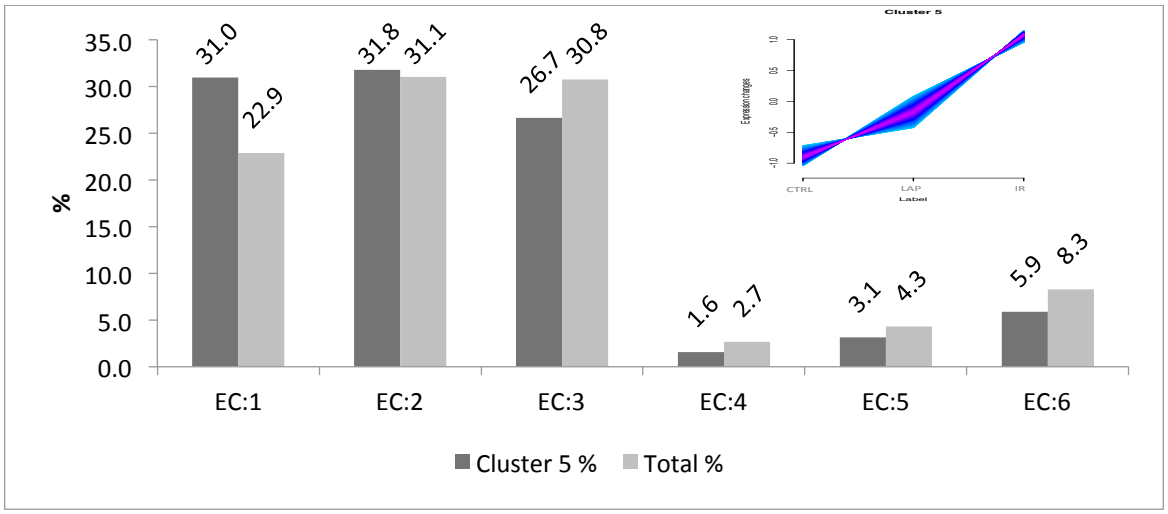

Figura 35 Predição enzimática das proteína do cluster 5. Predição de atividade enzimática baseada em similaridade de sequência de proteínas por B2GO das proteínas identificadas do *cluster* 5.

Aldose redutase (AR) (EC 1.1.1.21), que é uma enzima limitadora de taxa na via 3 do poliol, é um fator chave na injúria isquêmica de miocárdio e a sua elevação tem sido observada no coração durante isquemia que resulta em abertura de MTP [278, 279]. Em adição, foi demonstrado que AR medeia IRI em animais diabéticos e não diabéticos, que resulta em disfunção da microvasculatura [279, 280]. Inibição de AR preveniu a produção de citocinas inflamatórias e disfunção cardíaca induzidas por LPS em camundongos [281]. A estimulação de CD11b induzida por fMLP e a produção de superóxido são completamente impedidas por inibição de AR. Um estudo investigando o papel de AR na mediação de ALI mostrou que AR é necessária para que neutrófilos respondam à quimiocinas liberadas por ECs após a estimulação por TNFa. AR tem efeito também na estimulação de CD11b, na mudança de formato de neutrófilos e na adesão de neutrófilos à ECs [282]. Nossos dados sugerem o aumento na produção de AR durante IRI.

A análise proteômica da mucosa intestinal de ratos após pré-condicionamento isquêmico em um modelo de IRI identificou 10 proteínas por meio de 2DE em combinação com MALDI-TOF-MS e essas proteínas estavam envolvidas em anti-oxidação, inibição de apoptose e metabolismo energético. Esse estudo também revelou a estimulação de aldeído desidrogenase e aldose redutase no grupo IPC [152]. Outro estudo usou 2DE em combinação com MALDI-MS para analisar o proteoma de mucosa intestinal exposta à injúria de isquemia/reperfusão na presença e na ausência de pré-tratamento IPC em ratos. Um total de 16 proteínas estavam diferencialmente abundantes, às quais pertenciam proteínas envolvidas no metabolismo energético celular, anti-oxidação e anti-apoptose, dentre as quais a aldose redutase, que tem por função remover ROS, era significativamente suprimida em IR e estimulada em IPS [153]. À partir desses estudos e das nossas análises, parece interessante que a aldose redutase, sob condição de IR, encontra-se estimulada no neutrófilo e no miocárdio e suprimida na mucosa intestinal.

Lactato desidrogenase (LDH) (EC 1.1.1.27) é um conhecido marcador inespecífico de dano celular e necrose em tecidos cardíacos, hepáticos, musculares e renais, em uma variedade de infecções, linfomas, hemólise ou função tardia de enxertos [283]. A lactato

desidrogenase (LDH) é liberada de grânulos azurofílicos quando neutrófilos sofrem necrose [284].

6-Fosfogluconato desidrogenase (6PGDH) (EC 1.1.1.44), que converte 6-fosfogluconato em ribose 5-fosfato (segundo passo da PPP) com a liberação de uma segunda molécula de NAPDH. 6PGDH foi encontrada associada com o complexo oxidase de neutrófilo [285] e recentemente foi descoberta como fator de regulação da atividade de NADPH oxidase de fagócitos em neutrófilos [286].

Mieloperoxidase (MPO) (EC 1.11.1.7) é produzida e liberada em abundância à partir de grânulos azurofílicos de neutrófilos [287]. Ela catalisa a formação de ácido hipocloroso (HOCl), um agente oxidante com atividade bactericida in vitro [288]. Em adição, o sistema MPO-H2O2-cloreto por sua vez produz cloro, cloraminas, radicais hidroxil, oxigênio iônico e ozônio, que uma vez liberado para o exterior da célula pode atacar tecidos normais e assim contribuir para a patogênese da doença [289]. Outro estudo demonstrou que a ligação de MPO às integrinas CD11b/CD18 resulta em ativação de PMN por meio de mecanismo independente da atividade catalítica de MPO [290].

Araquidonato 5-lipoxigenase (EC 1.13.11.34) e Araquidonato 15-lipoxigenase 15-LO (EC 1.13.11.33) catalisam a inserção de oxigênio molecular no ácido araquidônico nos carbonos 5 e 15. Essas enzimas podem oxigenar também outros ácidos graxos polienóicos livres, assim como uma variedade de fosfolipídios [291]. Imunocitolocalização de 15-LO falhou em demonstrar a expressão de 15-LO em neutrófilos [292], e aqui nós demonstramos, pela primeira vez, o aumento na expressão dessas lipoxigenases em neutrófilos durante IRI.

Prostaglandina endoperoxidase sintase (EC 1.14.99.1), também conhecida como cicloxigenase (COX), que converte ácido araquidônico (AA) em Prostaglandina G2 (PGG2) e a redução de PGG2 em Prostaglandina H2 (PGH2), que é um precursor comum de todos os prostanóides [293]. Neutrófilos são capazes de sintetizar prostanóides em resposta a uma variedade de estímulos [294,295]. Em monócitos, a expressão de COX2 para a síntese de prostanóides necessita da ativação da p38MAPK [296]. Em neutrófilos tanto as vias de ERK e p38MAPK são envolvidas na expressão de COX2 e na produção

de prostaglandina E(2) PGE2 induzida por LPS, embora IL10 e IL4 possam inibir a síntese de prostanóides por neutrófilos por meio da supressão da ativação de p38MAPK [297].

Superóxido dismutase (SOD) (EC 1.15.1.1) está envolvida na regulação de apoptose de neutrófilos e pode levar a dano tecidual mediado por neutrófilos durante inflamação [298]. Recentemente foi descoberto que superóxido dismutase extracelular prejudica a função de neutrófilos e inibe a sua resposta imune inata, dessa forma levando à eliminação bacteriana prejudicada [299].

Xantina oxidase (XO) (EC 1.17.3.2) é uma enzima importante, tendo um papel no catabolismo de purinas. Em mamíferos a xantina desidrogenase endotelial (XDH) (EC 1.177.1.4) pode ser convertida em XO de forma reversível ou irreversível [300]. O estresse hipoxêmico também inicia a conversão de XDH em XO. O oxigênio molecular retorna aos tecidos durante a reperfusão dos intestinos, onde então reage com a hipoxantina e XO para produzir uma variedade de radicais livres de oxigênio, como ânion superóxido (O-2), peróxido de hidrogênio (H2O2) e óxidos nítricos [301]. Neutrófilos ativados também convertem XDH em XD em ECs, por meio da secreção de elastases de forma próximas às ECs [302]. Aqui nós estamos relatando pela primeira vez a presença e o consistente aumento da abundância XDH e XO em neutrófilos após isquemia e reperfusão.

Gliceraldeído-3-fosfato desidrogenase (GAPDH) (EC 2.1.12) é uma enzima glicolítica sendo que GAPDH de mamíferos também tem funções adicionais que incluem fusão de membranas, aglomeração de microtúbulos, atividade de fosfotransferase, exportação de RNA nuclear, replicação de DNA e reparo de DNA. Além disso, ela também participa de apoptose, de doenças neurodegenerativas relacionadas à idade, câncer de próstata e patogênese viral [303]. Foi provado que ela está envolvida em até 25% da desgranulação citosólica dependente de Ca em neutrófilos [304].

Retinal desidrogenase (RALDH) (EC 1.2.1.36) converte vitamina A em ácido retinóico (RA) em células dentríticas (DCs) e células estromais no intestino e induz a migração de células T para o intestino [305], como células T produtoras de Foxp3 [306] e células B

com expressão de IgA [307], assim como promove a supressão da diferenciação de células Th17 [308]. Aqui nós reportamos pela primeira vez um aumento na expressão de RALDH em neutrófilos após isquemia e reperfusão intestinal.

NADPH desidrogenase (quinona) (EC 1.6.5.2), também conhecida como NAD(P)H quinona oxiredutase 1 (NQO1) é uma flavoproteína que catalisa a redução metabólica de quinonas [309]. Níveis elevados de NQO1 foram observados em tecidos tumorais, quando comparados a tecidos normais [310], como em câncer pulmonar de células não-pequenas, câncer de cólon, câncer de mama, câncer de ovário e melanoma [310, 311]. Níveis elevados de NQO1 também foram encontrados em tumores de fígado, pulmão e cólon em pacientes humanos [312]. Aqui nós estamos relatando pela primeira vez a elevação da expressão de NQO1 em neutrófilos após isquemia/reperfusão.

Glutationa redutase (Gsr) (EC 1.8.1.7) catalisa a regeneração de glutationa a partir de glutationa disulfídica utilizando NADPH, onde a glutationa funciona como importante anti-oxidante, essencial para a remoção de H2O2 do citosol de granulócitos e leucócitos [313, 314]. Recentemente descobriu-se que Gsr facilita a defesa do hospedeiro por sustentar o burst oxidativo fagocítico e promover o desenvolvimento das armadilhas extracelulares de neutrófilos (NET) em camundongos [315].

Tioredoxina redutase NADPH dependente (TrxR) 1 (EC 1.8.1.9) está envolvida na denitrosilação de proteínas citosólicas [316]. Thom, S.R., et al. mostraram recentemente que TrxR está também envolvida no controle do citoesqueleto em neutrófilos através de associação com Adenosina Cinase Focal (FAK) [317].

Tabela 6 Enzimas do cluster 5 com função predita de oxidoredutase.

Acc	Gene	PD Description	Enzyme Codes
P07943	Akr1b1	Aldose reductase	EC:1.1.1.112
P07943	Akr1b1	Aldose reductase	EC:1.1.1.149
P22985	Xdh	Xanthine dehydrogenase/oxidase	EC:1.1.1.158
O70351	Hsd17b10	3-hydroxyacyl-CoA dehydrogenase type-2	EC:1.1.1.159
O70351	Hsd17b10	3-hydroxyacyl-CoA dehydrogenase type-2	EC:1.1.1.178
O70351	Hsd17b10	3-hydroxyacyl-CoA dehydrogenase type-2	EC:1.1.1.201
P07943	Akr1b1	Aldose reductase	EC:1.1.1.21
O70351	Hsd17b10	3-hydroxyacyl-CoA dehydrogenase type-2	EC:1.1.1.239
P04642	Ldha	L-lactate dehydrogenase A chain	EC:1.1.1.27
P19629	Ldhc	L-lactate dehydrogenase C chain	EC:1.1.1.27
Q811X6	Cryl1	Lambda-crystallin homolog	EC:1.1.1.35
O70351	Hsd17b10	3-hydroxyacyl-CoA dehydrogenase type-2	EC:1.1.1.35
O70351	Hsd17b10	3-hydroxyacyl-CoA dehydrogenase type-2	EC:1.1.1.36
Q99KE1	Me2	NAD-dependent malic enzyme, mitochondrial	EC:1.1.1.38
Q99KE1	Me2	NAD-dependent malic enzyme, mitochondrial	EC:1.1.1.39
P85968	Pgd	6-phosphogluconate dehydrogenase, decarboxylating	EC:1.1.1.43
P85968	Pgd	6-phosphogluconate dehydrogenase, decarboxylating	EC:1.1.1.44
O70351	Hsd17b10	3-hydroxyacyl-CoA dehydrogenase type-2	EC:1.1.1.51
O70351	Hsd17b10	3-hydroxyacyl-CoA dehydrogenase type-2	EC:1.1.1.62
P85968	Pgd	6-phosphogluconate dehydrogenase, decarboxylating	EC:1.1.1.95
Q3MID2	Cyp4f3	Leukotriene-B(4) omega-hydroxylase 2	EC:1.1.4.1
P11247	Mpo	Myeloperoxidase	EC:1.11.1.7
P49290	Epx	Eosinophil peroxidase	EC:1.11.1.7
P00406	Mtco2	Cytochrome c oxidase subunit 2	EC:1.11.1.7
Q63189	Prg2	Bone marrow proteoglycan	EC:1.11.1.7
P04041	Gpx1	Glutathione peroxidase 1	EC:1.11.1.9
Q02759	Alox15	Arachidonate 15-lipoxygenase	EC:1.13.11.33
P48999	Alox5	Arachidonate 5-lipoxygenase	EC:1.13.11.34
P00406	Mtco2	Cytochrome c oxidase subunit 2	EC:1.13.11
P48999	Alox5	Arachidonate 5-lipoxygenase	EC:1.13.11.34
Q02759	Alox15	Arachidonate 15-lipoxygenase	EC:1.13.11.33
Q02759	Alox15	Arachidonate 15-lipoxygenase	EC:1.13.11.33
P48999	Alox5	Arachidonate 5-lipoxygenase	EC:1.13.11.34
Q02759	Alox15	Arachidonate 15-lipoxygenase	EC:1.13.11.33
P48999	Alox5	Arachidonate 5-lipoxygenase	EC:1.13.11.34
P48999	Alox5	Arachidonate 5-lipoxygenase	EC:1.13.11.34
Q02759	Alox15	Arachidonate 15-lipoxygenase	EC:1.13.11.33
P00388	Por	NADPH--cytochrome P450 reductase	EC:1.14.12.17
Q99MS7	Ehbp1l1	EH domain-binding protein 1-like protein 1	EC:1.14.13
Q3MID2	Cyp4f3	Leukotriene-B(4) omega-hydroxylase 2	EC:1.14.13
P00388	Por	NADPH--cytochrome P450 reductase	EC:1.14.13
Q3MID2	Cyp4f3	Leukotriene-B(4) omega-hydroxylase 2	EC:1.14.13.30
Q3MID2	Cyp4f3	Leukotriene-B(4) omega-hydroxylase 2	EC:1.14.14.1
Q3MID2	Cyp4f3	Leukotriene-B(4) omega-hydroxylase 2	EC:1.14.15.3
P00406	Mtco2	Cytochrome c oxidase subunit 2	EC:1.14.99.1
P05982	Nqo1	NAD(P)H dehydrogenase 1	EC:1.15.1.1
Q4V8K1	Steap4	Metalloreductase STEAP4	EC:1.16.1

Q4V8K1	Steap4	Metalloreductase STEAP4	EC:1.16.1.7
Q4V8K1	Steap4	Metalloreductase STEAP4	EC:1.16.1.9
P09528	Fth1	Ferritin heavy chain	EC:1.16.3.1
P22985	Xdh	Xanthine dehydrogenase/oxidase	EC:1.17.1.4
P22985	Xdh	Xanthine dehydrogenase/oxidase	EC:1.17.3.2
P07943	Akr1b1	Aldose reductase	EC:1.2
P11884	Aldh2	Aldehyde dehydrogenase, mitochondrial	EC:1.2.1
Q4KYY3	GAPDH	Glyceraldehyde-3-phosphate dehydrogenase	EC:1.2.1.12
Q9Z2I8	Suclg2	Succinyl-CoA ligase subunit beta, mitochondrial	EC:1.2.1.24
P11884	Aldh2	Aldehyde dehydrogenase, mitochondrial	EC:1.2.1.3
P11884	Aldh2	Aldehyde dehydrogenase, mitochondrial	EC:1.2.1.36
P07943	Akr1b1	Aldose reductase	EC:1.2.1.36
Q5XI42	Aldh3b1	Aldehyde dehydrogenase family 3 member B1	EC:1.2.1.5
P11884	Aldh2	Aldehyde dehydrogenase, mitochondrial	EC:1.2.1.5
O08984	Lbr	Lamin-B receptor	EC:1.3.1.70
P11348	Qdpr	Dihydropteridine reductase	EC:1.5.1.34
Q63189	Prg2	Bone marrow proteoglycan	EC:1.5.5.1
P00388	Por	NADPH--cytochrome P450 reductase	EC:1.6.2.2
P05982	Nqo1	NAD(P)H dehydrogenase [quinone] 1	EC:1.6.2.2
P00388	Por	NADPH--cytochrome P450 reductase	EC:1.6.2.4
O70145	Ncf2	Neutrophil cytosol factor 2	EC:1.6.3
P05982	Nqo1	NAD(P)H dehydrogenase [quinone] 1	EC:1.6.5.10
P05982	Nqo1	NAD(P)H dehydrogenase [quinone] 1	EC:1.6.5.2
Q9DCZ1	Gmpr	GMP reductase 1	EC:1.7.1.7
P70619	Gsr	Glutathione reductase (Fragment)	EC:1.8.1.7
P47791	Gsr	Glutathione reductase, mitochondrial	EC:1.8.1.7
O89049	Txnrd1	Thioredoxin reductase 1, cytoplasmic	EC:1.8.1.9
Q9ESH6	Glrx	Glutaredoxin-1	EC:1.8.4.2
P00406	Mtco2	Cytochrome c oxidase subunit 2	EC:1.9.3.1
P00388	Por	NADPH--cytochrome P450 reductase	EC:1.9.99.1
P32577	Csk	Tyrosine-protein kinase CSK	EC:1.97.1
P09528	Fth1	Ferritin heavy chain	EC:1.97.1

5.7 Análise de vias metabólicas.

A Enciclopédia Kyoto de Genes e Genomas (KEGG) é utilizada como uma base de referência para a compreensão de transdução de sinal, processos celulares e das vias biológicas [318]. Os números de acesso UniProt das proteínas identificadas no presente trabalho foram mapeados para símbolos de genes pelo programa Proteína Center. Símbolos de genes de todas as proteínas diferencialmente abundantes dos cinco *cluster*s foram mapeados para o genoma de vias KEGG usando bases de dados online dos

programas WebGestalt e Enrichnet [197, 198]. A maioria das vias mostrou resultados significativos em diferentes clusters o que levou à análise e discussão dessas vias comuns em conjunto . A razão para a presença das mesmas vias em diferentes clusters é que, como a maioria das bases de dados, incluindo WebGestalt e Enrichnet, usa símbolos de genes em vez do padrão UniProt, o mapeamento de números de acesso UniProt para símbolos de genes resultou na atribuição de diferentes proteínas aos mesmos genes. Tal fato conduziu a uma duplicação de genes. Caso esses genes duplicados tivessem sido removidos de todos os cinco *cluster*s, cerca de 200 genes seriam eliminados além de uma diminuição no nível de significância, com pouca alteração na atribuição das vias . Então, nós removemos as duplicatas de vias de interesse em vez de remover todos os clusters. Na tabela. 7, os genes de sobreposição são genes no conjunto de genes carregados e também encontrados nos genes de referência na categoria. A Proporção é a relação de enriquecimento; P-valor bruto é o valor P do teste hipergeométrico e o p-valor foi ajustado pelo ajuste de testes múltiplos.

Tabela 7- Vias KEGG preditas para cada cluster.

PathwayName	Overlap Gene	Cluster No.	Reference Genes	Ratio	Raw P-value	Adjusted P-value
Ribosome	57	1	122	44.41	8.98E-80	1.11E-77
Spliceosome	28	1	135	19.72	4.74E-28	2.94E-26
Metabolic pathways	49	1	1169	3.98	3.16E-16	1.31E-14
Protein processing in endoplasmic reticulum	20	1	164	11.59	1.12E-15	3.47E-14
RNA transport	19	1	156	11.58	5.96E-15	1.48E-13
Phagosome	18	1	185	9.25	1.54E-12	3.18E-11
Proteasome	10	1	49	19.4	8.60E-11	1.52E-09
Neurotrophin signaling pathway	12	1	129	8.84	1.38E-08	2.14E-07
Focal adhesion	13	1	186	6.64	1.05E-07	1.45E-06
Lysosome	10	1	124	7.67	8.46E-07	9.54E-06
Regulation of actin cytoskeleton	24	2	208	11.53	1.78E-18	2.06E-16
Fc gamma R-mediated phagocytosis	17	2	91	18.67	4.37E-17	2.53E-15
Neurotrophin signaling pathway	18	2	129	13.94	1.15E-15	4.45E-14
Oocyte meiosis	17	2	115	14.77	2.67E-15	6.19E-14
Leukocyte transendothelial migration	17	2	114	14.9	2.29E-15	6.19E-14
Protein processing in endoplasmic reticulum	19	2	164	11.58	6.17E-15	1.19E-13
Long-term potentiation	14	2	69	20.27	7.74E-15	1.28E-13
Chemokine signaling pathway	18	2	178	10.1	3.45E-13	5.00E-12
Metabolic pathways	42	2	1169	3.59	1.38E-12	1.78E-11
Cell cycle	15	2	124	12.09	2.37E-12	2.75E-11
Metabolic pathways	109	3	1169	6.5	2.28E-55	3.58E-53
Spliceosome	36	3	135	18.59	3.41E-35	2.68E-33
Huntington's disease	41	3	218	13.11	2.87E-33	1.50E-31
Parkinson's disease	34	3	164	14.45	2.71E-29	1.06E-27
Oxidative phosphorylation	30	3	156	13.41	5.65E-25	1.77E-23
Proteasome	20	3	49	28.45	1.95E-24	5.10E-23
Citrate cycle (TCA cycle)	17	3	30	39.5	3.77E-24	8.46E-23
Alzheimer's disease	31	3	212	10.19	4.95E-22	9.71E-21
Protein processing in endoplasmic reticulum	26	3	164	11.05	1.34E-19	2.34E-18
Lysosome	22	3	124	12.37	7.00E-18	1.10E-16
Neurotrophin signaling pathway	22	4	129	21.85	3.75E-23	4.57E-21
Regulation of actin cytoskeleton	25	4	208	15.4	3.06E-22	1.87E-20
Long-term potentiation	16	4	69	29.71	1.77E-19	7.20E-18
Oocyte meiosis	17	4	115	18.94	4.39E-17	1.34E-15
Insulin signaling pathway	17	4	131	16.62	4.21E-16	1.03E-14
Metabolic pathways	41	4	1169	4.49	1.40E-15	2.85E-14
Fc gamma R-mediated phagocytosis	12	4	91	16.89	7.71E-12	1.18E-10
Leukocyte transendothelial migration	13	4	114	14.61	6.83E-12	1.18E-10
Chemokine signaling pathway	15	4	178	10.8	1.36E-11	1.84E-10
Glioma	10	4	62	20.66	5.55E-11	6.41E-10
Metabolic pathways	51	5	1169	4.77	3.39E-20	4.24E-18
Vasopressin-regulated water reabsorption	11	5	44	27.35	1.91E-13	1.19E-11
Chemokine signaling pathway	16	5	178	9.83	1.12E-11	4.67E-10
Systemic lupus erythematosus	14	5	132	11.6	2.35E-11	7.34E-10
Fc gamma R-mediated phagocytosis	12	5	91	14.43	4.77E-11	1.19E-09
Endocytosis	16	5	230	7.61	5.16E-10	1.08E-08
Regulation of actin cytoskeleton	15	5	208	7.89	1.09E-09	1.95E-08
Glycolysis / Gluconeogenesis	10	5	78	14.03	2.64E-09	4.03E-08
Neurotrophin signaling pathway	12	5	129	10.18	2.90E-09	4.03E-08
Oocyte meiosis	11	5	115	10.46	9.90E-09	1.24E-07

5.7.1 Via do Ribossoma:

A partir da tabela 6, observa-se que a via mais importante e significativa encontrada a partir da base de dados WebGestalt é a via ribossômica, com um valor P ajustado de 1.11e-77 e 57 proteínas superpostas a partir do nosso conjunto de dados que estão presentes nessa via (Fig. 36, 37).

Proteínas ribossomais são componentes fundamentais no metabolismo celular e a síntese no ribossoma é crítica para o crescimento e desenvolvimento celular. As proteínas (r-) ribossomais são responsáveis pelo dobramento correto e clivagem de rRNA, bem como para a montagem de subunidade [1]. O ribossoma eucariota consiste de duas subunidades, uma subunidade maior (60S) e outra menor (40S). A subunidade maior contém três RNAs e 46 proteínas e a subunidade menor é composta de um RNA e 33 proteínas. Proteínas ribossomais têm algumas atividades ribossomais extras, incluindo função catalítica, replicação, transcrição, processamento de RNA, reparo do DNA, e até mesmo inflamação (em monócitos), mas essas funções para cada proteína ribossômica ainda não foram elucidadas [319-321]. Durante condições normais, a mesma quantidade de rRNA e proteínas ribossomais são sintetizadas numa célula enquanto que as condições alteradas também alteram os níveis de síntese de proteínas ribossomais [322]. Como durante a diferenciação neuronal de células de carcinoma embrionário humano, proteínas da subunidade maior como L3, L7, L8, L10, L23a, L27a, L36a, e L39, mostraram diminuição da expressão, exibindo uma sub-regulação constante , juntamente com algumas proteínas da subunidade menor (S2, S3, S3a, S4X, S6, S9, S12, S13, S16, S19, S20, S23, e S27a).

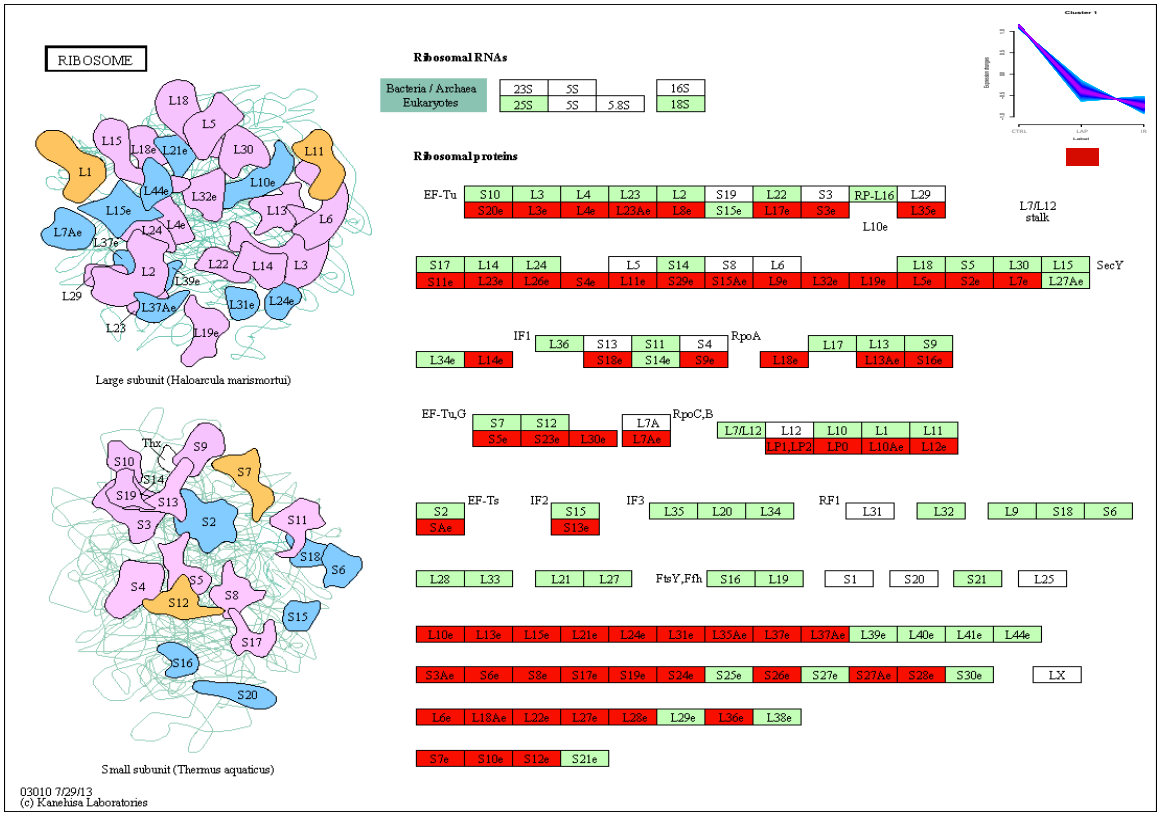

Figura 36- A via ribossomal enriquecida, mostrando as proteínas diferencialmente abundantes (DAPs) a partir do cluster 1. As proteínas sobrepostas com diminuição da abundância foram destacadas em vermelho.

Observou-se que enquanto L11, L32, S8 e S11 foram constantes inicialmente ou até com abundância aumentada, posteriormente apresentaram diminuição na abundância como L6, L15, L17, L31, e S27y [323]. Esta alteração independente na síntese de proteínas ribossomais sugere que essas proteínas possuem outras funções. Por exemplo P0 e S3 têm mostrado atividade de endonucleases, isso pode ter papel no reparo do DNA [324, 325] e L7 também pode atuar como co-reguladora do receptor de vitamina D [326]. L7 em células Jurkat de linfoma T [327], S20 na linha celular de leucemia humana CEM C7 [328], e S3a na célula tumoral [329] podem ter um papel na apoptose.

Oligômeros RP S19 atuam como quimiotáticos para a migração de monócitos / macrófagos para células em apoptose através da C5aR [330]. Oligômeros RP S19 tem duplo papel na C5aR de leucócitos fagocíticos; isso produz um efeito induzido pelo agonista na C5aR de monócitos mas por outro lado promove um efeito induzido pelo

antagonista sobre C5aR de neutrófilos [331]. C5a provoca a migração quimiotáctica e a secreção através da via clássica ERK1 / 2 mediada por C5aR.

Oligômeros RP S19 inibem vias quimiotácticas mediadas por C5aR neutrófilos. no entanto o mecanismo não é conhecido [332, 333]. Aqui estamos relatando pela primeira vez a diminuição da regulação de 57 proteínas ribossomais em neutrófilos após laparotomia e isquemia / reperfusão intestinal (Figura 36). RPS19 também está entre as proteínas com abundância diminuída, que podem estar envolvidos no aumento da quimiotaxia mediadas por C5aR em neutrófilos após IR.

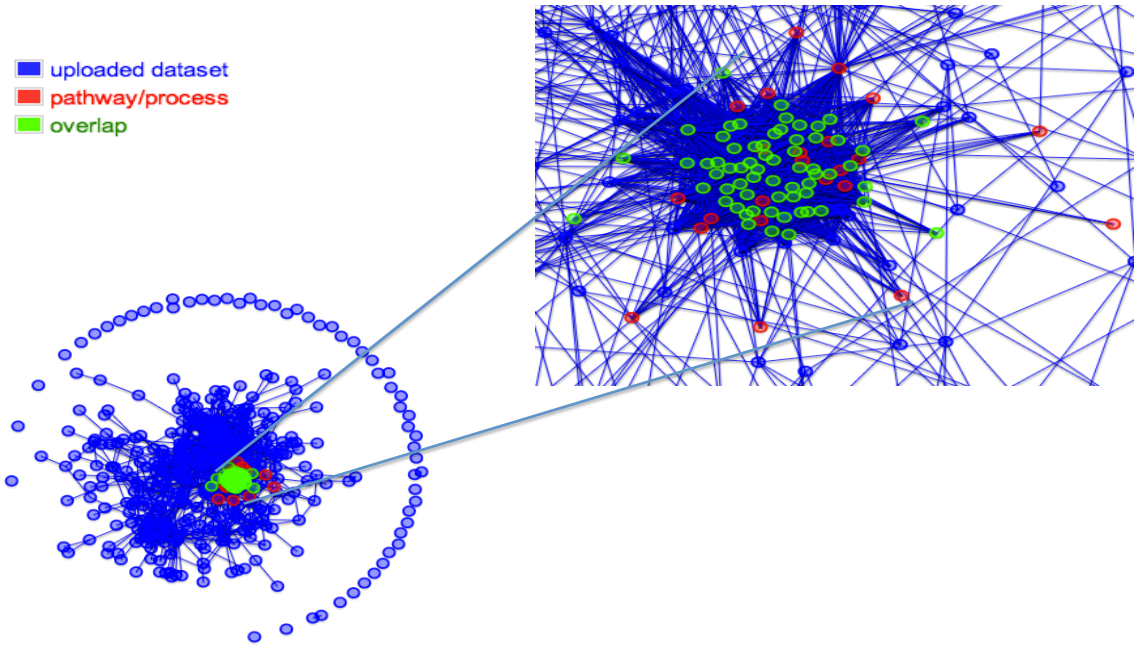

Figura 37 - visualização por Computação gráfica da Enrichnet do conjunto de dados do cluster 1. A sobreposição (verde) é mostrada para a regulação da via ribossômica.

A Interação em geral de proteínas identificadas no cluster 1 foi determinada utilizando o banco de dados STRING online. Para confirmação sobre a interação também foram analisadas as proteínas ribossomais em STRING e os resultados (Fig.38) mostraram forte ligação entre estas proteínas.

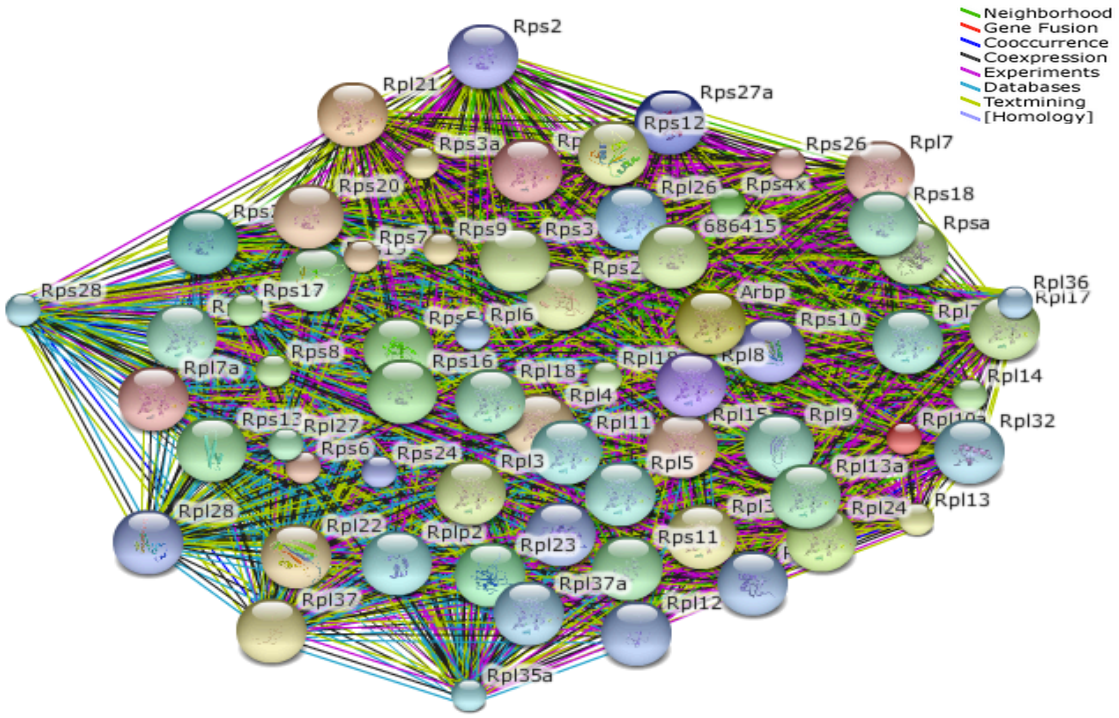

Figura 38- rede de interação de proteínas do cluster 1 identificados na via KEGG ribossômica.

5.7.2 Regulação das vias da actina do citoesqueleto

A regulação das vias da actina do citoesqueleto mostra proteínas comuns aos clusters 2, 4 e 5 com os valores-P, P = 2.06e-16 e 24 proteínas sobrepostas , P=1.87e-20 e 25 proteínas de sobreposição e P = 1.95e-08 com 15 proteínas com sobreposição respectivamente. Os valores de P desta via para cada cluster são significativos por isso fizemos uma comparação de todos os três grupos com diferentes cores para cada cluster, como mostrado na fig.39. A maior parte das proteínas apresentaram abundância aumentada (ouro e amarelo) e algumas apresentam abundância diminuída (vermelho) nesta via.

Neutrófilos circulantes normais não são polarizados. Uma vez que um quimioatrativo se liga ao seu receptor na superfície celular, a ativação do citoesqueleto ocorre depois de transduções de sinais citoplasmáticos que conduzem à formação de actina filamentosa lamelar ou de F-actina (frente=lamelipodia) e a uropodia rica em filamentos de actinomiosina (atrás) (polarização). Os neutrófilos podem alinhar sua polaridade de frente para trás com o gradiente quimioatrativo e começar a migração direcional [334].

Estudos demonstraram associação entre a PI-3-cinase e ativação de uma família de proteínas de ligação ao GTP Ras (pequenas) e de uma subfamília Ras incluindo Rho, Rac e CDC-42, que são importantes reguladores da motilidade e da morfologia da célula [335]. O complexo Arp2 / 3 localiza-se em regiões de polimerização ativa da actina em neutrófilos e está envolvido em vários vias de sinalização e organização da actina [336]. Regulação das vias da actina do citoesqueleto dos nossos dados mostraram que a maior parte destas proteínas incluindo Rho, Rac, Rac, Arp2 / 3 entre outros estão presentes. Essas proteínas apresentam abundância aumentada em neutrófilos durante IR em relação ao controle, levando a um aumento da motilidade, locomoção e quimiotaxia (Fig.39).

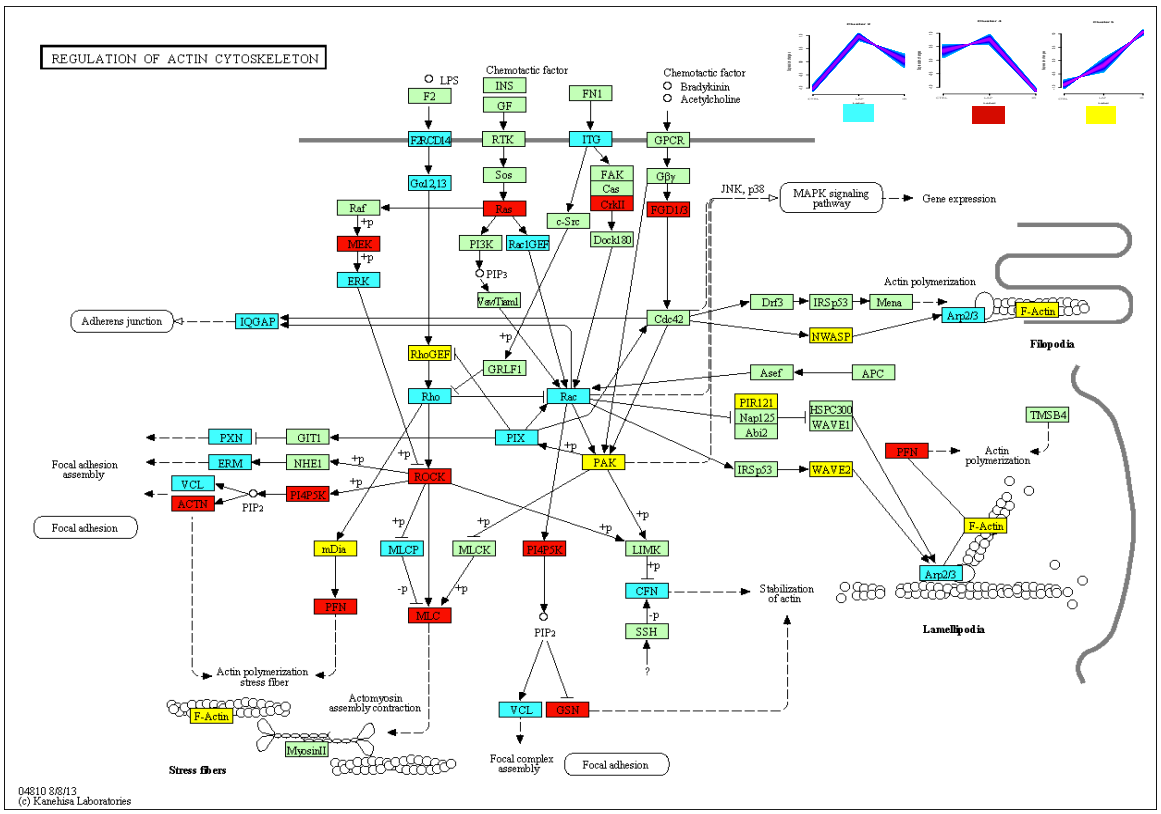

*Figura 39 O controle da via actina do citoesqueleto das proteínas diferencialmente abundantes (DAPs) de clusters de 2, 4 e 5. Azul (cluster 2) e amarelo (*cluster *5) mostram aumento da abundância , vermelho (*cluster *4) para abundância diminuída e verde não encontrada em nossa base de dados.*

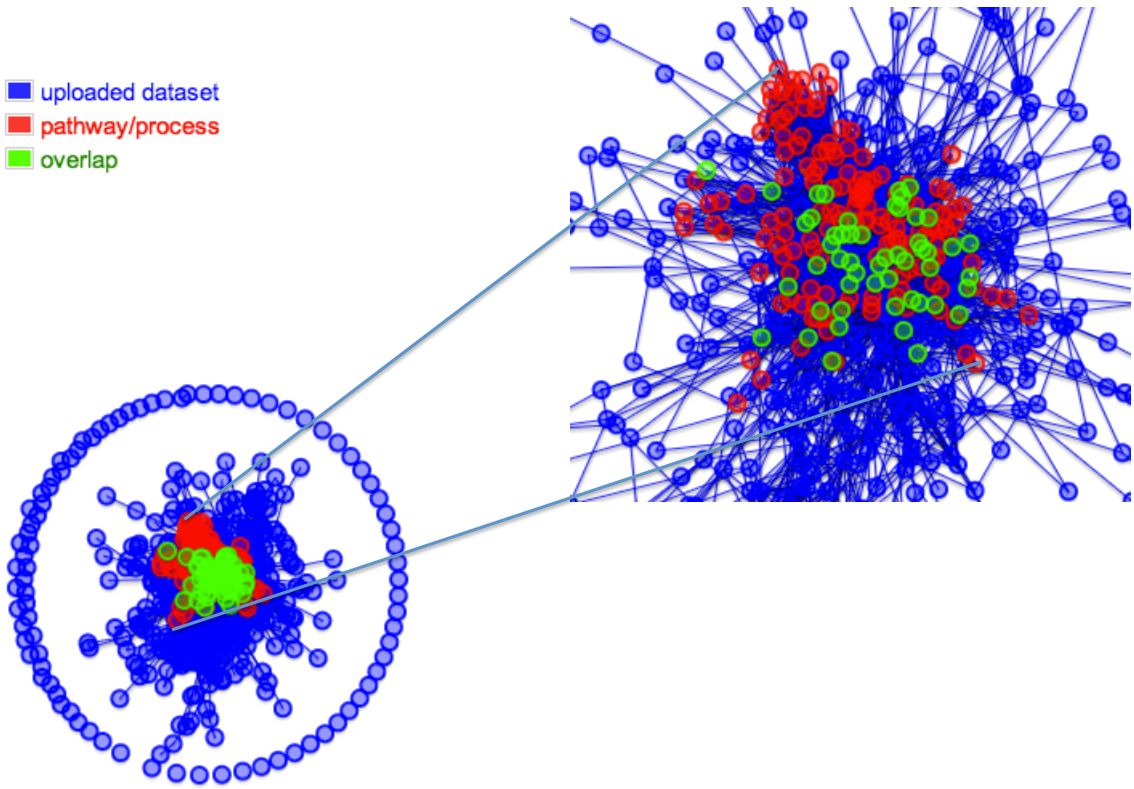

Figura 40- visualização gráfica de enrichnet.org de conjunto de dados enviados, para clusters de 2, 4 e 5 de sobreposição (verde) é mostrado para o controle da via da actina do citoesqueleto.

A visualização gráfica gerada por enrichnet.org do conjunto de dados enviado do cluster 2, 4 e 5. a sobreposição para a regulação da via da actina do citoesqueleto é mostrada na fig.40. Genes que se sobrepõem são mostrados em verde. Para as proteínas que se sobrepõem, uma análise de interação proteína-proteína uma STRING foi realizada para descobrir as interações entre as proteínas (Figura 41.).

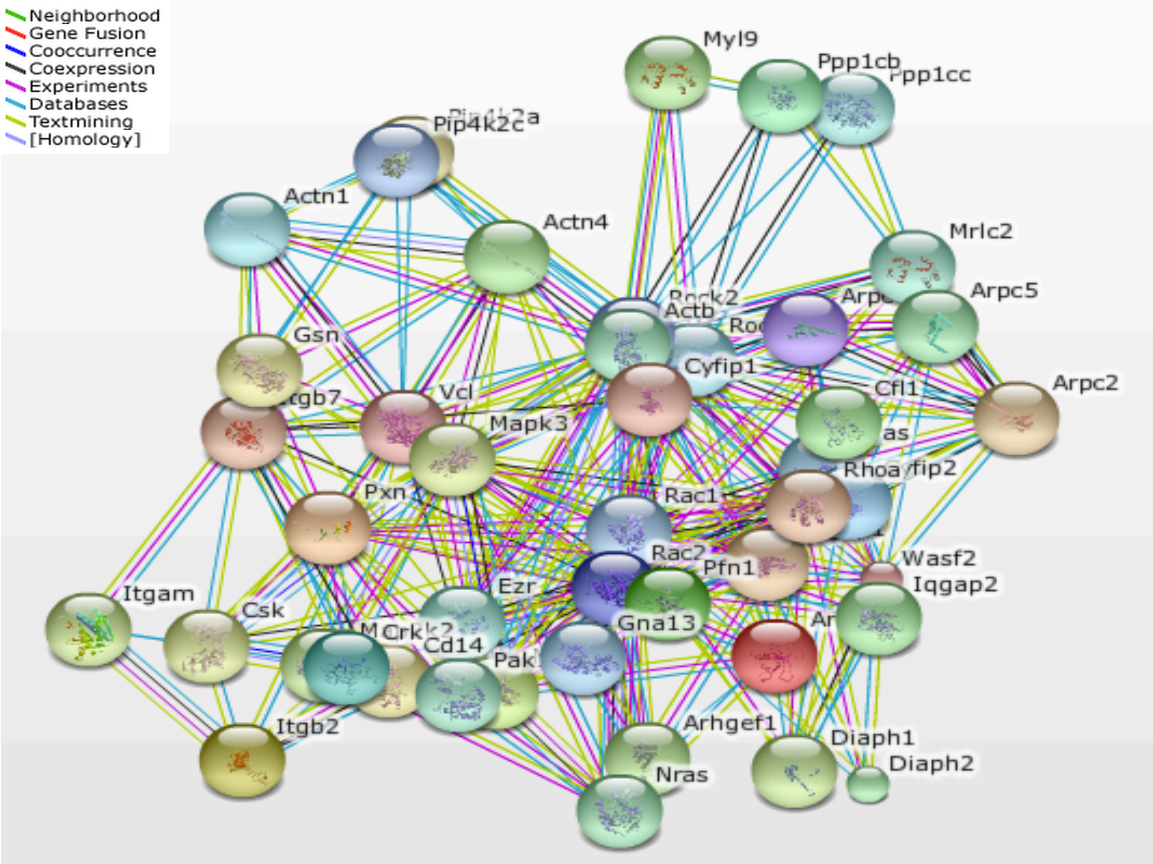

Figura 41- rede de interação de proteínas dos clusters 2, 4 e 5 identificados na via KEGG de organização da actina do citoesqueleto.

5.7.3 Via da fagocitose mediada por Fc gama R:

A Tabela 7 mostra que a outra via interessante predita por WebGestalt é a via da fagocitose mediada por Fc gamma R com valor P = 2.53e-15 e 17proteínas sobrepostas, P = 1.18e-10 e 12 proteínas sobrepostas e P = 1.19e- 09 com 12 proteínas sobrepostas dos clusters 2, 4 e 5, respectivamente (fig. 42) . As proteínas com aumento de abundância incluem Src, Syk, SPHK, WASP, PLC, ERK1 / 2, c PKC, p47phox, Arp2 / 3, Rac, PAG3, PAK1, WASP, WAVE e cofilina (amarelo e dourado) e poucas proteínas com diminuição da abundância , tais como a PKC, gelsolina, VASP, CrkII (vermelho). A visualização gráfica computacional feita pelo EnrichNet do conjunto de dados carregados a partir desses clusters mostra sobreposição de proteínas (verde) para fagocitose mediada pela via Fc gamma R na fig. 38. Em azul estão os conjuntos de todos os dados desses clusters das proteínas carregadas, e vermelho são as proteínas não sobrepostas dessa via.

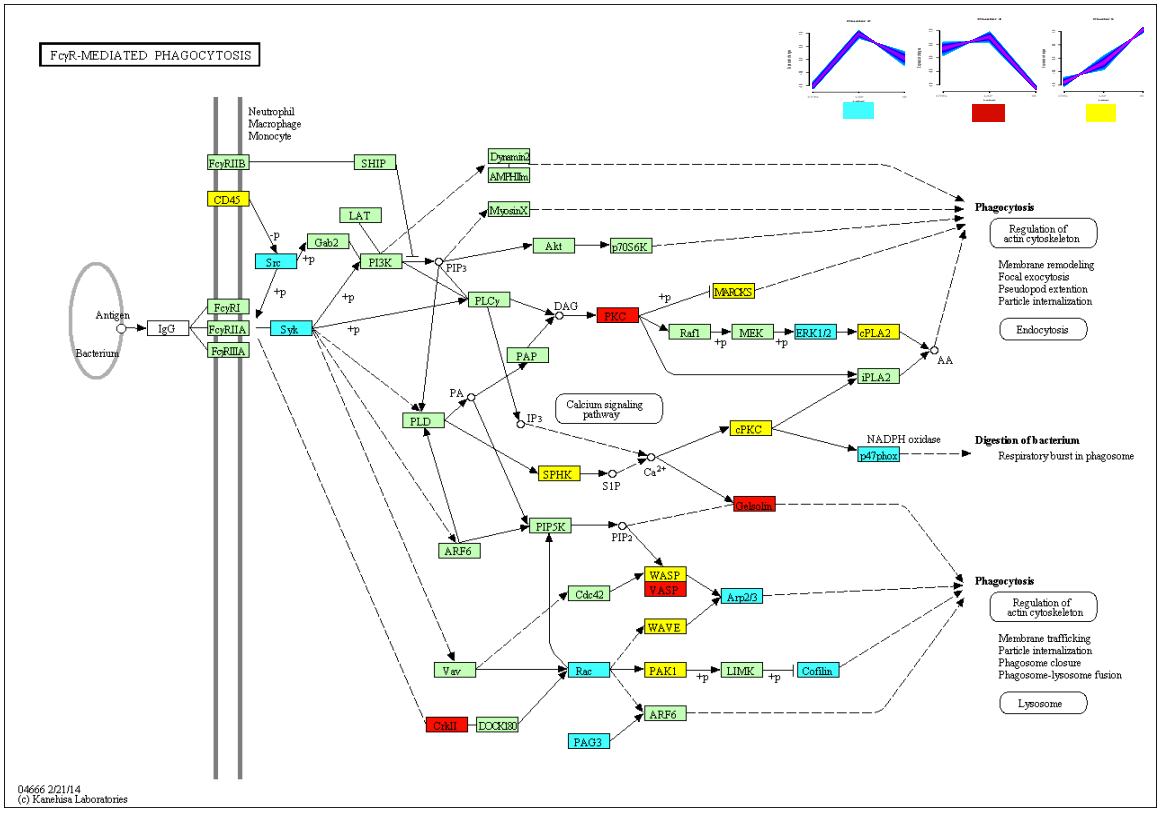

*Figura 42-A via de fagocitose por Fc gama mediada por R enriquecida para as proteínas diferencialmente abundantes (DEPs) dos clusters 2, 4 e 5. Azul (cluster 2) e amarelo (*cluster *5) estão com abundância aumentada e vermelho (*cluster *4) com abundância proteica diminuida.*

Como resultado da interação do FcR com os seus ligantes de Ig em leucócitos ocorre uma série de respostas, incluindo a fagocitose, citotoxicidade mediada por células dependente de anticorpos (ADCC), a liberação de mediadores pró-inflamatórios e produção de citocinas [337, 338]. A fosforilação de resíduos específicos de tirosina nos motivos de ativação de imunoreceptores ligados a tirosina (ITAMs) ocorre depois do agrupamento dos receptores e ligantes [339] e enzimas da família de tirosina-cinases Src estão envolvidas na fosforilação inicial das ITAMs [340]. Syk, uma tirosina cinase, é um importante componente dessa via, como em neutrófilos, a sua inibição repele a fagocitose de partículas revestidas com IgG [341]. Mas o papel exato da Syk neste processo permanece obscuro. Alguns estudos mostram o seu papel na formação de filamentos de actina durante a fagocitose mediada por FcRγ [341, 342].

PLCy (fosfolipase C gama) produz IP3 e diacilglicerol (DAG) a partir do PI- 4,5 bifosfato [PI(4,5)P2] . Isto leva à liberação de IP3, que medeia a liberação de cálcio e ativação de DAG dependente de várias isoformas de PKC. A inibição da PLCy resultou em fagocitose prejudicada em macrófagos e PLCy foi encontrada acumulada na área fagocítica [343].

Ativação de ERK ocorre após a translocação de PKC e Raf-1 para a membrana plasmática [344]. Raf-1 então ativa MAPK cinase (MEK), e ativação de MEK leva diretamente a ativação de ERK que medeia a ativação de fatores nucleares, como Elk e fator nuclear-B, importantes para a produção de citocinas [345]. Rac é também participante importante no presente processo, assim como a sua inibição em macrófagos leva à completa inibição da montagem de actina e internalização de partículas revestidas de IgG [346].

PAG3 (proteína de activação de GTPase para ARF6) foram encontradas acumuladas com ARF6 e F-actina em sítios fagocíticos [347]. Cofilina e gelsolina pertencem ao grupo de várias moléculas que fazem parte nesse tipo de fagocitose pela regulação da actina por vários mecanismos [348]. O complexo Arp2 / 3, também foi encontrado acumulado em fagossomas e é necessário para a ingestão de partículas pelo receptor [349]. Proteínas de Síndrome de Wiskott-Aldrich (WASP) ligam-se diretamente a Cdc42 e Rac de um modo dependente de GTP-[350], e são ativamente recrutados para o sítios fagocíticos durante a fagocitose mediada por IgG (. Figura 42) [351].

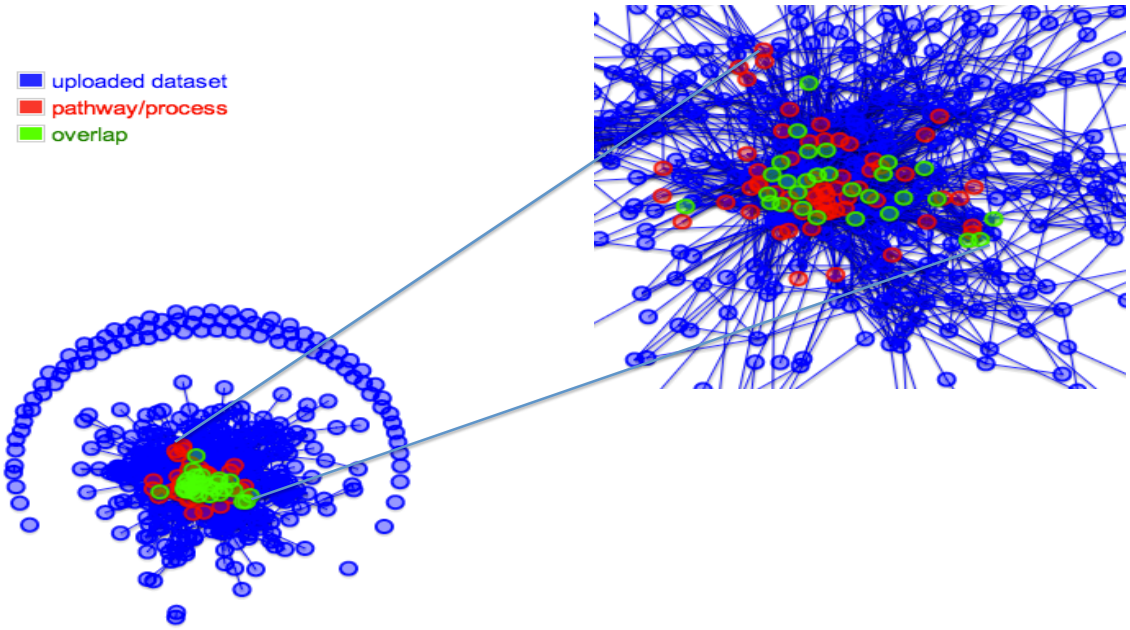

Figura 43- Visualização gráfica computacional gerada por EnrichNet do conjunto de dados enviado dos clusters 2, 4 e 5. A sobreposição (verde) é mostrada para a via da fagocitose mediada por Fc gama R.

Proteínas encontradas na via da fagocitose mediada por Fc gamma R foram analisados por STRING para interações proteína-proteína, que mostram fortes interações , fig. 44.

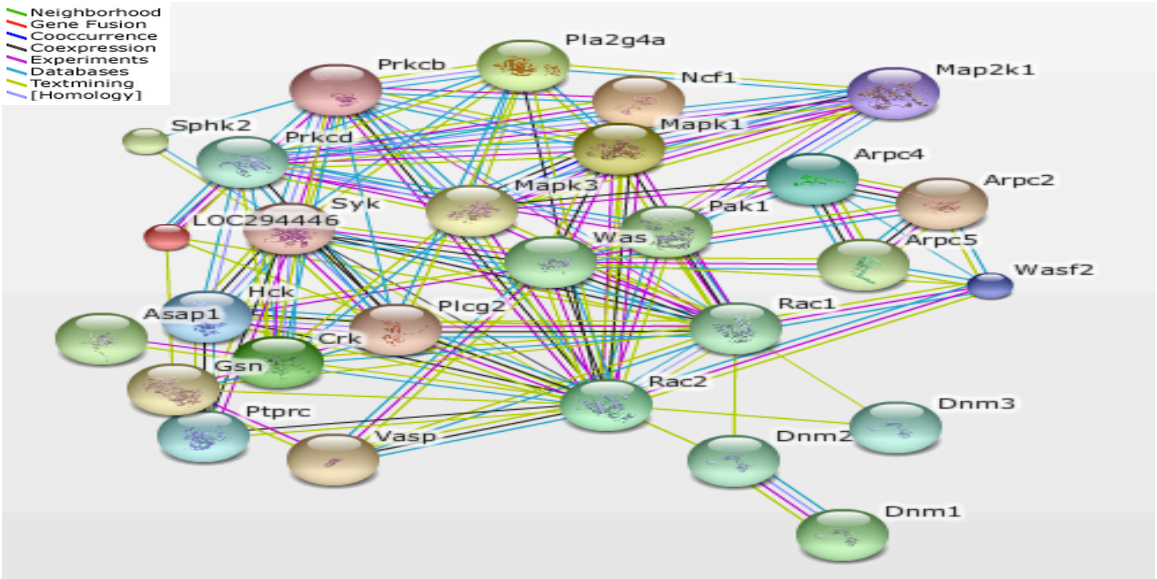

Figura 44 Análise por STRING da rede de proteínas da fagocitose mediada pela via Fc gamma R dos clusters 2, 4 e 5.

5.7.4 Via de sinalização de Quimiocinas :

A próxima via comum, significativa, interessante e relevante presente na tabela 7 é a via de sinalização da quimiocinas. Os valores P e proteínas que se sobrepõem para os clusters 2, 4 e 5 são P = 5.00e-12 e 18, P = 1.84e-10 e 15, e 4.67e-10 e 16, respectivamente. As proteínas desta via com aumento da abundância (amarelas douradas) e com abundância diminuída (vermelho) são mostradas na fig. 45.

Os neutrófilos migram para a fonte de agentes quimioatrativos como peptidios formilados, C5a, leucotrieno B4, e quimiocinas, como a IL-8 [352] e, depois da ligação ao seu receptor de superfície, uma série de eventos citoplasmáticos ocorrem ativando a máquina do citoesqueleto [353]. A interação com os respectivos ligantes resulta na alteração conformacional do receptor e consequente troca de GDP por GTP na subunidade alfa. Isso induz a liberação da subunidade α do par da subunidade βγ [354]. Dessa forma as subunidades α e βγ estarão livres para interagir com efetores *downstream*. [355]. Por sua vez, GTPases da Rac regulam diferentes funções dos neutrófilos, incluindo estrutura do citoesqueleto, a expressão dos genes e produção de espécies reativas de oxigênio (ROS) [356, 357]. Ainda, P-Rex1, um fator de troca de nucleotídeo de guanina (GEF) para Rac [358] deve vincular GPCRs e PI3Kγ a respostas de neutrófilos Rac-dependentes. Outro estudo mostrou o envolvimento de P-Rex1 na ativação de GPCR Rac2-dependente e formação de ROS em neutrófilos, bem como o recrutamento de neutrófilos a locais de inflamação e quimiotaxia, mas não em desgranulação [359]. Cinases ativadas por P21 (Paks) são cinases de serina / treonina, que têm sido identificadas como alvos de Rac e Cdc42 e afetam a actina do citoesqueleto [360]. Os receptores quimioatrativos acoplados a proteínas G e receptores Fc regulam a atividade de PAK em leucócitos humanos [361]. PAK1 foi também co-localizada com a actina polimerizada na região lamelipódia e nas áreas fagocíticas de neutrófilos humanos estimulados, consistentes com um papel para PAK na modulação da resposta dos leucócitos a estímulos fisiológicos [362]. Paxilina está presente em células cultivadas principalmente em locais de adesões focais, que são ligações estruturais entre a matriz extracelular (ECM) e da actina do citoesqueleto que também são importantes sítios de transdução de sinal. É importante notar que as proteínas de adesão focal incluindo paxilina também servem como um ponto de convergência de sinais resultantes da

estimulação de várias classes de receptores de fatores de crescimento [363]. Uma visualização gráfica computacional (Fig. 46) foi elaborada para a visualização das proteínas de sobreposição de conjunto de dados carregados e do conjunto de dados via. A análise STRING do conjunto de dados de sobreposição foi utilizada para as interações proteína-proteína que mostraram marcantes interações proteicas (47 Fig.).

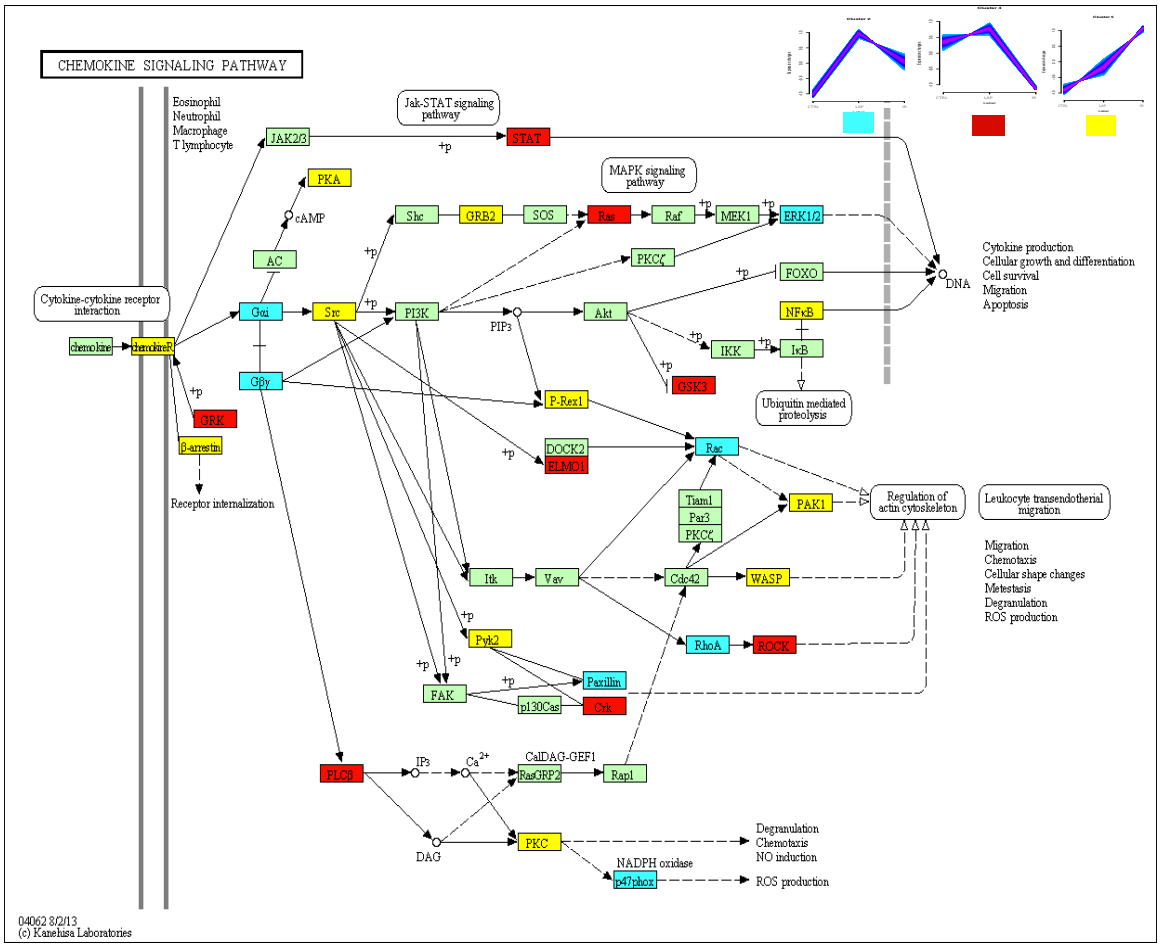

*Figura 45 A via de sinalização de quimiocinas enriquecida para as proteínas diferencialmente abundantes (DEPs) dos clusters 2, 4 e 5 Ciano (cluster 2) e amarelo (*cluster *5) apresentam abundância aumentada e vermelho (*cluster *4) para abundância diminuída.*

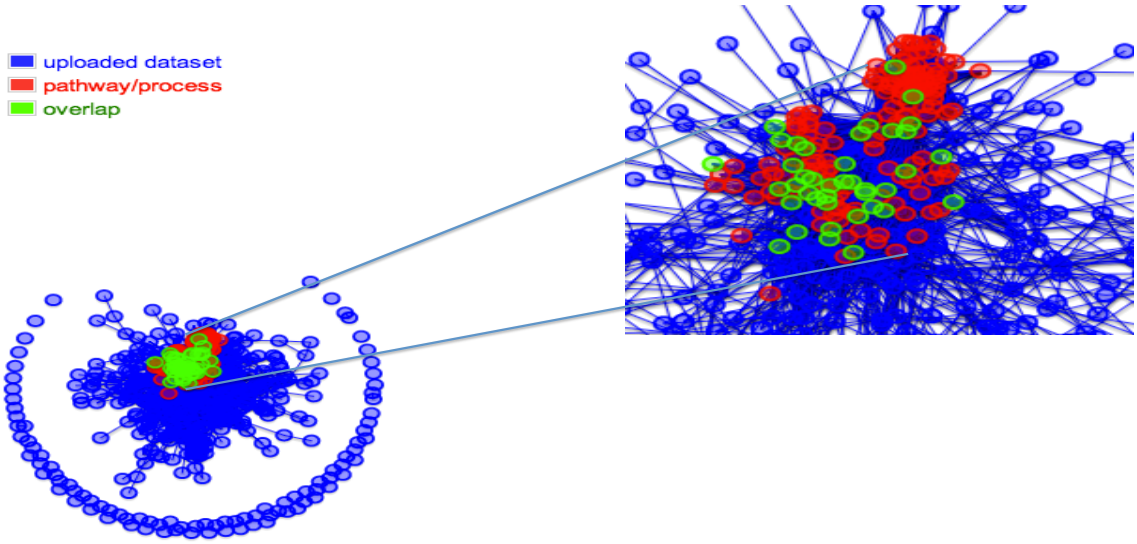

Figura 46 -visualização gráfica computacional obtida por meio de Enrichnet do conjunto de dados enviados dos clusters 2, 4 e 5 e os genes que se sobrepõem em verde para a via de sinalização de quimiocinas.

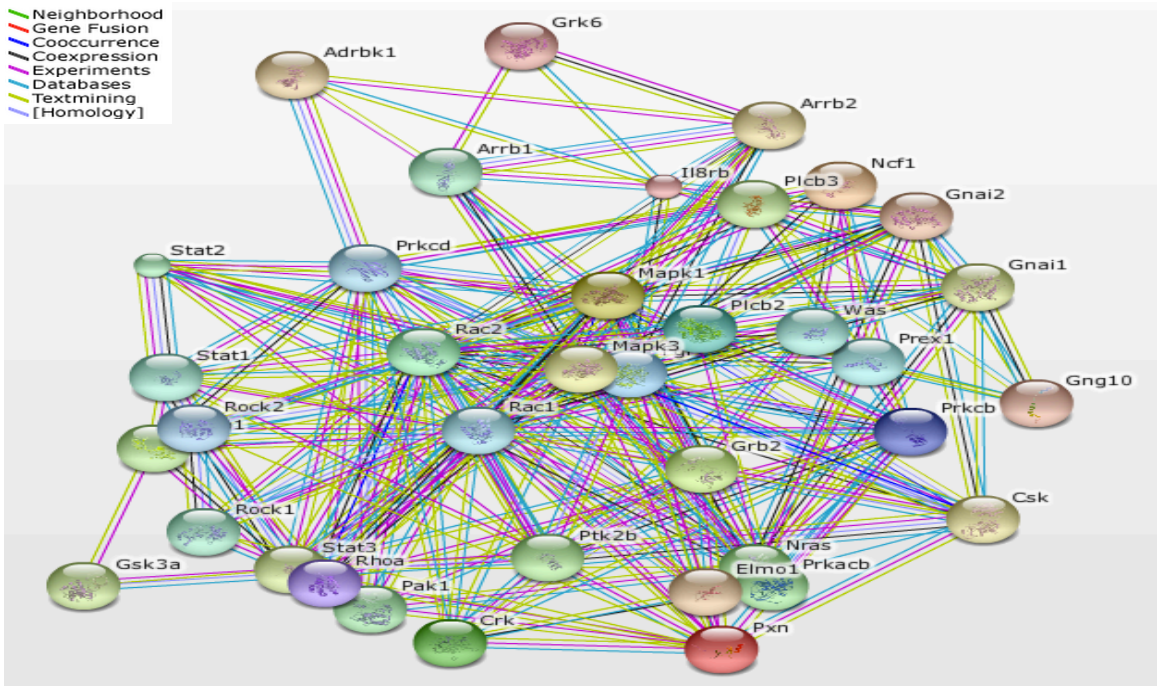

Figura 47- análise STRING da rede de proteínas da fagocitose mediada por receptores de Fc gamma dos clusters 2, 4 e 5.

5.7.5 Vias de Cluster 3

O grupo mais significativo das vias encontradas no *cluster* 3 compreende as vias metabólicas em neutrófilos com P valor P = 3.58e-53 e 109 proteínas que se sobrepõem. A visualização gráfica computacional da Enrichnet do conjunto de dados enviado do *cluster* 3 e das proteínas que se sobrepõem (verde) das vias metabólicas é mostrado na fig. 48. Essas proteínas pertencem ao metabolismo energético, de hidratos de carbono e metabolismo dos lípidos, incluindo também o metabolismo de nucleotídios e de aminoácidos e o metabolismo secundário. Análise STRING mostrou interações elevadas entre as proteínas de tais vias metabólicas Fig. 49.

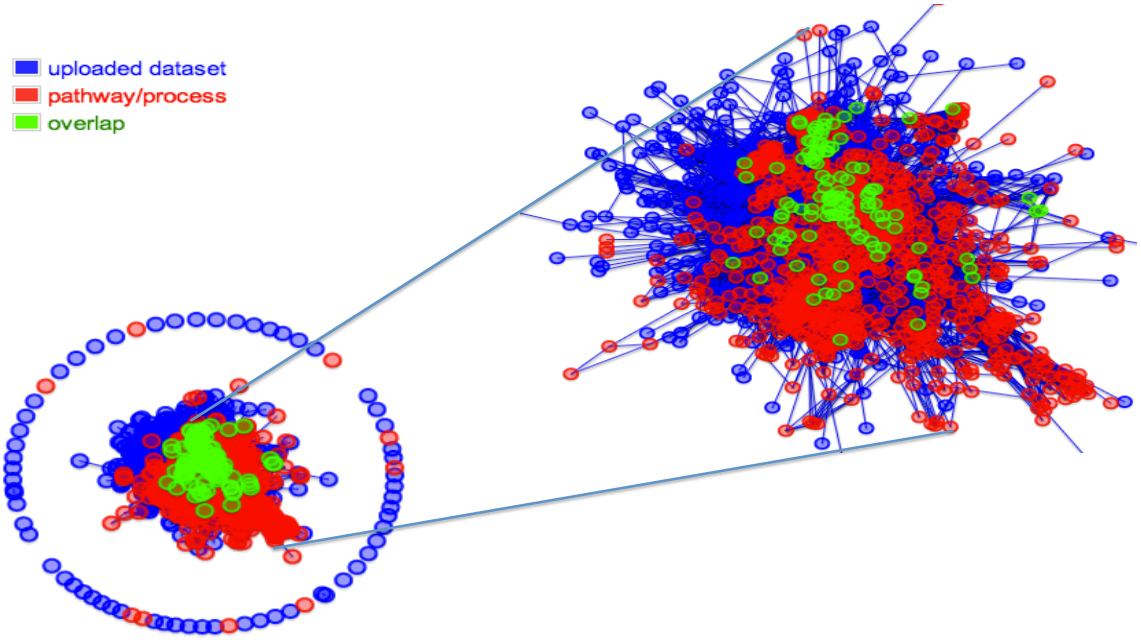

Figura 48- visualização gráfica da análise cmputacional do Enrichnet do conjunto de dados enviados do cluster *3.*

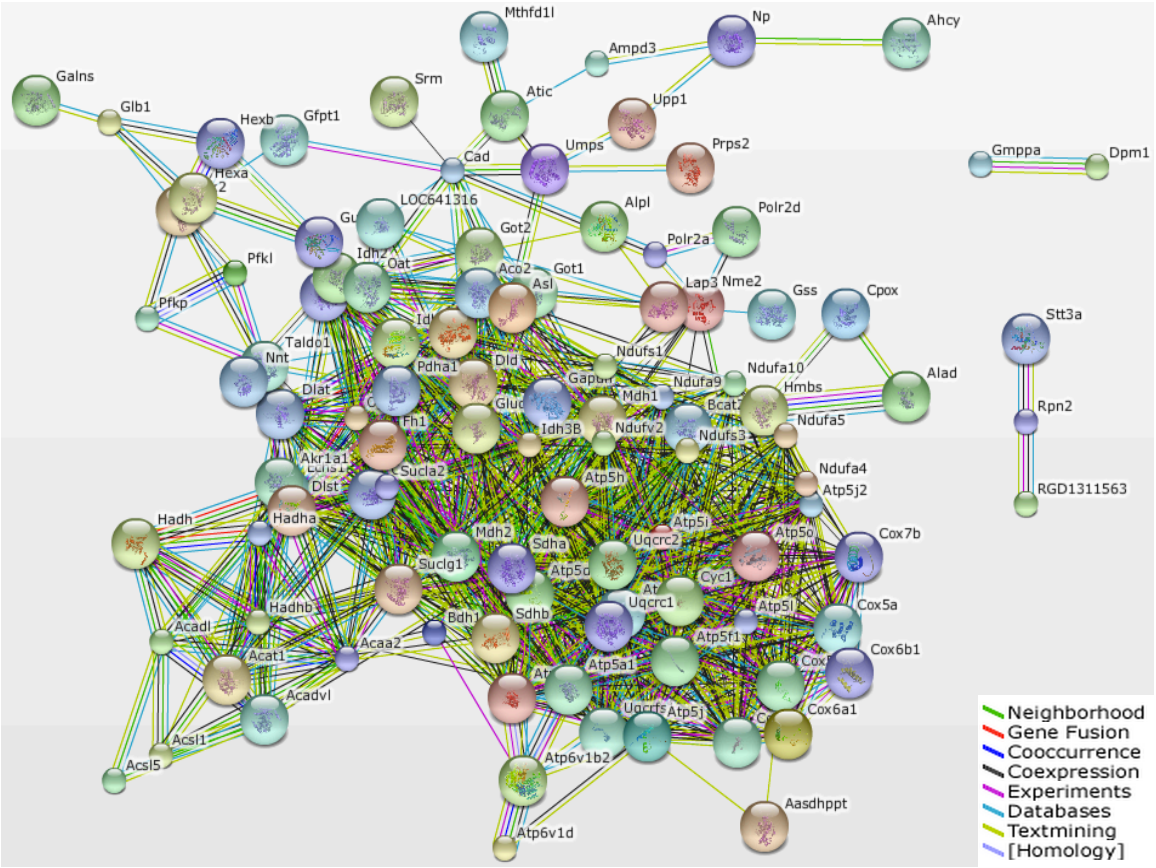

Figura 49- análise STRING da rede de proteínas de vias metabólicas de cluster *3.*

Outra via importante e significativa relacionada com as proteínas de cluster 3 é a fosforilação oxidativa tendo como valor P, P = 1.77e-23 com 30 proteínas sobrepostas, como mostrado na fig. 50.

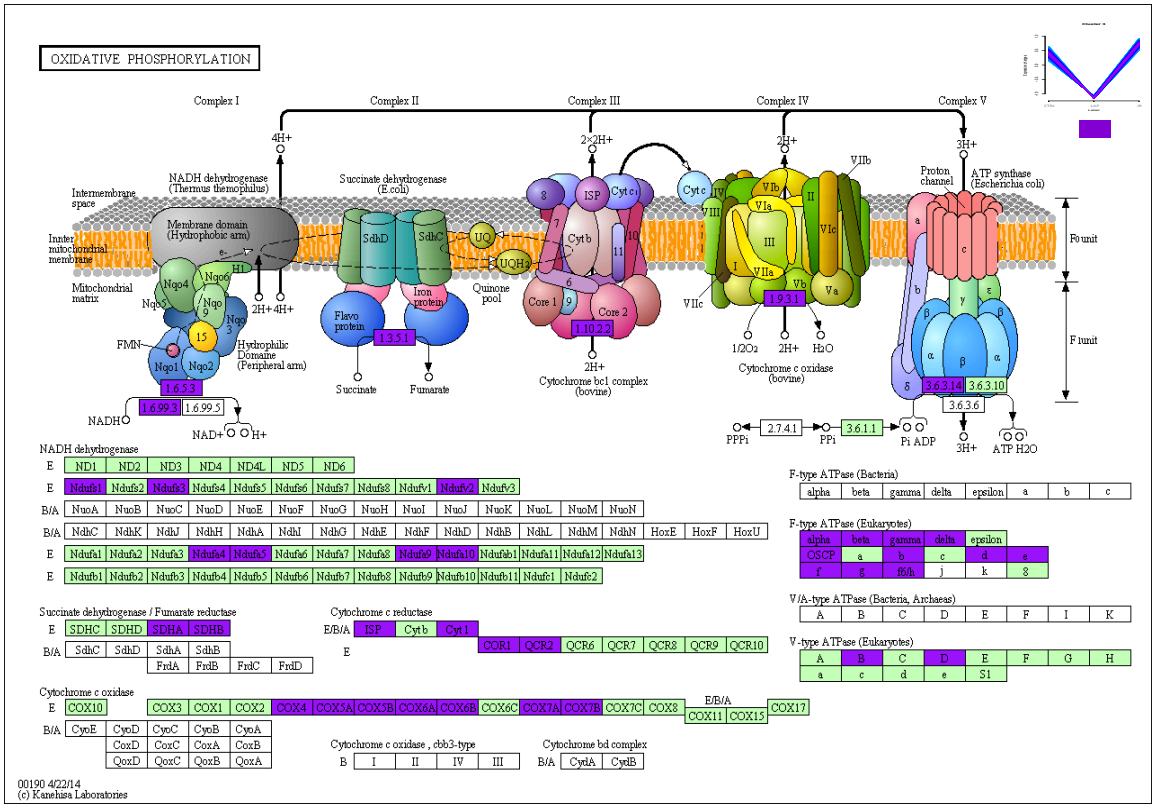

Figura 50 A via de fosforilação oxidativa enriquecida para proteínas diferencialmente abundantes (DAPs) do cluster 3. O destaque em roxo mostra as proteínas que se sobrepõem.

Acreditava-se que os neutrófilos maduros possuíssem nenhuma ou poucas mitocôndrias, não tendo nenhum papel na função celular [364], comprovado por microscopia eletrônica [365], e pela baixa taxa de respiração mitocondrial nos neutrófilos [366]. Mais tarde, os corantes fluorescentes específicos foram utilizados e as mitocôndrias foram identificadas como uma rede tubular nessas células [365, 367]. Além disso, os aglomerados de mitocôndrias foram mostrados em apoptose de neutrófilos espontânea ou induzida e a proteína Bax pró-apoptótica foi localizada [367-369]. No caso de isquemia e lesões de reperfusão, a perda do potencial e integridade da membrana mitocondrial, juntamente com o decréscimo na atividade mitocondrial foi observado [201, 370].

A importância das mitocôndrias na regulação de funções pró-inflamatórias de neutrófilos não é clara, embora a alteração da forma da célula e quimiotaxia ocorra como resultado de uma diminuição no potencial de membrana mitocondrial [365]. Algumas células do

sistema imunológico ativadas (e algumas inativas) preferem utilizar glicólise, já que esta é 100 vezes mais rápida do que a fosforilação oxidativa para a síntese de macromoléculas [371]. A glicólise fornece energia para a quimiotaxia, mas há pouco conhecimento sobre o papel regulador da mesma em condições normais e patológicas em neutrófilos [364]. Estudos mostram que os neutrófilos não dependem da fosforilação oxidativa e a glicólise surpreendentemente não é aumentada na inibição da sintase doATP mitocondrial [372]. Nossos dados também mostraram redução da abundância de proteínas da fosforilação oxidativa durante LAP e por outro lado aumento no grupo IR para quase o mesmo nível do grupo controle. O papel destas vias durante essas condições patológivcas não está claro na literatura. Observamos aumento na via da glicólise com P valor, P = 4.03e-08 e 10 proteínas sobrepostas (Tabela 7) que pode ser utilizado pelos neutrófilos para a produção de energia rápida em vez da fosforilação oxidativa, a qual está diminuída no cluster 3.

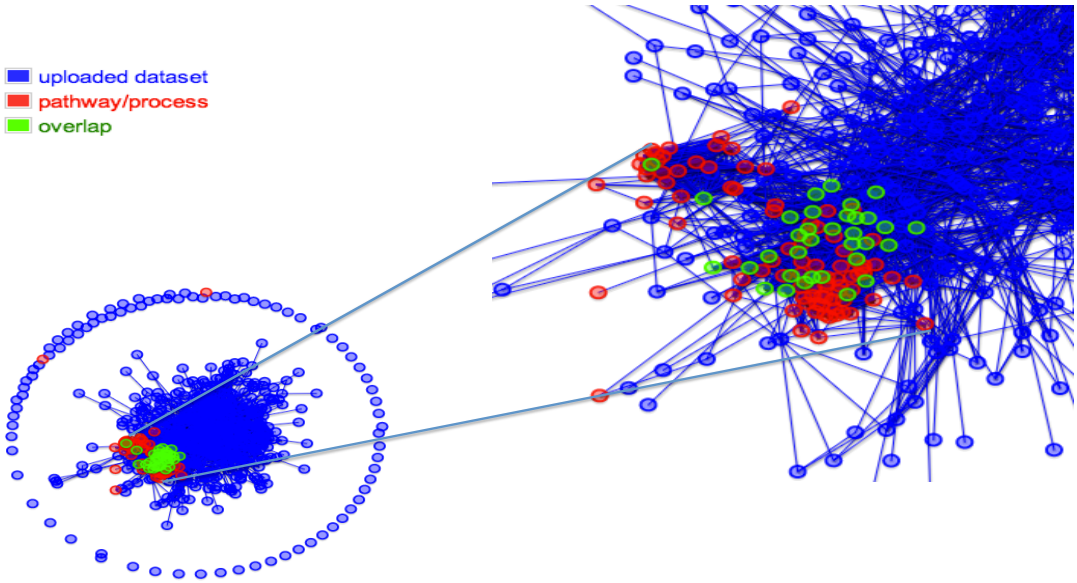

Figura 51 visualização gráfica por Enrichnet do conjunto de dados enviados do cluster *3 e mais proteínas sobrepostas (verde) para a via da fosforilação oxidativa.*

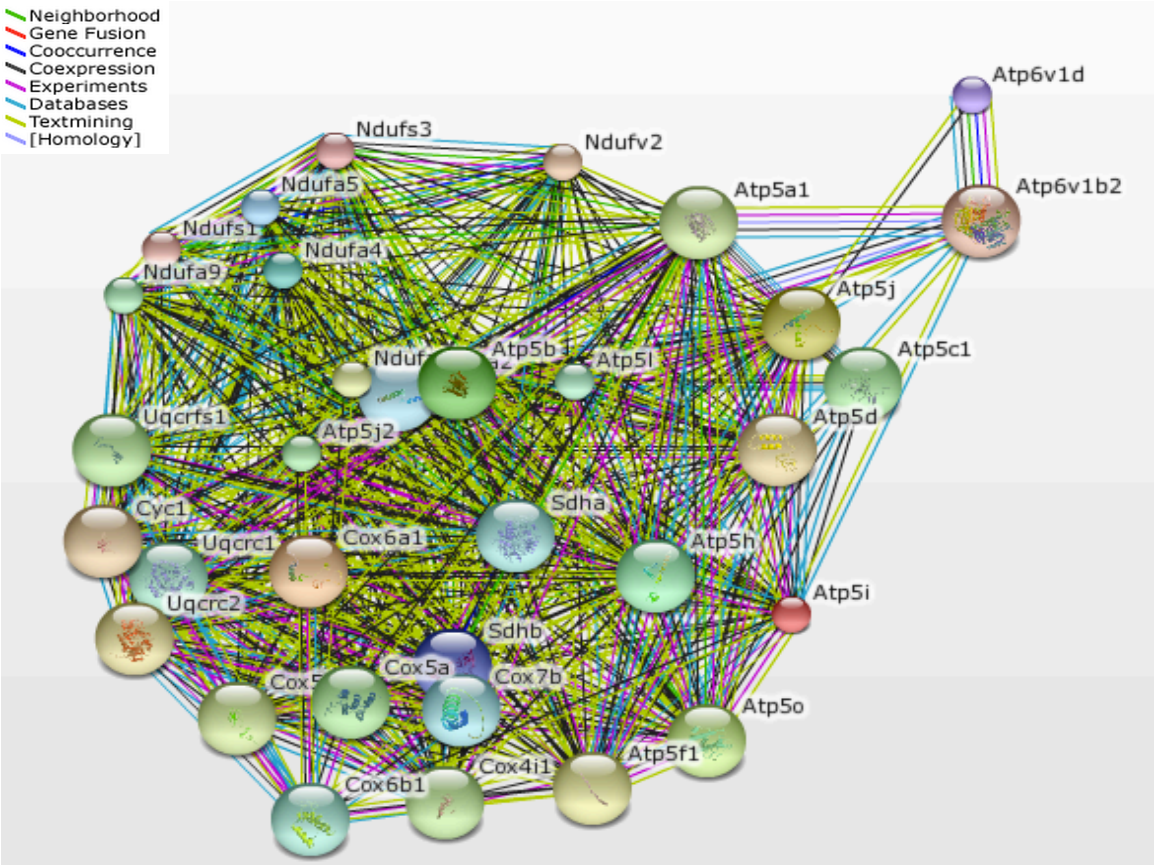

Figura 52 - análise da rede STRING para proteínas da via da fosforilação oxidativa do cluster 3.

Análise da visualização gráfica computacional foi realizada para via de fosforilação oxidativa usando Enrichnet (Fig. 51). A análise STRING das proteínas sobrepostas da via da fosforilação oxidativa mostra fortes interações proteína-proteína (Fig. 52).

5.8 Cinases e Fosfatases

Fosforilação de proteínas, uma modificação pós-translacional essencial, afeta a maioria das atividades celulares incluindo a transdução do sinal, a expressão gênica, a progressão do ciclo celular, a imunidade, aprendizagem e memória e outras funções biológicas [124, 217, 218]. É uma reação reversível, que é catalisada por proteínas cinases, transferindo o γ-fosfato do ATP para Ser, Thr e Tyr, enquanto que os resíduos de fosfatases agem de forma reversa para cinases (Fig. 53-A). As cinases proteicas têm ampla importância na transdução de sinal, estão entre as principais famílias de genes eucariotas, tornando-se a cerca de 2% do genoma e têm sido extensivamente estudados [218, 373, 374]. O genoma

humano contém cerca de 518 proteínas cinases putativas [375-377], que podem ser divididos em duas famílias: 428 de serina / treonina (Ser / Thr)-cinases (PSKs 90) e tirosina (Tyr)-cinases (PTK). Há cerca de 107 proteínas fosfatases putativas Tyr (DPT) e muito poucas, cerca de 30, proteínas Ser / Thr fosfatases (PSP) [378, 379]. Neste estudo foram identificados 188 sítios de fosforilação em 84 cinases proteicas perfazendo 2% e 107 sítios de fosforilação em 50 proteínas com o termo fosfatases compondo 1% do total identificado proteoma de neutrófilos de ratos, que mudou significativamente sua regulação nos controles, laparotomia e isquemia (Fig . 53-B).

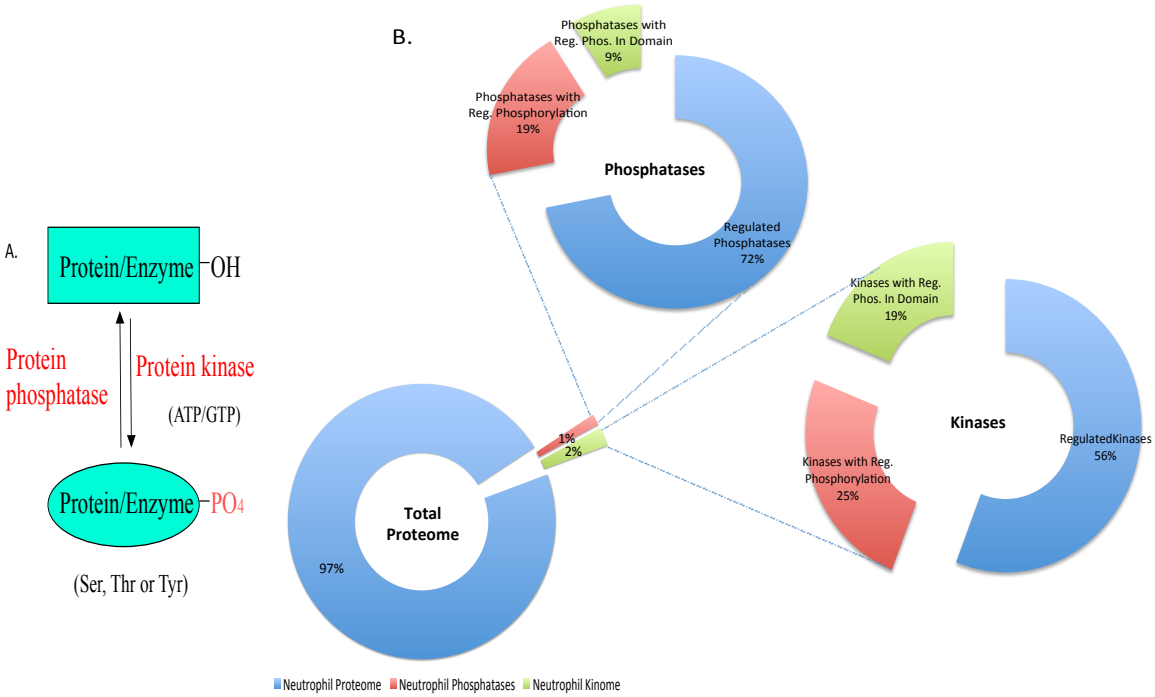

Figura 53- Em A, fosforilação e defosforilação pela cinase e fosfatase respectivamente. B, distribuição das cinases e fosfatases com abundância diferencial, com e sem abundância diferencial da fosforilação nos domínios identificados no proteoma total de neutrófilos de ratos.

5.8.1 Cinases fosforiladas em neutrófilos

Do proteoma total de neutrófilos, 84 proteínas foram encontradas com o uso do termo "*Kinase*", incluindo aquelas diferencialmente abundantes. Dessas 84 proteínas, 47 foram apenas diferencialmente abundantes, 21 diferencialmente abundantes tanto na fosforilação quanto na quantidade, mas estas fosforilações não foram encontradas nos

respectivos domínios de regulação, de modo que apenas 16 mostraram-se com a diferença tripla: abundância diferencial na quantidade, na fosforilação e nos respectivos sítios regulatórios. Cinases diferencialmente abundantes apenas na quantidade perfazem 56%, na fosrorilação representam 25% e aquelas cuja quantidade e fosforilação tiveram abundância diferencial correspondente nos domínios de regulação nos respectivos sítios abarcam 19% do total de cinases identificadas (Fig. 35-B). As cinases classificadas de acordo com os *clusters* são dadas na tabela 8, incluindo número de peptídeos fosforilados e seus domínios regulatórios que tiveram mudanças significativas na fosforilação.

5.8.1.1 Serina/treonina-proteína cinase, MARK2, (O08679)

A serina/treonina-proteína cinase, MARK2 (O08679), seguiu o padrão de abundância do *cluster* 2 e sua fosforilação seguiu o padrão de abundância do *cluster* 5 em S562. Curiosamente, esta fosforilação ocorreu num sítio APC, domínio básico que interage com os microtúbulos. MARK2 possui um domínio simples transmembrânico e está envolvida na regulação da estabilidade dos microtúbulos, a via de sinalização Wnt, e desempenha um papel no tráfico vesicular [380-388]. O papel dos microtúbulos na polaridade e migração de neutrófilos já é bem conhecido no peixe-zebra [389] e a via de sinalização Wnt regula a transmigração endotelial de monócitos [390]. Já o STE20-like serina/treonina-proteína cinase, slk (O08815), mostrou progressiva abundância diferencial no grupo Isquemia/reperfusão quando comparado aos controles (padrão do *cluster* 5). Também foram encontradas fosforilações nos residuos de serina S372, S780, S778 e S77.

Tabela 8 – Cinases fosforiladas com abundância diferencial após laparotomia e isquemia.

UNIPROT	No. of regulated phosphopeptides	Cluster	GENE Official symbol	TM	Description	Length	Enzyme Codes	Domain containing the phosphopeptide
O08679	1	2	Mark2	1	serine/threonine-protein kinase MARK2	722	EC:2.7.11.26; EC:2.7.11	APC basic domain.
O08815	4	5	Slk	1	STE20-like serine/threonine-protein kinase	1206	2.7.11.1	AAA ATPase containing von Willebrand factor type A (vWA) domain; RecF/RecN/SMC N terminal domain.
P09215	12	4	Prkcd	1	protein kinase C delta type	673	EC:2.7.11.13	STKc_nPKC_delta, Catalytic domain of the Protein Serine/Threonine Kinase, Novel Protein Kinase C delta; active site on conserved domain STKc_nPKC_delta; substrate binding site on conserved domain STKc_nPKC_delta; activation loop (A-loop) on conserved domain STKc_nPKC_delta; protein kinase A catalytic subunit; S_TK_X, Extension to Ser/Thr-type protein kinases; Pkinase_C domain; Protein kinase C terminal domain.
P11980	1	2	Pkm	0	pyruvate kinase PKM	531	EC:2.7.1.40	Pyruvate kinase (PK); domain interface.
P16879	2	3	Fes	0	tyrosine-protein kinase Fes/Fps	822	EC:2.7.10.2; EC:1.97.1	PTKc_Fes, Catalytic domain of the Protein Tyrosine Kinase, Fes; activation loop (A-loop) on conserved domain PTKc_Fes; active site on conserved domain PTKc_Fes; substrate binding site on conserved domain PTKc_Fes.
P18654	5	1	Rps6ka3	2	ribosomal protein S6 kinase alpha-3	740	EC:2.7.11	STKc_RSK_N[cd05582]; turn motif phosphorylation site on conserved domain STKc_RSK_N.
P26817	2	4	Adrbk1	0	beta-adrenergic receptor kinase 1	689	EC:2.7.11.16; EC:2.7.11.14; EC:2.7.11.15	G Protein-Coupled Receptor Kinase 2 subgroup pleckstrin homology (PH) domain.
P35991	5	4	Btk	0	tyrosine-protein kinase BTK	659	EC:2.7.10.2	
P36506	2	3	Map2k2	0	dual specificity mitogen-activated protein kinase kinase 2	400	EC:2.7.11.24; EC:2.7.11; EC:2.7.10	
P47811	3	2	Mapk14	1	mitogen-activated protein kinase 14 isoform 1	360	EC:2.7.11.24	Active site, substrate binding site, active loop (A-loop); KIM docking site; Catalytic domain of the Serine/Threonine Kinase, p38alpha Mitogen-Activated Protein Kinase ;Serine/Threonine Kinases (STKs), p38alpha subfamily, catalytic (c) domain.
P50545	6	2	Hck	2	tyrosine-protein kinase HCK	524	EC:2.7.10.2; EC:2.7.10	Hydrophobic binding pocket; autoinhibitory site; SH2_Src_HCK; active site; substrate binding site; active loop (A-loop); PTKc_Src_like domain; Pkinase_Tyr; STYKc; SPS1; PLN00034.
P54645	8	5	Prkaa1	1	5'-AMP-activated protein kinase catalytic subunit alpha-1	559	EC:2.7.11	AMPKA1_C, C-terminal regulatory domain of 5'-AMP-activated protein kinase (AMPK) alpha 1 catalytic subunit; AMPKA_C_like superfamily; beta/gamma subunit interface on conserved domain AMPKA1_C.
P67871	1	1	Csnk2b	0	casein kinase II subunit beta	215	EC:3.4.21; EC:2.7.11	
P68404	1	5	Prkcb	1	Protein kinase C beta type	671	EC:2.7.11	STKc_cPKC_beta; turn motif phosphorylation site.
P70600	5	5	Ptk2b	1	protein-tyrosine kinase 2-beta	1009	EC:2.7.10	
P81799	1	2	Nagk	0	N-acetyl-D-glucosamine kinase	343	EC:2.7.1.59; EC:2.7.1.60	Neucleotide binding site; NBD_sugar-kinase_HSP70_actin domain; BcrAD_BadFG; COG2971.
P97820	1	2	Map4k4	1	Mitogen-activated protein kinase kinase kinase kinase 4	1233	EC:2.7.11	
Q53UA7	5	4	Taok3	0	serine/threonine-protein kinase TAO3	898	EC:2.7.11	
Q5S006	1	3	Lrrk2	3	leucine-rich repeat serine/threonine-protein kinase 2	2527	EC:2.7.11	
Q5XIS9	2	2	Prkd2	1	serine/threonine-protein kinase D2	875	EC:2.7.11.13	
Q63433	10	3	Pkn1	0	serine/threonine-protein kinase N1	946	EC:2.7.11; EC:2.7.11.13	Catalytic domain of the Protein Serine/Threonine Kinase, Protein Kinase N ; Serine/Threonine Kinases (STKs), Protein Kinase N (PKN) subfamily, catalytic (c) domain.
Q63531	4	1	Rps6ka1	2	ribosomal protein S6 kinase alpha-1	735	EC:2.7.11	SPS1 Domain; STKc_RSK_N Domain; hydrophobic motif (HM) on conserved domain STKc_RSK_N; Protein kinase C terminal domain; protein kinase A catalytic subunit; turn motif phosphorylation site on conserved domain STKc_RSK_N.

Continue

Q64725	5	2	Syk	0	tyrosine-protein kinase SYK	629	EC:2.7.10.2; EC:2.7.10.1; EC:2.7.10	
Q6P6U0	17	5	Fgr	0	tyrosine-protein kinase Fgr	517	EC:2.7.10	PTKc_Src_like, Catalytic domain of Src kinase-like Protein Tyrosine Kinases; Protein Tyrosine Kinase (PTK) family; active site on conserved domain PTKc_Src_like; substrate binding site on conserved domain PTKc_Src_like; activation loop (A-loop) on conserved domain PTKc_Src_like; SH3/SH2 domain interface on conserved domain PTKc_Src_like; SH2_Src_Fgr, Src homology 2 (SH2) domain; SH2 domain; hydrophobic binding pocket on conserved domain SH2_Src_Fgr; autoinhibitory site on conserved domain SH2_Src_Fgr; phosphotyrosine binding pocket on conserved domain SH2_Src_Fgr.
Q6P9R2	5	5	Oxsr1	2	serine/threonine-protein kinase OSR1	527	EC:2.7.11	SPS1.
Q8K1R7	4	4	Nek9	2	serine/threonine-protein kinase Nek9	984	EC:2.7.11	
Q91XS8	3	5	Stk17b	1	serine/threonine-protein kinase 17B	371	EC:2.7.11.18; EC:2.7.11.17	
Q9JI11	3	4	Stk4	0	serine/threonine-protein kinase 4	487	EC:2.7.11; EC:2.7.11.13	
Q9JIH7	10	2	Wnk1	0	serine/threonine-protein kinase WNK1 isoform 3	2126	EC:2.7.11	
Q9WUT3	3	3	Rps6ka2	2	ribosomal protein S6 kinase alpha-2	733	EC:2.7.11	STKc_RSK_N, N-terminal catalytic domain of the Protein Serine/Threonine Kinase.
Q9Z277	2	5	Baz1b	2	tyrosine-protein kinase BAZ1B	1479	EC:2.7.10.2; EC:2.3.1.48	

As fosforilações em S372 e S780 mostraram-se reduzidas no grupo laparotomia (*cluster* 3), enquanto aquelas em S778 e S776 estavam reduzidas apenas no grupo isquemia (*cluster* 4). Recentemente foi descrito um domínio transmembrânico SLK mediado pela fosforilação da paxilina necessário para a adesão e migração celular [391]. Foram encontradas maiores quantidades de paxilina no *cluster* 2, com 22 diferentes sítios de fosforilação. SLK exarceba apoptose e pode regular a sobrevivência cellular nos casos de lesão e reparo [392]. Outros estudos também demonstraram uma papel da SLK na apoptose após sua expressão *in vitro* durante a lesão de isquemia e reperfusão [393-395].

5.8.1.2 Proteína cinase C tipo delta, prkcd, (P09215)

A proteína a cinase C tipo delta, prkcd (P09215), é uma cinase AGC específica da família cinase C serina-treonine (PKC) com um único domínio transmembrânico. Prkcd foi pouco abundante na isquemia quando comparada aos grupos controle e laparotomia (*cluster 4*) e foram encontrados 12 sítios de fosforilação diferencialmente expressos na prkcd. Blake et al, 1999, mostraram que o SRC promove a degradação de PKC delta por meio da sua fosforilação no resíduo Tyr311 [396] e o presente estudo reforça essa análise, ao encontrar baixa expressão de prkcd e de alta fosforilação de Y311. Também poderia ser interessante mencionar maiores quantidades de SRC fosfoproteína a-cinase 2

(Q920G0) no *cluster* 2 em nosso estudo com 14 sítios relacionados à fosforilação de prkcd no resíduo Y311, que pode resultar em degradação. Também ocorreu baixa fosforilação nos resíduos Ser504, Thr505 e Thr509, que estão em sítio ativo, em sítio de ligação a substrato e em alça de ativação (A-loop) do domínio STKc_nPKC_delta. Também foram encontradas baixas abundâncias dos sítios Ser643 e Ser662 no *cluster* 1 e alta abundância de Ser645 no *cluster* 5 no domínio C-terminal da PKC.

5.8.1.3 Piruvato cinase, pkm, (P11980)

A piruvato cinase, pkm, (P11980) catalisa a transferência do grupo fosfato do fosfoenolpiruvato (PEP) para o ADP resultando em ATP e molécula piruvato. Neste estudo foi encontrado aumento da abundância de pkm (*cluster* 2) e também aumento na fosforilação do resíduo Ser437 (*cluster* 5) – curiosamente essa fosforilação ocorreu no domínio PK_C. Oehler et al, 2000, relataram aumento da expressão de pkm in PMNs em pacientes politraumatizados [397] e nossos resultados estão de acordo com isso, uma vez que a expressão de pkm é maior no grupo laparotomia, que é um trauma cirúrgico, e pouco menor no grupo isquemia, porém ambos maiores que os respectivos controles. Adicionalmente, aquele estudo sugere que o aumento da expressão de pkm em neutrófilos de pacientes de politrauma resulta em amento de atividade da via pentose-fosfato (PPP), devido à alta na produção do NADPH envolvida na produção de espécies reativas de oxigênio (ROS) em neutrófilos quando expostos ao estímulo apropriado [398].

5.8.1.4 Proteína Tirosina-cinase Fes/Fps, fes, (P16879)

A Proteína tirosina-cinase Fes/Fps, fes, (P16879) teve baixa abundância no grupo laparotomia (*cluster* 3) e foram encontrados dois sítios com baixa fosforilação, nos resíduos Thr412 e Tyr713 (*cluster* 1). A baixa fosforilação no sítio Tyr713 estava presente na PTKc_Fes, domínio catalítico da tirosina cinase Fes, na alça de ativação (A-loop) na região conservada de PTKc_Fes; no sítio ativo da região conservada de PTKc_Fes e no sítio de ligação ao substrato da região conservada de PTKc_Fes. Movimentos direcionais e recrutamento de neutrófilos são extremamente importantes para a resposta imunitária inata. Parsons et al, 2007, mostraram que Fps/Fes cinase regula o recrutamento de leucócitos e seu extravasamento durante a inflamação. Também alta

aderência de leucócitos às vênulas e alta transmigração endotelial em camundongos fps/fes-knockout [399]. Outro recente estudo do mesmo grupo também aponta na mesma direção, que fer-cinase restringe a quimiotaxia de neutrófilos: observaram aumento da quimiotaxia de neutrófilos de camundongos cinase-inativados (FerDR/DR) em direção ao peptídeo quimioatraente (WKYMVm) e C5a comparado com o selvagem [400]. Ambos estudos amparam nossas análises e sugerem que fps/fes seja uma cinase inibitória para quimiotaxia em leucócitos e neutrófilos.

5.8.1.5 Proteína ribosomal S6 cinase alpha-3, Rps6ka3/RSK2, (P18654)

A proteína ribossomal S6 cinase alpha-3, Rps6ka3/RSK2 (P18654), uma cinase AGC da família RSK, com dois domínios transmembrânicos, sofre fosforilação e resulta em inativação de fatores de transcrição (por exemplo, cyclic AMP response element-binding proteína (CREB), inibidor de κBα/nuclear factor-κB, c-fos) [401-403]. Já foi relatado que, em neutrófilos, RSK2 fosforila e causa inativação da glycogen synthase cinase 3, um evento que melhora a sobrevida dessas células [404, 405]. Nossa análise mostra baixa abundância de RSK2 (*cluster* 1) e 5 sítios de fosforilação. A fosforilação no resíduo Thr365 mostrou-se maior que na região STKc_RSK_N, enquanto a fosforilação no resíduo Ser369 foi menor (*cluster* 4) que aquela encontrada no "*turn motif phosphorylation site*" da região STKc_RSK_N. A fosforilação em Ser369 já foi relacionada à ativação de RSK2 [406], e nós encontramos baixa abundância de RSK2 e baixa fosforilação em Ser369, provavelmente levando à ativação da glicogênio sintase cinase 3, envolvida na sobrevida de neutrófilos [404, 405]; e curiosamente encontramos glicogênio sintase cinase-3 alfa (P18265) aumentada (*cluster* 2).

5.8.1.6 Receptor Beta-adrenérgico cinase 1, Adrbk1/GRK2, (P26817)

O receptor beta-adrenérgico cinase 1, Adrbk1/GRK2, (P26817) é uma proteína cinase ubíqua da família GRK que fosforila o receptor beta-2 adrenérgico [407], pode regular quimiotaxia [408] e aumenta a mobilização de neutrófilos quando incompleta [409]. Foi demonstrado que neutrófilos ativados produzem radicais de oxigênio durante isquemia e reperfusão [410] e estudos *in vitro* mostraram a capacidade de mediadores inflamatórios, tais como citocinas pró-inflamatórias e radicais oxigênio, para reduzir a proteína GRK2 [411, 412]. Sua abundância estava diminuída (*cluster* 4) com dois sítios de fosforilação

em Ser666 e Ser670 no subgrupo PH_GRK2. Assim, provavelmente esta baixa abundância de GRK2 foi devido à alta produção de radicais oxigênio pelos neutrófilos durante a isquemia, facilitando sua migração.

5.8.1.7 Tirosina-proteína cinase, BTK/BPK, (P35991)

Tirosina-proteína cinase, BTK/BPK, (P35991) é uma tirosina cinase da família Tec-cinase, que são abundantes em linhagens celulares sanguíneas como monócitos, macrófagos, células B e neutrófilos [413]. Durante a isquemia tiveram baixa abundância (*cluster* 4) com 5 sítios de fosforilação, incluindo Ser180. Está claro da literatura que a fosforilação de Ser180 mediada por PKCβ causa baixa abundância de BTK resultando em sequestro do mesmo no citoplasma [414]. Nossos resultados sugerem baixa abundância de BTK, mas também baixa fosforilação de Ser180 (*Cluster* 1) mostrando outro resíduo candidato a regulador da abundância de BTK em neutrófilos. Em neutrófilos humanos, BTK regula negativamente a apoptose induzida por estímulos e a produção e espécies reativas de oxigênio [415].

5.8.1.7 Mitogen-activated proteína cinase 2 de dupla especificidade, Map2k2/MEK2, (P36506)

Já foi descrito que MEK2, membro da família STE7 cinase, é fosforilada e ativada por serina/treonina cinases como MEK e Raf cinase e essas MEK2 fosforilam e ativam ERK2 [416]. MEK2 teve a abundância reduzida (Cluster 3) em laparotomia e sua abundância não se alterou durante isquemia. Dois sítios de fosforiação Ser393 e Thr394 foram detectados reduzidos (Cluster 4) e aumentados (Cluster 2) respectivamente. Existem diversos anticorpos Anti-MEK2 fosfo-T394 disponíveis no mercado, mas nenhuma função conhecida para a abundância aumentada significativa na fosforilação em Thr394 [417].

5.8.1.8 Mitogen-activated proteína cinase 14 isoforma 1, Mapk14/ P38A/P38MAPK, (P47811)

P38MAPK pertence à família das MAPKs com dois domínios transmembranares e é ativada por fosforilações de resíduos de Thr e Tyr. Ela seguiu o padrão de abundância do *cluster* 2, com três sítios de fosforilação, Thr180, Thr185 e Tyr182. Todos esses sítios foram encontrados no sítio ativo, sítio de ligação a substrato, alça de ativação (A-loop),

sítio de ancoragem KIM do domínio catalítico Serina/Treonina Cinase, p38alpha Mitogen-Activated Proteína Cinase (STKc_p38alpha_MAPK14). Fosforilação em Thr185 foi diminuída (Cluster 1) enquanto que as outras duas foram aumentadas (Cluster 2). Essa fosforilação dupla na Thr180 e Tyr182 é causada por MAP2Ks MAP2K3/MKK3, MAP2K4/MKK4 e MAP2K6/MKK6 em resposta a estresse ambiental, fatores de crescimento ou citocinas inflamatórias e são importantes para a ativação da enzima [418, 419]. Além do mais, foi demonstrado que p38MAPK fosforilada em ambos resíduos de Thr180 e Tyr182 tem um incremento em sua atividade de 10-20 vezes maior que aquelas fosforiladas somente na Thr18, enquanto que p38MAPK fosforilada somente na Tyr182 é inativa [419]. Esse padrão de fosforilação não foi anteriormente descrito como resposta a IRI. Baseado na localização da Thr185 em sítios importantes, sua diminuição poderia ser de importância para a ativação de p38MAPK. Vários estudos mostraram que a inibição de p38MAPK por fármacos atenuam diversas funções de neutrófilos como adesão, quimiotaxia e desgranulação [420-422]. Mais ainda, alguns estudos em neutrófilos e outras células em geral mostraram o bloqueio da atividade da NADPH oxidase pela inibição de p38MAPK [420, 423-426].

5.8.1.9 Tirosina-proteína cinase, HCK, (P50545) e tirosina-proteína cinase, Fgr, (Q6P6U0)

Tirosina-proteína cinase, HCK, (P50545) e tirosina-proteína cinase, Fgr, (Q6P6U0) pertencem à família SCR que é predominantemente expressa em células do tipo hematopoiético. Ambas Hck e Fgr foram encontradas com abundância aumentada agrupadas nos clusters 2 e 5 com seis a dezenove sítios fosforilados respectivamente. Hck mostrou diminuição na fosforilação (Cluster 3) em laparotomia no resíduo Tyr207 que fica no sítio hidrofóbico de ligação e no domínio auto-inibitório SH2_Src_HCK. Fosforilação na Tyr409, Thr410 e Ser460 foi aumentada (Cluster 5). Tyr409 e Thr410 foram encontradas no sítio ativo, sítio de ligação a substrato, alça de ativação (A-loop) e na interface do domínio SH3/SH2 do domínio PTKc_Src_like enquanto que a fosforilação na Ser460 foi detectada em todos como também a Tyr409 e Thr410 exceto na alça de ativação. Fosforilação na Tyr400 de Fgr foi aumentada (Cluster 2) a qual é inibida por prévia fosforilação na Tyr511 [427], que não foi encontrada em nosso caso. Camundongos e neutrófilos humanos deficientes em Hck e Fgr resultam no fracasso da

explosão respiratória ativação e migração de neutrófilos em resposta a fMLP [428]. Dois estudos contraditórios sobre neutrófilos estimulados por fMLP, mas de camundongos deficientes em Hck e Fgr foram publicados atestando a incapacidade [421] e capacidade [429] das Hck e Fgr em ativar p38MAPK. Em neutrófilos, a enzima Hck foi mostrada desempenhando papéis importantes como regulação da quimiotaxia baseada em actina e adesão [430-432], assim como fagocitose mediada por integrina e FcRγ [433, 434].

5.8.1.10 Proteína cinase C beta type, Prkcb/pkcb, (P68404)

Pkcb é uma cinase do grupo AGC da família PKC. Ela possui um domínio transmembranar e mostrou aumento em sua abundância (Cluster 5) com uma fosforilação na Thr642 que também foi aumentada (Cluster 2) no sítio de fosforilação no domínio STKc_cPKC_beta. Foi demonstrado previamente que a fosforilação na Thr642 é muito importante da função enzimática da PKC [435]. Zhang et al mostrou que neutrófilos requerem aumento sustentável na concentração citosólica de Ca^{2+} para a produção de superóxidos devido à ativação dependente de Ca^{2+} de isoformas da proteína cinase C (PKCa and PKCb) [436] uma vez que essas isoformas são importantes para a fosforilação de componentes da NADPH oxidase [437, 438].

5.8.1.11 N-acetyl-D-glucosamina cinase, Nagk, (P81799)

Nagk pertence à superfamília das açúcar cinases/Hsp70/actina. Ela converte N-acetil-D-glicosamina em N-acetil-D-glicosamine-6-fosfato, convertendo ATP em ADP, [439]. Adicionalmente, como ATPases, Nagk também converte ATP em ADP e a superregulação de Nagk pode contribuir para a perda de energia [440]. Sua abundância foi aumentada (Cluster 2) com uma fosforilação na Ser76 que se mostrou diminuída (Cluster 4) em isquemia. Essa fosforilação na Ser76 foi encontrada no sítio de ligação a nucleotídeos do domínio NBD_açúcar-cinase_HSP70_actina, o qual é o domínio de ligação a nucleotídeos da superfamília açúcar-cinase/HSP70/actina. Essa fosforilação na Ser76, a qual pode ter algum papel na regulação da Nagk devido sua localização, não se encontra reportado na literatura apresentando papel regulatório nessa enzima, embora fosforilação na Tyr205 foi reportada tendo papel na ativação da Nagk [439].

5.8.1.12 Serina/treonina-proteína cinase N1, Pkn1/Prk1/Pak1, (Q63433)

Pkn1 é um membro da superfamília de proteínas cinase C das serina/treonina cinases que í um dos primeiros efetores da RhoA-GTPase existindo em um *pool* integral de membrana plasmática e em um *pool* citosólico/periférico [441]. Ela teve a abundância diminuída em laparotomia (Cluster 3). Um total de dez sítios fosforilados foram encontrados na Pkn1 e dois deles se mostraram aumentados (Cluster 5) na Thr918 e Ser920 e estes foram detectados no sítio do motivo de giro de fosforilação do domínio STKc_PKN, o qual é o domínio catalítico da Proteína Serina/Treonina Cinase, Proteína Cinase N. Outro aumento (Cluster 2) na fosforilação da Ser377 foi também emcontrada em nossa análise, que envolve a facilitação da integração da Pkn1 na membrana plasmática para funcionar como efetora da Rho [441].

5.8.1.13 Proteína S6 cinase alpha-1 ribosomal, Rps6ka1/Rsk1, (Q63531)

Rps6ka1 é uma AGC cinase da família RSK. Ela possui dois domínios transmembranares e mostrou-se com abundância reduzida (Cluster 1) com quatro sítios de fosforilação, um diminuindo (Cluster 1) na Ser732 e outros três na Tyr359, Ser363 e Ser380 aumentando (Cluster 2). Todas estas três fosforilações foram encontradas no domínio STKc_RSK_N, o qual é o domínio catalítico N-terminal da Proteína Serina/Treonina Cinase,da proteína ribosomal S6 cinase de 90kDa. Ser363 fosforilada pertence ao sítio do motivo de giro de fosforilação do domínio STKc_RSK_N, enquanto que a fosforilação na Ser380 foi encontrada no motivo hidrofóbico (HM) no domínio conservado STKc_RSK_N. Rps6ka1 pode interagir com fatores de transcrição como CREB em neutrófilose subunidades G da fosfatase 1 que regula a ativação da glicogênio sintetase [442, 443].

5.8.1.13 Proteína ribosomal S6 cinase alpha-2, Rps6ka2/Rsk3, (Q9WUT3)

Rps6ka2 é uma AGC cinase da família RSK. Ela possui dois domínios transmembranares e teve abundância diminuída na laparotomia (Cluster 3) e tem três sítios de fosforilação na Ser360 (Cluster 5), Ser377 (Cluster 2) e Ser716 (Cluster 1). Aumento na fosforilação da Ser360 foi encontrada no sítio do motivo de giro de fosforilação e na Ser377, no domínio hidrofóbico (HM) do domínio STKc_RSK_N, o qual é o domínio catalítico N-terminal da Proteína Serina/Treonina Cinase,da proteína ribosomal S6 cinase de 90kDa. Foi reportado que em condições similares *in vitro*, a atividade da RSK3 não é afetada por

RSK2 e também que Rsk3 fosforila proteínas-alvo nucleares como c-fos e histonas [444]. Ambas Rsk2 e Rsk3 são ativadas por Ngf e ativam CREB por fosforilação da Ser133 *in vitro* [445] e em nossos dados não detectamos fosforilação na Ser133 em (P15337) Creb (cyclic AMP-responsive element-binding proteína 1 isoform B), porém encontramos fosforilações em outros resíduos.

5.8.1.14 Proteína Serina/treonina cinase, Oxsr1/Osr1, (Q6P9R2)

Oxsr1 é uma proteína responsiva a estresse oxidativo 1 da família STE20. Ela tem dois domínios transmembranares e foi teve abundância aumentada (Cluster 5) com três sítios de fosforilação, um na Ser325 que diminuiu (Cluster 1) e na Ser324 e Ser359, que aumentaram (Cluster 5). Todos esses três sítios foram detectados em SPS1, que é um domínio proteína Serina/treonina proteína cinase. A Osr1 é estimulada por Wnk1 [446] que também foi encontrado mais abundante em nossos resultados com 10 sítios de fosforilação já previamente mencionados. Osr1 regula atividade de troca de Na^+/H^+, a qual participa na regulação do volume celular [447-449] e na produção de ROS [446] uma vez que a produção de ROS é paralela à geração de H^+ que inibem NADPH oxidase, as quais geram ROS [450].

5.8.2 Fosfatases fosforiladas em Neutrófilos

No proteoma de neutrófilos, descrevemos 50 proteínas reguladas contendo o termo "fosfatase". Entre elas, 13 apresentaram regulação em fosforilações e a regulações em sítios de fosforilação de 4 fosfatases foram encontradas e regiões de domínios conhecidos. Do 1% de fosfatases identificadas, aquelas que mostraram regulação na abundância compreendem 72%, aquelas que mostraram regulação de fosforilações compreenderam 19% e somente 9% das fosfatases mostraram fosforilações reguladas dentro de regiões de domínios (Fig. 35-B). Fosfatases e suas respectivas classificações em clusters de abundância , número de fosfopeptídeos e os domínios contendo mudanças significativas nas fosforilações estão mostradas na tabela 9.

5.8.2.1 Precursor de receptor tipo proteína tirosina fosfatase C isoforma 4, Ptprc/CD45, (P04157)

CD45 é um receptor tipo proteína tirosina fosfatase com dois domínios transmembranares e comumente conhecidas como CD45 ou LCA (antígeno comum de leucócitos). Foi

encontrada com abundância aumentada (Cluster 5) com 18 sítios de fosforilação. Regulação em fosforilação foi detectada no domínio catalítico Proteína tirosina fosfatase (PTPc). CD45 tem papel importante na adesão de neutrófilos, quimiotaxia, fagocitose, produção de ROS e lise bacterian [451]. A proteína tirosina fosfatase receptor-*like* (RPTPs) CD45 e CD148, tem papéis redundantes na atividade SFK em células B e macrófagos na estimulação de receptor imune ITAM [452]. Um estudo mostrou que ambas CD45 e CD 148 são essenciais na quimiotaxia mediada por quimioatrator em neutrófilos após infecção por *S. aureus*. CD45 positivamente enquanto CD148 positivamente e negativamente regulam a função GPCR e sinais proximais incluindo Ca^{2+}, PI3K, e atividade pERK. Ainda mais, CD45 e CD148 visam preferencialmente diferentes membros SFK (Hck e Fgr *versus* Lyn, respectivamente) durante a regulação da vias GPCR [451].

5.8.2.2 Proteína tirosina fosfatase tipo 6 não receptor, Ptpn6/Shp-1, (P81718)

Ptpn6 tem um domínio transmembranar e foi encontrada com o padrão de abundância do *cluster* 2, com dois sítios de fosforilação. A fosforilação na Ser12 foi aumentada no domínio SH2_N-SH2_SHP_like, N-terminal Src homologo 2 (N-SH2) encontrado em domínios SH2 de proteínas fosfatases (SHP).

O domínio Src homologo 2 (SH2)-contendo tirosina fosfatase-1 (SHP-1) é encontrado na rfegulação de diferenciação, proliferação e ativação de células hematopoiéticas. SHP-1 é também envolvido na modulação de vias de apoptose em neutrófilos. Baixos níveis de SHP-1 tem sido associados com aumento da sobrevivência de neutrófilos *in vitro* e camundongos deficientes em SHP-1 desenvolvem respostas inflamatórias neutrofílicas severas. Em contraste, alta abundância tem sido observada em pacientes neutropênicos [453]. Recentemente, a deleção de Ptpn6 em neutrófilos e células dendríticas de camundongo resultou em inflamação cutânea (dermatose neutrofílica) e autoimunidade severa, sem inflamação respectivamente [454]. Também foi proposto que SHP1 se liga a múltiplas cinases, tais como Jak2, Jak3, TAK1, ERK1/2, p38, JNK, cinase associada a IL-1R 1, e Lyn, através de um novo motivo inibidor de tirosil-cinase independente de fosforilação[455].

Tabela 9 Fosfatases fosforiladas com abundância regulada após laparotomia e isquemia.

UNIPROT	No. of regulated phosphopeptides	Cluster	GENE Official symbol	TM	Description	Length	Enzyme Codes	Domain containing the phosphopeptide
B2GV87	3	4	Ptpre	1	receptor-type tyrosine-protein phosphatase epsilon precursor	699	3.1.3.48	
P04157	18	5	Ptprc	2	receptor-type tyrosine-protein phosphatase C isoform 4 precursor	1273	EC:3.1.3.48	Protein tyrosine phosphatase (PTPc) catalytic domain
P20417	2	3	Ptpn1	0	tyrosine-protein phosphatase non-receptor type 1	432	-	
P81718	10	2	Ptpn6	1	tyrosine-protein phosphatase non-receptor type 6	613	EC:3.1.3.48	SH2_N-SH2_SHP_like[cd10340], N-terminal Src homology 2 (N-SH2) domain found in SH2 domain Phosphatases (SHP) proteins; SH2 domain; Src homology 2 domains
P97573	28	3	Inpp5d	0	phosphatidylinositol 3,4,5-trisphosphate 5-phosphatase 1	1190	EC:3.1.3; EC:3.1.3.56	PTZ00449, 104 kDa microneme/rhoptry antigen; Catalytic inositol polyphosphate 5-phosphatase (INPP5c) domain of SH2 domain; putative catalytic site; putative active site; putative MG binding site; putative PI/IP binding site
Q10728	29	4	Ppp1r12a	1	Protein phosphatase 1 regulatory subunit 12A	1032	EC:3.1.3.16	
Q5HZV9	2	2	Ppp1r7	0	protein phosphatase 1 regulatory subunit 7	360	-	
Q6PD03	4	3	Ppp2r5a	1	serine/threonine-protein phosphatase 2A 56 kDa regulatory subunit alpha isoform	486	-	
Q7TSI3	2	5	Ppp6r1	1	serine/threonine-protein phosphatase 6 regulatory subunit 1	856	-	CAF-1_p60_C, Chromatin assembly factor complex 1 subunit p60, C-terminal; PHA03247, large tegument protein UL36

5.8.2.3 Fosfatidilinositol 3,4,5-trisfosfato 5-fosfatase 1, Inpp5d/Ship, (P97573)

Inpp5d foi encontrada com abundância diminuída em laparotomia e sem mudança em isquemia (Cluster 3) com 28 sítios de fosforilação regulados na PTZ00449, um antígeno microneme/rhoptry de 104 kDa; domínio catalítico inositol polifosfato 5-fosfatase (INPP5c) do domínio SH2; dítio catalítico putativo; sítio ativo putativo; sítio de ligação MG putativo e sítio de ligação a PI/IP putativo. SHIP1 (Inpp5d) SHIP converte fosfatidilinositol 3, 4, 5 trifosfato em fosfatidil 3, 4 bifosfatoe e neutrófilos deficientes de SHIP1 mostraram polarização despareada e motilidade *in vitro*, sugerindo seu papel na motilidade de neutrófilos [456]. Recentemente um estudo com peixe-zebra mostrou que fosfatases SHIP limitam a motilidade de neutrófilos modulando a sinalização por PI3K. Depleção das fosfatases SHIP causou o aumento da motilidade 3D de neutrófilos e sua infiltração em feridas. Ais ainda, abundância aumentada de domínios de fosfatases SHIP em neutrófilos desparearam sua migração 3D [457]. SHIP é um regulador negativo na ativação de neutrófilos induzido por TLR2e no desenvolvimento de

processos inflamatórios dependentes de neutrófilos relacionadas *in vitro*, como dano agudo pulmonar [458].

5.8.2.4 Serina/treonina -proteína fosfatase 6 subunidade regulatória 1, Ppp6r1/Saps1, (Q7TSI3)

Ppp6r1 tem um domínio transmembranar e foi encontrada com o perfil de abunddância do *cluster* 5, com dois sítios de fosforilação nas Ser531 e Ser817. A fosforilação na Ser817 foi aumentada (Cluster 5) e localizada no CAF-1_p60_C, fator de montagem do complexo de cromatina 1 subunidade p60, C-terminal e PHA03247, grande proteína tegumentar UL36.

Proteína fosfatase 6 (PP6) é a principal T-loop fosfatase em Aurora A, que é uma importante cinase mitótica. Depleção de subunidades regulatórias ou catalíticas interfere com a formação do fuso e alinhamento cromossomal e resultam em perda de função da PP6 devido ao aumento da atividade da Aurora A. A holoenzima PP6 consiste da PPP6C catalítica, SAPS1–3 regulatória e subunidades ANKRD28–44 e todas estas são requeridas para mitose normal [459]. Nós reportamos aqui pela primeira vez a presença de subunidades regulatórias de SAPS1 (Ppp6r1) em neutrófilos. A literatura mostra que si quer foi reportada em qualquer outro tipo de célula do sistema imune anteriormente.

6 Resumo dos resultados das vias de sinalização

Resumindo os resultados da análise de vias de sinalização e enzimas, a figura 54 mostra que, no caso de isquemia e reperfusão, o sinal para a ativação de neutrófilos veio das células intestinais/endoteliais (ECs) na forma de quimiocinas e quimioatrativos. Como C5a e LTB4 são potentes quimioatrativos e levam a uma superregulação de moléculas de adesão vascular, ICAM-1, E-selectina endotelial, P-selectina, IL-8, MCP-1 [82, 83] e finalmente ativam a via de sinalização das quimiocinas. A maioria das proteínas da via de sinalização das quimiocinas foi encontrada superregulada após IR. Nós encontramos também subregulação de 57 proteínas ribosomais e o papel da maioria das proteínas não está claro em neutrófilos. No entanto RP19 tem um efeito antagonista induzido em neutrófilos C5aR e altera a quimiotaxia de leucócitos por causar diferenças funcionais na resposta do receptor C5a [333]. Neutrófilos migram em direção à fonte de quimioatrativos como peptídeos formilados, C5a, leucotrieno B4 e quimiocinas como IL-8 [352] e, após a ligação com seu receptor de superfície, diversos eventos citoplasmáticos ocorrem ativando a maquinaria do citoesqueleto [353]. Proteínas desta via também foram superreguladas após IR. A ativação de proteínas pertencentes a essa via levam ao aumento da motilidade, locomoção, quimiotaxia, adesão focal firme, migração trans-endotelial (TEM) através da formação de lamelopodia e filopodia. Como resultado da interação de FcR e seus ligantes Ig, em leucócitos, inicia-se um número de respostas incluindo fagocitose, citotoxicidade celular mediada dependente de anticorpos (ADCC, liberação de mediadores pró-inflamatórios e produção de citocinas [337, 338]. Lipoxigenases (5-LO e 15-LO) estão envolvidas no metabolismo do ácido araquidônico (AA) levando à produção de LTB4, que é outra fonte de recrutamento PMN em ECs. Após desgranulação e TEM, neutrófilos liberam citocinas e ROS dentro do endotélio que não somente resultam no recrutamento de mais PMNs, mas também causam dano endotelial. A energia requerida para ativação dos neutrófilos vem de vias metabólicas como 109 proteínas foram encontradas superreguladas em vias metabólicas. Nós também encontramos a via glicolítica superregulada, o que pode ser usado pelos neutrófilos para produção rápida de energia ao invés da fosforilação oxidativa que encontramos subregulada. Células do sistema imune ativadas preferem usar a glicólise, uma vez que esta é 100 vezes mais rápida que a fosforilação oxidativa para a síntese de macromoléculas e proliferação [371]. No entanto, o papel exato dessas vias metabólicas não é claro.

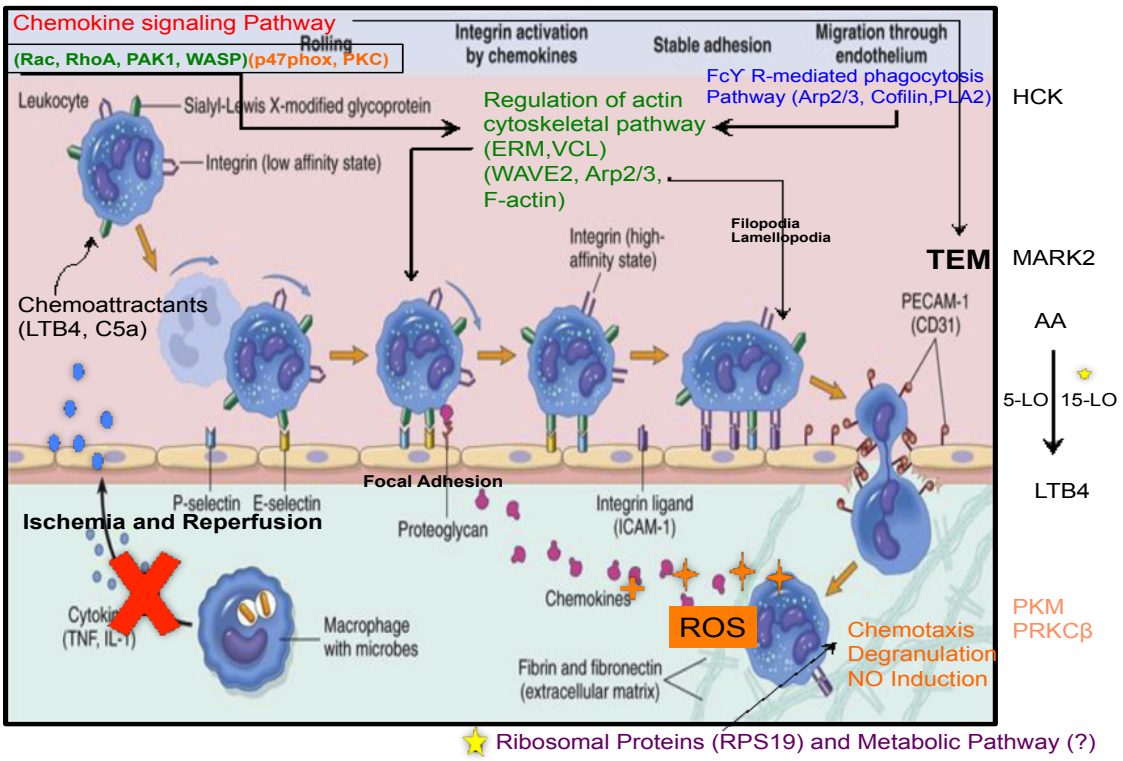

Figura 5 Resumo de alguns resultados mais relevantes e a interação entre diferentes vias de sinalização.

7 Conclusão e perspectivas futuras:

Em condições clínicas, o dano por isquemia/reperfusão é associado com alta morbidade e mortalidade. O papel de neutrófilos na patogênese da IRI é claro na literatura e não pudemos encontrar nenhum estudo mostrando os mecanismos subjacentes e abundância ou expressão diferencial de proteínas em neutrófilos nesses procedimentos cirúrgicos. Nosso estudo mostra a significância de estratégias proteômicas comparativas aplicadas a neutrófilos em diferentes grupos cirúrgicos. Nós reportamos a cobertura proteômica mais abrangente em neutrófilos até agora, mostrando adequação e sensibilidade de equipamentos e métodos usados aqui. As ferramentas aplicadas e estratégias discutidas são apropriadas para o alto nível de identificações do proteoma e fosfoproteoma de neutrófilos e para melhor compreender as facetas da biologia de neutrófilos. Nossos resultados contradizem alguns já reportados e corroboram outros e podem gerar novas ideias e hipóteses. Este trabalho sobre o proteoma de neutrófilos de ratos mostra a regulação de algumas enzimas importantes por análise de clusters. Algumas destas têm seu papel bem conhecido em neutrófilos, enquanto que poucas foram identificadas aqui pela primeira vez

em neutrófilos e a maioria do total encontra-se pouco caracterizada. Importantes proteínas cinases e fosfatases foram identificadas, juntamente com sua regulação de abundância e fosforilação em diferentes grupos cirúrgicos e podem ser consideradas como futuros alvos terapêuticos na biologia de neutrófilos.

Esse trabalho abre nova janela para melhor compreendermos o proteoma de neutrófilos e proporciona uma base de dados para futuros trabalhos. A validação dessas enzimas pode ser muito útil nesse sentido e ainda levar à descoberta de biomarcadores.

Nós reportamos alguns eventos interessantes preditos como a via ribossomal, a via de regulação da actina do citoesqueleto, a via de fagocitose mediada por Fc-gama-R, a via de sinalização de quimocina e a fosforilação oxidativa com padrão de regulação.

Como parte de uma linha de pesquisa em andamento do Laboratório de Bioquímica e Química de Proteínas da UnB, a análise realizada até hoje será estendida pelo estudo abrangente do proteoma de células ativadas em diferentes condições experimentais. O futuro exame de modificações pós-traducionais como glicosilações e acetilações proporcionará mais entendimento a respeito das vias de sinalização subjacentes e da biologia de neutrófilos.

Os resultados mostrados nesse trabalho também mostram diferenças nos parâmetros hematimétricos entre as condições avaliadas. Os parâmetros mais marcantes são aqueles relacionados a plaquetas e leucócitos; alguns desses, incluindo contagem de linfócitos e granulócitos e a razão granulócito/linfócito, sugerem que IPC atenua o efeito de IR nas células sanguíneas circulantes. Nosso trabalho proporciona dados que ajudam a melhorar a compreensão das respostas hematológicas do organismo após IR e IPC. Alguns desses parâmetros descritos aqui podem ser futuramente validados como marcadores preditivos de isquemia e podem dar base a futuros estudos visando reduzir o dano tecidual resultante de isquemia/reperfusão. A contagem de plaquetas, amplitude de distribuição de plaquetas (PDW), volume plaqutário médio (MPV) e plaquetócrito (PCT) mostram o envolvimento da ativação de plaquetas na IR e IPC. Como o papel das plaquetas não está elucidado em tais condições, o estudo proteômico das mesmas em um modelo similar pode ser útil. A descoberta de candidatos a biomarcadores, bem como as vias metabólicas de que participam, pode auxiliar na busca por formas de minimizar o dano tecidual.

References:

1. Hollmann, M.W., et al., *Local anesthetic effects on priming and activation of human neutrophils.* Anesthesiology, 2001. **95**(1): p. 113-22.

2. Lu, Y.Z., et al., *Neutrophil priming by hypoxic preconditioning protects against epithelial barrier damage and enteric bacterial translocation in intestinal ischemia/reperfusion.* Lab Invest, 2012. **92**(5): p. 783-96.

3. Rao, R.M., et al., *Endothelial-dependent mechanisms of leukocyte recruitment to the vascular wall.* Circ Res, 2007. **101**(3): p. 234-47.

4. http://www.studyblue.com.

5. Springer, T.A., *Traffic signals for lymphocyte recirculation and leukocyte emigration: the multistep paradigm.* Cell, 1994. **76**(2): p. 301-14.

6. Kuo, M.C., et al., *Ischemia-induced exocytosis of Weibel-Palade bodies mobilizes stem cells.* J Am Soc Nephrol, 2008. **19**(12): p. 2321-30.

7. Sluiter, W., et al., *Leukocyte adhesion molecules on the vascular endothelium: their role in the pathogenesis of cardiovascular disease and the mechanisms underlying their expression.* J Cardiovasc Pharmacol, 1993. **22 Suppl 4**: p. S37-44.

8. Kubes, P., M. Jutila, and D. Payne, *Therapeutic potential of inhibiting leukocyte rolling in ischemia/reperfusion.* J Clin Invest, 1995. **95**(6): p. 2510-9.

9. Granger, D.N. and P. Kubes, *The microcirculation and inflammation: modulation of leukocyte-endothelial cell adhesion.* J Leukoc Biol, 1994. **55**(5): p. 662-75.

10. Zimmerman, G.A., S.M. Prescott, and T.M. McIntyre, *Endothelial cell interactions with granulocytes: tethering and signaling molecules.* Immunol Today, 1992. **13**(3): p. 93-100.

11. Granger, D.N. and R.J. Korthuis, *Physiologic mechanisms of postischemic tissue injury.* Annu Rev Physiol, 1995. **57**: p. 311-32.

12. Gu, Q., et al., *Inhibition of TNF-alpha reduces myocardial injury and proinflammatory pathways following ischemia-reperfusion in the dog.* J Cardiovasc Pharmacol, 2006. **48**(6): p. 320-8.

13. Ikeda, U., et al., *Neutrophil adherence to rat cardiac myocyte by proinflammatory cytokines.* J Cardiovasc Pharmacol, 1994. **23**(4): p. 647-52.

14. Kuwabara, H., et al., *Antibody mediated ligation of platelet/endothelial cell adhesion molecule-1 (PECAM-1) on neutrophils enhances adhesion to cultured human dermal microvascular endothelial cells.* Kobe J Med Sci, 1996. **42**(4): p. 233-41.

15. Hierholzer, C., et al., *Molecular and functional contractile sequelae of rat intestinal ischemia/reperfusion injury.* Transplantation, 1999. **68**(9): p. 1244-54.

16. Alexander, J.S., et al., *Inflammatory mediators induce sequestration of VE-cadherin in cultured human endothelial cells.* Inflammation, 2000. **24**(2): p. 99-113.

17. Allingham, M.J., J.D. van Buul, and K. Burridge, *ICAM-1-mediated, Src- and Pyk2-dependent vascular endothelial cadherin tyrosine phosphorylation is required for leukocyte transendothelial migration.* J Immunol, 2007. **179**(6): p. 4053-64.

18. Ryan, G.B. and J.V. Hurley, *The chemotaxis of polymorphonuclear leucocytes towards damaged tissue.* Br J Exp Pathol, 1966. **47**(5): p. 530-6.

19. Ford-Hutchinson, A.W., et al., *Leukotriene B, a potent chemokinetic and aggregating substance released from polymorphonuclear leukocytes.* Nature, 1980. **286**(5770): p. 264-5.

20. Smart, S.J. and T.B. Casale, *TNF-alpha-induced transendothelial neutrophil migration is IL-8 dependent.* Am J Physiol, 1994. **266**(3 Pt 1): p. L238-45.

21. Strieter, R.M., et al., *The immunopathology of chemotactic cytokines: the role of interleukin-8 and monocyte chemoattractant protein-1.* J Lab Clin Med, 1994. **123**(2): p. 183-97.

22. Niessen, H.W., et al., *Upregulation of ICAM-1 on cardiomyocytes in jeopardized human myocardium during infarction.* Cardiovasc Res, 1999. **41**(3): p. 603-10.

23. Lacy, P., *The role of Rho GTPases and SNAREs in mediator release from granulocytes.* Pharmacol Ther, 2005. **107**(3): p. 358-76.

24. Faurschou, M. and N. Borregaard, *Neutrophil granules and secretory vesicles in inflammation.* Microbes Infect, 2003. **5**(14): p. 1317-27.

25. Borregaard, N., *Neutrophils, from marrow to microbes.* Immunity, 2010. **33**(5): p. 657-70.

26. Borregaard, N., O.E. Sorensen, and K. Theilgaard-Monch, *Neutrophil granules: a library of innate immunity proteins.* Trends Immunol, 2007. **28**(8): p. 340-5.

27. Amulic, B., et al., *Neutrophil function: from mechanisms to disease.* Annu Rev Immunol, 2012. **30**: p. 459-89.

28. Borregaard, N. and J.B. Cowland, *Granules of the human neutrophilic polymorphonuclear leukocyte.* Blood, 1997. **89**(10): p. 3503-21.

29. Delclaux, C., et al., *Role of gelatinase B and elastase in human polymorphonuclear neutrophil migration across basement membrane.* Am J Respir Cell Mol Biol, 1996. **14**(3): p. 288-95.

30. Jesaitis, A.J., et al., *Ultrastructural localization of cytochrome b in the membranes of resting and phagocytosing human granulocytes.* J Clin Invest, 1990. **85**(3): p. 821-35.

31. Guan, Y., et al., *Intestinal ischemia-reperfusion injury: reversible and irreversible damage imaged in vivo.* Am J Physiol Gastrointest Liver Physiol, 2009. **297**(1): p. G187-96.

32. Sanada, S., I. Komuro, and M. Kitakaze, *Pathophysiology of myocardial reperfusion injury: preconditioning, postconditioning, and translational aspects of protective measures.* Am J Physiol Heart Circ Physiol, 2011. **301**(5): p. H1723-41.

33. Bulkley, G.B., *Free radical-mediated reperfusion injury: a selective review.* Br J Cancer Suppl, 1987. **8**: p. 66-73.

34. Semenza, G.L., *HIF-1: mediator of physiological and pathophysiological responses to hypoxia.* J Appl Physiol (1985), 2000. **88**(4): p. 1474-80.

35. Stein, I., et al., *Translation of vascular endothelial growth factor mRNA by internal ribosome entry: implications for translation under hypoxia.* Mol Cell Biol, 1998. **18**(6): p. 3112-9.

36. Carden, D.L. and D.N. Granger, *Pathophysiology of ischaemia-reperfusion injury.* J Pathol, 2000. **190**(3): p. 255-66.

37. Lefer, A.M. and D.J. Lefer, *The role of nitric oxide and cell adhesion molecules on the microcirculation in ischaemia-reperfusion.* Cardiovasc Res, 1996. **32**(4): p. 743-51.

38. Heyderman, R.S., et al., *Induction of human endothelial tissue factor expression by Neisseria meningitidis: the influence of bacterial killing and adherence to the endothelium.* Microb Pathog, 1997. **22**(5): p. 265-74.

39. Levi, M., et al., *Pathogenesis of disseminated intravascular coagulation in sepsis.* Jama, 1993. **270**(8): p. 975-9.

40. Guneli, E., et al., *Erythropoietin protects the intestine against ischemia/ reperfusion injury in rats.* Mol Med, 2007. **13**(9-10): p. 509-17.

41. Mojzis, J., et al., *Protective effect of quercetin on ischemia/reperfusion-induced gastric mucosal injury in rats.* Physiol Res, 2001. **50**(5): p. 501-6.

42. Bradbury, A.W., et al., *Mesenteric ischaemia: a multidisciplinary approach.* Br J Surg, 1995. **82**(11): p. 1446-59.

43. Heys, S.D., J. Brittenden, and T.J. Crofts, *Acute mesenteric ischaemia: the continuing difficulty in early diagnosis.* Postgrad Med J, 1993. **69**(807): p. 48-51.

44. Sileri, P., et al., *Intestinal ischemia/reperfusion injury produces chronic abnormalities of absorptive function.* Transplant Proc, 2002. **34**(3): p. 984.

45. Cicalese, L., et al., *Bacterial translocation in clinical intestinal transplantation.* Transplantation, 2001. **71**(10): p. 1414-7.

46. Van Leeuwen, P.A., et al., *Clinical significance of translocation.* Gut, 1994. **35**(1 Suppl): p. S28-34.

47. Beutler, B. and E.T. Rietschel, *Innate immune sensing and its roots: the story of endotoxin.* Nat Rev Immunol, 2003. **3**(2): p. 169-76.

48. Fishbein, T.M., *Intestinal transplantation.* N Engl J Med, 2009. **361**(10): p. 998-1008.

49. Lenaerts, K., et al., *New insights in intestinal ischemia-reperfusion injury: implications for intestinal transplantation.* Curr Opin Organ Transplant, 2013. **18**(3): p. 298-303.

50. Ceppa, E.P., K.C. Fuh, and G.B. Bulkley, *Mesenteric hemodynamic response to circulatory shock.* Curr Opin Crit Care, 2003. **9**(2): p. 127-32.

51. Xiao, F., et al., *Lung neutrophil retention and injury after intestinal ischemia/reperfusion.* Microcirculation, 1997. **4**(3): p. 359-67.

52. Kong, S.E., et al., *Ischaemia-reperfusion injury to the intestine.* Aust N Z J Surg, 1998. **68**(8): p. 554-61.

53. Wang, Q., et al., *Endotoxemia in mice stimulates production of complement C3 and serum amyloid A in mucosa of small intestine.* Am J Physiol, 1998. **275**(5 Pt 2): p. R1584-92.

54. Zamir, O., et al., *Effect of sepsis or cytokine administration on release of gut peptides.* Am J Surg, 1992. **163**(1): p. 181-4; discussion 184-5.

55. Meyer, T.A., et al., *Sepsis and endotoxemia stimulate intestinal interleukin-6 production.* Surgery, 1995. **118**(2): p. 336-42.

56. Stark, M.E. and J.H. Szurszewski, *Role of nitric oxide in gastrointestinal and hepatic function and disease.* Gastroenterology, 1992. **103**(6): p. 1928-49.

57. Mangino, M.J., et al., *Mucosal arachidonate metabolism and intestinal ischemia-reperfusion injury.* Am J Physiol, 1989. **257**(2 Pt 1): p. G299-307.

58. Panes, J. and D.N. Granger, *Leukocyte-endothelial cell interactions: molecular mechanisms and implications in gastrointestinal disease.* Gastroenterology, 1998. **114**(5): p. 1066-90.

59. Zou, L., B. Attuwaybi, and B.C. Kone, *Effects of NF-kappa B inhibition on mesenteric ischemia-reperfusion injury.* Am J Physiol Gastrointest Liver Physiol, 2003. **284**(4): p. G713-21.

60. Massberg, S., et al., *In vivo assessment of the influence of cold preservation time on microvascular reperfusion injury after experimental small bowel transplantation.* Br J Surg, 1998. **85**(1): p. 127-33.

61. Sisley, A.C., et al., *Neutrophil depletion attenuates human intestinal reperfusion injury.* J Surg Res, 1994. **57**(1): p. 192-6.

62. Riaz, A.A., et al., *Fundamental and distinct roles of P-selectin and LFA-1 in ischemia/reperfusion-induced leukocyte-endothelium interactions in the mouse colon.* Ann Surg, 2002. **236**(6): p. 777-84; discussion 784.

63. Carden, D.L., J.K. Smith, and R.J. Korthuis, *Neutrophil-mediated microvascular dysfunction in postischemic canine skeletal muscle. Role of granulocyte adherence.* Circ Res, 1990. **66**(5): p. 1436-44.

64. Weiss, S.J., *Tissue destruction by neutrophils.* N Engl J Med, 1989. **320**(6): p. 365-76.

65. Bagge, U., B. Amundson, and C. Lauritzen, *White blood cell deformability and plugging of skeletal muscle capillaries in hemorrhagic shock.* Acta Physiol Scand, 1980. **108**(2): p. 159-63.

66. Nalini, S., M.M. Mathan, and K.A. Balasubramanian, *Oxygen free radical induced damage during intestinal ischemia/reperfusion in normal and xanthine oxidase deficient rats.* Mol Cell Biochem, 1993. **124**(1): p. 59-66.

67. Souza, D.G., et al., *Effects of the PAF receptor antagonist UK74505 on local and remote reperfusion injuries following ischaemia of the superior mesenteric artery in the rat.* Br J Pharmacol, 2000. **131**(8): p. 1800-8.

68. Willerson, J.T., *Pharmacologic approaches to reperfusion injury.* Adv Pharmacol, 1997. **39**: p. 291-312.

69. Souza, D.G., et al., *Effect of a BLT receptor antagonist in a model of severe ischemia and reperfusion injury in the rat.* Eur J Pharmacol, 2002. **440**(1): p. 61-9.

70. Crooks, S.W. and R.A. Stockley, *Leukotriene B4.* Int J Biochem Cell Biol, 1998. **30**(2): p. 173-8.

71. McDonald, P.P., et al., *Activation of the human neutrophil 5-lipoxygenase by leukotriene B4.* Br J Pharmacol, 1992. **107**(1): p. 226-32.

72. Tager, A.M. and A.D. Luster, *BLT1 and BLT2: the leukotriene B(4) receptors.* Prostaglandins Leukot Essent Fatty Acids, 2003. **69**(2-3): p. 123-34.

73. Souza, D.G. and M.M. Teixeira, *The balance between the production of tumor necrosis factor-alpha and interleukin-10 determines tissue injury and lethality during intestinal ischemia and reperfusion.* Mem Inst Oswaldo Cruz, 2005. **100 Suppl 1**: p. 59-66.

74. Kettritz, R., et al., *TNF-alpha-mediated neutrophil apoptosis involves Ly-GDI, a Rho GTPase regulator.* J Leukoc Biol, 2000. **68**(2): p. 277-83.

75. Ben, D.F., et al., *TLR4 mediates lung injury and inflammation in intestinal ischemia-reperfusion.* J Surg Res, 2012. **174**(2): p. 326-33.

76. Aytekin, F.O., et al., *Antithrombin III attenuates pulmonary tissue injury caused by mesenteric ischemia-reperfusion.* Am J Surg, 2005. **189**(2): p. 161-6.

77. Fessler, M.B., et al., *Lipopolysaccharide stimulation of the human neutrophil: an analysis of changes in gene transcription and protein expression by oligonucleotide microarrays and proteomics.* Chest, 2002. **121**(3 Suppl): p. 75s-76s.

78. Heitzmann, D. and R. Warth, *Physiology and pathophysiology of potassium channels in gastrointestinal epithelia.* Physiol Rev, 2008. **88**(3): p. 1119-82.

79. Pompermayer, K., et al., *Effects of the treatment with glibenclamide, an ATP-sensitive potassium channel blocker, on intestinal ischemia and reperfusion injury.* Eur J Pharmacol, 2007. **556**(1-3): p. 215-22.

80. Arumugam, T.V., et al., *Complement mediators in ischemia-reperfusion injury.* Clin Chim Acta, 2006. **374**(1-2): p. 33-45.

81. Eltzschig, H.K. and C.D. Collard, *Vascular ischaemia and reperfusion injury.* Br Med Bull, 2004. **70**: p. 71-86.

82. Monk, P.N., et al., *Function, structure and therapeutic potential of complement C5a receptors.* Br J Pharmacol, 2007. **152**(4): p. 429-48.

83. Xu, D.Z., et al., *Elimination of C5aR prevents intestinal mucosal damage and attenuates neutrophil infiltration in local and remote organs.* Shock, 2009. **31**(5): p. 493-9.

84. Zhelev, D.V., A.M. Alteraifi, and D. Chodniewicz, *Controlled pseudopod extension of human neutrophils stimulated with different chemoattractants.* Biophys J, 2004. **87**(1): p. 688-95.

85. Zhao, X., et al., *ELR-CXC chemokine receptor antagonism targets inflammatory responses at multiple levels.* J Immunol, 2009. **182**(5): p. 3213-22.

86. Zhao, X., et al., *A novel ELR-CXC chemokine antagonist reduces intestinal ischemia reperfusion-induced mortality, and local and remote organ injury.* J Surg Res, 2010. **162**(2): p. 264-73.

87. Takahashi, T., et al., *Activation of human neutrophil by cytokine-activated endothelial cells.* Circ Res, 2001. **88**(4): p. 422-9.

88. Takahashi, T., et al., *Neutrophil-activating activity and platelet-activating factor synthesis in cytokine-stimulated endothelial cells: reduced activity in growth-arrested cells.* Microvasc Res, 2007. **73**(1): p. 29-34.

89. Abramov, A.Y., A. Scorziello, and M.R. Duchen, *Three distinct mechanisms generate oxygen free radicals in neurons and contribute to cell death during anoxia and reoxygenation.* J Neurosci, 2007. **27**(5): p. 1129-38.

90. Szocs, K., *Endothelial dysfunction and reactive oxygen species production in ischemia/reperfusion and nitrate tolerance.* Gen Physiol Biophys, 2004. **23**(3): p. 265-95.

91. Giorgio, M., et al., *Electron transfer between cytochrome c and p66Shc generates reactive oxygen species that trigger mitochondrial apoptosis.* Cell, 2005. **122**(2): p. 221-33.

92. Di Girolamo, F., et al., *The Role of Mass Spectrometry in the "Omics" Era.* Curr Org Chem, 2013. **17**(23): p. 2891-2905.

93. Morris, H.R., et al., *Fast atom bombardment: a new mass spectrometric method for peptide sequence analysis.* Biochem Biophys Res Commun, 1981. **101**(2): p. 623-31.

94. Shackleton, C.H. and K.M. Straub, *Direct analysis of steroid conjugates: the use of secondary ion mass spectrometry.* Steroids, 1982. **40**(1): p. 35-51.

95. Yamashita M, F.J., *Negative ion source production with electrospray ion source.* J. Phys. Chem. , 1984. **88**: p. 4671–4675.

96. Hillenkamp, F. and M. Karas, *Mass spectrometry of peptides and proteins by matrix-assisted ultraviolet laser desorption/ionization.* Methods Enzymol, 1990. **193**: p. 280-95.

97. Hillenkamp, F., et al., *Matrix-assisted laser desorption/ionization mass spectrometry of biopolymers.* Anal Chem, 1991. **63**(24): p. 1193a-1203a.

98. Hillenkamp, F., Karas, M., Holtkamp, D. & Klüsener, P, *Energy deposition in ultraviolet laser desorption mass spectrometry of biomolecules.* International journal of mass spectrometry and ion processes, 1986. **69**: p. 265-276.

99. Fenn, J.B., et al., *Electrospray ionization for mass spectrometry of large biomolecules.* Science, 1989. **246**(4926): p. 64-71.

100. Aebersold, R. and M. Mann, *Mass spectrometry-based proteomics.* Nature, 2003. **422**(6928): p. 198-207.

101. Hu, Q., et al., *The Orbitrap: a new mass spectrometer.* J Mass Spectrom, 2005. **40**(4): p. 430-43.

102. Makarov, A., *Electrostatic axially harmonic orbital trapping: a high-performance technique of mass analysis.* Anal Chem, 2000. **72**(6): p. 1156-62.

103. Makarov, A., et al., *Performance evaluation of a hybrid linear ion trap/orbitrap mass spectrometer.* Anal Chem, 2006. **78**(7): p. 2113-20.

104. Whiteaker, J.R., *The increasing role of mass spectrometry in quantitative clinical proteomics.* Clin Chem, 2010. **56**(9): p. 1373-4.

105. http://biomed.brown.edu/epscor_proteomics/ltq-orbitrap-velos.

106. Biemann, K., *Appendix 5. Nomenclature for peptide fragment ions (positive ions).* Methods Enzymol, 1990. **193**: p. 886-7.

107. Roepstorff, P. and J. Fohlman, *Proposal for a common nomenclature for sequence ions in mass spectra of peptides.* Biomed Mass Spectrom, 1984. **11**(11): p. 601.

108. Chi, H., et al., *pNovo: de novo peptide sequencing and identification using HCD spectra.* J Proteome Res, 2010. **9**(5): p. 2713-24.

109. Frese, C.K., et al., *Improved peptide identification by targeted fragmentation using CID, HCD and ETD on an LTQ-Orbitrap Velos.* J Proteome Res, 2011. **10**(5): p. 2377-88.

110. Johnson, R.S., et al., *Novel fragmentation process of peptides by collision-induced decomposition in a tandem mass spectrometer: differentiation of leucine and isoleucine.* Anal Chem, 1987. **59**(21): p. 2621-5.

111. Schulze, W.X. and B. Usadel, *Quantitation in mass-spectrometry-based proteomics.* Annu Rev Plant Biol, 2010. **61**: p. 491-516.

112. Bantscheff, M., et al., *Quantitative mass spectrometry in proteomics: a critical review.* Anal Bioanal Chem, 2007. **389**(4): p. 1017-31.

113. Ong, S.E., et al., *Stable isotope labeling by amino acids in cell culture, SILAC, as a simple and accurate approach to expression proteomics.* Mol Cell Proteomics, 2002. **1**(5): p. 376-86.

114. Gygi, S.P., et al., *Quantitative analysis of complex protein mixtures using isotope-coded affinity tags.* Nat Biotechnol, 1999. **17**(10): p. 994-9.

115. Ross, P.L., et al., *Multiplexed protein quantitation in Saccharomyces cerevisiae using amine-reactive isobaric tagging reagents.* Mol Cell Proteomics, 2004. **3**(12): p. 1154-69.

116. Choe, L., et al., *8-plex quantitation of changes in cerebrospinal fluid protein expression in subjects undergoing intravenous immunoglobulin treatment for Alzheimer's disease.* Proteomics, 2007. **7**(20): p. 3651-60.

117. Wu, W.W., et al., *Comparative study of three proteomic quantitative methods, DIGE, cICAT, and iTRAQ, using 2D gel- or LC-MALDI TOF/TOF.* J Proteome Res, 2006. **5**(3): p. 651-8.

118. Shilov, I.V., et al., *The Paragon Algorithm, a next generation search engine that uses sequence temperature values and feature probabilities to identify peptides from tandem mass spectra.* Mol Cell Proteomics, 2007. **6**(9): p. 1638-55.

119. Washburn, M.P., D. Wolters, and J.R. Yates, 3rd, *Large-scale analysis of the yeast proteome by multidimensional protein identification technology.* Nat Biotechnol, 2001. **19**(3): p. 242-7.

120. Morris, H.R.F.a.G.E., *Quantitative Proteomics Using iTRAQ Labeling and Mass Spectrometry.* Integrative Proteomics, 2012. **Dr. Hon-Chiu Leung (Ed.)**(ISBN: 978-953-51-0070-6).

121. Bantscheff, M., et al., *Robust and sensitive iTRAQ quantification on an LTQ Orbitrap mass spectrometer.* Mol Cell Proteomics, 2008. **7**(9): p. 1702-13.

122. Zhang, Y., et al., *Optimized Orbitrap HCD for quantitative analysis of phosphopeptides.* J Am Soc Mass Spectrom, 2009. **20**(8): p. 1425-34.

123. Kocher, T., et al., *High precision quantitative proteomics using iTRAQ on an LTQ Orbitrap: a new mass spectrometric method combining the benefits of all.* J Proteome Res, 2009. **8**(10): p. 4743-52.

124. Cohen, P., *The regulation of protein function by multisite phosphorylation--a 25 year update.* Trends Biochem Sci, 2000. **25**(12): p. 596-601.

125. Manning, G., et al., *Evolution of protein kinase signaling from yeast to man.* Trends Biochem Sci, 2002. **27**(10): p. 514-20.

126. Attwood, P.V. and T. Wieland, *Nucleoside diphosphate kinase as protein histidine kinase.* Naunyn Schmiedebergs Arch Pharmacol, 2014.

127. Hunter, T. and B.M. Sefton, *Transforming gene product of Rous sarcoma virus phosphorylates tyrosine.* Proc Natl Acad Sci U S A, 1980. **77**(3): p. 1311-5.

128. Zhang, Z.Y., *Protein tyrosine phosphatases: structure and function, substrate specificity, and inhibitor development.* Annu Rev Pharmacol Toxicol, 2002. **42**: p. 209-34.

129. Tarrant, M.K. and P.A. Cole, *The chemical biology of protein phosphorylation.* Annu Rev Biochem, 2009. **78**: p. 797-825.

130. Steen, H., et al., *Phosphorylation analysis by mass spectrometry: myths, facts, and the consequences for qualitative and quantitative measurements.* Mol Cell Proteomics, 2006. **5**(1): p. 172-81.

131. Kim, J., D.G. Camp, 2nd, and R.D. Smith, *Improved detection of multi-phosphorylated peptides in the presence of phosphoric acid in liquid chromatography/mass spectrometry.* J Mass Spectrom, 2004. **39**(2): p. 208-15.

132. Liu, S., et al., *Formation of phosphopeptide-metal ion complexes in liquid chromatography/electrospray mass spectrometry and their influence on phosphopeptide detection.* Rapid Commun Mass Spectrom, 2005. **19**(19): p. 2747-56.

133. Tan, C.S., et al., *Positive selection of tyrosine loss in metazoan evolution.* Science, 2009. **325**(5948): p. 1686-8.

134. Collins, M.O., et al., *Proteomic analysis of in vivo phosphorylated synaptic proteins.* J Biol Chem, 2005. **280**(7): p. 5972-82.

135. Gronborg, M., et al., *A mass spectrometry-based proteomic approach for identification of serine/threonine-phosphorylated proteins by enrichment with phospho-specific antibodies: identification of a novel protein, Frigg, as a protein kinase A substrate.* Mol Cell Proteomics, 2002. **1**(7): p. 517-27.

136. Ficarro, S.B., et al., *Phosphoproteome analysis by mass spectrometry and its application to Saccharomyces cerevisiae.* Nat Biotechnol, 2002. **20**(3): p. 301-5.

137. Larsen, M.R., et al., *Highly selective enrichment of phosphorylated peptides from peptide mixtures using titanium dioxide microcolumns.* Mol Cell Proteomics, 2005. **4**(7): p. 873-86.

138. Beausoleil, S.A., et al., *Large-scale characterization of HeLa cell nuclear phosphoproteins.* Proc Natl Acad Sci U S A, 2004. **101**(33): p. 12130-5.

139. Pinkse, M.W., et al., *Selective isolation at the femtomole level of phosphopeptides from proteolytic digests using 2D-NanoLC-ESI-MS/MS and titanium oxide precolumns.* Anal Chem, 2004. **76**(14): p. 3935-43.

140. Li, Q.R., et al., *Effect of peptide-to-TiO2 beads ratio on phosphopeptide enrichment selectivity.* J Proteome Res, 2009. **8**(11): p. 5375-81.

141. Jensen, S.S. and M.R. Larsen, *Evaluation of the impact of some experimental procedures on different phosphopeptide enrichment techniques.* Rapid Commun Mass Spectrom, 2007. **21**(22): p. 3635-45.

142. Thingholm, T.E., et al., *SIMAC (sequential elution from IMAC), a phosphoproteomics strategy for the rapid separation of monophosphorylated from multiply phosphorylated peptides.* Mol Cell Proteomics, 2008. **7**(4): p. 661-71.

143. Rampitsch, C., et al., *The phosphoproteome of Fusarium graminearum at the onset of nitrogen starvation.* Proteomics, 2010. **10**(1): p. 124-40.

144. Fila, J. and D. Honys, *Enrichment techniques employed in phosphoproteomics.* Amino Acids, 2012. **43**(3): p. 1025-47.

145. Piubelli, C., et al., *Proteome analysis of rat polymorphonuclear leukocytes: a two-dimensional electrophoresis/mass spectrometry approach.* Electrophoresis, 2002. **23**(2): p. 298-310.

146. Lippolis, J.D. and T.A. Reinhardt, *Proteomic survey of bovine neutrophils.* Vet Immunol Immunopathol, 2005. **103**(1-2): p. 53-65.

147. Lominadze, G., et al., *Proteomic analysis of human neutrophil granules.* Mol Cell Proteomics, 2005. **4**(10): p. 1503-21.

148. Feuk-Lagerstedt, E., et al., *Lipid raft proteome of the human neutrophil azurophil granule.* Proteomics, 2007. **7**(2): p. 194-205.

149. Nebl, T., et al., *Proteomic analysis of a detergent-resistant membrane skeleton from neutrophil plasma membranes.* J Biol Chem, 2002. **277**(45): p. 43399-409.

150. Fessler, M.B., et al., *A genomic and proteomic analysis of activation of the human neutrophil by lipopolysaccharide and its mediation by p38 mitogen-activated protein kinase.* J Biol Chem, 2002. **277**(35): p. 31291-302.

151. Greenlee, K.J., et al., *Proteomic identification of in vivo substrates for matrix metalloproteinases 2 and 9 reveals a mechanism for resolution of inflammation.* J Immunol, 2006. **177**(10): p. 7312-21.

152. Liu, K.X., et al., *[Proteomics study of intestinal mucosa after ischemic preconditioning against intestinal ischemic reperfusion injury in rats].* Zhonghua Wei Chang Wai Ke Za Zhi, 2009. **12**(6): p. 598-602.

153. Liu, K.X., et al., *Proteomic analysis of intestinal ischemia/reperfusion injury and ischemic preconditioning in rats reveals the protective role of aldose reductase.* Proteomics, 2010. **10**(24): p. 4463-75.

154. de Souza Castro, M., et al., *Proteome analysis of resting human neutrophils.* Protein Pept Lett, 2006. **13**(5): p. 481-7.

155. Teles, L.M., et al., *Comparison of the neutrophil proteome in trauma patients and normal controls.* Protein Pept Lett, 2012. **19**(6): p. 663-72.

156. Powell, D.W., et al., *Proteomic identification of 14-3-3zeta as a mitogen-activated protein kinase-activated protein kinase 2 substrate: role in dimer formation and ligand binding.* Mol Cell Biol, 2003. **23**(15): p. 5376-87.

157. Singh, S., et al., *Identification of the p16-Arc subunit of the Arp 2/3 complex as a substrate of MAPK-activated protein kinase 2 by proteomic analysis.* J Biol Chem, 2003. **278**(38): p. 36410-7.

158. Lominadze, G., et al., *Myeloid-related protein-14 is a p38 MAPK substrate in human neutrophils.* J Immunol, 2005. **174**(11): p. 7257-67.

159. Pacquelet, S., et al., *Cross-talk between IRAK-4 and the NADPH oxidase.* Biochem J, 2007. **403**(3): p. 451-61.

160. Boldt, K., et al., *FPRL-1 induces modifications of migration-associated proteins in human neutrophils.* Proteomics, 2006. **6**(17): p. 4790-9.

161. Dang, P.M., et al., *A specific p47phox -serine phosphorylated by convergent MAPKs mediates neutrophil NADPH oxidase priming at inflammatory sites.* J Clin Invest, 2006. **116**(7): p. 2033-43.

162. Fukuda, M., *Versatile role of Rab27 in membrane trafficking: focus on the Rab27 effector families.* J Biochem, 2005. **137**(1): p. 9-16.

163. Ortega-Perez, I., et al., *c-Jun N-terminal kinase (JNK) positively regulates NFATc2 transactivation through phosphorylation within the N-terminal regulatory domain.* J Biol Chem, 2005. **280**(21): p. 20867-78.

164. Yamamoto, S., et al., *The role of tumor necrosis factor-alpha and interleukin-1beta in ischemia-reperfusion injury of the rat small intestine.* J Surg Res, 2001. **99**(1): p. 134-41.

165. Parks, D.A. and D.N. Granger, *Contributions of ischemia and reperfusion to mucosal lesion formation.* Am J Physiol, 1986. **250**(6 Pt 1): p. G749-53.

166. Collard, C.D. and S. Gelman, *Pathophysiology, clinical manifestations, and prevention of ischemia-reperfusion injury.* Anesthesiology, 2001. **94**(6): p. 1133-8.

167. Koksoy, C., et al., *Role of tumour necrosis factor in lung injury caused by intestinal ischaemia-reperfusion.* Br J Surg, 2001. **88**(3): p. 464-8.

168. Anaya-Prado, R., et al., *Ischemia/reperfusion injury.* J Surg Res, 2002. **105**(2): p. 248-58.

169. Blaisdell, F.W., *The pathophysiology of skeletal muscle ischemia and the reperfusion syndrome: a review.* Cardiovasc Surg, 2002. **10**(6): p. 620-30.

170. Kabaroudis, A., et al., *Metabolic alterations of skeletal muscle tissue after prolonged acute ischemia and reperfusion.* J Invest Surg, 2003. **16**(4): p. 219-28.

171. Yassin, M.M., et al., *Lower limb ischemia-reperfusion injury triggers a systemic inflammatory response and multiple organ dysfunction.* World J Surg, 2002. **26**(1): p. 115-21.

172. Castro, M.S., E.M. Cilli, and W. Fontes, *Combinatorial synthesis and directed evolution applied to the production of alpha-helix forming antimicrobial peptides analogues.* Curr Protein Pept Sci, 2006. **7**(6): p. 473-8.

173. Castro, M.S., et al., *Hylin a1, the first cytolytic peptide isolated from the arboreal South American frog Hypsiboas albopunctatus ("spotted treefrog").* Peptides, 2009. **30**(2): p. 291-6.

174. Abrahao, M.S., et al., *Biochemical and morphological evaluation of ischemia-reperfusion injury in rat small bowel modulated by ischemic preconditioning.* Transplant Proc, 2004. **36**(4): p. 860-2.

175. Mallick, I.H., et al., *Ischemia-reperfusion injury of the intestine and protective strategies against injury.* Dig Dis Sci, 2004. **49**(9): p. 1359-77.

176. Morris, C.F., M.S. Castro, and W. Fontes, *Neutrophil proteome: lessons from different standpoints.* Protein Pept Lett, 2008. **15**(9): p. 995-1001.

177. Houston, J.B. and D.J. Carlile, *Incorporation of in vitro drug metabolism data into physiologically-based pharmacokinetic models.* Toxicol In Vitro, 1997. **11**(5): p. 473-8.

178. Campbell, T.W. *Hematology of lower vertebrates*. in *In: Proceedings of the 55th Annual Meeting of the American College of Veterinary Pathologists (ACVPC) & 39th Annual Meeting of the American Society of Clinical Pathology (ASVCP).* USA: ACVP and ASVCP.

179. Di Giulio, R.a.D.H., *The Toxicology of Fishes.* Crc. Press, 2008: p. 1101.

180. E. M. S, R.-C., et al., *Comparative Study of Four Isolation Procedures to Obtain Rat Neutrophils.* Comparative Clinical Pathology, 2014. **11**: p. 71-76.

181. Wisniewski, J.R., et al., *Universal sample preparation method for proteome analysis.* Nat Methods, 2009. **6**(5): p. 359-62.

182. Laursen, I., et al., *Characterisation of the 1st SSI purified MBL standard.* Clin Chim Acta, 2008. **395**(1-2): p. 159-61.

183. Engholm-Keller, K., et al., *Multidimensional strategy for sensitive phosphoproteomics incorporating protein prefractionation combined with SIMAC, HILIC, and TiO(2) chromatography applied to proximal EGF signaling.* J Proteome Res, 2011. **10**(12): p. 5383-97.

184. Larsen, M.R., et al., *Exploring the sialiome using titanium dioxide chromatography and mass spectrometry.* Mol Cell Proteomics, 2007. **6**(10): p. 1778-87.

185. Melo-Braga, M.N., et al., *Comprehensive quantitative comparison of the membrane proteome, phosphoproteome, and sialiome of human embryonic and neural stem cells.* Mol Cell Proteomics, 2014. **13**(1): p. 311-28.

186. McNulty, D.E. and R.S. Annan, *Hydrophilic interaction chromatography reduces the complexity of the phosphoproteome and improves global phosphopeptide isolation and detection.* Mol Cell Proteomics, 2008. **7**(5): p. 971-80.

187. Spivak, M., et al., *Improvements to the percolator algorithm for Peptide identification from shotgun proteomics data sets.* J Proteome Res, 2009. **8**(7): p. 3737-45.

188. Taverner, T., et al., *DanteR: an extensible R-based tool for quantitative analysis of -omics data.* Bioinformatics, 2012. **28**(18): p. 2404-6.

189. Smyth, G.K., *Limma: linear models for microarray data.*, in *Bioinformatics and Computational Biology Solutions using R and Bioconductor*. 2005, Springer: New York.

190. Breitling, R., et al., *Rank products: a simple, yet powerful, new method to detect differentially regulated genes in replicated microarray experiments.* FEBS Lett, 2004. **573**(1-3): p. 83-92.

191. Schwammle, V., I.R. Leon, and O.N. Jensen, *Assessment and improvement of statistical tools for comparative proteomics analysis of sparse data sets with few experimental replicates.* J Proteome Res, 2013. **12**(9): p. 3874-83.

192. Storey, J.D., *A direct approach to false discovery rates.* J. R. Statist. Soc. B.,, 2002. **64**(3): p. 479-498.

193. Futschik, M.E. and B. Carlisle, *Noise-robust soft clustering of gene expression time-course data.* J Bioinform Comput Biol, 2005. **3**(4): p. 965-88.

194. Bezdek, J.C., *Cluster validity with fuzzy sets.* J. Cybernetics, 1973. **3**(3): p. 58-73.

195. Schwammle, V. and O.N. Jensen, *A simple and fast method to determine the parameters for fuzzy c-means cluster analysis.* Bioinformatics, 2010. **26**(22): p. 2841-8.

196. Conesa, A., et al., *Blast2GO: a universal tool for annotation, visualization and analysis in functional genomics research.* Bioinformatics, 2005. **21**(18): p. 3674-6.

197. Wang, J., et al., *WEB-based GEne SeT AnaLysis Toolkit (WebGestalt): update 2013.* Nucleic Acids Res, 2013. **41**(Web Server issue): p. W77-83.

198. Glaab, E., et al., *EnrichNet: network-based gene set enrichment analysis.* Bioinformatics, 2012. **28**(18): p. i451-i457.

199. Franceschini, A., et al., *STRING v9.1: protein-protein interaction networks, with increased coverage and integration.* Nucleic Acids Res, 2013. **41**(Database issue): p. D808-15.

200. Deitch, E.A., K.N. Landry, and J.C. McDonald, *Postburn impaired cell-mediated immunity may not be due to lazy lymphocytes but to overwork.* Ann Surg, 1985. **201**(6): p. 793-802.

201. Hotchkiss, R.S., et al., *Prevention of lymphocyte cell death in sepsis improves survival in mice.* Proc Natl Acad Sci U S A, 1999. **96**(25): p. 14541-6.

202. Deirmengian, G.K., et al., *Leukocytosis is common after total hip and knee arthroplasty.* Clin Orthop Relat Res, 2011. **469**(11): p. 3031-6.

203. Grau, A.J., et al., *Leukocyte count as an independent predictor of recurrent ischemic events.* Stroke, 2004. **35**(5): p. 1147-52.

204. Lantos, J., et al., *Leukocyte CD11a expression and granulocyte activation during experimental myocardial ischemia and long lasting reperfusion.* Exp Clin Cardiol, 2001. **6**(2): p. 72-6.

205. Grau, A.J., et al., *Granulocyte adhesion, deformability, and superoxide formation in acute stroke.* Stroke, 1992. **23**(1): p. 33-9.

206. Frangogiannis, N.G., C.W. Smith, and M.L. Entman, *The inflammatory response in myocardial infarction.* Cardiovasc Res, 2002. **53**(1): p. 31-47.

207. Hart, M.L., et al., *Gastrointestinal ischemia-reperfusion injury is lectin complement pathway dependent without involving C1q.* J Immunol, 2005. **174**(10): p. 6373-80.

208. Matthijsen, R.A., et al., *Myeloperoxidase is critically involved in the induction of organ damage after renal ischemia reperfusion.* Am J Pathol, 2007. **171**(6): p. 1743-52.

209. Szokoly, M., et al., *Hematological and hemostaseological alterations after warm and cold limb ischemia-reperfusion in a canine model.* Acta Cir Bras, 2009. **24**(5): p. 338-46.

210. Jackson, P.G. and M.T. Raiji, *Evaluation and management of intestinal obstruction.* Am Fam Physician, 2011. **83**(2): p. 159-65.

211. Dogdu, O., et al., *Assessment of red cell distribution width (RDW) in patients with coronary artery ectasia.* Clin Appl Thromb Hemost, 2012. **18**(2): p. 211-4.

212. Del Conde, I., et al., *Platelet activation leads to activation and propagation of the complement system.* J Exp Med, 2005. **201**(6): p. 871-9.

213. Hamad, O.A., et al., *Complement component C3 binds to activated normal platelets without preceding proteolytic activation and promotes binding to complement receptor 1.* J Immunol, 2010. **184**(5): p. 2686-92.

214. Lapchak, P.H., et al., *Platelets orchestrate remote tissue damage after mesenteric ischemia-reperfusion.* Am J Physiol Gastrointest Liver Physiol, 2012. **302**(8): p. G888-97.

215. Liu, S., et al., *Mean platelet volume: a controversial marker of disease activity in Crohn's disease.* Eur J Med Res, 2012. **17**: p. 27.

216. Ntaios, G., et al., *Mean platelet volume in the early phase of acute ischemic stroke is not associated with severity or functional outcome.* Cerebrovasc Dis, 2010. **29**(5): p. 484-9.

217. Manning, G., et al., *Evolution of protein kinase signaling from yeast to man.* (0968-0004 (Print)).

218. Manning, G., et al., *The protein kinase complement of the human genome.* (1095-9203 (Electronic)).

219. Hunter, T., *Protein kinases and phosphatases: the yin and yang of protein phosphorylation and signaling.* (0092-8674 (Print)).

220. Schlessinger, J., *Cell signaling by receptor tyrosine kinases.* (0092-8674 (Print)).

221. Macek, B., et al., *The serine/threonine/tyrosine phosphoproteome of the model bacterium Bacillus subtilis.* (1535-9476 (Print)).

222. Olsen, J.V., et al., *Global, in vivo, and site-specific phosphorylation dynamics in signaling networks.* (0092-8674 (Print)).

223. Hunter T Fau - Sefton, B.M. and B.M. Sefton, *Transforming gene product of Rous sarcoma virus phosphorylates tyrosine.* (0027-8424 (Print)).

224. Lundby, A., et al., *Quantitative maps of protein phosphorylation sites across 14 different rat organs and tissues.* (2041-1723 (Electronic)).

225. el Benna, J., J.M. Ruedi, and B.M. Babior, *Cytosolic guanine nucleotide-binding protein Rac2 operates in vivo as a component of the neutrophil respiratory burst oxidase. Transfer of Rac2 and the cytosolic oxidase components p47phox and p67phox to the submembranous actin cytoskeleton during oxidase activation.* J Biol Chem, 1994. **269**(9): p. 6729-34.

226. Nauseef, W.M., et al., *Assembly of the neutrophil respiratory burst oxidase. Protein kinase C promotes cytoskeletal and membrane association of cytosolic oxidase components.* J Biol Chem, 1991. **266**(9): p. 5911-7.

227. Jethwaney, D., et al., *Proteomic analysis of plasma membrane and secretory vesicles from human neutrophils.* Proteome Sci, 2007. **5**: p. 12.

228. Xu, P., et al., *Subproteome analysis of the neutrophil cytoskeleton.* Proteomics, 2009. **9**(7): p. 2037-49.

229. Fischer, G. and H. Bang, *The refolding of urea-denatured ribonuclease A is catalyzed by peptidyl-prolyl cis-trans isomerase.* Biochim Biophys Acta, 1985. **828**(1): p. 39-42.

230. Zhang, B., et al., *[The role of CyPA in chemotaxis of neutrophil in rheumatoid arthritis and secretion of interleukin-8].* Xi Bao Yu Fen Zi Mian Yi Xue Za Zhi, 2009. **25**(5): p. 423-5.

231. Gruber, C.W., et al., *Protein disulfide isomerase: the structure of oxidative folding.* Trends Biochem Sci, 2006. **31**(8): p. 455-64.

232. Laurindo, F.R., et al., *Novel role of protein disulfide isomerase in the regulation of NADPH oxidase activity: pathophysiological implications in vascular diseases.* Antioxid Redox Signal, 2008. **10**(6): p. 1101-13.

233. Hahm, E., et al., *Extracellular protein disulfide isomerase regulates ligand-binding activity of alphaMbeta2 integrin and neutrophil recruitment during vascular inflammation.* Blood, 2013. **121**(19): p. 3789-800, s1-15.

234. Daryadel, A., et al., *Apoptotic neutrophils release macrophage migration inhibitory factor upon stimulation with tumor necrosis factor-alpha.* J Biol Chem, 2006. **281**(37): p. 27653-61.

235. Jakobsson, P.J., et al., *Identification of human prostaglandin E synthase: a microsomal, glutathione-dependent, inducible enzyme, constituting a potential novel drug target.* Proc Natl Acad Sci U S A, 1999. **96**(13): p. 7220-5.

236. Tanioka, T., et al., *Molecular identification of cytosolic prostaglandin E2 synthase that is functionally coupled with cyclooxygenase-1 in immediate prostaglandin E2 biosynthesis.* J Biol Chem, 2000. **275**(42): p. 32775-82.

237. Tanikawa, N., et al., *Identification and characterization of a novel type of membrane-associated prostaglandin E synthase.* Biochem Biophys Res Commun, 2002. **291**(4): p. 884-9.

238. Murakami, M., et al., *Regulation of prostaglandin E2 biosynthesis by inducible membrane-associated prostaglandin E2 synthase that acts in concert with cyclooxygenase-2.* J Biol Chem, 2000. **275**(42): p. 32783-92.

239. Mosca, M., et al., *Regulation of the microsomal prostaglandin E synthase-1 in polarized mononuclear phagocytes and its constitutive expression in neutrophils.* J Leukoc Biol, 2007. **82**(2): p. 320-6.

240. Gangloff, J. and G. Dirheimer, *Studies on aspartyl-tRNA synthetase from Baker's yeast. I. Purification and properties of the enzyme.* Biochim Biophys Acta, 1973. **294**(1): p. 263-72.

241. Fraser, M.J., *Glycyl-RNA synthetase of rat liver: partial purification and effects of some metal ions on its activity.* Can J Biochem Physiol, 1963. **41**: p. 1123-33.

242. Norton, S.J., *PURIFICATION AND PROPERTIES OF THE PROLYL RNA SYNTHETASE OF ESCHERICHIA COLI.* Arch Biochem Biophys, 1964. **106**: p. 147-52.

243. Ravel, J.M., et al., *GLUTAMYL AND GLUTAMINYL RIBONUCLEIC ACID SYNTHETASES OF ESCHERICHIA COLI W. SEPARATION, PROPERTIES, AND STIMULATION OF ADENOSINE TRIPHOSPHATE-PYROPHOSPHATE EXCHANGE BY ACCEPTOR RIBONUCLEIC ACID.* J Biol Chem, 1965. **240**: p. 432-8.

244. Stulberg, M.P., *The isolation and properties of phenylalanyl ribonucleic acid synthetase from Escherichia coli B.* J Biol Chem, 1967. **242**(5): p. 1060-4.

245. Allen, E.H., E. Glassman, and R.S. Schweet, *Incorporation of amino acids into ribonucleic acid. I. The role of activating enzymes.* J Biol Chem, 1960. **235**: p. 1061-7.

246. Pickart, C.M. and M.J. Eddins, *Ubiquitin: structures, functions, mechanisms.* Biochim Biophys Acta, 2004. **1695**(1-3): p. 55-72.

247. Joazeiro, C.A. and A.M. Weissman, *RING finger proteins: mediators of ubiquitin ligase activity.* Cell, 2000. **102**(5): p. 549-52.

248. Petroski, M.D. and R.J. Deshaies, *Function and regulation of cullin-RING ubiquitin ligases.* Nat Rev Mol Cell Biol, 2005. **6**(1): p. 9-20.

249. Simmer, J.P., et al., *Mammalian carbamyl phosphate synthetase (CPS). DNA sequence and evolution of the CPS domain of the Syrian hamster multifunctional protein CAD.* J Biol Chem, 1990. **265**(18): p. 10395-402.

250. Lewis, J.P., D. Iyer, and C. Anaya-Bergman, *Adaptation of Porphyromonas gingivalis to microaerophilic conditions involves increased consumption of formate and reduced utilization of lactate.* Microbiology, 2009. **155**(Pt 11): p. 3758-74.

251. Honzatko, R.B. and H.J. Fromm, *Structure-function studies of adenylosuccinate synthetase from Escherichia coli.* Arch Biochem Biophys, 1999. **370**(1): p. 1-8.

252. Haines, R.J., L.C. Pendleton, and D.C. Eichler, *Argininosuccinate synthase: at the center of arginine metabolism.* Int J Biochem Mol Biol, 2011. **2**(1): p. 8-23.

253. Schendel, F.J., et al., *Formylglycinamide ribonucleotide synthetase from Escherichia coli: cloning, sequencing, overproduction, isolation, and characterization.* Biochemistry, 1989. **28**(6): p. 2459-71.

254. Silber, R., V.G. Malathi, and J. Hurwitz, *Purification and properties of bacteriophage T4-induced RNA ligase.* Proc Natl Acad Sci U S A, 1972. **69**(10): p. 3009-13.

255. Vaillancourt, M., et al., *The Src homology 2-containing inositol 5-phosphatase 1 (SHIP1) is involved in CD32a signaling in human neutrophils.* Cell Signal, 2006. **18**(11): p. 2022-32.

256. Toker, A., *The synthesis and cellular roles of phosphatidylinositol 4,5-bisphosphate.* Curr Opin Cell Biol, 1998. **10**(2): p. 254-61.

257. Noda, Y., et al., *Phosphatidylinositol 4-phosphate 5-kinase alpha (PIPKalpha) regulates neuronal microtubule depolymerase kinesin, KIF2A and suppresses elongation of axon branches.* Proc Natl Acad Sci U S A, 2012. **109**(5): p. 1725-30.

258. Coppolino, M.G., et al., *Inhibition of phosphatidylinositol-4-phosphate 5-kinase Ialpha impairs localized actin remodeling and suppresses phagocytosis.* J Biol Chem, 2002. **277**(46): p. 43849-57.

259. Rincon, E., et al., *Diacylglycerol kinase zeta: at the crossroads of lipid signaling and protein complex organization.* Prog Lipid Res, 2012. **51**(1): p. 1-10.

260. Chen, M.Z., et al., *Oxidative stress decreases phosphatidylinositol 4,5-bisphosphate levels by deactivating phosphatidylinositol- 4-phosphate 5-kinase beta in a Syk-dependent manner.* J Biol Chem, 2009. **284**(35): p. 23743-53.

261. Lacalle, R.A., et al., *Type I phosphatidylinositol 4-phosphate 5-kinase controls neutrophil polarity and directional movement.* J Cell Biol, 2007. **179**(7): p. 1539-53.

262. Manes, S., et al., *An isoform-specific PDZ-binding motif targets type I PIP5 kinase beta to the uropod and controls polarization of neutrophil-like HL60 cells.* Faseb j, 2010. **24**(9): p. 3381-92.

263. Paone, G., et al., *ADP-ribosyltransferase-specific modification of human neutrophil peptide-1.* J Biol Chem, 2006. **281**(25): p. 17054-60.

264. Cardenas, M.L., A. Cornish-Bowden, and T. Ureta, *Evolution and regulatory role of the hexokinases.* Biochim Biophys Acta, 1998. **1401**(3): p. 242-64.

265. Wilson, J.E., *Hexokinases.* Rev Physiol Biochem Pharmacol, 1995. **126**: p. 65-198.

266. Rijksen, G., et al., *Compartmentation of hexokinase in human blood cells. Characterization of soluble and particulate enzymes.* Biochim Biophys Acta, 1982. **719**(3): p. 431-7.

267. Federzoni, E.A., et al., *PU.1 is linking the glycolytic enzyme HK3 in neutrophil differentiation and survival of APL cells.* Blood, 2012. **119**(21): p. 4963-70.

268. Zarbock, A. and K. Ley, *Protein tyrosine kinases in neutrophil activation and recruitment.* Arch Biochem Biophys, 2011. **510**(2): p. 112-9.

269. Fiedler, K., et al., *Neutrophil development and function critically depend on Bruton tyrosine kinase in a mouse model of X-linked agammaglobulinemia.* Blood, 2011. **117**(4): p. 1329-39.

270. Ding, J., et al., *The renaturable 69- and 63-kDa protein kinases that undergo rapid activation in chemoattractant-stimulated guinea pig neutrophils are p21-activated kinases.* J Biol Chem, 1996. **271**(40): p. 24869-73.

271. Huang, R., et al., *Neutrophils stimulated with a variety of chemoattractants exhibit rapid activation of p21-activated kinases (Paks): separate signals are required for activation and inactivation of paks.* Mol Cell Biol, 1998. **18**(12): p. 7130-8.

272. Manser, E., et al., *A brain serine/threonine protein kinase activated by Cdc42 and Rac1*. Nature, 1994. **367**(6458): p. 40-6.

273. Kumar, R. and R.K. Vadlamudi, *Emerging functions of p21-activated kinases in human cancer cells.* J Cell Physiol, 2002. **193**(2): p. 133-44.

274. Stokoe, D., et al., *MAPKAP kinase-2; a novel protein kinase activated by mitogen-activated protein kinase.* Embo j, 1992. **11**(11): p. 3985-94.

275. Zu, Y.L., et al., *Activation of MAP kinase-activated protein kinase 2 in human neutrophils after phorbol ester or fMLP peptide stimulation.* Blood, 1996. **87**(12): p. 5287-96.

276. Gaines, P., et al., *A cascade of Ca(2+)/calmodulin-dependent protein kinases regulates the differentiation and functional activation of murine neutrophils.* Exp Hematol, 2008. **36**(7): p. 832-44.

277. Johnson, G.L. and R. Lapadat, *Mitogen-activated protein kinase pathways mediated by ERK, JNK, and p38 protein kinases.* Science, 2002. **298**(5600): p. 1911-2.

278. Ananthakrishnan, R., et al., *Aldose reductase mediates myocardial ischemia-reperfusion injury in part by opening mitochondrial permeability transition pore.* Am J Physiol Heart Circ Physiol, 2009. **296**(2): p. H333-41.

279. Kaneko, M., et al., *Aldose reductase and AGE-RAGE pathways: key players in myocardial ischemic injury.* Ann N Y Acad Sci, 2005. **1043**: p. 702-9.

280. Hwang, Y.C., et al., *Central role for aldose reductase pathway in myocardial ischemic injury.* Faseb j, 2004. **18**(11): p. 1192-9.

281. Ramana, K.V., et al., *Endotoxin-induced cardiomyopathy and systemic inflammation in mice is prevented by aldose reductase inhibition.* Circulation, 2006. **114**(17): p. 1838-46.

282. Ravindranath, T.M., et al., *Novel role for aldose reductase in mediating acute inflammatory responses in the lung.* J Immunol, 2009. **183**(12): p. 8128-37.

283. Boothpur, R. and D.C. Brennan, *Didactic lessons from the serum lactate dehydrogenase posttransplant: a clinical vignette.* Am J Transplant, 2008. **8**(4): p. 862-5.

284. Haslett, C., *Granulocyte apoptosis and inflammatory disease.* Br Med Bull, 1997. **53**(3): p. 669-83.

285. Paclet, M.H., et al., *Regulation of phagocyte NADPH oxidase activity: identification of two cytochrome b558 activation states.* Faseb j, 2007. **21**(4): p. 1244-55.

286. Baillet, A., et al., *Coupling of 6-phosphogluconate dehydrogenase with NADPH oxidase in neutrophils: Nox2 activity regulation by NADPH availability.* Faseb j, 2011. **25**(7): p. 2333-43.

287. Klebanoff, S.J., *Myeloperoxidase.* Proc Assoc Am Physicians, 1999. **111**(5): p. 383-9.

288. Winterbourn, C.C., *Biological reactivity and biomarkers of the neutrophil oxidant, hypochlorous acid.* Toxicology, 2002. **181-182**: p. 223-7.

289. Klebanoff, S.J., *Myeloperoxidase: friend and foe.* J Leukoc Biol, 2005. **77**(5): p. 598-625.

290. Lau, D., et al., *Myeloperoxidase mediates neutrophil activation by association with CD11b/CD18 integrins.* Proc Natl Acad Sci U S A, 2005. **102**(2): p. 431-6.

291. Murray, J.J. and A.R. Brash, *Rabbit reticulocyte lipoxygenase catalyzes specific 12(S) and 15(S) oxygenation of arachidonoyl-phosphatidylcholine.* Arch Biochem Biophys, 1988. **265**(2): p. 514-23.

292. Nadel, J.A., et al., *Immunocytochemical localization of arachidonate 15-lipoxygenase in erythrocytes, leukocytes, and airway cells.* J Clin Invest, 1991. **87**(4): p. 1139-45.

293. Vane, J.R. and R.M. Botting, *Mechanism of action of anti-inflammatory drugs.* Scand J Rheumatol Suppl, 1996. **102**: p. 9-21.

294. Maloney, C.G., et al., *Inflammatory agonists induce cyclooxygenase type 2 expression by human neutrophils.* J Immunol, 1998. **160**(3): p. 1402-10.

295. Pouliot, M., et al., *Expression and activity of prostaglandin endoperoxide synthase-2 in agonist-activated human neutrophils.* Faseb j, 1998. **12**(12): p. 1109-23.

296. Niiro, H., et al., *MAP kinase pathways as a route for regulatory mechanisms of IL-10 and IL-4 which inhibit COX-2 expression in human monocytes.* Biochem Biophys Res Commun, 1998. **250**(2): p. 200-5.

297. Nagano, S., et al., *Molecular mechanisms of lipopolysaccharide-induced cyclooxygenase-2 expression in human neutrophils: involvement of the mitogen-activated protein kinase pathway and regulation by anti-inflammatory cytokines.* Int Immunol, 2002. **14**(7): p. 733-40.

298. Yasui, K., et al., *Superoxide dismutase (SOD) as a potential inhibitory mediator of inflammation via neutrophil apoptosis.* Free Radic Res, 2005. **39**(7): p. 755-62.

299. Break, T.J., et al., *Extracellular superoxide dismutase inhibits innate immune responses and clearance of an intracellular bacterial infection.* J Immunol, 2012. **188**(7): p. 3342-50.

300. Meneshian, A. and G.B. Bulkley, *The physiology of endothelial xanthine oxidase: from urate catabolism to reperfusion injury to inflammatory signal transduction.* Microcirculation, 2002. **9**(3): p. 161-75.

301. Harrison, R., *Structure and function of xanthine oxidoreductase: where are we now?* Free Radic Biol Med, 2002. **33**(6): p. 774-97.

302. Phan, S.H., et al., *Mechanism of neutrophil-induced xanthine dehydrogenase to xanthine oxidase conversion in endothelial cells: evidence of a role for elastase.* Am J Respir Cell Mol Biol, 1992. **6**(3): p. 270-8.

303. Sirover, M.A., *New insights into an old protein: the functional diversity of mammalian glyceraldehyde-3-phosphate dehydrogenase.* Biochim Biophys Acta, 1999. **1432**(2): p. 159-84.

304. Hessler, R.J., et al., *Identification of glyceraldehyde-3-phosphate dehydrogenase as a Ca2+-dependent fusogen in human neutrophil cytosol.* J Leukoc Biol, 1998. **63**(3): p. 331-6.

305. Molenaar, R., et al., *Lymph node stromal cells support dendritic cell-induced gut-homing of T cells.* J Immunol, 2009. **183**(10): p. 6395-402.

306. Elias, K.M., et al., *Retinoic acid inhibits Th17 polarization and enhances FoxP3 expression through a Stat-3/Stat-5 independent signaling pathway.* Blood, 2008. **111**(3): p. 1013-20.

307. Massacand, J.C., et al., *Intestinal bacteria condition dendritic cells to promote IgA production.* PLoS One, 2008. **3**(7): p. e2588.

308. Mucida, D., et al., *Reciprocal TH17 and regulatory T cell differentiation mediated by retinoic acid.* Science, 2007. **317**(5835): p. 256-60.

309. Belinsky, M. and A.K. Jaiswal, *NAD(P)H:quinone oxidoreductase1 (DT-diaphorase) expression in normal and tumor tissues.* Cancer Metastasis Rev, 1993. **12**(2): p. 103-17.

310. Joseph, P., et al., *NAD(P)H:quinone oxidoreductase1 (DT-diaphorase): expression, regulation, and role in cancer.* Oncol Res, 1994. **6**(10-11): p. 525-32.

311. Workman, P., *Enzyme-directed bioreductive drug development revisited: a commentary on recent progress and future prospects with emphasis on quinone anticancer agents and quinone metabolizing enzymes, particularly DT-diaphorase.* Oncol Res, 1994. **6**(10-11): p. 461-75.

312. Cresteil, T. and A.K. Jaiswal, *High levels of expression of the NAD(P)H:quinone oxidoreductase (NQO1) gene in tumor cells compared to normal cells of the same origin.* Biochem Pharmacol, 1991. **42**(5): p. 1021-7.

313. Cohen, H.J., et al., *The role of glutathione reductase in maintaining human granulocyte function and sensitivity to exogenous H2O2.* Blood, 1987. **69**(2): p. 493-500.

314. Strauss, R.R., et al., *The role of the phagocyte in host-parasite interactions. XIX. Leukocytic glutathione reductase and its involvement in phagocytosis.* Arch Biochem Biophys, 1969. **135**(1): p. 265-71.

315. Yan, J., et al., *Glutathione reductase facilitates host defense by sustaining phagocytic oxidative burst and promoting the development of neutrophil extracellular traps.* J Immunol, 2012. **188**(5): p. 2316-27.

316. Sun, Q.A., et al., *Reaction mechanism and regulation of mammalian thioredoxin/glutathione reductase.* Biochemistry, 2005. **44**(44): p. 14528-37.

317. Thom, S.R., et al., *Thioredoxin reductase linked to cytoskeleton by focal adhesion kinase reverses actin S-nitrosylation and restores neutrophil beta(2) integrin function.* J Biol Chem, 2012. **287**(36): p. 30346-57.

318. Zhang, J.D. and S. Wiemann, *KEGGgraph: a graph approach to KEGG PATHWAY in R and bioconductor.* Bioinformatics, 2009. **25**(11): p. 1470-1.

319. Wool, I.G., *Extraribosomal functions of ribosomal proteins.* Trends Biochem Sci, 1996. **21**(5): p. 164-5.

320. Wool, I.G., Y.L. Chan, and A. Gluck, *Structure and evolution of mammalian ribosomal proteins.* Biochem Cell Biol, 1995. **73**(11-12): p. 933-47.

321. Yamamoto, T., *Molecular mechanism of monocyte predominant infiltration in chronic inflammation: mediation by a novel monocyte chemotactic factor, S19 ribosomal protein dimer.* Pathol Int, 2000. **50**(11): p. 863-71.

322. Chester, K.A., et al., *Identification of a human ribosomal protein mRNA with increased expression in colorectal tumours.* Biochim Biophys Acta, 1989. **1009**(3): p. 297-300.

323. Bevort, M. and H. Leffers, *Down regulation of ribosomal protein mRNAs during neuronal differentiation of human NTERA2 cells.* Differentiation, 2000. **66**(2-3): p. 81-92.

324. Grabowski, D.T., et al., *Drosophila AP3, a presumptive DNA repair protein, is homologous to human ribosomal associated protein P0.* Nucleic Acids Res, 1991. **19**(15): p. 4297.

325. Kim, J., et al., *Implication of mammalian ribosomal protein S3 in the processing of DNA damage.* J Biol Chem, 1995. **270**(23): p. 13620-9.

326. Berghofer-Hochheimer, Y., et al., *L7 protein is a coregulator of vitamin D receptor-retinoid X receptor-mediated transactivation.* J Cell Biochem, 1998. **69**(1): p. 1-12.

327. Neumann, F. and U. Krawinkel, *Constitutive expression of human ribosomal protein L7 arrests the cell cycle in G1 and induces apoptosis in Jurkat T-lymphoma cells.* Exp Cell Res, 1997. **230**(2): p. 252-61.

328. Naora, H., et al., *Altered cellular responses by varying expression of a ribosomal protein gene: sequential coordination of enhancement and suppression of ribosomal protein S3a gene expression induces apoptosis.* J Cell Biol, 1998. **141**(3): p. 741-53.

329. Goldstone, S.D. and M.F. Lavin, *Isolation of a cDNA clone, encoding the ribosomal protein S20, downregulated during the onset of apoptosis in a human leukaemic cell line.* Biochem Biophys Res Commun, 1993. **196**(2): p. 619-23.

330. Gregory, C.D. and J.D. Pound, *Microenvironmental influences of apoptosis in vivo and in vitro.* Apoptosis, 2010. **15**(9): p. 1029-49.

331. Nishiura, H., et al., *Determination of the cross-linked residues in homo-dimerization of S19 ribosomal protein concomitant with exhibition of monocyte chemotactic activity.* Lab Invest, 1999. **79**(8): p. 915-23.

332. Nishiura, H., et al., *The role of the ribosomal protein S19 C-terminus in Gi protein-dependent alternative activation of p38 MAP kinase via the C5a receptor in HMC-1 cells.* Apoptosis, 2010. **15**(8): p. 966-81.

333. Nishiura, H., R. Zhao, and T. Yamamoto, *The role of the ribosomal protein S19 C-terminus in altering the chemotaxis of leucocytes by causing functional differences in the C5a receptor response.* J Biochem, 2011. **150**(3): p. 271-7.

334. Tang, W., et al., *A PLCbeta/PI3Kgamma-GSK3 signaling pathway regulates cofilin phosphatase slingshot2 and neutrophil polarization and chemotaxis.* Dev Cell, 2011. **21**(6): p. 1038-50.

335. Quilliam, L.A., et al., *Guanine nucleotide exchange factors: activators of the Ras superfamily of proteins.* Bioessays, 1995. **17**(5): p. 395-404.

336. Machesky, L.M., et al., *Mammalian actin-related protein 2/3 complex localizes to regions of lamellipodial protrusion and is composed of evolutionarily conserved proteins.* Biochem J, 1997. **328 (Pt 1)**: p. 105-12.

337. Daeron, M., *Fc receptor biology.* Annu Rev Immunol, 1997. **15**: p. 203-34.

338. Sanchez-Mejorada, G. and C. Rosales, *Signal transduction by immunoglobulin Fc receptors.* J Leukoc Biol, 1998. **63**(5): p. 521-33.

339. Isakov, N., *Immunoreceptor tyrosine-based activation motif (ITAM), a unique module linking antigen and Fc receptors to their signaling cascades.* J Leukoc Biol, 1997. **61**(1): p. 6-16.

340. Korade-Mirnics, Z. and S.J. Corey, *Src kinase-mediated signaling in leukocytes.* J Leukoc Biol, 2000. **68**(5): p. 603-13.

341. Raeder, E.M., et al., *Syk activation initiates downstream signaling events during human polymorphonuclear leukocyte phagocytosis.* J Immunol, 1999. **163**(12): p. 6785-93.

342. Cox, D., et al., *Syk tyrosine kinase is required for immunoreceptor tyrosine activation motif-dependent actin assembly*. J Biol Chem, 1996. **271**(28): p. 16597-602.

343. Botelho, R.J., et al., *Localized biphasic changes in phosphatidylinositol-4,5-bisphosphate at sites of phagocytosis.* J Cell Biol, 2000. **151**(7): p. 1353-68.

344. Raeder, E.M., et al., *Sphingosine blocks human polymorphonuclear leukocyte phagocytosis through inhibition of mitogen-activated protein kinase activation.* Blood, 1999. **93**(2): p. 686-93.

345. Marshall, C.J., *MAP kinase kinase kinase, MAP kinase kinase and MAP kinase.* Curr Opin Genet Dev, 1994. **4**(1): p. 82-9.

346. Cox, D., et al., *Requirements for both Rac1 and Cdc42 in membrane ruffling and phagocytosis in leukocytes.* J Exp Med, 1997. **186**(9): p. 1487-94.

347. Uchida, H., et al., *PAG3/Papalpha/KIAA0400, a GTPase-activating protein for ADP-ribosylation factor (ARF), regulates ARF6 in Fcgamma receptor-mediated phagocytosis of macrophages.* J Exp Med, 2001. **193**(8): p. 955-66.

348. May, R.C. and L.M. Machesky, *Phagocytosis and the actin cytoskeleton.* J Cell Sci, 2001. **114**(Pt 6): p. 1061-77.

349. May, R.C., et al., *Involvement of the Arp2/3 complex in phagocytosis mediated by FcgammaR or CR3.* Nat Cell Biol, 2000. **2**(4): p. 246-8.

350. Aspenstrom, P., U. Lindberg, and A. Hall, *Two GTPases, Cdc42 and Rac, bind directly to a protein implicated in the immunodeficiency disorder Wiskott-Aldrich syndrome.* Curr Biol, 1996. **6**(1): p. 70-5.

351. Lorenzi, R., et al., *Wiskott-Aldrich syndrome protein is necessary for efficient IgG-mediated phagocytosis.* Blood, 2000. **95**(9): p. 2943-6.

352. Zachariae, C.O., *Chemotactic cytokines and inflammation. Biological properties of the lymphocyte and monocyte chemotactic factors ELCF, MCAF and IL-8.* Acta Derm Venereol Suppl (Stockh), 1993. **181**: p. 1-37.

353. Benard, V., G.M. Bokoch, and B.A. Diebold, *Potential drug targets: small GTPases that regulate leukocyte function.* Trends Pharmacol Sci, 1999. **20**(9): p. 365-70.

354. Wieland, T. and C.K. Chen, *Regulators of G-protein signalling: a novel protein family involved in timely deactivation and desensitization of signalling via heterotrimeric G proteins.* Naunyn Schmiedebergs Arch Pharmacol, 1999. **360**(1): p. 14-26.

355. Park, D., et al., *Activation of phospholipase C isozymes by G protein beta gamma subunits.* J Biol Chem, 1993. **268**(7): p. 4573-6.

356. Dinauer, M.C., *Regulation of neutrophil function by Rac GTPases.* Curr Opin Hematol, 2003. **10**(1): p. 8-15.

357. Etienne-Manneville, S. and A. Hall, *Rho GTPases in cell biology.* Nature, 2002. **420**(6916): p. 629-35.

358. Welch, H.C., et al., *P-Rex1, a PtdIns(3,4,5)P3- and Gbetagamma-regulated guanine-nucleotide exchange factor for Rac.* Cell, 2002. **108**(6): p. 809-21.

359. Welch, H.C., et al., *P-Rex1 regulates neutrophil function.* Curr Biol, 2005. **15**(20): p. 1867-73.

360. Sells, M.A. and J. Chernoff, *Emerging from the Pak: the p21-activated protein kinase family.* Trends Cell Biol, 1997. **7**(4): p. 162-7.

361. Jones, S.L., et al., *Two signaling mechanisms for activation of alphaM beta2 avidity in polymorphonuclear neutrophils.* J Biol Chem, 1998. **273**(17): p. 10556-66.

362. Dharmawardhane, S., et al., *Localization of p21-activated kinase 1 (PAK1) to pseudopodia, membrane ruffles, and phagocytic cups in activated human neutrophils.* J Leukoc Biol, 1999. **66**(3): p. 521-7.

363. Turner, C.E., *Paxillin interactions.* J Cell Sci, 2000. **113 Pt 23**: p. 4139-40.

364. Borregaard, N. and T. Herlin, *Energy metabolism of human neutrophils during phagocytosis.* J Clin Invest, 1982. **70**(3): p. 550-7.

365. Fossati, G., et al., *The mitochondrial network of human neutrophils: role in chemotaxis, phagocytosis, respiratory burst activation, and commitment to apoptosis.* J Immunol, 2003. **170**(4): p. 1964-72.

366. Peachman, K.K., D.S. Lyles, and D.A. Bass, *Mitochondria in eosinophils: functional role in apoptosis but not respiration.* Proc Natl Acad Sci U S A, 2001. **98**(4): p. 1717-22.

367. Maianski, N.A., et al., *Granulocyte colony-stimulating factor inhibits the mitochondria-dependent activation of caspase-3 in neutrophils.* Blood, 2002. **99**(2): p. 672-9.

368. Maianski, N.A., D. Roos, and T.W. Kuijpers, *Tumor necrosis factor alpha induces a caspase-independent death pathway in human neutrophils.* Blood, 2003. **101**(5): p. 1987-95.

369. Pryde, J.G., et al., *Temperature-dependent arrest of neutrophil apoptosis. Failure of Bax insertion into mitochondria at 15 degrees C prevents the release of cytochrome c.* J Biol Chem, 2000. **275**(43): p. 33574-84.

370. Ogawa, S., et al., *Hypoxia-induced increased permeability of endothelial monolayers occurs through lowering of cellular cAMP levels.* Am J Physiol, 1992. **262**(3 Pt 1): p. C546-54.

371. Pfeiffer, T., S. Schuster, and S. Bonhoeffer, *Cooperation and competition in the evolution of ATP-producing pathways.* Science, 2001. **292**(5516): p. 504-7.

372. Chacko, B.K., et al., *Methods for defining distinct bioenergetic profiles in platelets, lymphocytes, monocytes, and neutrophils, and the oxidative burst from human blood.* Lab Invest, 2013. **93**(6): p. 690-700.

373. Caenepeel, S., et al., *The mouse kinome: discovery and comparative genomics of all mouse protein kinases.* Proc Natl Acad Sci U S A, 2004. **101**(32): p. 11707-12.

374. Zhu, H., et al., *Analysis of yeast protein kinases using protein chips.* Nat Genet, 2000. **26**(3): p. 283-9.

375. Johnson, S.A. and T. Hunter, *Kinomics: methods for deciphering the kinome.* Nat Methods, 2005. **2**(1): p. 17-25.

376. Lander, E.S., et al., *Initial sequencing and analysis of the human genome.* Nature, 2001. **409**(6822): p. 860-921.

377. Jurkowska, M. and J. Bal, *[Biomedical science in the era of complete sequence of human genome]*. Med Wieku Rozwoj, 2001. **5**(3): p. 197-212.

378. Alonso, A., et al., *Protein tyrosine phosphatases in the human genome.* Cell, 2004. **117**(6): p. 699-711.

379. Shi, Y., *Serine/threonine phosphatases: mechanism through structure.* Cell, 2009. **139**(3): p. 468-84.

380. Elbert, M., G. Rossi, and P. Brennwald, *The yeast par-1 homologs kin1 and kin2 show genetic and physical interactions with components of the exocytic machinery.* Mol Biol Cell, 2005. **16**(2): p. 532-49.

381. Ossipova, O., et al., *Distinct PAR-1 proteins function in different branches of Wnt signaling during vertebrate development.* Dev Cell, 2005. **8**(6): p. 829-41.

382. Cohen, D., E. Rodriguez-Boulan, and A. Musch, *Par-1 promotes a hepatic mode of apical protein trafficking in MDCK cells.* Proc Natl Acad Sci U S A, 2004. **101**(38): p. 13792-7.

383. Drewes, G., et al., *Microtubule-associated protein/microtubule affinity-regulating kinase (p110mark). A novel protein kinase that regulates tau-microtubule interactions and dynamic instability by phosphorylation at the Alzheimer-specific site serine 262.* J Biol Chem, 1995. **270**(13): p. 7679-88.

384. Drewes, G., et al., *MARK, a novel family of protein kinases that phosphorylate microtubule-associated proteins and trigger microtubule disruption.* Cell, 1997. **89**(2): p. 297-308.

385. Nishimura, I., Y. Yang, and B. Lu, *PAR-1 kinase plays an initiator role in a temporally ordered phosphorylation process that confers tau toxicity in Drosophila.* Cell, 2004. **116**(5): p. 671-82.

386. Doerflinger, H., et al., *The role of PAR-1 in regulating the polarised microtubule cytoskeleton in the Drosophila follicular epithelium.* Development, 2003. **130**(17): p. 3965-75.

387. Sun, T.Q., et al., *PAR-1 is a Dishevelled-associated kinase and a positive regulator of Wnt signalling.* Nat Cell Biol, 2001. **3**(7): p. 628-36.

388. Ducharme, N.A., et al., *MARK2/EMK1/Par-1Balpha phosphorylation of Rab11-family interacting protein 2 is necessary for the timely establishment of polarity in Madin-Darby canine kidney cells.* Mol Biol Cell, 2006. **17**(8): p. 3625-37.

389. Yoo, S.K., et al., *The role of microtubules in neutrophil polarity and migration in live zebrafish.* J Cell Sci, 2012. **125**(Pt 23): p. 5702-10.

390. Tickenbrock, L., et al., *Wnt signaling regulates transendothelial migration of monocytes.* J Leukoc Biol, 2006. **79**(6): p. 1306-13.

391. Quizi, J.L., et al., *SLK-mediated phosphorylation of paxillin is required for focal adhesion turnover and cell migration.* (1476-5594 (Electronic)).

392. Luhovy, A.Y., et al., *Regulation of the Ste20-like kinase, SLK: involvement of activation segment phosphorylation.* (1083-351X (Electronic)).

393. Cybulsky, A.V., et al., *Renal expression and activity of the germinal center kinase SK2.* Am J Physiol Renal Physiol, 2004. **286**(1): p. F16-25.

394. Cybulsky, A.V., et al., *The Ste20-like kinase SLK promotes p53 transactivation and apoptosis.* Am J Physiol Renal Physiol, 2009. **297**(4): p. F971-80.

395. Hao, W., et al., *Induction of apoptosis by the Ste20-like kinase SLK, a germinal center kinase that activates apoptosis signal-regulating kinase and p38.* (0021-9258 (Print)).

396. Blake, R.A., et al., *Src promotes PKCdelta degradation.* Cell Growth Differ, 1999. **10**(4): p. 231-41.

397. Oehler, R., et al., *Polytrauma induces increased expression of pyruvate kinase in neutrophils.* Blood, 2000. **95**(3): p. 1086-92.

398. Chanock, S.J., et al., *The respiratory burst oxidase.* J Biol Chem, 1994. **269**(40): p. 24519-22.

399. Parsons, S.A., et al., *The Fps/Fes kinase regulates leucocyte recruitment and extravasation during inflammation.* Immunology, 2007. **122**(4): p. 542-50.

400. Khajah, M., et al., *Fer kinase limits neutrophil chemotaxis toward end target chemoattractants.* J Immunol, 2013. **190**(5): p. 2208-16.

401. Chen, R.H., J. Abate C Fau - Blenis, and J. Blenis, *Phosphorylation of the c-Fos transrepression domain by mitogen-activated protein kinase and 90-kDa ribosomal S6 kinase.* (0027-8424 (Print)).

402. Schouten, G.J., et al., *IkappaB alpha is a target for the mitogen-activated 90 kDa ribosomal S6 kinase.* (0261-4189 (Print)).

403. Xing, J., M.E. Ginty Dd Fau - Greenberg, and M.E. Greenberg, *Coupling of the RAS-MAPK pathway to gene activation by RSK2, a growth factor-regulated CREB kinase.* (0036-8075 (Print)).

404. De Mesquita, D.D., et al., *p90-RSK and Akt may promote rapid phosphorylation/inactivation of glycogen synthase kinase 3 in chemoattractant-stimulated neutrophils.* (0014-5793 (Print)).

405. Pap, M. and G.M. Cooper, *Role of glycogen synthase kinase-3 in the phosphatidylinositol 3-Kinase/Akt cell survival pathway.* (0021-9258 (Print)).

406. Hauge, C., et al., *Mechanism for activation of the growth factor-activated AGC kinases by turn motif phosphorylation.* EMBO J, 2007. **26**(9): p. 2251-61.

407. Salazar, N.C., et al., *GRK2 blockade with betaARKct is essential for cardiac beta2-adrenergic receptor signaling towards increased contractility.* Cell Commun Signal, 2013. **11**: p. 64.

408. Vroon, A., C.J. Heijnen, and A. Kavelaars, *GRKs and arrestins: regulators of migration and inflammation.* J Leukoc Biol, 2006. **80**(6): p. 1214-21.

409. Nijboer, C.H., et al., *Low endogenous G-protein-coupled receptor kinase 2 sensitizes the immature brain to hypoxia-ischemia-induced gray and white matter damage.* J Neurosci, 2008. **28**(13): p. 3324-32.

410. Matsuo, Y., et al., *Role of neutrophils in radical production during ischemia and reperfusion of the rat brain: effect of neutrophil depletion on extracellular ascorbyl radical formation.* J Cereb Blood Flow Metab, 1995. **15**(6): p. 941-7.

411. Lombardi, M.S., et al., *Decreased expression and activity of G-protein-coupled receptor kinases in peripheral blood mononuclear cells of patients with rheumatoid arthritis.* FASEB J, 1999. **13**(6): p. 715-25.

412. Lombardi, M.S., et al., *Oxidative stress decreases G protein-coupled receptor kinase 2 in lymphocytes via a calpain-dependent mechanism.* Mol Pharmacol, 2002. **62**(2): p. 379-88.

413. Mohamed, A.J., et al., *Bruton's tyrosine kinase (Btk): function, regulation, and transformation with special emphasis on the PH domain.* Immunol Rev, 2009. **228**(1): p. 58-73.

414. Kang, S.W., et al., *PKCbeta modulates antigen receptor signaling via regulation of Btk membrane localization.* EMBO J, 2001. **20**(20): p. 5692-702.

415. Honda, F., et al., *The kinase Btk negatively regulates the production of reactive oxygen species and stimulation-induced apoptosis in human neutrophils.* Nat Immunol, 2012. **13**(4): p. 369-78.

416. Suzuki, K., et al., *Cytokine-specific activation of distinct mitogen-activated protein kinase subtype cascades in human neutrophils stimulated by granulocyte colony-stimulating factor, granulocyte-macrophage colony-stimulating factor, and tumor necrosis factor-alpha.* Blood, 1999. **93**(1): p. 341-9.

417. Britton, D., et al., *Quantification of pancreatic cancer proteome and phosphorylome: indicates molecular events likely contributing to cancer and activity of drug targets.* PLoS One, 2014. **9**(3): p. e90948.

418. Salvador, J.M., et al., *The autoimmune suppressor Gadd45alpha inhibits the T cell alternative p38 activation pathway.* Nat Immunol, 2005. **6**(4): p. 396-402.

419. Zhang, Y.Y., et al., *Enzymatic activity and substrate specificity of mitogen-activated protein kinase p38alpha in different phosphorylation states.* J Biol Chem, 2008. **283**(39): p. 26591-601.

420. Nick, J.A., et al., *Common and distinct intracellular signaling pathways in human neutrophils utilized by platelet activating factor and FMLP.* J Clin Invest, 1997. **99**(5): p. 975-86.

421. Mocsai, A., et al., *Kinase pathways in chemoattractant-induced degranulation of neutrophils: the role of p38 mitogen-activated protein kinase activated by Src family kinases.* J Immunol, 2000. **164**(8): p. 4321-31.

422. Detmers, P.A., et al., *Role of stress-activated mitogen-activated protein kinase (p38) in beta 2-integrin-dependent neutrophil adhesion and the adhesion-dependent oxidative burst.* J Immunol, 1998. **161**(4): p. 1921-9.

423. Lal, A.S., et al., *Activation of the neutrophil NADPH oxidase is inhibited by SB 203580, a specific inhibitor of SAPK2/p38.* Biochem Biophys Res Commun, 1999. **259**(2): p. 465-70.

424. Cui, Y.D., et al., *FMLP-induced formation of F-actin in HL60 cells is dependent on PI3-K but not on intracellular Ca2+, PKC, ERK or p38 MAPK.* Inflamm Res, 2000. **49**(12): p. 684-91.

425. Yamamori, T., et al., *Roles of p38 MAPK, PKC and PI3-K in the signaling pathways of NADPH oxidase activation and phagocytosis in bovine polymorphonuclear leukocytes.* FEBS Lett, 2000. **467**(2-3): p. 253-8.

426. Dolado, I., et al., *p38alpha MAP kinase as a sensor of reactive oxygen species in tumorigenesis.* Cancer Cell, 2007. **11**(2): p. 191-205.

427. Ruzzene, M., et al., *Regulation of c-Fgr protein kinase by c-Src kinase (CSK) and by polycationic effectors.* J Biol Chem, 1994. **269**(22): p. 15885-91.

428. Fumagalli, L., et al., *The Src family kinases Hck and Fgr regulate neutrophil responses to N-formyl-methionyl-leucyl-phenylalanine.* J Immunol, 2007. **178**(6): p. 3874-85.

429. Nijhuis, E., et al., *Src kinases regulate PKB activation and modulate cytokine and chemoattractant-controlled neutrophil functioning.* J Leukoc Biol, 2002. **71**(1): p. 115-24.

430. Scholz, G., K. Cartledge, and A.R. Dunn, *Hck enhances the adherence of lipopolysaccharide-stimulated macrophages via Cbl and phosphatidylinositol 3-kinase.* J Biol Chem, 2000. **275**(19): p. 14615-23.

431. Giagulli, C., et al., *The Src family kinases Hck and Fgr are dispensable for inside-out, chemoattractant-induced signaling regulating beta 2 integrin affinity and*

valency in neutrophils, but are required for beta 2 integrin-mediated outside-in signaling involved in sustained adhesion. J Immunol, 2006. **177**(1): p. 604-11.

432. Evangelista, V., et al., *Src family kinases mediate neutrophil adhesion to adherent platelets.* Blood, 2007. **109**(6): p. 2461-9.

433. Suzuki, T., et al., *Differential involvement of Src family kinases in Fc gamma receptor-mediated phagocytosis.* J Immunol, 2000. **165**(1): p. 473-82.

434. Wang, A.V., P.R. Scholl, and R.S. Geha, *Physical and functional association of the high affinity immunoglobulin G receptor (Fc gamma RI) with the kinases Hck and Lyn.* J Exp Med, 1994. **180**(3): p. 1165-70.

435. Zhang, J., et al., *Phosphorylation of Thr642 is an early event in the processing of newly synthesized protein kinase C beta 1 and is essential for its activation.* (0021-9258 (Print)).

436. Zhang, H., et al., *STIM1 calcium sensor is required for activation of the phagocyte oxidase during inflammation and host defense.* Blood, 2014. **123**(14): p. 2238-49.

437. El-Benna, J., et al., *p47phox, the phagocyte NADPH oxidase/NOX2 organizer: structure, phosphorylation and implication in diseases.* Exp Mol Med, 2009. **41**(4): p. 217-25.

438. Makni-Maalej, K., et al., *The TLR7/8 agonist CL097 primes N-formyl-methionyl-leucyl-phenylalanine-stimulated NADPH oxidase activation in human neutrophils: critical role of p47phox phosphorylation and the proline isomerase Pin1.* J Immunol, 2012. **189**(9): p. 4657-65.

439. Weihofen, W.A., et al., *Structures of human N-Acetylglucosamine kinase in two complexes with N-Acetylglucosamine and with ADP/glucose: insights into substrate specificity and regulation.* J Mol Biol, 2006. **364**(3): p. 388-99.

440. Zhan, X., et al., *Brief focal cerebral ischemia that simulates transient ischemic attacks in humans regulates gene expression in rat peripheral blood.* J Cereb Blood Flow Metab, 2010. **30**(1): p. 110-8.

441. Zhu, Y., et al., *Signaling via a novel integral plasma membrane pool of a serine/threonine protein kinase PRK1 in mammalian cells.* FASEB J, 2004. **18**(14): p. 1722-4.

442. Dent, P., et al., *The molecular mechanism by which insulin stimulates glycogen synthesis in mammalian skeletal muscle.* (0028-0836 (Print)).

443. Lian, J.P., et al., *Activation of p90RSK and cAMP response element binding protein in stimulated neutrophils: novel effects of the pyridinyl imidazole SB 203580 on activation of the extracellular signal-regulated kinase cascade.* J Immunol, 1999. **163**(8): p. 4527-36.

444. Zhao, Y., et al., *RSK3 encodes a novel pp90rsk isoform with a unique N-terminal sequence: growth factor-stimulated kinase function and nuclear translocation.* Mol Cell Biol, 1995. **15**(8): p. 4353-63.

445. Xing, J., et al., *Nerve growth factor activates extracellular signal-regulated kinase and p38 mitogen-activated protein kinase pathways to stimulate CREB serine 133 phosphorylation.* Mol Cell Biol, 1998. **18**(4): p. 1946-55.

446. Pasham, V., et al., *OSR1-sensitive regulation of Na+/H+ exchanger activity in dendritic cells.* Am J Physiol Cell Physiol, 2012. **303**(4): p. C416-26.

447. Hoffmann, E.K., I.H. Lambert, and S.F. Pedersen, *Physiology of cell volume regulation in vertebrates.* Physiol Rev, 2009. **89**(1): p. 193-277.

448. Lang, F., et al., *Altered cell volume regulation in ras oncogene expressing NIH fibroblasts.* Pflugers Arch, 1992. **420**(5-6): p. 424-7.

449. Pedersen, S.F., *The Na+/H+ exchanger NHE1 in stress-induced signal transduction: implications for cell proliferation and cell death.* Pflugers Arch, 2006. **452**(3): p. 249-59.

450. Henderson, L.M., J.B. Chappell, and O.T. Jones, *Internal pH changes associated with the activity of NADPH oxidase of human neutrophils. Further evidence for the presence of an H+ conducting channel.* Biochem J, 1988. **251**(2): p. 563-7.

451. Zhu, J.W., et al., *Receptor-like tyrosine phosphatases CD45 and CD148 have distinct functions in chemoattractant-mediated neutrophil migration and response to S. aureus.* Immunity, 2011. **35**(5): p. 757-69.

452. Zhu, J.W., et al., *Structurally distinct phosphatases CD45 and CD148 both regulate B cell and macrophage immunoreceptor signaling.* Immunity, 2008. **28**(2): p. 183-96.

453. Yousefi, S. and H.U. Simon, *SHP-1: a regulator of neutrophil apoptosis.* Semin Immunol, 2003. **15**(3): p. 195-9.

454. Abram, C.L., et al., *Distinct roles for neutrophils and dendritic cells in inflammation and autoimmunity in motheaten mice.* Immunity, 2013. **38**(3): p. 489-501.

455. Abu-Dayyeh, I., et al., *Leishmania-induced IRAK-1 inactivation is mediated by SHP-1 interacting with an evolutionarily conserved KTIM motif.* PLoS Negl Trop Dis, 2008. **2**(12): p. e305.

456. Nishio, M., et al., *Control of cell polarity and motility by the PtdIns(3,4,5)P3 phosphatase SHIP1.* Nat Cell Biol, 2007. **9**(1): p. 36-44.

457. Lam, P.Y., et al., *The SH2-domain-containing inositol 5-phosphatase (SHIP) limits the motility of neutrophils and their recruitment to wounds in zebrafish.* J Cell Sci, 2012. **125**(Pt 21): p. 4973-8.

458. Strassheim, D., et al., *Involvement of SHIP in TLR2-induced neutrophil activation and acute lung injury.* J Immunol, 2005. **174**(12): p. 8064-71.

459. Zeng, K., et al., *Protein phosphatase 6 regulates mitotic spindle formation by controlling the T-loop phosphorylation state of Aurora A bound to its activator TPX2.* J Cell Biol, 2010. **191**(7): p. 1315-32.

ABSTRACTS PUBLISHED

Samina Arshid, **Muhammad Tahir**, Belchor Fontes, Mariana S. Castro, Simone Sidoli, Veit Schwammle, Peter Roepstorff, Wagner Fontes,*"Quantitative proteomic analysis of rat neutrophils after intestinal ischemia reperfusion and preconditioning".* 2nd Proteomics Meeting of the Brazilian Proteomics Society jointly with the 2nd Pan American HUPO Meeting December 7th and 10th , 2014, Búzios – Rio de Janeiro – Brazil.

Fontes, W. **Tahir, M.**, Arshid, S., Montero, E., Fontes, B., Castro, M.S., Sidoli, S., Roepstorff, P. *"Quantitative proteomic analysis of rat neutrophils after intestinal ischemia and reperfusion"*. International Symposium NEUTROPHIL 2014 - May 31st - June 3rd , 2014, Montréal - Canada.

Fontes, W., **Tahir, M.**, Arshid, S., Heimbecker, A.M.C., Castro, M.S., Montero, E.F.S., Fontes, B. *"Effects of the ischemic preconditioning on the hematological parameters"*. International Symposium NEUTROPHIL 2014 - May 31st - June 3rd , 2014, Montréal - Canada.

Muhammad Tahir, Samina Arshid, Mariana S. Castro, Belchor Fontes, Peter Roepstorff, Wagner Fontes, *"Proteomic characterization of ischemia activated neutrophils"*. 5th BrMASS Conference, December 7th – 11th, 2013, São Paulo – Brazil.

ARTICLES PUBLISHED

Muhammad Tahir, Samina Arshid, Ana Maria C. Heimbecker, Mariana S. Castro, Edna Frasson de Souza Montero, Belchor Fontes, Wagner Fontes.*"Evaluation of the effects of ischemic preconditioning on the hematological parameters of rats subjected to intestinal ischemia and reperfusion"*.

Quantitative proteomic analysis of rat neutrophils after intestinal ischemia reperfusion and preconditioning

Samina Arshid 3, Muhammad Tahir 1, Belchor Fontes 3, Mariana S. Castro 1, Simone Sidoli 2, Veit Schwammle 2, Peter Roepstorff 2, Wagner Fontes 1

1 University of Brasilia, 2 University of Southern Denmark, 3 University of São Paulo

Introduction: Intestinal Ischemia reperfusion results in tissues injury and multiple organ dysfunction, development of acute respiratory distress syndrome and acute lung injury caused by infiltration of activated neutrophils whereas ischemic preconditioning is one of the several known modalities to attenuate this damage. **Objective:** The objective of our study was to analyze the effect of intestinal ischemia reperfusion and preconditioning on the rat neutrophil proteome. **Methodology:** The experimental design includes forty rats that were randomly assigned to four experimental groups, i.e control, laparotomy, intestinal ischemia reperfusion and ischemic preconditioning. After experimental procedures and neutrophils isolation, proteins were extracted from neutrophils by using FASP protocol. After trypsin digestion and quantification the peptides were labeled by iTRAQ TM. HILIC fractionation was performed and fractions were analyzed by a nLC-MS LTQ Orbitrap Velos and Proteome Discoverer was used to process the raw files. For data normalization, statistical analysis and cluster development a statistical program R was used. GO slim analysis was performed for the final results by using ProteinCenter and enzymes prediction was carried out by Blast2GO. **Results:** A total of 2508 proteins were identified and were classified in 6 clusters based on their expression. The GO analysis of cluster 5 shows enrichment for cellular component ribosome and cluster 1 for mitochondria. Molecular function GO analysis showed cluster 5 enrichment for RNA binding and structural molecule activity. Blast2GO analysis revealed that most of the Transferases and Hydrolases belong to cluster 1 that shows more up regulation in Ischemia than in Laparotomy and Preconditioning group of rat neutrophils.

QUANTITATIVE PROTEOMIC ANALYSIS OF RAT NEUTROPHILS AFTER INTESTINAL ISCHEMIA AND REPERFUSION

Fontes,W.[1]; Tahir, M.[1,2];Arshid,S.[1,3];Montero,E.[3];Fontes,B.[3];Castro,M.S.[1];Sidoli, S.[2];Roepstorff,P.[1]
[1]Laboratory of Biochemistry and Protein Chemistry, University of Brasilia, Brazil
[2]Biochemistry and Molecular Biology Institute, University of Southern Denmark
[3]Laboratory of Surgical Physiopathology (LIM-62), University of São Paulo, Brazil

Ischemic reperfusion (IR) injury leads to tissue damage. Polymorphonuclear neutrophils (PMNs) are involved in intestinal tissue damage after ischemia and reperfusion, which often leads to acute lung injury and multiple organ failure. **Objective:** The objective of our study was to analyze the effect of intestinal IR on the neutrophil protein profile. **Methods:** After intestinal IR and neutrophils isolation, proteins were extracted from neutrophils by FASP method and trypsin digested. Peptides were labeled by iTRAQ™ and phospho enrichment was performed via TiSH. HILIC fractions were analyzed by a nLC-MS LTQ-Orbitrap Velos. Files were processed using Proteome Discoverer and proteins of interest were analyzed by Blast2GO for gene ontologies. **Results:** We identified 2924 proteins in total, of which 653 proteins showed significant regulation while 367 and 286 were up and down regulated respectively. Up regulated proteins showed enrichment in cytoplasm, nucleus and ribosomes while membrane proteins showed down regulation in IR. Phosphorylation analysis revealed 433 proteins significantly more phosphorylated in which 300 proteins were mono, 75 di, 36 tri, 16 tetra, 4 penta, 1 octa and 1 trideca phosphorylated. Most of the oxidoreductases were down regulated whereas isomerases and ligases showed up regulation in rat neutrophils after intestinal IR. **Conclusion:** Our analysis revealed pronounced effect of intestinal ischemia on the rat neutrophil proteome. The phospho enrichment method provided 95% enrichment of phosphorylated peptides.

EFFECTS OF THE ISCHEMIC PRECONDITIONING ON THE HEMATOLOGICAL PARAMETERS

Fontes, W. 2; **Tahir, M. 2**; Arshid, S. 1,2; Heimbecker, A.M.C 1; Castro, M.S. 2; Montero, E.F.S. 1; Fontes, B. 1

1 Laboratory of Surgical Physiopathology (LIM-62), Faculty of Medicine, University of São Paulo, Brazil
2 Laboratory of Biochemistry and Protein Chemistry, University of Brasilia, Brazil

Intestinal ischemia and reperfusion (IR) results in tissue damage mediated by neutrophils, often leading to acute lung injury and multiple organ failure. Ischemic preconditioning (IPC) has been shown to be protective in nature and reduced tissue injuries in animal and human models of different organs. **Objective:** To evaluate the hematological changes during IR and IPC in rats. **Methodology:** Forty Wistar rats were divided into four groups: control, laparotomy, IR and IPC. The IR group received 45 min of superior mesenteric artery occlusion (SMAO), while the IPC group had 10 min of short ischemia and reperfusion before 45 min of prolonged SMAO. An automated cell counter was used to analyze the blood from all rats before and after the surgical procedures, and the hematological results were compared among the groups. **Results:** We found significant differences in the hematimetric parameters among all conditions. The major significant differences in values among groups regarded lymphocytes, white blood cells, granulocytes, hematocrit, mean corpuscular hemoglobin concentration, mean platelet volume, plateletcrit, platelet distribution width and platelet and red cell deviation width. **Conclusion:** The most remarkable parameters were those related to leukocytes and platelets. The lymphocyte and granulocytes counts and the granulocytes/lymphocytes ratio suggest that IPC attenuates the effect of the IR in the circulating blood cells. Our work provides knowledge toward a better understanding of the hematological responses after IR and IPC.

Proteomic characterization of ischemia activated neutrophils

Muhammad Tahir [1], Samina Arshid [1], Mariana S. Castro [1], Belchor Fontes [3], Peter Roepstorff [2], Wagner Fontes [1]

wagnerf@unb.br

[1]University of Brasilia, [2]University of Southern Denmark, [3]University of São Paulo

Neutrophils have an impressive array of microbicidal weapons, and in the presence of a pathogen or damaged tissue, progress from a quiescent state in the bloodstream to a completely activated state. Failure to regulate this activation, for example, when the blood is flooded with cytokines after hypovolemic shock, causes inappropriate neutrophil activation that paradoxically, is associated with tissue and organ damage.

Interruption of blood supply results in ischemic injury which rapidly damages metabolically active tissues. Paradoxically, restoration of blood flow to the ischemic tissue initiates a cascade of events that may lead to additional cell injury known as ischemic reperfusion injury (IRI). IRI to the intestine results in production of molecules such as hydrogen peroxide, superoxide, and inflammatory cytokines that can enhance inflammation and harm distant organs. This leads to the development of systemic inflammatory response syndrome (SIRS), which can progress to multiple organ failure (MOF), with a high morbidity and mortality in both surgical and trauma patients. The effect of IRI on neutrophils proteome has not yet been elucidated. The identification of a wide group of proteins has become practicable for many laboratories in recent years, largely due to improvements in mass spectrometry (MS) and development of chromatography and bioinformatics methods.

In this work we present the proteomic characterization of rat neutrophils activated by intestinal ischemia and reperfusion highlighting protein groups that show significant abundance difference to the control groups.

Methods: Healthy rats were divided in three groups, control (CTRL), laparotomy (LAP) and ischemia/reperfusion (I/R). The I/R group was submitted to anesthesia, laparotomy, isolation of the mesenteric artery, clamping for 45 min and reperfusion for 120 min. After that the blood was collected from the right atrium. The LAP group was not submitted to the clamping and the CTRL group was not submitted to laparotomy. Neutrophils were isolated, lysed in SDS+protease inhibitors, the proteins were digested with trypsin, the peptides were desalted and subjected to a discovery proteomics workflow using label free analysis. Chromatography was performed on a RP C18 two-column system, eluted to an Orbitrap Velos operating in DDA high/low mode to fragment the top 10 more intense ions. The collected data was analyzed using the Progenesis software for chromatogram alignment and feature quantitation, then using Mascot for proteins identification.

Results: In this work we achieved the identification of 2345 proteins, being 220 potentially involved in inflammatory signaling after ischemia and reperfusion, as well as proteins described for the first time in neutrophils. Among the proteins presenting significantly different abundance, 62 were more abundant in the CTRL group and 15 predominant in the I/R group. The analysis of these proteins suggests the participation of the PAF pathway in the IRI process.

CLINICS

BASIC RESEARCH

Evaluation of the effects of ischemic preconditioning on the hematological parameters of rats subjected to intestinal ischemia and reperfusion

Muhammad Tahir,[II,**] Samina Arshid,[I,II,**] Ana Maria C. Heimbecker,[I] Mariana S. Castro,[II] Edna Frasson de Souza Montero,[I] Belchor Fontes,[I] Wagner Fontes[II,*]

[I]Faculdade de Medicina da Universidade de São Paulo, Laboratory of Surgical Physiopathology (LIM-62), São Paulo, Brazil. [II]University of Brasilia, Cell Biology Dept, Laboratory of Biochemistry and Protein Chemistry, Brasilia/DF, Brazil.

OBJECTIVES: Intestinal ischemia/reperfusion often leads to acute lung injury and multiple organ failure. Ischemic preconditioning is protective in nature and reduces tissue injuries in animal and human models. Although hematimetric parameters are widely used as diagnostic tools, there is no report of the influence of intestinal ischemia/reperfusion and ischemic preconditioning on such parameters. We evaluated the hematological changes during ischemia/reperfusion and preconditioning in rats.

METHODS: Forty healthy rats were divided into four groups: control, laparotomy, intestinal ischemia/reperfusion and ischemic preconditioning. The intestinal ischemia/reperfusion group received 45 min of superior mesenteric artery occlusion, while the ischemic preconditioning group received 10 min of short ischemia and reperfusion before 45 min of prolonged occlusion. A cell counter was used to analyze blood obtained from rats before and after the surgical procedures and the hematological results were compared among the groups.

RESULTS: The results showed significant differences in hematimetric parameters among the groups. The parameters that showed significant differences included lymphocyte, white blood cells and granulocyte counts; hematocrit; mean corpuscular hemoglobin concentration; red cell deviation width; platelet count; mean platelet volume; plateletcrit and platelet distribution width.

CONCLUSION: The most remarkable parameters were those related to leukocytes and platelets. Some of the data, including the lymphocyte and granulocytes counts, suggest that ischemic preconditioning attenuates the effect of intestinal ischemia/reperfusion on circulating blood cells. Our work contributes to a better understanding of the hematological responses after intestinal ischemia/reperfusion and IPC, and the present findings may also be used as predictive values.

KEYWORDS: Ischemic Reperfusion Injury; Ischemic Preconditioning; Systemic Inflammatory Response; Intestinal Ischemia; Hemocytometry; Superior Mesenteric Artery Occlusion.

Tahir M, Arshid S, Heimbecker AM, Castro MS, Montero EF, Fontes B, et al. Evaluation of the effects of ischemic preconditioning on the hematological parameters of rats subjected to intestinal ischemia and reperfusion. Clinics. 2015;70(1):61-68.

Received for publication on August 1, 2014; **First review completed on** September 22, 2014; **Accepted for publication on** October 14, 2014

E-mail: wagnerf@unb.br

*corresponding author

**contributed equally to the study

INTRODUCTION

Ischemic injury results from the interruption of blood flow and causes damage to active tissues; ischemic reperfusion injury (IRI) occurs after the restoration of blood flow, leading to additional tissue injury (1). In 1986, Parks and Granger (2) reported that reperfusion is more harmful than ischemia alone. In particular, the tissue damage that is caused by ischemia and reperfusion in the intestine is associated with high morbidity and mortality in surgical patients. IRI occurs in cases of abdominal aortic aneurysm surgery, hemorrhagic shock, acute mesenteric ischemia (AMI), strangulated hernia, neonatal necrotizing enterocolitis, cardiopulmonary bypass and organ transplantation (3). Among the internal organs, the intestine is most sensitive to IRI (1). Intestinal IRI can lead to damage in the intestinal mucosa and the release of various inflammatory mediators, potentially resulting in the development of systemic inflammatory response syndrome (SIRS) and further leading to multiple organ failure (MOF), especially acute lung

No potential conflict of interest was reported.

DOI: 10.6061/clinics/2015(01)11

injury (ALI) (4-7). Ischemia-reperfusion causes local and systemic changes in hemodynamics, endothelial function, microcirculation, fluid equilibrium and metabolic homeostasis while also inducing the complement and inflammatory pathways (8-14). In an attempt to attenuate this damage, several treatment modalities have been applied in various animal models of IRI, such as hypothermia, antioxidants, ischemic preconditioning (IPC) and modulation of inflammatory mediators and adhesion molecules. Among these approaches, IPC seems to be the most promising against reperfusion injury, as it increases the bowel's tolerance against the damage caused by ischemia followed by reperfusion (15-17).

In 1986, Murry et al. introduced the concept of IPC as short episodes of ischemia followed by short periods of reperfusion preceding a prolonged ischemia; this approach was shown to protect organs against subsequent longer ischemia (18). IPC of the intestine was first described by Hotter et al. in 1996 (19) and subsequent studies have confirmed this phenomenon. Studies in shock models show that IPC before intestinal ischemia causes a significant reduction in the inflammatory response in the lungs and intestinal injuries due to hemorrhagic shock (20). However, the precise mechanism by which IPC confers protection to the intestine remains unclear.

Blood is the most accessible component of the vertebrate body fluid system and has frequently been examined to assess physiological status (21). Hematimetric parameters have long been used as diagnostic tools for a large number of diseases, such as leukemias, anemias and infectious diseases. However, few studies have collectively addressed the prognostic values of these parameters using multivariate analysis and to our knowledge, no studies have addressed IPC. The purpose of this study was to obtain a basic knowledge of the hematological factors after IRI and IPC in rats. In this prospective study, we evaluated the significance of routine blood parameters after intestinal ischemia and preconditioning in rats, the results of which could help in the early diagnosis of IRI and in understanding how IPC affects blood components.

MATERIALS AND METHODS

Experimental subjects and sample collection

Male Wistar rats without inflammatory disease and weighing 250–350 g were collected from the animal house of the Faculdade de Medicina da Universidade de São Paulo (FMUSP), São Paulo State, Brazil. The project was approved by the Ethics Committee of FMUSP (Protocol No. 8186) for the use of rats as experimental subjects. The animals were provided access to food and water ad libitum until the time of the experiment.

Experimental groups

Forty rats were randomly allocated into the following four groups (Figure 1), where n represents the number of animals per group:

1- The control group (C) (n = 10), without any surgical procedure.
2- The sham laparotomy group (LAP) (n = 10), without clamping of any artery, but receiving the same surgical procedure except for the clamping.
3- Ischemia/reperfusion (IR) group (n = 10), submitted to superior mesenteric artery occlusion (SMAO) for 45 min followed by 120 min of reperfusion.
4- Ischemic preconditioning (IPC) group (n = 10), submitted to a 10-min period of SMAO followed by 10-min reperfusion immediately before 45 min of ischemia and 120 min of reperfusion, as in the IR group.

Hematological analyses

We collected 20 µl of blood from the tails of all animals before and after surgery and injected the samples into a

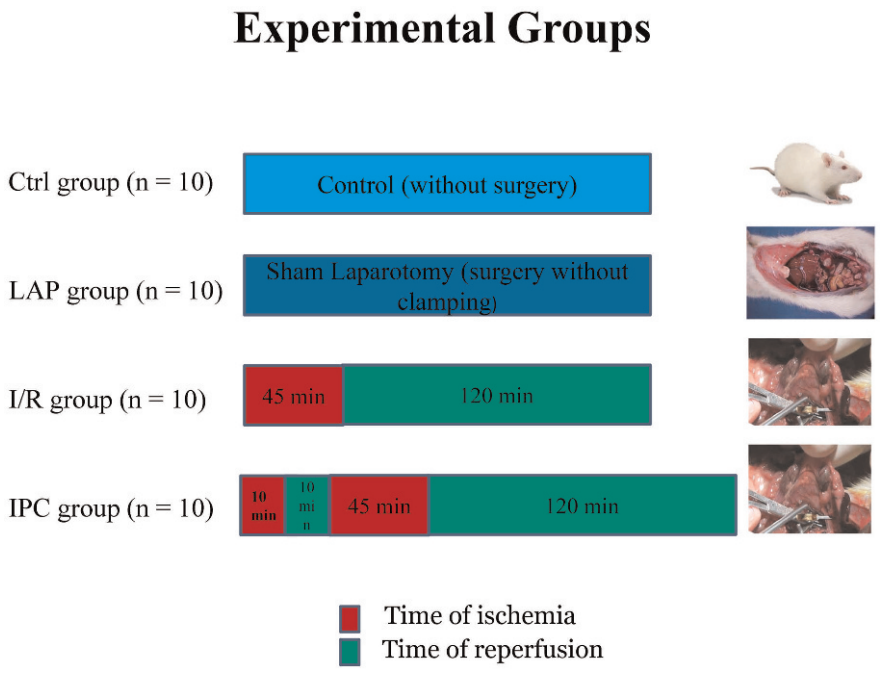

Figure 1 - Experimental groups and their times of ischemia and reperfusion, where n represents the number of animals per group.

veterinary automated cell counter (BC-2800Vet, Shenzhen Mindray Bio-Medical Electronics Co., Nanshan, China). The analyzed hematimetric parameters included the total erythrocyte count (RBC), total white blood cell (WBC) count, hematocrit (HCT) level, hemoglobin (Hb) concentration, erythrocyte indices as mean corpuscular volume (MCV), mean corpuscular hemoglobin (MCH), mean corpuscular hemoglobin concentration (MCHC), platelet (PLT) count, mean platelet volume (MPV), platelet distribution widths (PDW), plateletcrit (PCT) and WBC differential count (22,23).

Surgical procedures

The surgical procedures were performed in the Laboratory of Surgical Physiopathology (LIM-62), department of Surgery, FMUSP. Rats from all of the groups were anesthetized with intraperitoneal (i.p.) injections of sodium pentobarbital (45 mg/kg) and ketamine (80 mg/kg) + xylazine (7 mg/kg) and their core body temperatures were maintained at 37℃. After midline laparotomy, the superior mesenteric artery was isolated near its aortic origin. During this procedure, the intestinal tract was placed between gauze pads that had been soaked with warmed 0.9% NaCl solution. In rats from the IR group, the superior mesenteric artery was clamped, resulting in total occlusion of the artery for 45 min. After the time of occlusion, the clamps were removed and blood samples were collected from the tail after 120 min of reperfusion. In the rats of the IPC group, the ischemic procedure described above was preceded by 10 min of clamping followed by 10 min of reperfusion.

Statistical analysis

For statistical analysis, the data were first checked for normality by applying the D'Agostino & Pearson omnibus normality test. The data were normalized and outliers were removed, based on the Thompson tau technique; then, normality was reconfirmed with the above-mentioned normality test. Variance analysis (one-way ANOVA) was used to determine the difference between the groups and the Tukey-Kramer test was used to compare and determine the means that differed significantly from each other using the Graph Pad Prism program (V.6.0c). Values with $p<0.05$ were considered significant.

RESULTS

The hematological parameters of the control, laparotomy, ischemia/reperfusion and IPC groups are summarized in Supplementary Table 1.

All of the surgical groups (LAP, IR and IPC) showed a remarkably smaller amount of lymphocytes than did the control group. Among the surgical groups, the IR group showed a decrease in lymphocyte count ($p=0.0021$) compared with the LAP group; however, an increase was noted in the IPC group ($p=0.0171$) compared with IR group (Figure 2-A).

The WBC counts showed a significant increase in both the IR ($p=0.0005$) and the IPC ($p=0.0074$) groups compared with the control group (Figure 2-B). The elevation in WBCs was more prominent in the IR group than in the IPC group. A significant increase in the granulocyte count was observed in the LAP, IR and IPC groups compared with the controls; there was also an increase in the IR group compared with the LAP group ($p=0.0015$), whereas the IPC group showed a significant reduction ($p=0.0168$) compared with the IR group, almost approaching the level of the LAP group (Figure 2-C).

Platelets showed a significant difference between the IR and IPC groups. The PLT counts were higher ($p=0.0340$) in the IR group than in the IPC group (Figure 2-D) and the MPV also showed a significantly increased value in the IR ($p=0.0096$) and IPC ($p=<0.0001$) groups compared with the controls. In preconditioned rats, the MPV was higher than that in LAP ($p=0.0004$) and IR rats ($p=0.0485$) (Figure 2-E). The PDW was significantly greater in IPC rats compared to all of the other groups. The p-values for the IPC group compared with the control, LAP and IR groups are 0.0003, 0.0015 and 0.0011, respectively (Figure 2-F).

The levels of monocytes, RBCs, Hb, MCV and MCH were not influenced significantly in any experimental group. The HCT level was increased ($p=0.0082$) in the IR group compared with the control group (Figure 1-A, supplementary). The MCHC was decreased in the IR group ($p=0.0111$) compared with the controls, whereas there was an increase in the MCHC value in the IPC group ($p=0.0111$) compared with the IR group, which restored the MCHC value to a normal level (Figure 1-B, supplementary). The red cell deviation width was higher ($p=0.0152$) in the IPC group than the control group, although no other group showed a significant difference (Figure 1-C, supplementary). Both the IR and IPC groups showed significant differences regarding their PCT levels, whereas the remaining groups did not show any significant differences. The PCT level was higher ($p=0.0264$) in the IR group compared with the IPC group (Figure 2-D).

DISCUSSION

IPC has been studied as a protective strategy against IRI in intestinal models (19,20). In humans, prolonged jejunal ischemia (45 min) followed by reperfusion results in intestinal barrier integrity loss, which is accompanied by a significant translocation of endotoxins. These phenomena result in an inflammatory response that is characterized by complement activation, endothelial activation, neutrophil sequestration and the release of pro-inflammatory mediators into circulation (24). A comparison of the effect of IR and IPC on blood parameters has not been made using the 45-min SMAO model in rats. Lymphocyte loss and dysfunction have been consistently reported in animal models of both SIRS and sepsis (25) and preventing lymphocyte dysfunction, specifically lymphocyte apoptosis following sepsis, has been shown to improve survival after sepsis (26). Recently, a decrease in the lymphocyte percentage was observed following IR and local and remote IPC in a rat model with temporary supraceliac aortic clamping (27). IPC also prevented lymphocyte loss compared with that observed in the IR group in our study.

We observed a significant increase in the WBC count after IR. Postoperative leukocytosis represents a normal physiologic response to surgery (28). However, an augmentation in the WBC count has been viewed as a predictor of ischemic stroke (29). This increase is due to the marked elevation of leukocyte activation, as previously described in myocardial ischemia and reperfusion in dogs (30). The increased number of granulocytes after ischemic strokes leads to tissue damage, as these cells are implicated in the early responses of the hemostatic and inflammatory processes (31). Intestinal

CLINICS 2015;70(1):61-68

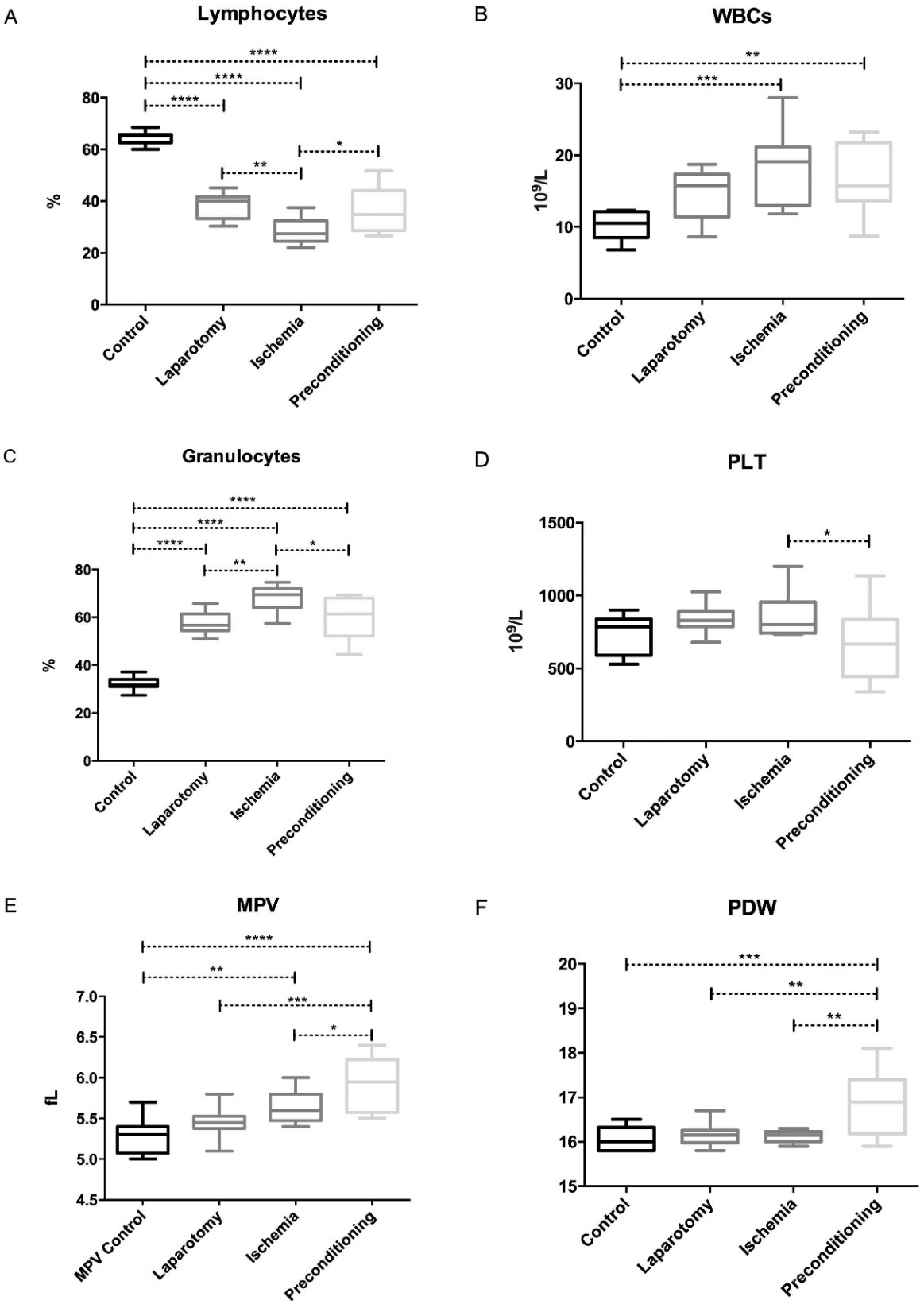

Figure 2 - Distribution of the hematimetric parameters in the four experimental groups. (A) Lymphocyte count, (B) WBC count (C) Granulocyte count, (D) Platelet count, (E) MPV and (F) PDW. (***$p<0.001$; **$p<0.001$ to 0.01; *$p<0.01$ to 0.05).

ischemia is characterized by the production of cytokines (32) and the sequestration of polymorphonuclear neutrophils (PMNs) into the ischemically damaged tissue. The complement system also contributes to the attraction of neutrophils to ischemically damaged areas (33), where neutrophil-released myeloperoxidase (MPO) and other proinflammatory mediators further contribute to IR-induced tissue damage (34). Figure 2-C clearly shows a significant reduction in circulating granulocytes of the IPC group compared with the IR group, suggesting a protective aspect of IPC.

With the exception of the MCHC values, our results concerning RBCs, Hb, MCV, MCH and HCT are similar to those of a study using a canine model to investigate limb IR, with or without cooling (35). Dehydration during surgery or fluid sequestration due to edema can result in a higher-than-normal HCT level (36). This increase was more prominent in the IR group and showed no significant difference in any other group. Similarly, an increase in HCT was observed in the IR compared with local IPC and remote IPC groups in a similar model using temporary supraceliac aortic clamping (27).

Platelets also participate in ischemic strokes (37) and IR-mediated tissue damage (38) through the modulation of leukocyte function and the generation of free radicals and proinflammatory mediators, such as thromboxane (TxA2), leukotrienes, serotonin, platelet factor-4 and platelet-derived growth factor (PDGF) (39,40). Similar to leukocytes, the expression of P-selectin on the platelet surface contributes to rolling and firm adherence to the vascular endothelium and in the interaction with leukocytes during post-ischemic reperfusion, resulting in increased expression of adhesion molecules, the generation of superoxide and the phagocytic activity of leukocytes (39,41). The inhibition of platelet adhesion by the administration of an anti-fibrinogen antibody was shown to decrease short-term liver injury after ischemia. In addition, platelet-derived serotonin is a mediator of tissue repair after hepatic normothermic ischemia in mice (42,43). We observed a significant decrease in platelets in the IPC group compared with the IR group. However, the role of platelets in the progression of tissue damage after IR injury remains unclear. A recent study showed that platelet-deficient mice showed significant reductions in damage to their villi in response to IR compared with mice with normal platelet counts (44).

Previous studies showed that the MPV was higher when there was destruction of platelets associated with inflammatory bowel disease (45), whereas other studies showed that the MPV was not associated with stroke severity or functional outcomes (46). The activation of platelets leads to morphologic changes, including pseudopodia formation and the development of a spherical shape. Platelets with an increased number and size of pseudopodia differ in size, possibly affecting the PDW. Indeed, we found an inverse relationship between the PLT count and MPV value after IR and IPC, which suggests that IPC lowers the PLT count but increases the MPV value. However, a recent study in patients who underwent surgical intervention for acute mesenteric ischemia showed an increase in MPV and a decrease in PLT count in non-surviving patients compared with surviving patients (47). In the IR group, we found an increase in the PLT count and a decrease in the MPV value, in contrast to this previous study. This discrepancy could be attributed to different occlusion models because AMI patients can present partial vascular occlusions that last for less-precise amounts of time. In addition, we cannot correlate this change with mortality rate, as the model involving 45 min of intestinal ischemia in rats has been considered to be free of mortality (48), whereas the ischemic period and severity varies among clinical conditions, leading to higher morbidity and mortality. For example, AMI has an overall mortality of 60% to 80% and the reported incidence increases over time (49,50), mostly because of the continued difficulty in recognizing this condition (50). The effect of IPC on these parameters with AMI requires further validation in humans.

In summary, our results demonstrate that IPC before intestinal IR provoked significant alterations in hematimetric parameters in the IPC group compared with that in the IR group, mainly comprising decreases in the granulocyte count and PCT count and increases in the lymphocyte count and the MPV.

The results of the present study indicate that 10 min of IPC before 45 min of intestinal IR alter the hematimetric parameters, suggesting that IPC attenuates the effect of IR in circulating blood cells.

■ ACKNOWLEDGMENTS

The authors acknowledge TWAS, CNPq, CAPES, FAPESP, FAP-DF and FUB-UnB for financial support. We also thank Prof. Dr. Paulina Sonnomiya from the Laboratory of Cardio-Pneumology (LIM-11) of the Faculty of Medicine of the University of São Paulo LIM11 for allowing access to the hemocytometer.

■ AUTHOR CONTRIBUTIONS

Tahir M, Arshid S and Montero EF were responsible for the hematimetric parameter analysis and surgical procedures. Heimbecker AM and Fontes B were responsible for the surgical procedures. Castro MS and Fontes W were responsible for the experimental design and statistical analysis. All of the authors contributed to the discussion of the results and to the writing of the article.

■ REFERENCES

1. Yamamoto S, Tanabe M, Wakabayashi G, Shimazu M, Matsumoto K, Kitajima M. The role of tumor necrosis factor-alpha and interleukin-1beta in ischemia-reperfusion injury of the rat small intestine. J Surg Res. 2001;99(1):134-41, http://dx.doi.org/10.1006/jsre.2001.6106.
2. Parks DA, Granger DN. Contributions of ischemia and reperfusion to mucosal lesion formation. Am J Physiol. 1986;250(6 Pt 1):G749-53.
3. Collard CD, Gelman S. Pathophysiology, clinical manifestations, and prevention of ischemia-reperfusion injury. Anesthesiology. 2001;94(6):1133-8, http://dx.doi.org/10.1097/00000542-200106000-00030.
4. Ceppa EP, Fuh KC, Bulkley GB. Mesenteric hemodynamic response to circulatory shock. Curr Opin Crit Care. 2003;9(2):127-32, http://dx.doi.org/10.1097/00075198-200304000-00008.
5. Koksoy C, Kuzu MA, Kuzu I, Ergun H, Gurhan I. Role of tumour necrosis factor in lung injury caused by intestinal ischaemia-reperfusion. Br J Surg. 2001;88(3):464-8.
6. Xiao F, Eppihimer MJ, Young JA, Nguyen K, Carden DL. Lung neutrophil retention and injury after intestinal ischemia/reperfusion. Microcirculation. 1997;4(3):359-67, http://dx.doi.org/10.3109/10739689709146800.
7. Teles LM, Aquino EN, Neves AC, Garcia CH, Roepstorff P, Fontes B, et al. Comparison of the neutrophil proteome in trauma patients and normal controls. Protein Pept Lett. 2012;19(6):663-72, http://dx.doi.org/10.2174/092986612800493977.
8. Anaya-Prado R, Toledo-Pereyra LH, Lentsch AB, Ward PA. Ischemia/reperfusion injury. J Surg Res. 2002;105(2):248-58, http://dx.doi.org/10.1006/jsre.2002.6385.
9. Blaisdell FW: The pathophysiology of skeletal muscle ischemia and the reperfusion syndrome: a review. Cardiovasc Surg. 2002;10(6):620-30, http://dx.doi.org/10.1016/S0967-2109(02)00070-4.
10. Kabaroudis A, Gerassimidis T, Karamanos D, Papaziogas B, Antonopoulos V, Sakantamis A. Metabolic alterations of skeletal muscle tissue after prolonged acute ischemia and reperfusion. J Invest Surg. 2003;16(4):219-28, http://dx.doi.org/10.1080/08941930390215015.

11. Yassin MM, Harkin DW, Barros D'Sa AA, Halliday MI, Rowlands BJ. Lower limb ischemia-reperfusion injury triggers a systemic inflammatory response and multiple organ dysfunction. World J Surg. 2002;26(1):115-21.
12. Castro MS, Ferreira TC, Cilli EM, Crusca E, Jr., Mendes-Giannini MJ, Sebben A, et al. Hylin a1, the first cytolytic peptide isolated from the arboreal South American frog Hypsiboas albopunctatus (''spotted treefrog''). Peptides. 2009;30(2):291-6, http://dx.doi.org/10.1016/j.peptides.2008.11.003.
13. de Souza Castro M, de Sa NM, Gadelha RP, de Sousa MV, Ricart CA, Fontes B, et al. Proteome analysis of resting human neutrophils. Protein and peptide letters 2006;13(5):481-487, http://dx.doi.org/10.2174/092986606776819529.
14. Nascimento A, Chapeaurouge A, Perales J, Sebben A, Sousa MV, Fontes W, et al. Purification, characterization and homology analysis of ocellatin 4, a cytolytic peptide from the skin secretion of the frog Leptodactylus ocellatus. Toxicon. 2007;50(8):1095-104, http://dx.doi.org/10.1016/j.toxicon.2007.07.014.
15. Abrahao MS, Montero EF, Junqueira VB, Giavarotti L, Juliano Y, Fagundes DJ. Biochemical and morphological evaluation of ischemia-reperfusion injury in rat small bowel modulated by ischemic preconditioning. Transplant Proc. 2004;36(4):860-2, http://dx.doi.org/10.1016/j.transproceed.2004.03.046.
16. Mallick IH, Yang W, Winslet MC, Seifalian AM. Ischemia-reperfusion injury of the intestine and protective strategies against injury. Dig Dis Sci. 2004;49(9):1359-77, http://dx.doi.org/10.1023/B:DDAS.0000042232.98927.91.
17. Morris CF, Castro MS, Fontes W. Neutrophil proteome: lessons from different standpoints. Protein Pept Lett. 2008;15(9):995-1001, http://dx.doi.org/10.2174/092986608785849371.
18. Murry CE, Jennings RB, Reimer KA. Preconditioning with ischemia: a delay of lethal cell injury in ischemic myocardium. Circulation. 1986;74(5):1124-36, http://dx.doi.org/10.1161/01.CIR.74.5.1124.
19. Hotter G, Closa D, Prados M, Fernandez-Cruz L, Prats N, Gelpi E, et al. Intestinal preconditioning is mediated by a transient increase in nitric oxide. Biochem Biophys Res Commun. 1996;222(1):27-32, http://dx.doi.org/10.1006/bbrc.1996.0692.
20. Tamion F, Richard V, Lacoume Y, Thuillez C. Intestinal preconditioning prevents systemic inflammatory response in hemorrhagic shock. Role of HO-1. Am J Physiol Gastrointest Liver Physiol. 2002;283(2):G408-14.
21. Houston JB, Carlile DJ. Incorporation of in vitro drug metabolism data into physiologically-based pharmacokinetic models. Toxicol In Vitro. 1997;11(5):473-8, http://dx.doi.org/10.1016/S0887-2333(97)00056-8.
22. Campbell TW. Hematology of lower vertebrates. In: In: Proceedings of the 55th Annual Meeting of the American College of Veterinary Pathologists (ACVPC) & 39th Annual Meeting of the American Society of Clinical Pathology (ASVCP); USA: ACVP and ASVCP.
23. Di Giulio RT, Hinton DE. The Toxicology of Fishes. Crc Press 2008:1101.
24. Grootjans J, Lenaerts K, Derikx JP, Matthijsen RA, de Bruine AP, van Bijnen AA, et al. Human intestinal ischemia-reperfusion-induced inflammation characterized: experiences from a new translational model. Am J Pathol. 2010;176(5):2283-91.
25. Deitch EA, Landry KN, McDonald JC. Postburn impaired cell-mediated immunity may not be due to lazy lymphocytes but to overwork. Ann Surg. 1985;201(6):793-802, http://dx.doi.org/10.1097/00000658-198506000-00018.
26. Hotchkiss RS, Tinsley KW, Swanson PE, Chang KC, Cobb JP, Buchman TG, Korsmeyer SJ, Karl IE. Prevention of lymphocyte cell death in sepsis improves survival in mice. Proc Natl Acad Sci U S A. 1999;96(25):14541-6, http://dx.doi.org/10.1073/pnas.96.25.14541.
27. Erling Junior N, Montero EF, Sannomiya P, Poli-de-Figueiredo LF. Local and remote ischemic preconditioning protect against intestinal ischemic/reperfusion injury after supraceliac aortic clamping. Clinics. 2013;68(12):1548-54, http://dx.doi.org/10.6061/clinics/2013(12)12.
28. Deirmengian GK, Zmistowski B, Jacovides C, O'Neil J, Parvizi J. Leukocytosis is common after total hip and knee arthroplasty. Clin Orthop Relat Res. 2011;469(11):3031-6, http://dx.doi.org/10.1007/s11999-011-1887-x.
29. Grau AJ, Boddy AW, Dukovic DA, Buggle F, Lichy C, Brandt T, et al. Leukocyte count as an independent predictor of recurrent ischemic events. Stroke. 2004;35(5):1147-52, http://dx.doi.org/10.1161/01.STR.0000124122.71702.64.
30. Lantos J, Grama L, Orosz T, Temes G, Roth E. Leukocyte CD11a expression and granulocyte activation during experimental myocardial ischemia and long lasting reperfusion. Exp Clin Cardiol. 2001;Summer;6(2):72-6.
31. Grau AJ, Berger E, Sung KL, Schmid-Schonbein GW. Granulocyte adhesion, deformability, and superoxide formation in acute stroke. Stroke. 1992;23(1):33-9, http://dx.doi.org/10.1161/01.STR.23.1.33.
32. Frangogiannis NG, Smith CW, Entman ML. The inflammatory response in myocardial infarction. Cardiovasc Res. 2002;53(1):31-47, http://dx.doi.org/10.1016/S0008-6363(01)00434-5.
33. Hart ML, Ceonzo KA, Shaffer LA, Takahashi K, Rother RP, Reenstra WR, et al. Gastrointestinal ischemia-reperfusion injury is lectin complement pathway dependent without involving C1q. J Immunol. 2005;174(10):6373-80, http://dx.doi.org/10.4049/jimmunol.174.10.6373.
34. Matthijsen RA, Huugen D, Hoebers NT, de Vries B, Peutz-Kootstra CJ, Aratani Y, et al. Myeloperoxidase is critically involved in the induction of organ damage after renal ischemia reperfusion. Am J Pathol. 2007;171(6):1743-52.
35. Szokoly M, Nemeth N, Furka I, Miko I. Hematological and hemostaseological alterations after warm and cold limb ischemia-reperfusion in a canine model. Acta Cir Bras. 2009;24(5):338-46, http://dx.doi.org/10.1590/S0102-86502009000500002.
36. Jackson PG, Raiji MT. Evaluation and management of intestinal obstruction. Am Fam Physician. 2011;83(2):159-65.
37. Del Conde I, Cruz MA, Zhang H, Lopez JA, Afshar-Kharghan V. Platelet activation leads to activation and propagation of the complement system. J Exp Med. 2005;201(6):871-9, http://dx.doi.org/10.1084/jem.20041497.
38. Hamad OA, Nilsson PH, Wouters D, Lambris JD, Ekdahl KN, Nilsson B. Complement component C3 binds to activated normal platelets without preceding proteolytic activation and promotes binding to complement receptor 1. J Immunol. 2010;184(5):2686-92, http://dx.doi.org/10.4049/jimmunol.0902810.
39. Massberg S, Enders G, Leiderer R, Eisenmenger S, Vestweber D, Krombach F, et al. Platelet-endothelial cell interactions during ischemia/reperfusion: the role of P-selectin. Blood. 1998;92(2):507-15.
40. Massberg S, Messmer K. The nature of ischemia/reperfusion injury. Transplant Proc. 1998;30(8):4217-23, http://dx.doi.org/10.1016/S0041-1345(98)01397-9.
41. Cooper D, Chitman KD, Williams MC, Granger DN. Time-dependent platelet-vessel wall interactions induced by intestinal ischemia-reperfusion. Am J Physiol Gastrointest Liver Physiol. 2003;284(6):G1027-33.
42. Khandoga A, Biberthaler P, Enders G, Axmann S, Hutter J, Messmer K, et al. Platelet adhesion mediated by fibrinogen-intercelllular adhesion molecule-1 binding induces tissue injury in the postischemic liver in vivo. Transplantation. 2002;74(5):681-8, http://dx.doi.org/10.1097/00007890-200209150-00016.
43. Nocito A, Georgiev P, Dahm F, Jochum W, Bader M, Graf R, et al. Platelets and platelet-derived serotonin promote tissue repair after normothermic hepatic ischemia in mice. Hepatology. 2007;45(2):369-76, http://dx.doi.org/10.1002/hep.21516.
44. Lapchak PH, Kannan L, Ioannou A, Rani P, Karian P, Dalle Lucca JJ, et al. Platelets orchestrate remote tissue damage after mesenteric ischemia-reperfusion. Am J Physiol Gastrointest Liver Physiol. 2012;302(8):G888-97, http://dx.doi.org/10.1152/ajpgi.00499.2011.
45. Liu S, Ren J, Han G, Wang G, Gu G, Xia Q, Li J. Mean platelet volume: a controversial marker of disease activity in Crohn's disease. Eur J Med Res. 2012;17:27.
46. Ntaios G, Gurer O, Faouzi M, Aubert C, Michel P. Mean platelet volume in the early phase of acute ischemic stroke is not associated with severity or functional outcome. Cerebrovasc Dis. 2010;29(5):484-9, http://dx.doi.org/10.1159/000297964.
47. Altintoprak F, Arslan Y, Yalkin O, Uzunoglu Y, Ozkan OV. Mean platelet volume as a potential prognostic marker in patients with acute mesenteric ischemia-retrospective study. World J Emerg Surg. 2013;8(1):49.
48. Kozar RA, Holcomb JB, Hassoun HT, Macaitis J, DeSoignie R, Moore FA. Superior mesenteric artery occlusion models shock-induced gut ischemia-reperfusion. J Surg Res. 2004;116(1):145-50, http://dx.doi.org/10.1016/S0022-4804(03)00301-9.
49. Bradbury AW, Brittenden J, McBride K, Ruckley CV. Mesenteric ischaemia: a multidisciplinary approach. Br J Surg. 1995;82(11):1446-59.
50. Heys SD, Brittenden J, Crofts TJ. Acute mesenteric ischaemia: the continuing difficulty in early diagnosis. Postgrad Med J. 1993;69(807):48-51, http://dx.doi.org/10.1136/pgmj.69.807.48.

Supplementary Table 1 - Hematological analyses, expressed as the mean ± standard deviation, median and range (min. - max.) of the four groups.

	Control group			Laparotomy group			Ischemia/Reperfusion group			Preconditioning group		
Parameters	Mean ± std dev	Median	Range Min - Max	Mean ± std dev	Median	Range Min - Max	Mean ± std dev	Median	Range Min - Max	Mean ± std dev	Median	Range Min - Max
WBC (10^9/L)	10.27±2.04	10.85	6.8-12.3	14.71±3.4	15.75	8.6-18.7	18.13±5.16	19.1	11.8-15.75	16.39±4.67	15.7	8.7-23.2
Lymphocytes (10^9/L)	6.79±1.59	7.2	4.1-8.8	5.6±1.42	5.3	3.5-7.7	5.65±1.28	5.65	3.7-8.8	5.61±2.24	5.05	3.9-11.6
Monocytes (10^9/L)	0.31±0.07	0.3	0.2-0.4	0.6±0.28	0.5	0.3-1.2	0.71±0.29	0.6	0.4-0.6	0.57±0.19	0.6	0.3-0.8
Granulocytes (10^9/L)	3.17±0.59	3.1	2.3-3.9	8.51±2.11	9.15	4.7-10.7	13.36±6.31	12.85	5-9.15	10.21±3.7	9.85	4.5-17.6
Lymphocytes (%)	64.76±2.96	65.1	60-70.8	38.26±4.98	39.95	30.3-45.1	28.47±5.23	27.35	22-70.8	36.33±8.19	34.85	26.7-51.8
Monocytes (%)	3.25±0.36	3.1	2.9-3.9	3.68±0.6	3.6	2.9-4.7	3.36±0.28	3.35	3-3.9	3.81±0.43	3.85	3.2-4.7
Granulocytes (%)	32.1±2.86	31.65	26.2-37.1	57.63±4.61	56.75	51.1-65.9	67.87±5.74	69.5	57.5-57.63	59.89±8.25	61.45	44.5-69.3
RBC (10^{12}/L)	6.528±0.55	6.58	5.49-7.52	7.38±0.72	7.65	6.1-8.3	7.66±0.52	7.665	6.88-7.65	7.32±1.38	7.63	4.62-9.58
Hb (g/L)	128±6.94	126.5	120-142	138.5±12.03	138.5	120-156	143.3±7.69	144	134-142	141±20.02	147.5	107-167
HCT (%)	40.83±1.86	40.45	38.8-44.4	44.63±3.63	44.95	38.7-49.8	47.07±2.61	46.85	43.3-44.95	45.14±6.31	47.65	34.2-54.2
MCV (fL)	61.39±2.46	61.1	57.2-65.1	60.41±1.95	59.95	58-63.7	61.57±2.34	61.2	58.2-65.1	60.8±2.39	60.75	56.6-64.7
MCH	19.16±0.75	19.15	17.6-20.3	18.6±0.67	18.6	17.8-19.7	18.7±0.8	18.8	17.5-20.3	18.98±0.73	19.05	17.4-20.1
MCHC (g/L)	312.8±4.61	312.5	307-320	308.7±5.89	308.5	301-320	304.1±5.36	302.5	297-320	312.7±7.12	313.5	303-325
RDW (%)	11.46±0.72	11.2	10.7-12.7	11.96±0.65	11.95	10.5-12.9	12.52±1.35	12.15	11-12.7	12.87±1.32	12.7	11.5-15.2
PLT (10^9/L)	746.6±148.32	785.5	529-943	837.3±92.71	828	679-1024	867.2±154.25	800.5	734-943	653.1±248.34	665	341-1135
MPV (fL)	5.3±0.2	5.3	5-5.7	5.45±0.18	5.45	5.1-5.8	5.64±0.2	5.6	5.4-5.7	5.93±0.33	5.95	5.5-6.4
PDW	16.1±0.24	16.05	15.8-16.5	16.15±0.26	16.15	15.8-16.7	16.13±0.13	16.15	15.9-16.5	16.86±0.68	16.9	15.9-18.1
PCT (%)	0.3946±0.08	0.412	0.275-0.49	0.46±0.03	0.456	0.418-0.52	0.49±0.09	0.441	0.401-0.49	0.3763±0.12	0.3945	0.218-0.578

CLINICS 2015;70(1):61-68

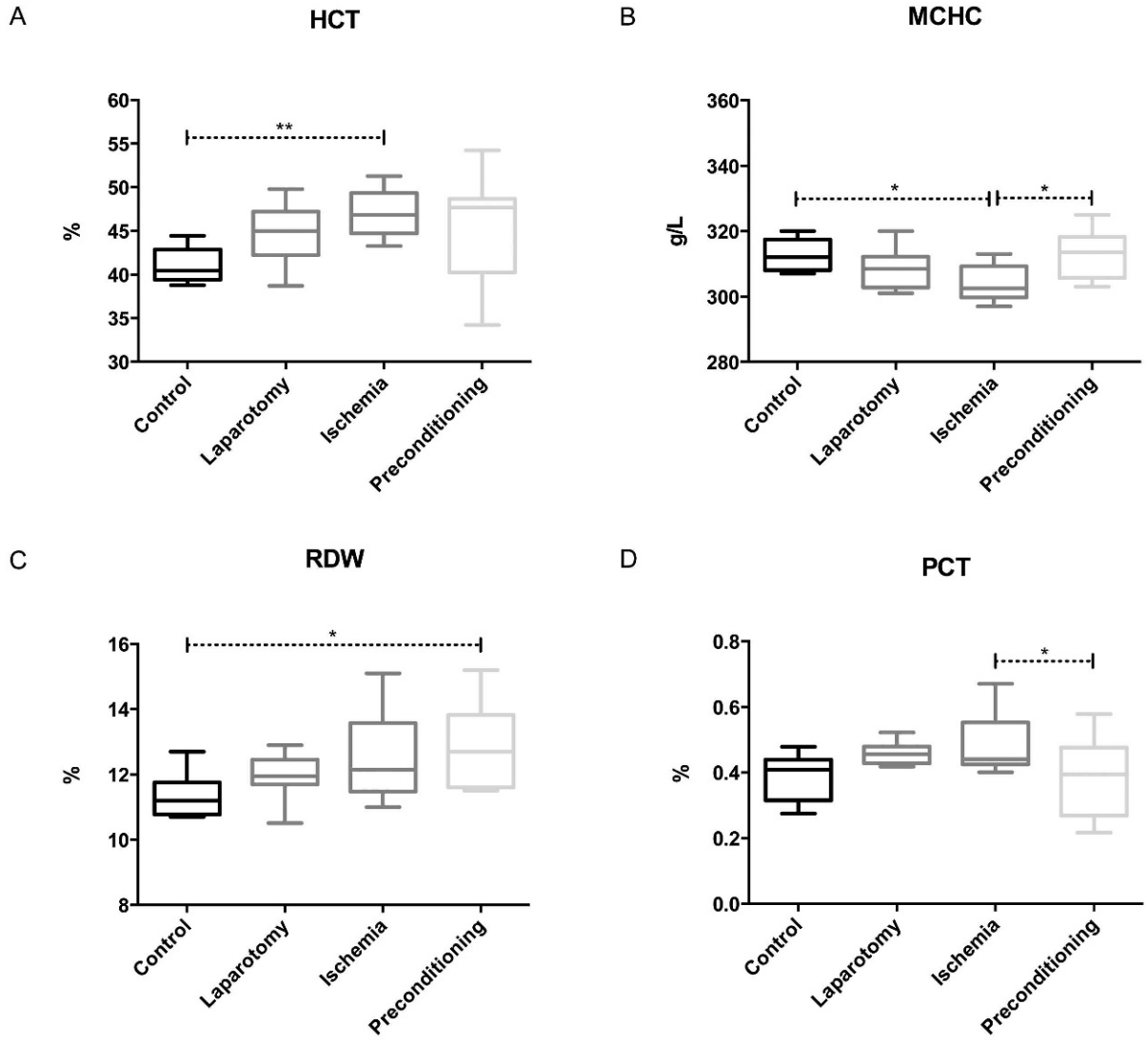

Supplementary Figure 1 - supplementary. Distribution of hematimetric parameters in the four experimental groups. (A) HCT, (B) MCHC, (C) Red cell distribution width and (D) PCT. (**$p<0.001$ to 0.01; *$p<0.01$ to 0.05).